Aus dem Institut für Molekulare Medizin
des Universitätsklinikums Schleswig-Holstein
Campus Lübeck
Direktor: Prof. Dr. Georg Sczakiel

The Hexanucleotide UCGUGU as a Lead Compound against the Reverse Transcriptase of HIV-1: a Proof of Concept

Dissertation

zur Erlangung des akademischen Grades einer
Doktorin der Naturwissenschaften
(Dr. rer. nat.)
der
Technisch-Naturwissenschaftlichen Fakultät
der
Universität zu Lübeck

vorgelegt von
Alessandra Mescalchin
geboren am 13.10.1975 in Dolo (Ve), Italien

Lübeck, 19. Juni 2007

This work was performed in the period from May 2004 to June 2007 at the ´Institut für Molekulare Medizin der Universität zu Lübeck´ under the supervision of Prof. Dr. Georg Sczakiel.

1. Gutachter: Prof. Dr. G. Sczakiel
2. Gutachter: Prof. Dr. R. Hilgenfeld

Publications

The main part of this thesis has been published in the following publications:

A. Mescalchin, W. Wünsche, S.D. Laufer, D. Grohmann, T. Restle, G. Sczakiel. Specific binding of a hexanucleotide to HIV-1 reverse transcriptase: a novel class of bioactive molecules. Nucleic Acids Research (2006) 34:5631-5637.

A. Mescalchin, W. Wünsche, S.D. Laufer, D. Grohmann, T. Restle, G. Sczakiel. Oligonucleotide active substances. Patent: Publication No.: WO/2006/122701, International Application No.: PCT/EP2006/004439, Publication Date: 23.11.2006, International Filing Date: 11.05.2006.

Further manuscripts published or submitted during the period of the Ph.D. study:

B. Havlickova, T. Bíró, A. Mescalchin, P. Arenberger, R. Paus. Towards optimization of an organotypic assay system that imitates human hair follicle-like epithelial-mesenchymal interactions. British Journal of Dermatology (2004) 151:753-765.

E. Bodó, T. Bíró, A. Telek, G. Czifra, Z. Griger, B.I. Tóth, A. Mescalchin, T. Ito, A. Bettermann, L. Kovács, R. Paus. A hot new twist to hair biology involvement of vanilloid receptor-1 (VR1/TRPV1) signaling in human hair growth control. American Journal of Pathology (2005) 166:985-998.

A. Mescalchin, A. Detzer, M. Wecke, M. Overhoff, W. Wünsche, G. Sczakiel. Delivery and intracellular release are major obstacles to the therapeutic application of siRNA: novel options by phosphorothioate-stimulated delivery. Manuscript submitted.

B. Havlickova, T. Bíró, A. Mescalchin, M. Tschirschmann, H. Mollenkopf, A. Bettermann, P. Pertile, R. Lauster, R. Paus. A novel human folliculoid microsphere assay for exploring epithelial-mesenchymal interactions that mimic intrafollicular communication pathways. Manuscript submitted.

Abbreviations

2´-F	2´-deoxy-2´-fluoro
2´-H	2´-deoxy
2´-O-Me	2´-O-methyl
2´-O-MOE	2´-O-methoxyethyl
3D	three-dimensional
4´-thio U	4-thio uracil
^{125}I	iodine-125
Ab	antibody
A_i	absorbance (i= wavelength in nm)
AIDS	acquired immunodeficiency syndrome
Amp	ampicillin
AP	alkaline phosphatase
APS	ammonium peroxodisulphate
AZT	3´-azido-3´-deoxythymidine (zidovudine)
BCIP	5-bromo-4-chloro-3-indolylphosphate
BJA-B	human Burkitt-lymphoma
bp	base pair(s)
BSA	bovine serum albumin
C-terminus	carboxy-terminus
CA	capsid protein (protein 24, p24)
cfu	colony-forming units
ChIP-chip	on-chip chromatin immunoprecipitation
Ci	Curie
CIP	calf intestinal alkaline phosphatase
CNBr	cyanogen bromide
cpm	counts per minute
cPPT	central polypurine tract
Cy	cyanin
D	aspartate
Dam	DNA adenine methyltransferase
DDDP	DNA-dependent DNA polymerase activity
ddNTP	dideoxynucleoside triphosphate
DEA	diethanolamine
DEAE	diethylaminoethyl
DMSO	dimethyl sulphoxide
DNA	deoxyribonucleic acid
DNase	deoxyribonuclease
dNTP	deoxynucleoside triphosphate
ds	double-stranded
DTT	dithiothreitol
E. coli	*Escherichia coli*
ECL	enhanced chemiluminescence
EDTA	ethylenediaminetetraacetic acid
EGTA	ethyleneglycoltetraacetic acid

EIAV	equine infectious anaemia virus
ELISA	enzyme-linked immunosorbant assay
EMSA	electrophoretic mobility shift assay
env	envelope of HIV-1
EtBr	ethidium bromide
FAM	carboxyfluorescein
FCS	fetal calf serum
FDA	fluorescein diacetate
Fig.	figure
FITC	fluorescein isothio-cyanate
FIV	feline immunodeficiency virus
FPLC	fast protein liquid chromatography
Gag	group-specific antigen precursor of HIV-1
GagPol	group-specific antigen precursor polymerase of HIV-1
gp120	120 kDa glycoprotein of HIV-1, glycoprotein 120
gp41	41 kDa glycoprotein of HIV-1, glycoprotein 41
HAV	hepatitis A virus
HBS	HEPES-buffered saline
HCV	hepatitis C virus
HEK	human embryonic kidney
HIV	human immunodeficiency virus
HPLC	high performance liquid chromatography
hPrP	human prion protein
HRP	horseradish peroxidise
IC_{50}	half-maximal inhibitory concentration
ICAM-1	intercellular adhesion molecule-1
IgG	immunoglobulin G
IN	integrase
IPTG	isopropyl-β-D-thiogalactopyranoside
K_d	dissociation constant
LB	Luria-Bertani
LNA	locked nucleic acid
LTR	long terminal repeat
MA	matrix protein
miRNA	micro RNA
mRNA	messenger RNA
MWCO	molecular weight cut-off
NBT	nitroblue tetrazolium
nc	non-coding
NC	nucleocapsid protein of HIV-1
Nef	negative regulatory factor
NHS-fluorescein	5-(and 6-)carboxyfluorescein succinimidyl ester
Ni-NTA	nickel-nitrilotriacetic acid
NMR	nuclear magnetic resonance
NNRTIs	non-nucleoside reverse transcriptase inhibitors
NRTIs	nucleoside reverse transcriptase inhibitors

nt	nucleotide(s)
NtRTIs	nucleotide reverse transcriptase inhibitors
OH	hydroxyl
p24	24 kDa protein of HIV-1, protein 24 (capsid protein)
p/t	primer/template
PAGE	polyacrylamide gel electrophoresis
PBS	primer binding sequence
PBS_b	phosphate buffered saline
PCR	polymerase chain reaction
PDB	protein bata bank
PEG	polyethylene glycol
PMSF	phenyl methyl sulforyl fluoride
PPT	RNA polypurine tract
PR	protease
PS	phosphorothioate
PVDF	polyvinyl difluoride
R regions	regions of homology
RDDP	RNA-dependent DNA polymerase activity
Rev	regulator of virion expression
RISC	RNA-induced silencing complex
RITS	RNA-induced transcriptional silencing
RNA	ribonucleic acid
RNAi	RNA interference
RNase	ribonuclease
rRNA	ribosomal RNA
RT	reverse transcriptase
SCC	sodium chloride/sodium citrate
SDS	sodium dodecylsulphate
SELEX	systematic evolution of ligands by exponential enrichment
siRNA	small interfering RNA
SIV	simian immunodeficiency virus
ss	single-stranded
STD	saturation transfer difference
S-TIBO	tetrahydro-imidazo[4,5,1-jk][1,4]-benzodiazepin-2(1H)-one
$t_{1/2}$	half-life time
TAE	triethanolamine
Taq	*Thermophilus aquaticus*
TAR	transactivation response element
Tat	transactivator protein
TBE	tris-borate-EDTA
TBS	tris-buffered saline
TCA	trichloroacetic acid
TLC	thin layer chromatography
TE	tris-EDTA
TEMED	N,N,N´,N´,-tetramethylethylendiamin
TFO	triple-helix-forming oligodeoxynucleotide
TLR9	toll-like receptor 9

TMAE	trimethylaminoethyl
Tris	trihydroxymethylaminomethane
tRNA	transfer RNA
UV	ultraviolet
Vif	virus infectivity factor of HIV-1
Vpr	viral protein R of HIV-1
Vpu	viral protein U of HIV-1
v/v	volume/volume
w/v	weight/volume
X-Gal	5-bromo-4-chloro-3-indolyl β-D-galactopyranoside
ε	molar extinction coefficient

Table of Contents

1 Introduction

1.1 Nucleic acids and their biological functions

The fundamental role of the deoxyribonucleic acid (DNA) as the depository of the genetic information for life was discovered in 1952 by A. Hershey and M. Chase (1). In eukaryotes the DNA is organised in chromosomes, 23 homologous pairs in humans, whereas in prokaryotes it usually consists of a single circular DNA molecule (2). The DNA undergoes a replication process, which enables the genetic information of an organism to be passed to the two daughter cells created after cell division, and to a recombination process, which allows chromosomes to exchange genetic information producing new combinations of genes. This reshuffling of genetic information on chromosomes permits a damaged chromosome to repair itself by using a second copy (allel) as a guide and it furthermore increases the genetic variation, which is important for a rapid evolution (2). DNA can also excert important biological functions and, as an example, bacterial DNA containing unmethylated CpG motifs is able to activate immune responses through the interaction with a specific cellular receptor, the toll-like receptor 9 (TLR9) (3;4). The DNA also specifies non-coding ribonucleic acids (ncRNAs) through the process of transcription. Importantly, the genetic sequence information is also transcribed into coding messenger RNAs (mRNAs), which after further processing are translated into proteins. This process involves the ribosomal RNAs (rRNAs) as structural and functional components of the ribosomes and the transfer RNAs (tRNAs). The translation of the nucleotide (nt) sequence is accomplished at the ribosome through a specific recognition-based system in which specific amino acids are transferred from tRNAs into a growing polypeptide chain using the mRNA as template.

In recent years it turned out that in addition to protein biosynthesis, a variety of ncRNAs play important or essential roles in the cell, e.g. the regulation of gene expression, protein trafficking, RNA processing and modification. The class of ncRNA molecules includes catalytic RNAs (ribozymes), which catalyse chemical reactions and the group-I and group-II introns which perform self-splicing (5;6). An example of the former is the RNA subunit of the ribonucleoprotein ribonuclease P (RNase P) which is essential for the 5´-end maturation of precursor tRNAs. It has recently been discovered that even the ribosome can be regarded a ribozyme, since the center of the peptidyl-transferase activity is located on the RNA component (7-9).

Moreover, several RNAs have been discovered which bind small metabolites and, as a consequence, switch their conformation and function. They are called riboswitches (10-12). These molecules possess a specific domain, sometimes referred to as ´aptamer

domain´, which functions as a sensor and presents the ligand binding site, and a second domain, called expression platform, that transduces ligand binding events into conformational changes leading to the control of gene expression (10;13). Most of the riboswitches occur in bacteria, but functional riboswitches of one type, the thiamine pyrophosphate riboswitches, which are involved in controlling gene expression via mRNA splicing, have been discovered also in eukaryotes (10;14).

Other ncRNAs include small nucleolar RNAs, which are essential for rRNA processing and modification (pseudouridylation and methylation), small nuclear RNAs that compose the pre-mRNA splicing machinery, as well as U7 snRNA, which is essential for the histone mRNA 3´-end formation (15). In addition, studies suggest that U1-U6 and 7SK ncRNAs play an important role in the regulation of transcription via an association with specific transcriptional factors (16;17). In bacteria, the 6S ncRNA was also found to be involved in the transcriptional regulation by a direct interaction with the RNA polymerase (18).

Other ncRNAs involved in ´housekeeping´ functions include the telomerase RNA, required for chromosome end replication, the signal recognition particle RNA, involved in protein sorting within the cell, and the guide RNAs, which direct insertion or deletion of uridine residues in mRNA (15;18;19). In addition it has been shown that antisense RNAs regulate gene expression (4).

Only in the late 1990s and early 2000, a new class of ncRNA was discovered and named micro RNA (miRNA). The miRNAs are involved in gene regulation and have been found in many metazoans, from *Caenorhabditis elegans* to *Homo sapiens* (20). Endogenous miRNAs or exogenously introduced small interfering RNAs (siRNAs) are loaded into the RNA-induced silencing complex (RISC) after having been processed by the protein Dicer. This complex partially or fully recognises complementary mRNA molecules via base-pairing, and leads to a suppression of protein biosynthesis (20). This mechanism of the regulation of gene expression is called RNA interference (RNAi). It has been shown that miRNAs suppress translation via both the direct block of protein synthesis or the induction of target mRNA degradation, whereas siRNAs act only through target mRNA destruction (20;21). In addition, miRNAs and siRNAs were found to be involved in a form of RNA interference by which they trigger the downregulation of transcription of a particular gene or genomic region. This is usually accomplished by a modification of histones, often methylation or by the induction of heterochromatin formation. In this case, the complex that binds the small RNA and interacts with the DNA is called the RNA-induced transcriptional silencing (RITS) complex (22-24).

In addition, a new and unexpected role of the ncRNAs has been described very recently by Rassoulzadegan *et al.* (25), in which a novel mode of epigenetic inheritance was associated with the zygotic transfer of RNA molecules.

1.2 Nucleic acids as therapeutics and as tools in molecular biology

Based on the natural functions of nucleic acids, new synthetic drugs and tools to explore biological systems have been developed. So far, a great number of ribozymes, deoxyribozymes, siRNAs, miRNAs, antisense oligonucleotides, triple-helix-forming oligodeoxynucleotides (TFOs), CpG-containing oligonucleotides, decoys and aptamers, has been produced synthetically and applied successfully for therapeutic purposes and for understanding and manipulating biological processes (4;26).

1.2.1 Catalytic nucleic acids, antisense oligonucleotides, siRNAs and miRNAs

The catalytic potential of RNA has been employed in therapeutic applications and for target validation. Ribozymes bind to a substrate RNA through Watson-Crick base pairing and cleave the target transcripts in a sequence-specific fashion. Based on the discovery that even DNA possesses a catalytic activity, deoxyribozymes have been developed (27). Those molecules showed high similarity with their RNA homologues presenting some advantages, such as an increased stability, an easier synthesis and in some cases higher turnover rates (4). These catalytic nucleic acids can be delivered or expressed in cells, in which they direct the cleavage events.

Similarly, the targeted inactivation of gene expression *in vitro* and *in vivo* has been achieved by using siRNAs, miRNAs and antisense oligonucleotides. The high inhibitory effect of siRNAs on their target mRNAs expression, make them very useful drugs for targeting specific transcripts involved in diseases (28;29). The miRNA class present less sequence specificity towards their targets than the siRNA class. This is due to the mechanism of action of the miRNAs which does not require a perfect sequence complementarity with their targeted sequence (28).

Like the two classes described above, the reverse-complementary antisense oligonucleotides are used in living cells to manipulate gene expression at the mRNA level. They are known to find their target unassisted, and once bound they can block expression via a steric mechanism by obstructing the ribosome. Alternatively, they can form an RNA-DNA hybrid that can be a substrate for ribonuclease H (RNase H), thereby leading to target degradation (29;30).

1.2.2 Triple-helix-forming oligodeoxynucleotides

A strategy based on the regulation of gene expression at the gene-level employs the TFOs that target a given gene by homologous recombination. In a sequence-specific fashion these molecules bind to the major groove of the (double-stranded DNA) dsDNA and, for stable hybridisation and Hoogsteen bonds formation, require in their sequence a series of purines (10 to 30 nt) on one strand and pyrimidines on the other. The formation of a triple helix by these oligonucleotides is limited to polypurine tracts of dsDNA. TFOs are used *in vitro* and *in vivo*, to block transcription and to induce site-specific mutations (4;31;32).

1.2.3 CpG-containing oligonucleotides, decoys and aptamers

Chemically synthesised oligonucleotides containing CpG motifs have been used for therapeutic purposes. The targeted activation of TLR9 using these synthetic oligonucleotides improves the treatment of infectious diseases and also of cancer, as demonstrated by the results obtained in human clinical trials (3;4). It was also shown that CpG-containing oligonucleotides should be at least 18 nt in length in order to exploit their function effectively (33).

Decoys are usually 30-100 nt in length and fold in complex three-dimensional (3D) structures and shapes, which are required for the interaction with and recognition of their targets. They are widely used for target validation and for therapeutic application, and their function is based on their ability to compete with the real ligand of the target protein or structure (34). They present a structure which mimics or is identical to the real ligand, thus acting as ligand antagonists (35).

The observation that decoys can be used to inhibit target functionality, suggested that other highly structured RNA molecules might be able to bind and inhibit a given target. Concurrent with this observation, synthetic high-affinity nucleic acids ligands, named aptamers (36), were selected from a large pool of randomised sequences by a process called systematic evolution of ligands by exponential enrichment (SELEX), described in detail in section 1.5.2 (37). So far, the SELEX process has been used to successfully select high-affinity DNA or RNA ligands against a variety of targets (35;38;39). Like decoys, aptamers are 30-200 nt long molecules, and their high affinity and specificity of aptamers is based on their ability to fold into complex, 3D shapes rivalling those of the targets (26;40;41). Aptamers have a very broad application range, since they are used for target validation, for clinical application and as well as diagnostic agents (42-47). Additionally, due to their high similarity in function and affinity towards the targets, aptamers are used as substitutes for antibodies and applied in several systems as

capture agents, to monitor protein-nucleic acids and protein-protein interactions (48). Recently, a high-affinity ligand selected against a plasma membrane receptor, the prostate-specific membrane antigen receptor, has been coupled to siRNAs and used to mediate siRNA cell type-specific delivery (49). These molecules possess a number of advantages which make them good candidates for therapeutic applications, such as their very high affinity and specificity towards their targets, the possibility to be selected against almost any molecule, the high inhibitory potential, the lack of toxicity and immunogenicity (34;43).

1.3 Advantages and disadvantages in the use of nucleic acid-based tools and drugs

Nucleic acid-based drugs and tools are routinely used *in vitro*, and in some cases their *in vivo* application has been successful, as confirmed by the number of nucleic acid-based therapeutics applied in clinical trials and approved by the regulatory agencies (4;28;50;51). Chemically synthesised nucleic acids can be delivered into cells, alternatively they be can be expressed endogenously from a vector, thus allowing a continued production of these molecules intracellularly (52). However, their instability in physiological fluids and their poor cellular uptake limit their use *in vivo*. To overcome these limitations several strategies have been adopted, such as the use of improved delivery systems, and the insertion of chemical modifications (Fig. 1.3.1) that confers stability against exo- and endonucleases without affecting their biological activity (28;53;54).

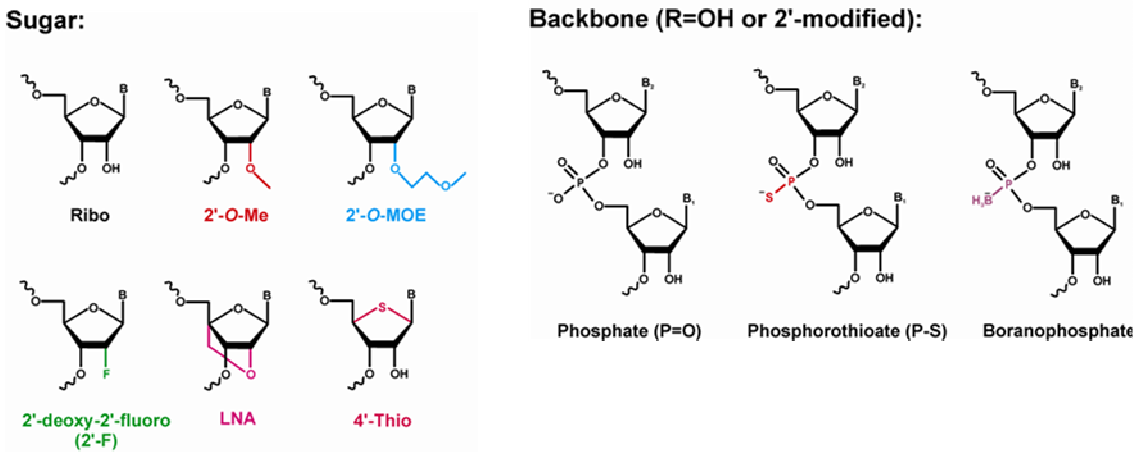

Fig. 1.3.1: Chemical modifications of nucleic acids: 2´-O-methyl (2´-O-Me), 2´-O-methoxyethyl (2´-O-MOE), 2´-deoxy-2´-fluoro (2´-F), locked nucleic acid (LNA), 4´-Thio sugars and backbone modifications are shown.

The delivery of nucleic acid-based therapeutics is one of the most challenging aspects of their *in vivo* application, and has to fulfil a number of criteria: (i) the delivery should be cell

type-specific, (ii) the nucleic acid should be able to gain entry to the cell through the plasma membrane, and (iii) once intracellular, it should encounter its target. Several approaches have been used to achieve delivery efficiency, namely complexation or conjugation of nucleic acids with lipids, polymers, cell-penetrating peptides, small molecules, aptamers and antibodies (55-57). Besides the local administration of nucleic acid-based therapeutics that allows a site-specific localisation of the drugs, the systemic application of nucleic acids conjugated to aptamers or antibodies also has led to an extremely high cell type-specific and efficient delivery *in vivo* (49;58).

1.4 Nucleic acid-protein interactions

The interactions between nucleic acids and proteins are of fundamental importance for the survival of cells. Most proteins bind to nucleic acids in an evolved sequence-dependent fashion (59;60). Major characteristics of protein-nucleic acid interaction include high specificity for the interacting polypeptide domain and the recognised nucleic acid sequence motif. Also the binding strength of both partners may be of great importance for biological activity as, for example, in case of repressor-operator interactions (61). The sequence-specific binding proteins are capable of selecting the correct sequence out of a huge number of potential sequences. This remarkable ability is still poorly understood, despite a variety of models which have been proposed (60).

1.4.1 DNA-protein interactions

Many proteins which are involved in DNA replication, recombination and repair, but also structural proteins exert their functions via interactions with DNA in a sequence-independent way. Others are able to precisely define sites for DNA replication, DNA methylation, DNA cleavage, or transcription initiation and termination by sequence-specific recognition. The latter is the result of interactions between defined DNA sequences and proteins with stringent binding selectivity (62). Examples of sequence-specific binding proteins are the repressors and the transcription factors, which regulate gene transcription by binding to a particular set of DNA sequences, and thus activating or inhibiting the transcription of genes (61). Other proteins which recognise specific DNA sequences include the TATA box-binding proteins, and restriction enzymes which bind to specific motifs, and cut the double helix (63).

The structure of the dsDNA is relatively uniform, and consists of a negatively charged sugar-phosphate backbone and a core of stacked base pairs whose edges are exposed in major and minor grooves. The pattern of functional groups exposed in the DNA grooves

provides each DNA sequence its chemical signature which is recognised by the sequence-specific binding proteins, allowing them to read the DNA sequence. Most proteins bind the DNA by interactions with bases located in the major groove, where they are more accessible (59;64).

The surfaces of these proteins are chemically complementary to their cognate DNA sequences, and the stabilisation of the complexes is given by a series of favourable electrostatic and van der Waals interactions between the molecules. In addition, all protein-DNA complexes contain a large number of contacts with the negatively charged phosphates that include salt bridges with positively charged amino acid side chains and hydrogen bonds with the uncharged backbone or side chain atoms in the proteins (59). A combined analysis of protein sequence and protein structural data showed that the sugar-phosphate DNA backbone contacts are well conserved among all DNA-binding protein families, while in most cases the base contacts are highly conserved only among the sequence-specific proteins belonging to the same family (63).

1.4.2 RNA-protein interactions

RNA molecules are flexible structures that display a variety of structures, including a short stretch of double helix (A-form), hairpin loops, bulges and pseudoknots (65). The motifs which stabilise the tertiary structures are relatively small and often involve backbone functional groups and non-canonical base pairs, creating geometries and surfaces used in RNA-protein recognition (66).

Several proteins bind to RNA in a sequence-independent fashion, as the heterogeneous nuclear ribonucleoprotein and serine-arginine-rich protein families which associate non-specifically with nascent transcripts or have redundant activities in splicing (62). Others display very high sequence specificity, as the aminoacyl-tRNA synthetases which directly recognise the anticodon sequence of their respective tRNAs (67).

Information concerning RNA structures and the basis of the molecular interactions with proteins has been obtained after solving the crystal structures of the ribosome and its subunits. The structure of the big subunit proves that the site of peptide-bond formation, is composed entirely of RNA and that the proteic component contributes to the neutralisation of negative charges on the rRNA backbone and stabilises certain tertiary folds (8;9).
The interface properties of the protein-RNA complexes reveal that proteins tend to interact with RNA where it forms complex secondary structure elements such as stem-loops and bulges. In addition, non-canonical base pairing, which may occur in loop regions of RNA structures, are also features which are preferentially recognised by proteins (65). In RNA binding sites van der Waals interactions play a more relevant role than hydrogen bonds,

and a preferential binding to guanine and uracil was observed. Moreover, the positively charged residue arginine and the single aromatic residues phenylalanine and tyrosine, play important roles in the binding to RNA molecules (65).

Despite the ability of the RNA molecules to adopt a great variety of non-canonical and tertiary structures when compared to the DNA molecules, it appears that most of the base and backbone contacts (both hydrogen bonding and van der Waals), as well as the modes of secondary structure interactions observed for RNA recognition are similar to the ones observed for duplex- and single-stranded-specific DNA binding proteins (67).

1.5 Approaches for identifying nucleic acid ligands to proteins

Nucleic acid-binding proteins, as described above, often possess a high affinity and in some cases, a high specificity for their target sequences.

Several strategies have been developed to identify sequences, which are naturally bound by nucleic acid-binding proteins. These comprise deoxyribonuclease (DNase) footprinting (68), enzyme-linked immunosorbant assay (ELISA) (69), phage display (70), analysis of chromatin immunoprecipitated DNA by polymerase chain reaction (PCR) (71), and screenings in which duplex DNA molecules are immobilised on surfaces and protein binding is detected by plasmon resonance (72) or fluorescence (73). However, for the identification of nucleic acid ligands to a variety of targets, including proteins and other molecules, which naturally lack the nucleic acid-binding ability, primarily two methods are employed, namely a selection on microarrays and SELEX (37). These two approaches are described in more detail below.

1.5.1 The microarray approach

Since its introduction as a technique for large-scale DNA mapping, sequencing, and for transcriptional profile analyses, the microarray technology has been applied to many other areas by adapting the basic concept and combining it with other techniques (74-76). For example, the interaction between proteins, such as transcription factors, and DNA has been studied using on-chip chromatin immunoprecipitation (ChIP-chip) (Fig. 1.5.1), whereby a protein is ultraviolet- (UV-) crosslinked to DNA, and immunoprecipitated via a specific antibody (Ab) (77-79). The hybridisation of the isolated DNA to a genomic DNA fragments identifies its position, and therefore the genomic position of the protein binding site. This method is the most widely used for identifying *in vivo* transcriptional factor-binding sites in a high-throughput fashion, and has recently been applied as well to study histone modifications, histone-modifying proteins and chromatin remodelling (76).

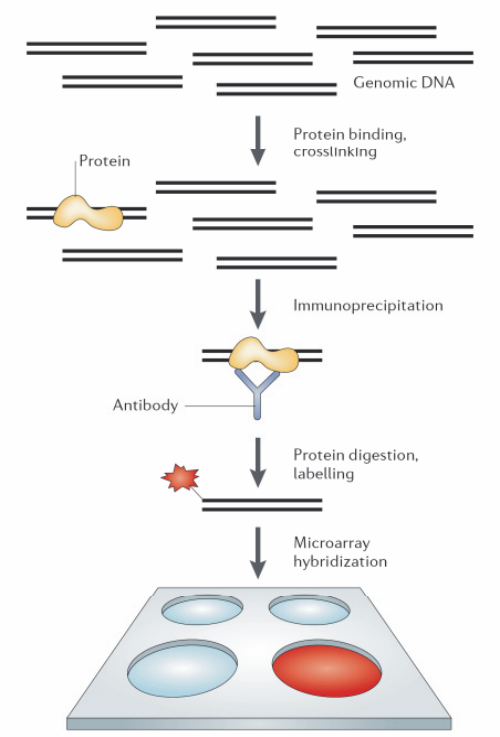

Fig. 1.5.1: ChIP-chip technique. The genomic DNA is incubated in the presence of the DNA-binding protein. The DNA-protein complexes are stabilised by UV-crosslinking, followed by immunoprecipitation of the complexes using a specific Ab. The protein is then removed by digestion and the DNA molecules after labelling are hybridised to a DNA microarray. The origin of the precipitated DNA-fragments is deduced from their binding positions. Figure taken from Hoheisel (74)

Another method for the *in vivo* identification of binding sites utilises a DNA-binding protein fused to DNA adenine methyltransferase (Dam), which marks DNA near the target sites of the protein (76). In this approach, the protein of interest and Dam are co-expressed as a fusion construct. When the protein binds its specific sequence on DNA, Dam methylates the adenines within GATC sites in the vicinity of the binding sites. The methylated sites are detected by digestion with a methyl-specific restriction enzyme, followed by amplification, labelling and hybridisation to a microarray. This approach has been used to identify binding sites for sequence-specific transcriptional factors, DNA methyltransferase, chromatin and chromatin-associated proteins (76). Compared to the ChIP-chip approach, this method has the advantage of not requiring the use of specific antibodies. However, it is not suitable for the detection of post-translational modifications, and does not permit high-resolution mapping of binding sites, because methylation by the Dam extends over a few kilobases from the targeted-binding site.

As an alternative to the *in vivo* approaches, the binding of protein to nucleic acid sequences can be analysed *in vitro* directly by using epitope-tagged proteins (74;80). With this method, the proteins are incubated with microarrays that contain spots of nucleic acid, and once bound to their binding sites, they are detected with a labelled Ab. This technique allows the determination of *in vitro* binding specificities of individual proteins in a single day, and has been used successfully to study the recognition via transcription factors of specific sequences (80).

In addition to the strategies described above, several aptamer-based microarrays have been developed to analyse potential aptamer-protein interactions (81), or as protein capture agents for the detection and quantification of the level of individual proteins in complex biological mixtures (82;83). This approach presents the advantages of screening a pool of potential aptamers for binding affinity to a specific target protein conveniently in a single measurement. Additionally, any protein bound to an aptamer microarray can be easily removed by denaturation, allowing the reuse of the microarray. Despite these benefits, this approach is not widely used. The number of different sequences that an aptamer-based array contains is in a range of 10^{15}, making the production of such an array difficult and costly.

1.5.2 The SELEX approach

The process of the systematic evolution of ligands by exponential enrichment, SELEX, was introduced for the first time in 1990 by Tuerk *et al.* (37) who selected high-affinity RNA ligands for the T4 DNA polymerase.

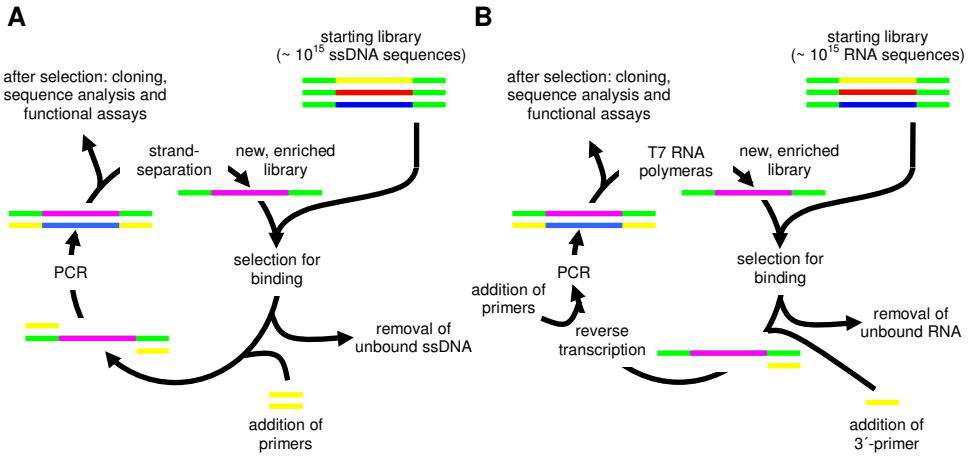

Fig. 1.5.2: Schematic representation of the SELEX process. (A) SELEX procedure for DNA aptamers. A pool of randomised DNA sequences flanked by constant primer sites (green) is subjected to a selection process, the unbound species are removed and the selected species are amplified and analysed. The enriched library is used to repeat the selection cycle. (B) The SELEX procedure for RNA aptamers is similar to the method used for DNA aptamers but includes two additional steps, namely a reverse transcription and a T7 RNA polymerase transcription. Over iterative rounds, high-affinity and specific aptamers can be selected.

Using this approach RNA and DNA aptamers are selected *in vitro* from libraries containing random sequences of up to a few hundred nt (Fig. 1.5.2 A and B). The selection is based on the ability of the nucleic acids to bind target molecules with high affinity and specificity. Therefore the 3D structures of selected aptamers reveal highly optimised scaffolds for specific target recognition (38;44).

Over the last few years, a large number of aptamers have been evolved against a variety of targets such as amino acids, oligosaccharides, proteins, organic dyes, antibiotics, biological cofactors, cell surface epitopes and even complex structures such as whole virus particles, red blood cell membrane, live African trypanosomes and mammalian endothelial cells (38;39;41;46;84).

The selection of high-affinity ligands, which are able to discriminate between even very closely related targets, such as the amino acids arginine and citrulline, or different conformational states of the same protein, revealed an exceptional specificity of aptamers (38;44). The target discrimination by aptamers is based on different effects, and the network of specific hydrogen bonds plays a key role in the discrimination of arginine and citrulline. In the protein-aptamer complexes, the ligands are structurally more complex, and this results in a high number of discriminatory interactions, which include stacking, shape complementarity, electrostatic interactions, and hydrogen bonds (38).

Although the basic principles of SELEX have remained mostly unaltered since its conception, the original protocol was modified to allow the isolation of aptamers with specific desired properties (40). The toggle-SELEX, for instance, permits the isolation of aptamers with a broader range of specificities by selecting against related targets in alternating cycles (34). The tailored-SELEX, instead, involves the ligation and cleavage of primer sites before and after amplification, allowing the isolation of shorter aptamer sequences that are more readily synthesised chemically (85). In the photo-SELEX, aptamers containing light-sensitive nt are UV-crosslinked to their targets, increasing binding affinity (43;86). Recently, a non-SELEX approach has been described (87), whereby aptamers were selected against the human Ras protein. In the non-SELEX approach, the steps of amplification and strand separation are omitted leading to a faster and simpler selection method compared to the original protocol.

The SELEX approach allows the selection of aptamers against targets that do not normally bind nucleic acids, and this possibility increases the potential functions and applications of nucleic acids, as therapeutics and tools in molecular biology. However, using this method only very tight binders can be selected, with an extremely high affinity towards their targets (dissociation constant values, K_d, in the low nanomolar to picomolar range) (44), making this system not suitable for the identification of natural binding motifs of nucleic acid-binding proteins, since such interactions need to be reversible to allow gene regulation. Selected aptamers bind at sites on their targets that cannot be predicted in theory. Usually they show epitope dominance, but only in some cases the dominant epitopes overlap with the functional domains of the target protein, e.g. substrate binding pockets or allosteric sites, thereby modulating the biological function of the molecule (40;44;48). Additionally, the application of aptamers is hampered by technical problems

that are related to their size and ways of syntheses or endogenous expression, respectively.

1.6 Recognition of proteins by short oligonucleotides

Short oligonucleotides, below 12 nt in length, have been shown to specifically interact with target proteins (88;89). Due to their small size, these short nucleic acids lack the disadvantage of a costly chemical synthesis, which is the main limiting factor in the use of aptamers, while preserving advantages, such as the possibility of screening libraries systematically to identify binders, and of a rational drug design. Pinskaya *et al.* (88) showed that a phosphorothioate- (PS-) modified octanucleotide bound to the human immunodeficiency virus type 1 (HIV-1) integrase (IN). This oligonucleotide was derived from the long terminal repeats (LTRs) of HIV-1. The binding to the IN was sequence-specific, although the high affinity of this short oligonucleotide for the protein was due to its PS-modified backbone. Furthermore, Wyatt *et al.* (89) showed that an 11mer oligonucleotide, which was coupled with an acridine group, bound with high specificity to the surface glycoprotein 120 (gp120) of HIV-1 and was able to inhibit gp120-mediated cell fusion. Even though the specificity was due to the sequence, also in this case the high affinity was due to the presence of a hydrophobic moiety, which played a key role for the interaction with this protein by forming additional contacts between the enzyme and the oligonucleotide.

Although these two examples are highly specialised cases that cannot be generalised, they indicate that short oligonucleotides may be able to specifically bind to polypeptides. For this reason, I considered to investigate in a ´proof of concept study´ whether very short oligonucleotides may bind in a specific and biologically meaningful way to a given target protein of interest.

The reverse transcriptase (RT) of HIV-1, described in detail below, was chosen as a target because it naturally binds to nucleic acids and is an essential component of the HIV-1 life cycle. Furthermore, previous studies have proved that long oligonucleotides (aptamers) can be selected which are highly specific for this protein and which have been shown to interfere with the enzymatic activity leading to a reduction of viral replication (84;90-97). A technical advantage was the fact that large amounts of highly pure HIV-1 RT could be obtained from recombinant bacteria. In addition, the 3D structure is known and could be used for modeling studies, and cell-based infectivity assays for testing potential inhibitors are available.

1.7 HIV and the reverse transcriptase

The HIV is a member of the *Lentivirus* genus, which belongs to the *Retroviridae* family. As all other retroviruses, HIV presents an RNA genome, which is reverse-transcribed to viral dsDNA by the viral RT upon entering a new host cell. However, the lentiviruses present a number of unique aspects that are not common to the other members of the *Retroviridae* family, such as their long incubation period (*Lenti*-, latin for ´slow´), their ability to infect some types of non-dividing cells, the target receptors and co-receptors which are distinct from those used by other retroviruses, and additional regulatory and accessory proteins which are not encoded by the genome of other retroviruses (98;99). Other members of the *Lentivirus* genus are the simian immunodeficiency virus (SIV), the equine infectious anaemia virus (EIAV) and the feline immunodeficiency virus (FIV).

In 1983, the HIV-1 was identified as the causative agent for acquired immunodeficiency syndrome (AIDS) (100;101), and only three years later a second type of HIV, called HIV-2, was discovered. Like the original virus, HIV-2 also leads to AIDS, but with a longer incubation time and a lower morbidity (99).

The HIV-1 RT was employed as model target in this study. Therefore, in the following sections, the HIV-1 and in particular its encoded RT will be described.

1.7.1 The HIV-1 and its replication cycle

The HIV-1 mature virion is a roughly spherical particle (approximately 100 nm in diameter) (Fig. 1.7.1). As all other lentiviruses, HIV-1 is enveloped by a lipid bilayer derived from the membrane of the host cell. The glycoprotein gp120 is exposed on the surface and anchored to the lipid bilayer via interactions with the transmembrane glycoprotein 41 (gp41). In addition to the virally encoded proteins, the envelope also contains several cellular membrane proteins which are derived from the host cell, including major histocompatibility antigens, actin and ubiquitin (102;103). A matrix, formed by the matrix protein (MA), lines the inner surface of the viral membrane and surrounds the capsid, which located in the center of the virus and is composed by the capsid protein (CA or protein 24, p24). Included in the capsid are two copies of the RNA viral genome (~ 9 kb), stabilised by interaction with the nucleocapsid protein (NC), and also three virally encoded enzymes, namely the protease (PR), the RT and the IN. In addition, virus particles also package the accessory proteins, negative regulatory factor (Nef), virus infectivity factor (Vif) and viral protein R (Vpr) (102;104).

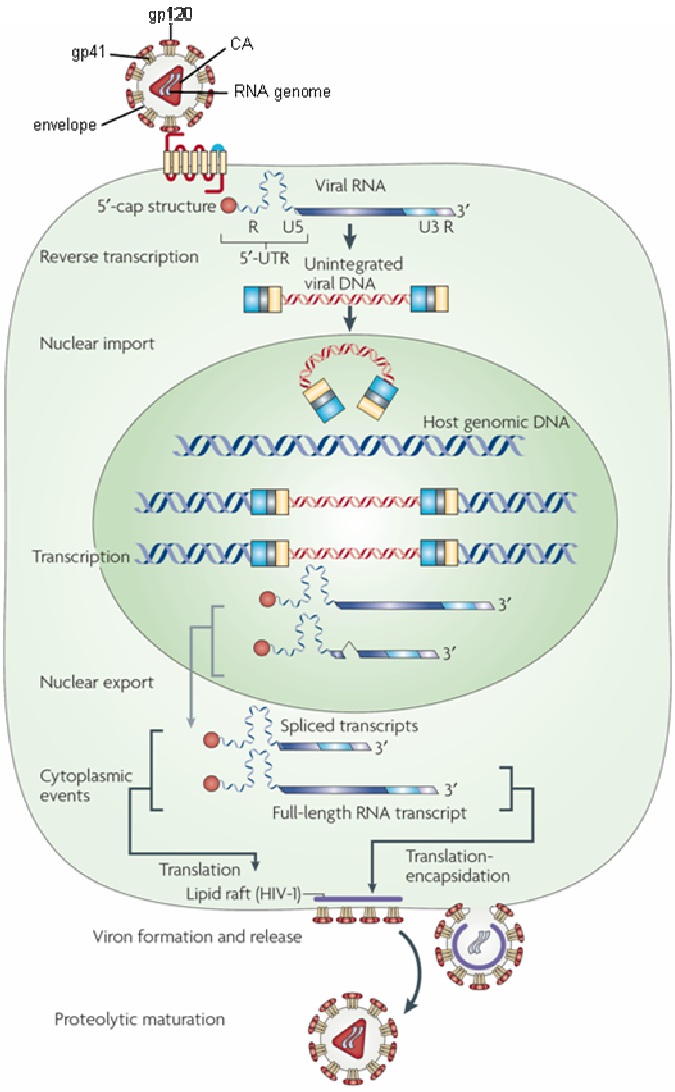

Fig. 1.7.1: Schematic drawing of the HIV-1 virion organisation and the HIV-1 replication cycle. The general features of the mature HIV virion are shown (top), in which the approximate locations of the gp120, the gp41, the envelope, the CA, and the dimeric RNA genome are indicated. Upon recognition of the target cell, the virus envelope fuses with the host plasma membrane and the virus capsid is released into the cell. The RNA genome undergoes a reverse transcription by the RT. The viral DNA is then integrated into the chromosome of the host cell. The transcription of the integrated viral DNA leads to full-length genomic RNAs, which in part undergo a splicing process. All transcripts are exported to the cytoplasm. Viral proteins are then translated and transported to the plasma membrane. Progeny virions are released from the infected cell by budding, followed by a proteolytic maturation of the virions. Figure modified from Balvay *et al.* (105).

The HIV-1 primarily infects cells in the human immune system which bear the CD4 receptor, such as helper T cells (specifically $CD4^+$ T cells), macrophages and dendritic cells (106), and its replication cycle is shown in Fig. 1.7.1.

The first stage of the HIV-1 entry process involves the binding of HIV-1 gp120 glycoprotein to the cell surface CD4 antigen. After the virus has attached to CD4, gp120 glycoprotein undergoes conformational changes and displays a co-receptor-binding site, which allows its binding to co-receptors, such as the chemokine receptors CCR5 and CXCR4 (107-110). Once the virus has fused with the target cell, the uncoating event occurs, resulting in the release of the viral nucleic acids from the capsid into the host cell cytoplasm (102;111). This process has not yet been satisfactorily elucidated. The viral RNA genome, is reverse transcribed by the viral RT, which catalyses the conversion of viral RNA into double-stranded complementary DNA (see 1.7.2). Once synthesised, the viral DNA is transported to the nucleus as part of a pre-integration complex which includes

the IN, and seems to include the MA, the RT, the Vpr viral proteins, as well as the cellular host protein high-mobility-group I (102).

After its translocation to the nucleus, the viral DNA is integrated into the chromosome of the host cell by the viral IN enzyme. Here, the IN interacts with sequences at the end of the LTRs (102;111). Following the integration into the host chromosome, the transcription of the integrated provirus leads to the generation of a large number of viral RNAs, which fall into three main classes: (i) unspliced full-length genomic mRNAs which are first translated to the group-specific antigen precursor (Gag) as well as the group-specific antigen precursor polymerase (GagPol) polyproteins and are then packaged into progeny virions as genomic RNA, (ii) partially spliced mRNAs (~ 5 kb) which encode for the gp120, gp41, Vif, the viral protein U (Vpu) and Vpr proteins, and (iii) the small (< 2 kb) mRNAs which are translated into the regulator of virion expression (Rev), the transactivator protein (Tat) and Nef (98;102). The full-length and partially spliced mRNA transcripts are exported into the cytoplasm via a mechanism which is mediated by the virus protein Rev. Once in the cytoplasm the Gag polyprotein is translated from the unspliced mRNA, and a translational frame-shift results in the generation of GagPol precursor proteins (105). The formation of viral particles requires the multimerisation of the precursor proteins Gag and GagPol. The MA, CA, and NC domains drive the multimerisation of retroviral precursor proteins (112). In addition, experimental evidence showed that viral RNA might function as a scaffold in this multimerisation process (113).

The amino- (N-) terminally myristoylated matrix domain of the polyproteins directs the binding to the cellular membrane where it interacts with the cytoplasmic tail of gp41 (98;102). Two copies of the viral RNA genome are packaged in a budding viral particle, and this process is mediated by the NC domain of the assembling viral Gag polyproteins (114;115). The $tRNA^{Lys3}$, used as a primer during the reverse transcription, is also selectively packaged into the virus by the Gag, and the ´thumb´ subdomain within the GagPol precursor (116). During or shortly after virus release from the plasma membrane, the viral particles undergo to a maturation process, in which the polyproteins are cleaved by the viral PR to produce the viral enzymes, as well as the MA, CA and NC structural proteins, followed by a rearrangement of the structural proteins to form the infectious virus particle (102;103).

The accessory proteins encoded by HIV-1, namely Nef, Vif, Vpr and Vpu are usually dispensable for viral growth in many *in vitro* systems (104;117). However, these proteins play important roles during the viral life cycle *in vivo*. Nef, for example, has been shown to be involved in the modulation of cellular receptors, including CD4, MHCI, MHCII and CD28, to enhance viral infectivity, and to interfere with the host cell signal transduction. Vif stimulates the reverse transcription and plays a role in counteracting host anti-virus

factors (118;119), while Vpr is involved, as described above, in the nuclear import of the pre-integration complex, in the induction of apoptosis and it interferes with the host cell cycle progression. The Vpu instead plays a role in the CD4 degradation and promotion of the virus release.

1.7.2 The HIV-1 RT and the reverse transcription

The RT derives from a proteolytic processing of the GagPol precursor by the viral PR (120). Initially the cleavage produces a homodimer of two p66 (66 kDa) molecules, and the subsequent proteolytic removal of carboxy(C)-terminus of one of the subunits results in the mature p66/p51 RT heterodimer (Fig. 1.7.2 A). The larger subunit, p66, contains both polymerase and RNase H domains, while the smaller subunit, p51 (51 kDa), lacks the RNase H domain.

Several crystal structures of RT non-complexed (121;122), and complexed with non-nucleoside inhibitors (123-127) or with nucleic acids (128-131) have been solved in the last years, therefore detailed structural data are available.

Based on its resemblance of the polymerase domain to a right hand, the four subdomains have been designated as fingers, palm, thumb, and connection (Fig. 1.7.2 A) (129). The finger subdomain is composed of mixed β-strands and three α-helices, and the palm includes five β-strands that form hydrogen bonds with four β-strands positioned at the base of the thumb. A helical bundle forms the thumb subdomain of the enzyme, whereas the connection subdomain, which connects the polymerase and RNase H domains, is composed of a large β-sheet and two α-helices.

Although the subdomains of p66 and p51 are folded similarly, they have a completely different spatial arrangement (132). The p51 subunit has a compact structure, and is assumed to play a largely structural role in the RT heterodimer (128), while the p66 has a more extended structure and forms a large cleft (Fig. 1.7.2 A).

The HIV-1 RT is enzymatically active only as a dimer (133;134), and the dimerisation involves first the rapid association of the two subunits, followed by a slow conformational change yielding a fully active form (135). Experimental data show that the interaction between the thumb domain of p51 and the RNase H domain of p66 plays a major role in the conformational change required for the proper folding of the binding sites for the primer/template (p/t) and the tRNA, for the maturation and the activation of the heterodimeric RT. The thumb subdomain of the p51 is rotated away from the palm, allowing significant interactions with the RNase H subdomain.

A comparison of the structure of RT complexed with dsDNA and the unliganded RT revealed a rotation of the thumb domain of about 30-40° closing off the DNA-binding cleft

and representing a transition from an open to a closed state (121;128). Additionally, minor structural changes occur in the RNase H domain.

The adoption of an open conformation by the p66 subunit results in the formation of a large cleft in the polymerase site that exposes the three catalytic residues aspartate (D)110, D185, and D186 (128). This is the catalytically competent conformation of RT, which can accommodate a nucleic acid template.

The RT is conformationally flexible, and experimental evidence described by Kensch *et al.* (136) shows that the unliganded RT can exist in two different conformations, and the equilibrium between these two states is temperature-dependent. At physiological temperatures the open/closed equilibrium is shifted towards the closed conformation whereas at low temperatures the open conformation is energetically favoured.

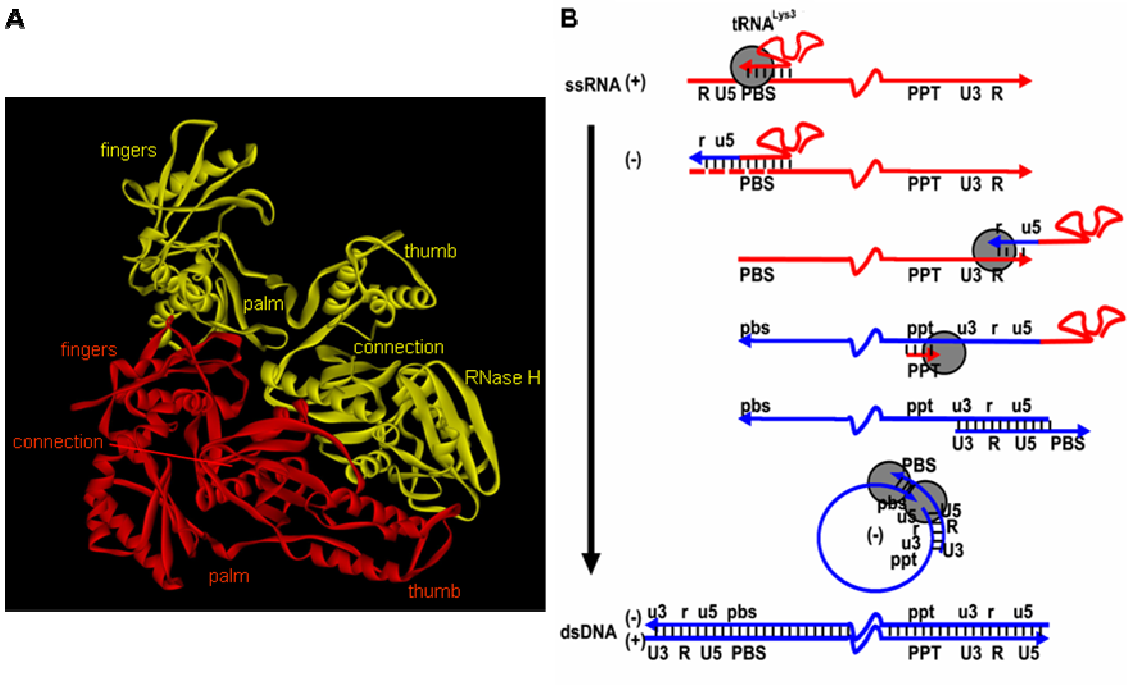

Fig. 1.7.2: HIV-1 RT and the process of reverse transcription. (A) Ribbon diagram of HIV-1 RT [protein data bank (PDB): 1RTD] in an open conformation. The p66 and p51 subunits are shown in yellow and red, respectively. Indicated are the fingers, palm, thumb, and connection subdomains of the two subunits and the RNase H domain of p66 subunit. (B) Reverse transcription process. The RNA is shown in red and the DNA in blue. Figure modified from Held *et al.* (137).

The HIV-1 RT, as described above, catalyses the conversion of the viral RNA genome into dsDNA (98;138). To perform this process, the RT has a RNA- and DNA-dependent polymerase activity as well as an RNase H activity to cleave the template RNA during the reverse transcription.

The reverse transcription occurs in serial steps shown in Fig. 1.7.2 (B), and is initiated by using the host cell $tRNA^{Lys3}$ as a primer which is annealed to the viral RNA primer binding sequence (PBS). The PBS is complementary to the 18 3´-terminal nt of the

$tRNA^{Lys3}$ (139). The RT bound to the RNA/tRNA hybrid starts the DNA synthesis, which proceeds to the 5´-end of the RNA molecule, generating a DNA/RNA hybrid. The RNase H degradation of the copied 5´-end of the RNA genome by RT releases the DNA fragment known as the minus-strand strong stop DNA. By using short regions of homology (R regions), the minus-strand strong stop DNA is transferred from the 5´- to the 3´-end of the genome. The 3´-end of the minus-strand strong stop DNA is used to prime the synthesis of the minus-strand DNA. This transfer step is chaperoned by the NC, which has been shown to facilitate the annealing between the transactivation response element (TAR) RNA and complementary TAR DNA stem-loop structures. This is achieved by binding and destabilisation of the secondary structure of the cTAR DNA by NC, to inhibit self-priming, and to promote the annealing of cTAR to TAR RNA (140;141).

The RNase H degradation of the RNA genome during minus-strand synthesis leaves behind an RNA polypurine tract (PPT) fragment and a central polypurine tract (cPPT), which prime the plus-strand DNA synthesis. The $tRNA^{Lys3}$ bound to the PBS is removed by RNaseH, thereby allowing second-strand transfer to take place, followed by strand displacement synthesis, which allows complete extension of both DNA copies. The DNA product also contains a duplicated U3-R-U5 region, called LTRs, as a result of the two strand transfer reactions.

The viral accessory protein Vif has been found to modulate the RNA- and DNA-dependent DNA polymerase activity of RT via a stimulation of the binding of the viral RT to the primer by increasing the association rate and by decreasing the thermodynamic barrier for complex formation, and finally via increasing the polymerisation rate of HIV-1 RT (142).

1.7.3 The HIV-1 RT as a target for therapeutic intervention

During the last two decades, many efforts have been made to keep the AIDS disease under control and several compounds have been formally approved as anti-HIV drugs. These compounds can be divided into: (i) the RT inhibitors, (ii) the PR inhibitors and the (iii) fusion inhibitors (143;144).

In addition, a variety of new anti-HIV agents are at present in clinical or preclinical development. Some of the new agents are directed against already therapeutically validated viral targets such as RT, PR, gp120 and gp41 targets, others instead are developed to interfere with other fundamental viral processes such as the viral adsorption and entry, the proviral DNA integration, the transcription transactivation, or the viral particles budding and maturation (107;111;143;145-147).

Furthermore, several attempts have been made to regulate viral replication by using nucleic-acid based inhibitors. For example, synthetic siRNAs have been used *in vitro* to degrade the viral RNA genome (148-150), others strategies employ decoys, antisense oligonucleotides, ribozymes or aptamers towards regulatory regions of the viral genome (151-153).

The RT is one of the most attractive targets for inhibiting HIV replication since: (i) it is a crucial enzyme in the viral replication cycle; (ii) its properties are different from those of the other cellular DNA polymerases; and (iii) it is active in the cytoplasmic compartment of the infected cell, separate from the nuclear and mitochondrial DNA polymerases (154).

The first drug approved by the U.S. Food and Drug Administration for the treatment of AIDS was the RT inhibitor 3´-azido-3´-deoxythymidine (AZT or zidovudine) (155). The AZT belongs to the class of nucleoside RT inhibitors (NRTIs), which also includes the didanosine, zalcitabine, stavudine, lamivudine, abacavir and emtricitabine. Other RT inhibitors are the nucleotide RT inhibitors (NtRTIs), such as tenofovir disoproxil fumarate, and the non-nucleoside RT inhibitors (NNRTIs), such as nevirapine, delavirdine and efavirenz (143).

The NRTIs are administered as unphosphorylated pro-drugs, and consequently recognised by cellular kinases after their entry into the host cell. Once phosphorylated, the NRTIs and the NtRTIs act as competitive inhibitors with respect to the natural deoxynucleotide triphosphates (dNTPs). They are incorporated into the growing DNA chain, and act as chain terminators because they lack a 3´-hydroxyl (3´-OH) group on the ribose or pseudo-ribose moiety. This prevents 3´-5´ phosphodiester bond formation, blocking further extension of the DNA (102;156).

The NNRTIs are allosteric non-competitive inhibitors. They bind to a hydrophobic pocket adjacent to the polymerase active site on the p66 subunit and induce structural modifications that decrease the nt incorporation rate by displacement of the catalytic D residues, thus inhibiting catalysis without blocking substrate binding (102;156;157).

Although these drugs delay the progression of the disease, they do not cure it, as the infection readily leads to drug-resistant mutants (158-160). In addition, long-term treatment with antiretroviral NRTI has revealed important adverse effects ranging from mild (myopathy) to fatal in some cases (pancreatitis, liver failure and lactic acidosis). Most of these side-effects are due to the inhibition of the mitochondrial DNA polymerase γ by the NRTI, which leads to a decreased mitochondrial energy-generating capacity (161;162).

As an alternative to the currently used anti-RT drugs, a variety of RT-directed high-affinity ligands have been developed and tested for their inhibitory potential (84;90-97). Tuerk *et al.* (163), applying the SELEX procedure to the HIV-1 RT, has identified an

RNA pseudoknot which displayed both an extremely high affinity (K_d = 25 pM) and a strong inhibitory effect (164;165). Most of the selected aptamers prove to interfere with more than one step during the reverse transcription process (137). Hannoush *et al.* (97) selected aptamers that proved to inhibit the RNase H activity of RT without a measurable inhibitory effect on polymerase activity by directly screening a limited library of chemically synthesised RNAs designed to adopt hairpin and ´dumb-bell´ configurations.

In addition, many new approaches have been developed to inhibit the RT function by modulation of the interfaces between the subunits of the enzyme (166). These strategies employ peptides and small molecules as RT dimerisation inhibitors (167;168).

1.8 Aim of the study

The aim of my study was to investigate whether (i) specific interactions between very short non-structured oligonucleotides and proteins do occur and if so, (ii) the binding affinity is strong enough to be biologically relevant.

As a model system I chose hexameric oligonucleotides and the HIV-1 RT for the following reasons: oligonucleotide species should be as short as possible, on the other hand; a certain minimal sequence space of 4^6 (4,096) seemed to be necessary for a combinatorial approach. The HIV-1 RT was chosen as model target since the 3D structure of RT is known allowing detailed modeling studies and the binding of high-affinity aptamers shows that RT can interact with non-substrate like nucleic acids. Additionally, highly pure and active enzyme can be obtained in large amounts and several cell-based systems for testing potential viral inhibitors are available.

Hexanucleotides which exhibit high specificity and affinity towards HIV-1 RT should then be studied in order to characterise their mode of binding, to locate their binding site on the protein, and to analyse their biological effects on protein function and virus replication.

Finally, the feasibility of combinatorial selection approaches for the search of hexanucleotides which specifically bind to a given target protein was investigated.

2 Materials and Methods

2.1 Materials

2.1.1 Devices

Axioskop 2	Carl Zeiss, Göttingen
Biotrap Gel chamber	Schleicher & Schuell, Dassel
Blotting device	GE-Healthcare, Chalfont St. Gilles (UK)
CO_2 incubator	Thermo electron corp., Waltham, MA (USA)
Centrifuge Beckman Avanti J-25	Beckman, Fullerton, CA (USA)
Centrifuge Hettich Rotixa 120R	Hettich, Tuttlingen
Dewar flask	Schott, Mitterteich
DNA Thermal Cycler	Biometra, Göttingen
Electroporation apparatus	Bio-Rad, München
Electroporation cuvette (2 mm)	Bio-Rad, München
Electrophoresis Power Supply-EPS 3500	GE-Healthcare, Chalfont St. Gilles (UK)
ELISA-Reader	Bio-Rad, München
FPLC[a)] system	GE-Healthcare, Chalfont St. Gilles (UK)
Fluoroskan Microplate Reader	Labsystems, Helsinki (Finland)
Hand-held fluotest lamp	Heraeus, Hanau
HPLC[b)] Waters 510	Waters, Milford, CA (USA)
Gel chamber for agarose gels Mini-Sub® Cell GT	Bio-Rad, München
Gel dryer	Bio-Rad, München
GradiFrac fraction collector	GE-Healthcare, Chalfont St. Gilles (UK)
Hoefer SG30 gradient maker	GE-Healthcare, Chalfont St. Gilles (UK)
Image Eraser	GE-Healthcare, Chalfont St. Gilles (UK)
Incubator (bacteria)	Heraeus, Hanau
NanoDrop® spectrophotometer ND-1000	Nanodrop, Wilmington, DE (USA)
Peristaltic pump Minipuls3	Gilson, Middleton, WI (USA)
pH meter 761 Calimatic	Knick, Berlin
PhosphorImager screen	GE-Healthcare (Chalfont St. Gilles, UK)
Precision balance METTLER PM 480	Delta Range Mettler-Toledo, Giessen
Power supply	GE-Healthcare, Chalfont St. Gilles (UK)
Rotors JA-25.50 and JLA-10.500	Beckman, Fullerton, CA (USA)
Scintillation counter (liquid) Wallac 1409	Perkin Elmer, Boston, MA (USA)
Spectrophotometer Beckman DU-600	Beckman, Fullerton, CA (USA)
Sequencing gel electrophoresis apparatus	Bio-Rad, München
Shaker KS 250 basic	IKA Labortechnik, Staufen
Speed Vac SC 110-A	Faust, Bochum
Spectrophotometer DU 650	Beckman, Fullerton, CA (USA)
Table centrifuge 5415 C	Eppendorf, Hamburg
Thermocycler Uno II	Biometra, Göttingen
TRIO-Thermoblock	Biometra, Göttingen
Typhoon 8600 Variable Mode Imager	GE-Healthcare, Chalfont St. Gilles (UK)
Ultrasonicator Sonorex Super RK 103 H	Bandelin, Berlin

Vacuum pump	Werner Hassa, Lübeck
Vortex Vibrofix VF1	IKA Labortechnik, Staufen
Water bath W22	Prufgerate-Werk, Medingen

[a)] FPLC, fast protein liquid chromatography; HPLC, [b)] high performance liquid chromatography.

2.1.2 Chemicals

All solutions were prepared with ultra pure Milli-Q water which had been distilled using an ion exchange cartridge (Millipore, Witten, Germany). All reagents used were molecular biology grade unless otherwise stated. All chemicals not listed below were purchased from the companies Merck (Darmstadt, Germany), Roth (Karlsruhe, Germany) and Sigma-Aldrich (Deisenhofen, Germany).

Acetic acid	Roth, Karlsruhe
Acetone	Roth, Karlsruhe
Agarose	Cambrex Bioscience, Rockland, ME (USA)
Ammonium peroxodisulphate (APS)	Serva, Heidelberg
Ammonium sulphate [$(NH_4)_2SO_4$]	Gerbu Biochemicals, Gaiberg
Ampicillin (Amp)	Serva, Heidelberg
AZT	T. Restle
β-Mercaptoethanol	Sigma-Aldrich, Deisenhofen
1,3-Bis[tris-(hydroxymethyl)-methylamino]-propane	Sigma-Aldrich, Deisenhofen
Boric acid	Sigma-Aldrich, Deisenhofen
Bromophenol blue	Sigma-Aldrich, Deisenhofen
Calcium chloride ($CaCl_2$)	Roth, Karlsruhe
NHS-fluorescein[a)]	Pierce, Rockford, IL (USA)
Chloroform/isoamyl alcohol (24:1, v/v)	Roth, Karlsruhe
Coenzyme A	Sigma-Aldrich, Deisenhofen
Coomassie brilliant blue R-250	Sigma-Aldrich, Deisenhofen
Cyanogen bromide (CNBr)	Sigma-Aldrich, Deisenhofen
Diethanolamine	Merck, Darmstadt
Dimethyl sulphoxide (DMSO)	Serva, Heidelberg
Dithiothreitol (DTT)	Sigma-Aldrich, Deisenhofen
D-Luciferin	Sigma-Aldrich, Deisenhofen
Ethanol	Merck, Darmstadt
Ethidium bromide (EtBr)	Serva, Heidelberg
Ethylenediaminetetraacetic acid (EDTA)	Merck, Darmstadt
Ethyleneglycoltetraacetic acid (EGTA)	Merck, Darmstadt
Ficoll 400	Sigma-Aldrich, Deisenhofen
Fluorescein diacetate (FDA)	Invitrogen, Carlsbard, CA (USA)
Fluorescein-5-maleimide	Pierce, Rockford, IL (USA)
Formic acid	Roth, Karlsruhe
Glutaraldehyde (pentanedial)	Sigma-Aldrich, Deisenhofen
Glycerol	Merck, Darmstadt

Glycine	Roth, Karlsruhe
Isopropyl-β- D-thiogalactopyranoside (IPTG)	Gerbu Biochemicals, Gaiberg
Isopropanol	Merck, Darmstadt
Kanamycin	Sigma-Aldrich, Deisenhofen
Lithium chloride (LiCl)	Merck, Darmstadt
Magnesium chloride ($MgCl_2$)	Merck, Darmstadt
Magnesium sulphate ($MgSO_4$)	Sigma-Aldrich, Deisenhofen
Methanol	Merck, Darmstadt
N,N,N´,N´,-tetramethylethylendiamin (TEMED)	Roth, Karlsruhe
NP-40 (detergent)	LKB, Bromma (Sweden)
Phenol/chloroform (1:1, v/v)	Roth, Karlsruhe
Phenyl methyl sulforyl fluoride (PMSF)	Roth, Karlsruhe
Polyethylene glycol 8000 (PEG 8000)	Sigma-Aldrich, Deisenhofen
Potassium chloride (KCl)	Merck, Darmstadt
Potassium dihydrogen phosphate (KH_2PO_4)	Merck, Darmstadt
Potassium hexacyanoferrate (III) [$K_3Fe(CN)_6$]	Sigma-Aldrich, Deisenhofen
Potassium hexacyanoferrate (II) trihydrate[b)]	Sigma-Aldrich, Deisenhofen
Roti-Block	Roth, Karlsruhe
Rotiphorese gel 40%[c)]	Roth, Karlsruhe
Rotiphorese gel 30%[d)]	Roth, Karlsruhe
Scintillation cocktail	Roth, Karlsruhe
SideStep lysis and stabilisation buffer	Stratagene, La Jolla, CA (USA)
Silane	GE-Healthcare, Chalfont St. Gilles (UK)
Skim milk	DIFCO, Detroit, MI (USA)
Sodium acetate ($NaC_2H_3O_2 \cdot 3H_2O$)	Merck, Darmstadt
Sodium chloride (NaCl)	Roth, Karlsruhe
Sodium dodecylsulphate (SDS)	Sigma-Aldrich, Deisenhofen
Sodium-^{125}iodide ($Na^{125}I$)	Hartmann Analytic, Braunschweig
Sodium phosphate dibasic (Na_2HPO_4)	Roth, Karlsruhe
Stains-All	Sigma-Aldrich, Deisenhofen
Streptomycin sulphate ($C_{21}H_{39}N_7O_{12} \cdot 1.5H_2O_4S$)	Sigma-Aldrich, Deisenhofen
S-TIBO[e)]	T. Restle
SYBR gold	Invitrogen, Carlsbard, CA (USA)
Trihydroxymethylaminomethane (Tris)	Sigma-Aldrich, Deisenhofen
Trichloroacetic acid (TCA)	Sigma-Aldrich, Deisenhofen
Triton-X 100	Sigma-Aldrich, Deisenhofen
Tween 20 (detergent)	Roth, Karlsruhe
Urea	Sigma-Aldrich, Deisenhofen
X-Gal[f)]	Sigma-Aldrich, Deisenhofen
Xylene cyanol	Roth, Karlsruhe

[a)] NHS-fluorescein, 5-(and 6-)carboxyfluorescein succinimidyl ester; [b)] Potassium hexacyanoferrate (II) trihydrate, [$K_4Fe(CN)_6 \cdot 3H_2O$]; [c)] Rotiphorese gel 30%, acrylamide/bisacrylamide (37.5:1); [d)] acrylamide/bisacrylamide (19:1); [e)] S-TIBO, tetrahydro-imidazo[4,5,1-jk][1,4]-benzodiazepin-2(1H)-one; [f)] X-Gal, 5-Bromo-4-chloro-3-indolyl β-D-galactopyranoside.

2.1.3 Columns for HIV-1 RT purification

Diethylaminoethyl- (DEAE-) Sephacel	GE-Healthcare, Chalfont St. Gilles (UK)
Fractogel EMD Trimethylaminoethyl (TMAE)	Merck, Darmstadt
Heparin Sepharose CL-6B	GE-Healthcare, Chalfont St. Gilles (UK)
HiLoad 26/60 Superdex 75 prep grade	GE-Healthcare, Chalfont St. Gilles (UK)

2.1.4 Kits

Bio-Rad protein assay	Bio-Rad, München
BCIP/NBT[a)] solution	Calbiochem, Darmstadt
Developing and fixative solutions	Kodak, Rochester, NY (USA)
ECL™[b)] western blotting reagent	Pierce, Rockford, IL (USA)
INNOTEST™ HIV Ag monoclonal Ab	Innogenetics, Ghent (Belgium)
QIAfilter plasmid maxi kit	Qiagen, Hilden
Miniprep kit	Sigma-Aldrich, Deisenhofen
pGEM-T easy vector system	Promega, Madison, WI (USA)
TOPO-TA cloning system	Invitrogen, Carlsbard, CA (USA)
Silver stain kit	Bio-Rad, München

[a)] BCIP, 5-bromo-4-chloro-3-indolylphosphate and NBT, nitroblue tetrazolium; [b)] ECL, enhanced chemiluminescence.

2.1.5 Consumables

Oligonucleotide-based arrays	BF-BIOlabs, Freiburg
Cell culture flasks (25, 75 and 162 cm^2)	Greiner, Frickenhausen
Cell culture plates (24-, 12-, 6-well)	Greiner, Frickenhausen
Cell scraper	Greiner, Frickenhausen
Centrifuge tubes (15 or 50 ml)	Greiner, Frickenhausen
Dialysis tube (MWCO[a)] 12.0-14.0 kDa)	Spectrum, Breda (The Netherlands)
DEAE paper	Whatman, Brentford (UK)
Gel filtration micro columns (NICK, G-50, G-25)	GE-Healthcare, Chalfont St. Gilles (UK)
GenElute plasmid miniprep kit	Sigma-Aldrich, Deisenhofen
Hyperfilm™ ECL	GE-Healthcare, Chalfont St. Gilles (UK)
Immobilon-P membrane (PVDF[b)] membrane)	Millipore, Witten
IODOGEN-tubes	Pierce, Rockford, IL (USA)
Membrane filters (0.45 µm)	Schleicher & Schuell, Dassel
3MM paper	Whatman, Brentford (UK)
Ni-NTA magnetic agarose beads	Qiagen, Hilden
Phase lock gel	Eppendorf, Hamburg
Plastic visible cuvette	Brand, Wertheim
Polygram CEL 300 PEI/UV_{254}	Macherey & Nagel, Düren
Protran nitrocellulose filter BA85 (0.45 µm)	Schleicher & Schuell, Dassel
Scalpels	Feather, Köln
Specra/Por micro dialyzer (MWCO[a)] 25 and 3 kDa)	Spectrum ,Breda (The Netherlands)
Syringes	Becton Dickinson, Franklin Lak., NJ (USA)

Ultra centrifugal filters 30 MWCO[a)] (Amicon)	Millipore, Witten
Ultrafree centrifugal filter device (Biomax-100)	Millipore, Witten
96-well luminometer plates (white)	Greiner, Frickenhausen

[a)] MWCO, molecular weight cut-off; [b)] PVDF, polyvinyl difluoride.

2.1.6 Cell lines, cell culture media and cell culture reagents

Human Burkitt-lymphoma (BJA-B) (169), Human Embryonic Kidney (HEK)293 T (170) and HEK293 (171) cell lines were obtained from the Institute of Molecular Medicine, Lübeck, Germany.

DMEM with GlutaMAX I and sodium pyruvate	Invitrogen, Carlsbard, CA (USA)
Fetal calf serum (FCS)	Gibco-BRL, Eggestein
Fibronectin from bovine plasma	Calbiochem, Darmstadt
Lipofectamine 2000	Invitrogen, Carlsbard, CA (USA)
199 medium	Invitrogen, Carlsbard, CA (USA)
Opti-MEM I	Invitrogen, Carlsbard, CA (USA)
RPMI 1640	Invitrogen, Carlsbard, CA (USA)
Trypan blue	Invitrogen, Carlsbard, CA (USA)
Trypsin/EDTA (0.05% Trypsin, 0.025% EDTA)	Linaris, Wertheim-Bettingen

2.1.7 Bacterial strains and bacterial culture medium

Escherichia coli (*E. coli*) JM109
Genotype: *rec*A1, *end*A1, *gyr*A96, *thi*, *hsd*R17 (rK.,mK+), *rel*A1, supE44, Δ(*lac-pro*AB), [F´, *tra*D36, *pro*AB, *lac*I^{q}ZΔM15]
Source: Promega, Madison, WI (USA)

E. coli TOP10
Genotype: F- *mcr*A Δ(*mrr-hsd*RMS-*mcr*BC) ϕ80*lac*ZΔM15 Δ*lac*X74 *rec*A1 *ara*D139 (*ara-leu*)7697 *gal*U galK *rps*L (Str^R) *end*A1 *nup*G
Source: Invitrogen, Carlsbard, CA (USA)

E. coli XL1 blue
Genotype: *rec*A1 *end*A1 *gyr*A96 *thi-l hsd*R17 *sup*E44 *rel*A1 *lac*
Source: T. Restle

Luria-Bertani (LB) medium	0.5% (w/v) yeast extract
(pH 7.5)	1.0% (w/v) tryptone
	1.0% (w/v) NaCl

For agar plates 15g/l agarose were added to LB medium

SOC medium	2% (w/v) tryptone
(pH 7.0)	0.5% (w/v) yeast extract
	10 mM NaCl
	2.5 mM KCl
	10 mM $MgCl_2$
	20 mM $MgSO_4$
	20 mM glucose

2.1.8 Enzymes, molecular weight markers and antibodies

BenchMark pre-stained protein ladder	Invitrogen, Carlsbard, CA (USA)
Calf intestinal alkaline phosphatase (CIP)	New England Biolabs, Beverly, MA (USA)
DNA ladder (10 bp, 100 bp and 1 kb)	Invitrogen, Carlsbard, CA (USA)
Kaleidoscope prestained standard	Bio-Rad, München
Lysozyme	Serva, Heidelberg
Mark12 unstained protein standard	Invitrogen, Carlsbard, CA (USA)
Monoclonal HIV-1 RT-directed Ab (MAb 20)	T. Restle (172)
Monoclonal TLR9-directed Ab FITC-conjugated	IMGENEX, San Diego, CA (USA)
Mung Bean nuclease	Promega, Madison, WI (USA)
PageRuler prestained protein ladder	Fermentas, Burlington, Ontario (Canada)
Polyclonal donkey anti-rabbit IgG FITC-conjugated	Jackson ImmunoResearch, Suffolk (UK)
Polyclonal goat anti-firefly luciferase Ab	Promega, Madison, WI (USA)
Polyclonal goat anti-HIV-1 Ab	Acris, Herford
Polyclonal goat anti-rabbit IgG AP-conjugated Ab	Dako, Hamburg
Polyclonal goat anti-rabbit IgG HRP-conjugated Ab	Dako, Hamburg
Polyclonal rabbit anti-goat IgG Ab	Jackson ImmunoResearch, Suffolk (UK)
Polyclonal rabbit anti-goat IgG HRP-conjugated Ab	Dako, Hamburg
Polyclonal rabbit anti-HIV-2 RT (K38)	T. Restle
Polyclonal rabbit anti-human β-actin Ab	Abcam, Cambridge (UK)
Polyclonal rabbit anti-p24 Ab	B. Müller
Proteinase K	Fermentas, Burlington, Ontario (Canada)
RNase A/T1 Mix	Fermentas, Burlington, Ontario (Canada)
RNasin	Promega, Madison, WI (USA)
S1 nuclease	GE-Healthcare, Chalfont St. Gilles (UK)
Thermophilus aquaticus (*Taq*) DNA polymerase	New England Biolabs, Beverly, MA (USA)
Terminal deoxynucleotidyl transferase	Fermentas, Burlington, Ontario (Canada)
T4 polynucleotide kinase	Fermentas, Burlington, Ontario (Canada)
T4 RNA ligase	Fermentas, Burlington, Ontario (Canada)

Abbreviations: IgG, immunoglobulin G; FITC, fluorescein isothio-cyanate; AP, alkaline phosphatase; HRP, horseradish peroxidise.

2.1.9 Proteins

Alexa^{488}-labelled HIV-1 RT:	p66^{194C}Alexa^{488}/p51	T. Restle
	p66^{K287C}Alexa^{488}/p51	T. Restle
	p66/p51^{K281C}Alexa^{488}	T. Restle

Bovine serum albumin (BSA)	Promega, Madison, WI (USA)
Casein from bovine milk	Sigma-Aldrich, Deisenhofen
EIAV RT	T. Restle
HIV-1 RT	see 2.2.4 and from T.Restle
6xHis-tagged HIV-1 RT	T. Restle (173)
HIV-2 RT	T. Restle
Human prion protein (hPrP)	T. Restle
p51 subunit of HIV-1 RT	T. Restle
TLR9	E. Latz
T7 RNA polymerase	T. Restle

2.1.10 Nucleotides

[γ-^{32}P]-dATP, 3000 Ci/mmol, 10 mCi/ml	Perkin Elmer, Boston, MA (USA)
[^{3}H]-dTTP, 110 Ci/mmol, 2.5 mCi/ml	Perkin Elmer, Boston, MA (USA)
[5,6-^{3}H]-UTP, 35 Ci/mmol, 2.5 mCi/ml	Perkin Elmer, Boston, MA (USA)
ddNTP	Fermentas, Burlington, Ontario (Canada)
dNTP	Peqlab Biotechnologie, Erlangen
Fluorescein-12-ddCTP[a)]	Perkin Elmer, Boston, MA (USA)

[a)] ddCTP, dideoxycytidine triphosphate.

2.1.11 Nucleic acids

2.1.11.1 Plasmids/vectors

M13mp18
Features: single-stranded DNA (ssDNA), *lac*Z
Source: New England Biolabs, Beverly, MA (USA)

pDMI.1
Features: *kan*^{r}, lac I^{Q}-repressor
Source: T. Restle (175)

pcDNA 3.1 (-)/Myc-His/*lac*Z
Features: *amp*^{r}, *neo*^{r}*, lac*Z, *f1* ori, *pUC* ori, *SV40* ori,
Source: Invitrogen, Carlsbard, CA (USA)

Pcz VSV-G wt
Features: *amp*^{r}, *vsv-g*, *zeo*^{r}
Source: G.J. Jármy (174)

pGEM-T
Features: *amp*^{r}, *f1* ori, *lac*Z
Source: Promega, Madison, WI (USA)

pGJ3-Luci

Features: *amp*^{r}, *gag*, *pol*, *rev*1, δ*env*, *rev*2, *luc*, *zeo*^{r}
Source: G.J. Jármy (174)

pRT1 66/51.1
Features: *amp*^{r}, coexpression of p66 and p51 subunits of HIV-1 RT
Vector: pKK 233-2
Source: T. Restle (175)

pCR®II-TOPO®
Features: *amp*^{r}, *kan*^{r}, *lac*Z, *f1* ori, *pUC* ori
Source: Invitrogen, Carlsbard, CA (USA)

2.1.11.2 Chemically synthesised and *in vitro* transcribed nucleic acids

Table 2.1.1: Primers used in this study

name	sequence (5´ to 3´)	supplier
M13 forward primer	d(GTA AAA CGA CGG CCA G)	Metabion, Martinsried
M13 reverse primer	d(CAG GAA ACA GCT ATG AC)	Metabion, Martinsried
M13/pUC (-47)	d(CGC CAG GGT TTT CCC AGT CAC GAC)	New England Biolabs, Beverly, MA (USA)
Primer Flo1	d(TCC CTG TTC GGG CGC CAC)	IBA, Göttingen
Primer PA	d(TGC AGG CTC GAG TTA ATT AAC TGA)	IBA, Göttingen
Primer PB	d(TGT ATT GCG GCC GCT GAT CTA GA)	IBA, Göttingen
Adaptor PB	d[TGT ATT GCG GCC GCT GAT CTA GA$(G)_{14}$]	IBA, Göttingen
Poly(rA)/oligo$(dT)_{12-18}$	Poly(rA)/oligo$(dT)_{12-18}$ p/t	GE-Healthcare, Chalfont St. Gilles (UK)
Primer sara	r(GGG UUA AUC UCU GCA UGG CGC CCG AAC AGG GAC AA)	T. Restle
Primer T7	d(TAA ATA CGA CTC ACT ATA)	T. Restle

Table 2.1.2: Oligodeoxyribonucleotides (DNA) used in this study

name	sequence (5´ to 3´)	supplier
Hex-0	AGA GAG	IBA, Göttingen
Hex-1	TCA AAA	IBA, Göttingen
Hex-2	TCA TGA	IBA, Göttingen
Hex-4	GTC TAA	IBA, Göttingen
Hex-5	GGC AAC	IBA, Göttingen
Hex-FB1	ATA GAG	IBA, Göttingen
Hex-FB2	GCT TAT	IBA, Göttingen
Hex-FB3	TCG TGA	IBA, Göttingen
Hex-FB4	GTA GAG	IBA, Göttingen
Hex-FB5	TTT TTT	IBA, Göttingen
Hex-S1	CGA CCG	IBA, Göttingen
Hex-S3	TCG TGT	IBA, Göttingen
Elongated derivatives	ATC GTG T	IBA, Göttingen
of Hex-S3	TTC GTG T	IBA, Göttingen
	CTC GTG T	IBA, Göttingen
	GTC GTG T	IBA, Göttingen
	TCG TGT A	IBA, Göttingen
	TCG TGT T	IBA, Göttingen
	TCG TGT C	IBA, Göttingen
	TCG TGT G	IBA, Göttingen
	$(TCG\ TGT)_2$	IBA, Göttingen
	$(TCG\ TGT)_3$	IBA, Göttingen
	$(TCG\ TGT)_4$	IBA, Göttingen
	$(TCG\ TGT)_5$	IBA, Göttingen
	$(TCG\ TGT)_6$	IBA, Göttingen
Pentamer-FB1	CCG GG	IBA, Göttingen
Pentamer-FB2	CAT GA	IBA, Göttingen
Polyadenylic acid	PolyA (Mw~ 900,000, Length~ 2,500 b)	Sigma-Aldrich, Deisenhofen
RT1t49 aptamer (92)	ATC CGC CTG ATT AGC GAT ACT CAG AAG GAT AAA CTG TCC AGA ACT TGG A	T. Restle
Sense si2B	GCC TCA GCA CGT ACC TCT ATT	Biomers, Ulm
Template Flo6	TGT GGA AAA TCT CTA GAC GTG GCG CCC GAA CAG GGA	IBA, Göttingen
Template sara (52mer)	TTG TCC CTG TTC GGG CGC CAT GCA GAG ATT AAC CCT ATA GTG AGT CGT ATT A	T. Restle
Template T7	GGG GCG GAC ATT GAT AAG CAG CGA GTG ACA TTC CCT GTC ACC TAT AGT GAG TCG TAT TA	T. Restle

Table 2.1.3: Oligoribonucleotides (RNA) used in this study

name	sequence (5´ to 3´)	supplier
antisense 2B	UAG AGG UAC GUG CUG AGG CTT	Biomers, Ulm
Hex-0	AGA GAG	IBA, Göttingen
Hex-1	UCA AAA	IBA, Göttingen
Hex-2	UCA UGA	IBA, Göttingen
Hex-4	GUC UAA	IBA, Göttingen
Hex-5	GGC AAC	IBA, Göttingen
Hex-S3	UCG UGU	IBA, Göttingen
Derivatives of Hex-S3	ACG UGU	IBA, Göttingen
(positional mutants)	UAG UGU	IBA, Göttingen
	UCA UGU	IBA, Göttingen
	UCG AGU	IBA, Göttingen
	UCG UAU	IBA, Göttingen
	UCG UGA	IBA, Göttingen
Shortened derivatives of	UCG UG	IBA, Göttingen
Hex-S3	CGU GU	IBA, Göttingen
	UCG U	IBA, Göttingen
	CGU G	IBA, Göttingen
	GUG U	IBA, Göttingen
	GUG	IBA, Göttingen
Pseudoknot aptamer (163)	GGG AGA UUC CGU UUU CAG UCG GGA AAA ACU GAA	T. Restle
RNA MS2	-	Roche Applied Science, Penzberg

Table 2.1.4: Chemically modified oligonucleotides used in this study

name	sequence (5´ to 3´)	supplier
5´-end 6-FAM Hex-$S3_R$	*UCGUGU	IBA, Göttingen
3´-end 6-FAM Hex-$S3_R$	UCGUGU*	IBA, Göttingen
3´-end Cy5 Hex-$S3_R$	UCGUGU*	IBA, Göttingen
Hex-1_R-2´-F	UCAAAA	IBA, Göttingen
Hex-$S3_R$-2´-F	UCG UGU	IBA, Göttingen
Hex-$S3_D$-LNA	TCG TGT	IBA, Göttingen
Hex-1_D-2´-O-Me	TCAAAA	IBA, Göttingen
Hex-$S3_D$-2´-O-Me	TCG TGT	IBA, Göttingen
Hex-1_D-PS	TCAAAA	IBA, Göttingen
Hex-$S3_D$-PS	TCG TGT	IBA, Göttingen
4-thio U-Hex-$S3_R$	UCGUGU	IBA, Göttingen

Abbreviations: 6-FAM, 6-carboxyfluorescein; Cy5, cyanin, 4-thio uracil, 4-thio U. Labels are indicated with * and chemically modified nt are underlined.

2.1.12 Buffers

2.1.12.1 Staining, destaining solutions and buffers used in this study

Coomassie blue staining solution (gel)	40% (v/v) methanol 10% (v/v) acetic acid 0.01% (w/v) Coomassie brilliant blue R-250
Coomassie blue staining solution (PVDF)	40% (v/v) methanol 1.0% (v/v) acetic acid 0.01% (w/v) Coomassie brilliant blue R-250
2x Denaturing loading buffer (PAGE)	7.0 M urea, 0.1% (w/v) bromophenol blue 0.1% (w/v) xylene cyanol in 1x TBE buffer pH 8.0
Destaining solution for Coomassie (gel)	40% (v/v) methanol 10% (v/v) acetic acid
Destaining solution for Coomassie (PVDF)	40% (v/v) methanol 1.0% (v/v) acetic acid
2x HEPES-buffered saline (HBS) (pH 7.1)	50 mM HEPES 280 mM NaCl 1.5 mM Na_2HPO_4
10x Hybridisation buffer	0.25 M NaCl 0.20 M Tris-HCl pH 7.5
6x Non-denaturating loading buffer (PAGE)	0.25% (w/v) bromophenol blue 0.25% (w/v) xylene cyanol 25% (w/v) Ficoll 400 in 1x TAE buffer pH 7.4
10x Phosphate buffered saline (PBS_b) (pH 7.4)	1.37 M NaCl 0.027 M KCl 0.081 M Na_2HPO_4 0.0147 M KH_2PO_4
1x RT binding buffer	50 mM Tris-HCl pH 8.0 5 mM KCl 5 mM $MgCl_2$ 1 mM DTT
10x Running buffer (SDS-PAGE)	0.25 M Tris-HCl pH 8.3 2.50 M glycine 10% (w/v) SDS

2x Sample buffer (SDS-PAGE)	0.10 M Tris-HCl pH 6.8 0.02 M DTT (or 10% (v/v) β-Mercaptoethanol) 4% (w/v) SDS 20% (v/v) glycerol 0.2% (w/v) bromophenol blue
1x Sodium chloride/Sodium citrate (SCC) buffer (pH 7.0)	0.3 M NaCl 30 mM sodium citrate
10x Tris-buffered saline (TBS) buffer (pH 7.6)	1.37 M NaCl 0.20 M Tris-HCl 3.8% (v/v) HCl

1x TBS-T buffer is 1x TBS buffer with 0.1% (v/v) Tween-20

1x Transfer buffer (Western blotting)	0.025 M Tris-HCl pH 8.3 0.190 M glycine 20% (v/v) methanol
10x Tris-borate-EDTA (TBE) buffer (pH 8.0)	0.89 M Tris 0.02 M EDTA 0.89 M boric acid
10x Triethanolamine (TAE) buffer (pH 8.5)	0.40 M Tris 0.01 M EDTA 0.20 M acetic acid
10x Tris-EDTA (TE) buffer (pH 7.5)	0.10 M Tris 0.01 M EDTA

2.1.12.2 Buffers used for HIV-1 RT purification

Lysis buffer	25 mM Tris-HCl, pH 8.0 5 mM DTT 1 mM EDTA 0.4 mM PMSF	Buffer A	50 mM Tris-HCl, pH 8.0 25 mM NaCl 1 mM DTT 1 mM EDTA 6% (v/v) glycerol
Buffer B	50 mM Tris-HCl, pH 8.0 1 mM NaCl 1 mM DTT 1 mM EDTA	1x RT storage buffer	20 mM Tris-HCl pH 8.0 10% (v/v) glycerol 1 mM EDTA 1 mM DTT 6% (v/v) glycerol

Diethanolamine (DEA) buffer A	50 mM diethanolamine, pH 8.0
DEA buffer B	50 mM diethanolamine, pH 8.0 1 M NaCl
Gel filtration buffer (pH 7.0)	10 mM 1,3-bis[tris-(hydroxymethyl)-methylamino]-propane-HCl 250 mM ammonium sulphate

2.2 Methods

2.2.1 Microbiological techniques - cloning techniques

2.2.1.1 Cloning of PCR products

PCR products were cloned into pGEM-T easy and TOPO-TA cloning vectors according to the protocol of the manufacturers (Promega, Madison, WI, USA; Invitrogen, Carlsbard, CA, USA). They are based on the terminal-transferase activity of the *Taq* DNA polymerase which creates 3´-deoxyadenosine (A) overhangs on the PCR products. The cloning site contains 5´-deoxythymidine (T) overhangs and topoisomerase I enzyme (TOPO-TA) or T4 DNA ligase (pGEM-T easy).

2.2.1.2 Transformation of *E. coli* JM109 and TOP10 cells

Ligated products (see 2.2.1.1) were used to transform commercially available chemical-competent *E. coli* JM109 (Promega, Madison, WI, USA) or *E. coli* TOP10 (Invitrogen, Carlsbard, CA, USA) cells as described in the following protocol. *E. coli* JM109 or *E. coli* TOP10 cells (50 µl) were mixed with ligation reaction (2 µl), and incubated on ice (20 min). Cells were then heat-shocked in a water bath at 42°C for 45 s and immediately chilled on ice (2 min). SOC medium (950 µl) was added, followed by incubation in an orbital shaker (1.5 h, 200 rpm, 37°C). The transformed cells were plated onto LB agar containing 100 µg/ml Amp and 80 µg/ml X-Gal. Plates were incubated for 16 h at 37°C. White colonies, which generally contained inserts, were picked for further analysis. The transformation efficiency was in the order of 1×10^7 colony-forming units (cfu)/µg plasmid.

2.2.1.3 Transformation of *E. coli* by electroporation

An amount of 100 ng of plasmid DNA was mixed with 80 µl of *E. coli* XL1 blue cells, incubated on ice (1 min), and transferred to a pre-cooled 0.1 cm electroporation cuvette, and immediately pulsed in the electroporator (Gene Amp II from Bio-Rad, München, Germany) at 1.8 kV, 25 µF, 200 Ω for 5 ms. LB medium (1 ml) was added to the bacteria and incubated under shaking (1 h, 200 rpm, 37ºC) to allow the bacteria to recover. Bacteria were concentrated by centrifugation (2 min, 4,000 x g, 23°C), the cell pellet was resuspended in 100 µl LB medium and spread onto agar plates containing Amp and X-Gal. Plates were incubated overnight at 37°C. The transformation efficiency was in the order of 1 x 10^8 cfu/µg plasmid.

2.2.1.4 Screening of colonies by PCR

For the rapid detection of transformation efficiency and to verify the presence of ligated DNA, single colonies of transformed bacteria were picked with a sterile toothpick and suspended into the PCR solution containing primers, buffer, *Taq* DNA polymerase, dNTP and buffer (see 2.2.2.5). In this case an initial step for 10 min at 95°C was introduced into the PCR program (see 2.2.2.5) in order to lyse the cells. The PCR products were analysed by TAE-agarose gel electrophoresis.

2.2.1.5 Preparation of bacterial glycerol stocks

To 1 ml of a bacteria culture [optical density at 600 nm (OD_{600}) = 0.7], 20% (v/v) glycerol was added, the suspension was mixed gently, and then frozen rapidly in liquid nitrogen. The bacterial stock cultures were kept at - 80°C until further use.

2.2.1.6 Preparation of plasmid DNA

The LB medium (5 ml) supplemented with 100 µg/ml Amp was inoculated with a little amount of bacteria, collected from glycerol stocks with the tip of a sterile toothpick, and incubated (16 h, 37°C) in an orbital shaker. The culture was used for small scale DNA preparation (Miniprep kit from Sigma-Aldrich, Deisenhofen, Germany) or to inoculate 200 ml of LB medium supplemented with 100 µg/ml Amp, followed by incubation (16 h, 37°C) in an orbital shaker, for large scale DNA preparation (QIAfilter plasmid maxi kit from Qiagen, Hilden, Germany). Purification of plasmid DNA was performed following the supplier's recommendations (Sigma-Aldrich and Qiagen). A Miniprep kit was used to isolate up to 20 µg of plasmid DNA, alternatively the QIAfilter plasmid maxi kit was used for obtaining pure plasmid DNA up to 500 µg from 200 ml bacterial culture.

2.2.1.7 Sequencing of DNA

Plasmid DNA was sequenced at the company SeqLab (Göttingen, Germany) using sequencing primers M13 forward (16mer) or M13 reverse (17mer).

2.2.2 Methods for nucleic acids

2.2.2.1 Determination of nucleic acid concentration

To determine the concentration of DNA or RNA in solution the absorbance was measured at a wavelength of 260 nm (A_{260}) in a quartz cuvette (d = 1 cm) with a Beckmann spectrophotometer. The concentration of nucleic acids was determined by using the following conversions:

1 A_{260} = 50 µg/ml dsDNA
1 A_{260} = 37 µg/ml ssDNA
1 A_{260} = 40 µg/ml ssRNA

When the sequence of the nucleic acid and consequently the molar extinction coefficient were known, the concentration could be determined by the Lambert-Beer's law:

$$A = \varepsilon \cdot c \cdot d$$

In which A is the absorbance, ε is the molar extinction coefficient, c is the concentration and d is the path length of the cuvette. The concentration of nucleic acids was as well determined using a NanoDrop® spectrophotometer ND-1000, which allows the analysis of 1 µl of sample volume.

2.2.2.2 Purification of nucleic acids by phenol/chloroform extraction

For removal of contaminating proteins from nucleic acid solutions, one volume of phenol/chloroform (1:1, v/v) solution was added to the sample, mixed vigorously and centrifuged (5 min, 20,000 x g, 4°C) to separate the phases. The aqueous phase was transferred to a new tube and an equal volume of a chloroform/isoamyl alcohol (24:1, v/v) solution was added to remove any trace phenol followed by centrifugation (5 min, 20,000 x g, 4°C). The aqueous phase was transferred into a new tube and the nucleic acids were precipitated by sodium acetate/ethanol precipitation (see 2.2.2.3).
Phase lock gel vials were used in order to improve the recovery of the nucleic acids and to reduce the contamination by the organic phase.

2.2.2.3 Sodium acetate/ethanol precipitation

Sodium acetate was added to the sample to a final concentration of 0.3 M, the solution was mixed and 3 volumes of 96% (v/v) ethanol in water were added. The sample was placed on ice for at least 30 min. The precipitated nucleic acid was recovered by centrifugation (15 min, 20,000 x g, 4°C), the supernatant discarded, and the nucleic acid pellet rinsed with a 70% (v/v) ethanol/water solution. After a second centrifugation step, the supernatant was discarded, and the pellet dried in the Speed Vac SC 110-A. The lyophilised nucleic acids were then dissolved in water or TE buffer.

2.2.2.4 Isopropanol precipitation

RNA was precipitated by adding 0.4 M lithium chloride and an equal volume of 96% (v/v) isopropanol to the sample. After incubation (30 min, -20°C), the sample was centrifuged (30 min, 20,000 x g, 4°C). The pellet was washed with 70% (v/v) ethanol in water, centrifuged, the supernatant discarded, and the pellet dried in the Speed Vac SC 110-A. The lyophilised RNA was then dissolved in water or TE buffer.

2.2.2.5 Polymerase chain reaction

For amplification of DNA fragments a PCR was performed using the *Taq* DNA polymerase. An amount of 25 ng DNA was used as template, 0.5 µM each of forward and reverse primers, 200 µM of each dNTP and 1.0 U of *Taq* DNA polymerase. The steps of the PCR are listed below:

denaturing	94°C	2 min	
denaturing	94°C	15 s	⎫
annealing	T°C *	45 s	⎬ 25x
elongation	72°C	45 s	⎭
elongation	72°C	10 min	
cooling	4°C	∞	

The annealing temperatures and the corresponding p/t hybrids are listed below:

Table 2.2.1: Primers and annealing temperature

forward primer	reverse primer	annealing T°C
Primer PA	Primer PB	60°C
Primer B	M13 reverse primer	50°C

PCR products were analysed by TAE-agarose gel electrophoresis (see 2.2.2.6).

2.2.2.6 Non-denaturing TAE-agarose gel electrophoresis

PCR products and plasmids were analysed by non-denaturing agarose gel electrophoresis. The concentration of agarose was adapted to the length of the DNA samples (Table 2.2.2). The required amount of agarose was dissolved by heating (usually 2 min at 800 W in a microwave oven) into a suitable volume (usually 100 ml) of 1x TAE buffer, and 0.006% (w/v) EtBr was added. The agarose solution was then poured into a gel casting chamber and allowed to solidify. Samples were diluted in non-denaturing loading buffer and gels were run horizontally at 8 V/cm length of gel, for about 1 h in 1x TAE running buffer. The DNA bands were visualised under UV light.

Table 2.2.2: Concentration of agarose used for non-denaturing agarose gel electrophoresis

agarose (%)	DNA fragment sizes (bp)
0.5	1,000-30,000
0.7	800-12,000
1.0	500-10,000
1.2	400-7,000
1.5	200-3,000
2.0	50-2,000

2.2.2.7 Polyacrylamide gel electrophoresis (PAGE)

Stock solutions for the preparation of polyacrylamide gels were filtered via a 0.45 µm filter and degassed under vacuum prior to addition of APS and TEMED.
Radio- or fluorescent-labelled samples investigated by denaturing or non-denaturing PAGE were visualised by autoradiography or by fluorescence-detection, respectively.

In the case of radiolabelled probes, the gels were exposed to PhosphorImager screens for about 1 h, followed by scanning with the Typhoon 8600 scanner. For the fluorescent-labelled probes, the gels could be directly scanned on the Typhoon 8600 without prior exposure to a screen. When the nucleic acids were not labelled, gels were stained with Stains-All.

Denaturing PAGE

Single-stranded nucleic acids were analysed by PAGE under denaturing conditions. The gel solution was prepared by mixing a solution of acrylamide/bisacrylamide (19:1) to 7 M Urea, 0.05% (w/v) APS and 0.1% (v/v) TEMED in 1x TBE. The final concentration of acrylamide was adjusted depending on the length of the samples to be analysed (Table 2.2.3). The gel solution was poured into a chamber, formed by two glass plates separated

by spacers, 0.1-1.0 mm in thickness, and polymerised. Gels were pre-run for 30 min in order to achieve a temperature of 55°C. An equal volume of denaturing loading buffer was added to the samples which were heated (5 min, 95°C) before loading. Gels were generally run (0.5-1 h), using 1x TBE as running buffer, at 20 V/cm (gels were 1.0 mm thick and 15 cm long). Sequencing gels were run at a voltage of 30 mV/cm (gels were 0.1 mm thick and 45 cm long), followed by fixation in 10% (v/v) acetic acid (5 min at 23°C), and dried for 2 h at 80°C.

Table 2.2.3: Concentration of acrylamide used for PAGE

denaturing PAGE		non-denaturing PAGE	
acrilamide (%)	**fragment sizes (nt)**	**acrylamide (%)**	**fragment sizes (bp)**
4.0	100-500	3.5	100-2,000
5.0	70-300	5.0	75-500
6.0	45-70	8.0	50-400
8.0	35-45	12.0	35-250
10.0	25-35	15.0	20-150
20.0	8-25	20.0	5-100

Non-denaturing PAGE

Double-stranded nucleic acids were analysed by PAGE under non-denaturing conditions.

A solution of acrylamide/bisacrylamide (19:1) containing 0.05% (w/v) APS and 0.1% (v/v) TEMED was prepared in 1x TBE and used to prepare 1.0 mm thick gels. The final concentration of acrylamide was adjusted depending on the length of the samples to be analysed (Table 2.2.3). The samples were diluted into non-denaturing loading buffer and loaded onto the gel. Gels were run, using 1x TBE as running buffer at 4°C, at 10 V/cm, for about 2 h. One of the two strands was radio- or fluorescent-labelled for detection by autoradiography or fluorescence measurement.

2.2.2.8 Hybridisation of nucleic acids

This procedure was used in order to hybridise complementary single-stranded nucleic acids to form double-stranded nucleic acids. The two matching single strands were mixed in a molar ratio 1:1 in hybridisation buffer. The samples were then denatured (5 min, 95°C), and allowed to cool down to 23°C. To test the hybridisation efficiency, samples were resolved by non-denaturing PAGE (see 2.2.2.7). In the case of the p/t hybridisation procedure, the template strand was used in a 1.3 molar excess over the primer, to achieve the complete annealing.

2.2.2.9 Radiolabelling of the 5´-termini of single-stranded nucleic acids

Synthetic single-stranded nucleic acids have a free 5´-OH group and can be directly labelled by T4 polynucleotide kinase as described below. Instead *in vitro* transcribed RNA was subjected to 5´-dephosphorylation by CIP prior to 5´-end-radiolabelling with polynucleotide kinase.

Radiolabelling of synthetic single-stranded nucleic acids

Single-stranded nucleic acids were 5´-end-labelled by an incubation of 10 pmol of DNA or RNA, 30 mCi of [γ-^{32}P]-dATP with T4 polynucleotide kinase (30 min, 37°C). Reactions were stopped by heating the samples (5 min, 95°C). Labelled short oligonucleotides (< 10 nt) were directly analysed by denaturing PAGE, since, due to their small size, a separation from the contaminating [γ-^{32}P]-dATP by a phenol/chloroform extraction was impossible. Gels were analysed by exposure to a PhosphorImager screen. The screen was scanned on the Typhoon 8600 scanner and the relative amount of radioactivity was determined by the program ImageQuant 5.2 (Molecular Dynamics, Sunnyvale, CA, USA). The percentage of radioactivity of the short oligonucleotide was determined by comparing the counts per min (cpm) of the labelled short oligonucleotides and the free [γ-^{32}P]-dATP.

Labelled long oligonucleotides (> 10 nt) were purified by phenol/chloroform extraction (see 2.2.2.2). The aqueous supernatant was gel-filtrated on a G-25 micro column in order to remove the contaminating excess [γ-^{32}P]-dATP. The determination of the amount of labelled oligonucleotide was performed by thin layer chromatography (TLC) (see 2.2.2.10).

Radiolabelling at the 5´-termini of RNA transcribed *in vitro*

Prior to the labelling of the 5´-end of RNA with polynucleotide kinase, CIP was used to ´cleave off´ the 5´-terminal phosphate groups of the *in vitro* transcribed RNA. Five nmol of RNA were incubated (1 h, 37°C) with 20 units of CIP following the supplier's instructions (New England Biolabs, Beverly, MA, USA). The reaction was stopped by heating (10 min, 70°C). Dephosphorylated RNA could then be used as substrate for the 5´-end labelling by T4 polynucleotide kinase (see above).

2.2.2.10 Thin layer chromatography (TLC)

In order to quantify the amount of radiolabelled oligonucleotide, 2 µl of collected samples (see 2.2.2.9) were loaded onto a TCL plate (Polygram CEL 300 PEI/UV_{254}), and TCL was performed in 0.6 M potassium dihydrogen phosphate, pH 3.5. When the leading front of

the buffer had reached the end of the plate, the plate was dried and exposed to a PhosphorImager screen for 15 min. The screen was scanned on the Typhoon 8600 scanner and the relative amount of radioactivity was quantified by the program ImageQuant 5.2 (Molecular Dynamics, Sunnyvale, CA, USA). By comparing the cpm of the labelled oligonucleotides before and after the purification from excess [γ-^{32}P]-dATP, the concentration of the labelled probe was determined.

2.2.2.11 Extraction of DNA fragments from non-denaturing polyacrylamide gels

Radiolabelled DNA (see 2.2.2.9) was visualised by autoradiography and the gel slice containing the DNA band was excised with a scalpel. The slice was cut into small pieces and 400 µl of water was added, followed by vortexing for 1 min and incubation at 37°C for 3 h. The elution of DNA was further continued for 12 h at 4°C. The fragments of polyacrylamide were removed by centrifugation (20 min, 20,000 x g, 23°C). The supernatant was carefully transferred to a fresh tube and the DNA was dried in the Speed Vac SC 110-A. The lyophilised DNA was then dissolved in water or TE buffer and stored at -20°C.

2.2.3 Methods for proteins

2.2.3.1 Determination of protein concentration by measuring A_{280}

The absorbance of proteins in solution was measured at a wavelength of 280 nm in a quartz cuvette (d = 1 cm) with a Beckmann Spectrophotometer. The protein concentration was calculated on the base of the Lambert-Beer's law (see 2.2.2.1) and the extinction coefficients (Table 2.2.4) were calculated using the amino acid composition of the proteins and the computer program ´Protein Identification and Analysis Tools on the ExPASy server´ (http://www.expasy.org/tools/protparam.html) (176).

Table 2.2.4: Molar extinction coefficients of proteins used in this study

Protein	ε ($M^{-1}cm^{-1}$)
HIV-1 RT	260,450
HIV-2 RT	238,150
EIAV RT	223,180
p51 subunit of HIV 1 RT	124,180
T7 RNA polymerase	140,000

2.2.3.2 Determination of protein concentration by the Bradford method

For mixtures of proteins and when the primary structure was not available, the concentration was determined by the Bradford assay (Bio-Rad protein assay kit from Bio-Rad, München, Germany), which is based on the binding of the Coomassie Blue G250 dye to proteins. The protein solution (200 µl) was mixed to 800 µl of Bradford reagent followed by incubation at 23°C for 5 min and the measurement of the absorption at 595 nm. The concentration was obtained from a calibration curve with known amounts of BSA.

2.2.3.3 Concentration and dialysis of proteins

For concentration, buffer exchange, and desalting, ultrafiltration centrifugal filters (MWCO 30,000 kDa) were used following manufacturer's instructions (Spectrum, Breda, The Netherlands). The dialysis of protein solutions was done using Specra/Por micro dialyzers (MWCO 25.0 and 3.5 kDa) for small (< 50 µl) volumes, and Spectrum Dialysis tubes (MWCO 12.0-14.0 kDa) for large volumes.

2.2.3.4 SDS-PAGE

The SDS-PAGE was performed according to Laemmli (177) to analyse purity, molecular mass, and concentration of proteins, under denaturing conditions. The discontinuous SDS-PAGE was conducted on a vertical gel casting system in 0.75 mm gels. Gels were run in 1x running buffer at 5 V/cm until the samples reached the resolving gel, then a higher voltage (15 V/cm) was applied. Prior to electrophoresis, samples were diluted in 1x sample buffer and heated (5 min, 95°C). Stacking and resolving gels were prepared as summarised in Table 2.2.5.

To generate 10-20% (w/v) linear gradient SDS-PAGE, equal volumes of the solutions of the two concentrations [10 and 20% (w/v)] were poured into the two chambers of the Hoefer SG30 gradient maker. The denser solution was poured into the mixing chamber. The gradient was created as described in the supplier manual. The gel solution from the mixing chamber was pumped by a peristaltic pump into the gel casting system.

After SDS-PAGE, proteins were stained using Coomassie blue staining solution for about 1 h at 23°C and destained for about 2 h in destaining solution. Alternatively, when the protein amount was very low, a Silver stain kit (Bio-Rad, München, Germany) was used for staining. This method allowed the detection of 1 ng/band of protein as compared to 30-100 ng/band detected by Coomassie blue staining. Silver staining of SDS-PAGE gels was performed following supplier's recommendations (Bio-Rad, München, Germany).

Table 2.2.5: Stacking and resolving gels used in this study

	stacking gel	**resolving gel**			
	5% (w/v)	10% (w/v)	12% (w/v)	15% (w/v)	20% (w/v)
Rotiphorese gel 30%	0.5 ml	1.7 ml	2.0 ml	2.5 ml	3.3 ml
1.5 M Tris-HCl, pH 8.8	-	1.3 ml	1.3 ml	1.3 ml	1.3 ml
1.0 M Tris-HCl, pH 6.8	0.38 ml	-	-	-	-
10% (w/v) SDS	30 µl	50 µl	50 µl	50 µl	50 µl
H_2O	2.1 ml	1.9 ml	1.6 ml	1.1 ml	0.3 ml
TEMED	3 µl	5 µl	5 µl	5 µl	5 µl
10% (w/v) APS	30 µl	50 µl	50 µl	50 µl	50 µl

2.2.3.5 Western blotting of SDS-PAGE gels

For western blotting, unstained SDS-PAGE gels were used (see 2.2.3.4). This protocol was performed using specific antibodies directed against the proteins of interest. A piece of Immobilon-P membrane of the same size of the SDS-PAGE gel was hydrated in methanol for 1 min and washed in distilled water for 5 min. The gel and the membrane were soaked in 1x transfer buffer for 10 min to remove electrophoresis salts and detergents.

For each gel, 6 pieces of 3MM paper were soaked in 1x transfer buffer and the transfer cassette was then assembled as follows:

(-) anode
3 layers of 3MM paper
SDS-PAGE gel
Immobilon-P membrane
3 layers of 3MM paper
(+) cathode

The blotting was performed at 0.8 mA per cm^2 gel area, for 2 h at 23°C, using a blotting device from GE-Healthcare (Chalfont St. Gilles, UK).

For the detection of proteins, the membrane was rinsed for 15 min in 1x TBS-T buffer to remove contaminating SDS followed by blocking in 1x Roti-block solution under shaking (1 h, 200 rpm, 23°C). The blocking solution was removed, and the membrane rinsed in TBS-T for 15 min. The primary Ab was added in TBS-T and the membrane was incubated under shaking (for conditions see Table 2.2.6). The membrane was washed (3 times,

5 min each) with TBS-T and the AP- or HRP-conjugated secondary Ab in TBS-T was added and incubated under shaking (for conditions see Table 2.2.6).

Table 2.2.6: Antibodies tested and suitable conditions

Antibody	dilution in TBS-T (v/v)	incubation conditions
goat anti-HIV-1 Ab	1/2,000	16 h at 4°C
goat anti-rabbit IgG HRP-conjugated Ab	1/2,000	1 h at 23°C
goat anti-rabbit IgG AP-conjugated Ab	1/10,000	1 h at 23°C
rabbit anti-goat IgG Ab	1/10,000	1 h at 23°C
rabbit anti-goat IgG HRP-conjugated Ab	1/2,000	1 h at 23°C
rabbit anti-human β-actin Ab	1/5,000	1 h at 23°C
rabbit anti-p24 Ab	1/2,000	16 h at 4°C

As substrate for AP a BCIP/NBT solution was used as described by the supplier (Calbiochem, Darmstadt, Germany). The membrane was incubated until the bands appeared (about 15 min). The reaction was stopped by rinsing the membrane with water. Stained membranes were photographed and stained with Coomassie blue staining (1 h, 23°C), and destained for 2 h in destaining solution.

Alternatively, in the case of the HRP-conjugated secondary Ab, an ECL™ western blotting reagent was used. The staining protocol was performed as described by the supplier (Pierce, Rockford, IL, USA). After 1 min of incubation with the substrate, the membrane was exposed to a Hyperfilm™ ECL for a maximum of 30 min followed by the development of the film using developing and fixative solutions. After their development the membranes were stained with Coomassie blue.

2.2.3.6 Radioactive labelling of HIV-1 RT

The procedure of the radiolabelling of protein was performed by W. Wünsche. HIV-1 RT was radiolabelled with iodine-125 (^{125}I) by using a commercial Na^{125}I solution (Hartmann Analytic, Braunschweig, Germany). Briefly, 100 µl of 5 µM Na^{125}I solution (pH 8.0) were placed in an IODOGEN-tube and incubated for 6 min at 23°C to oxidise the iodide to reactive periodate. A volume of 96 µl of reaction mixture was incubated with 60 µg of protein for 6 min at 23°C followed by incubation on ice for 10 min. Iodinated HIV-1 RT was analysed by SDS-PAGE (see 2.2.3.4).

2.2.3.7 Fluorescent labelling of proteins

The NHS-fluorescein was used for labelling proteins at lysine residues. The protocol was performed according to the supplier's instructions (Pierce, Rockford, IL, USA). The protein

(1 mg) was dialysed against a solution containing 20 mM sodium phosphate and 150 mM NaCl (pH 7.0), for 12 h at 4°C. A 24-fold molar excess of the fluorescent dye was added to the protein solution and incubated 2 h on ice. Contaminating free NHS-fluorescein was removed from the labelled proteins by gel-filtration (G-50 or G-25 micro columns).
Fluorescein-5-Maleimide was used for the labelling of cysteine residues on proteins. The protein (1 mg) was dialysed against Tris-HCl buffer (pH 7.0) for 12 h at 4°C. The fluorescent dye was added in a 25-fold molar excess to the protein to be labelled, followed by incubation for 12 h at 4°C. Excess of dye was removed by gel-filtration (G-50 or G-25 micro columns).
Labelled proteins were analysed by SDS-PAGE (see 2.2.3.4). The absorbances of the protein and of the fluorophore were determined by the NanoDrop® spectrophotometer ND-1000 and the labelling efficiency was calculated as described by the manufacturer (Pierce, Rockford, IL, USA).

2.2.4 Expression and purification of recombinant HIV-1 RT

The HIV-1 RT was expressed in *E. coli* and purified using the protocol originally described in reference (175).

Briefly, LB medium, supplemented with 100 µg/ml Amp and 25 µg/ml Kanamycin, was inoculated with bacteria (*E. coli* M15/pRT1 66/51.1, pDMI.1) from glycerol stock and grown for 16 h at 37°C in an orbital shaker. The bacterial culture was used to inoculate 6 l of LB medium (0.5 l medium per 1 l Erlmeyer flask) containing 100 µg/ml Amp and 25 µg/ml Kanamycin such that the OD_{600} of the final bacterial culture reached a value of 0.1. The 6 l bacterial culture were incubated in an orbital shaker (200 rpm, 37°C) until the OD_{600} reached a value of about 0.8-1.0 and then p66 and p51 (gene) expression was induced by adding IPTG to a final concentration of 0.4 mM. Induced bacteria were further cultivated in Erlmeyer flasks for additional 4 h at 37°C under shaking (200 rpm) and harvested by centrifugation (30 min, 5,000 x g, 4°C). The culture supernatant was discarded and the bacterial stored at -80°C.

2.2.4.1 Bacterial lysis

Frozen bacteria were thawed and resuspended in lysis buffer (see 2.1.12.2) (3 ml lysis buffer/g wet bacteria), and the suspension incubated on ice for 30 min. An amount of 3 mg lysozyme per ml of bacterial solution was added, followed by stirring (20 min, 4°C). The solution was subjected to sonication by Ultrasonicator Sonorex Super RK 103 H using a TT 13 Titanium flat tip (Bandelin, Berlin, Germany) (continuous mode, 17 times for 20 s,

40% duty cycle) and centrifuged (45 min, 27,000 x g, 4°C). The supernatant was collected and NaCl added (final conc. of 1 M).

2.2.4.2 Precipitation of proteins by ammonium sulphate (I)

From the supernatant, proteins were precipitated by the addition of ammonium sulphate (390 g/l). After incubation for 30 min on ice, the precipitate was collected by centrifugation (20 min, 27,000 x g, 4°C), and the pellet resuspended in 3 ml buffer A (see 2.1.12.2) per 1 g of pellet.

2.2.4.3 Precipitation of nucleic acids by streptomycin sulphate

An amount of 40 mg/ml (final concentration) streptomycin sulphate was added to the solution, followed by incubation on ice for 30 min under slow stirring. The solution was then centrifuged (40 min, 27,000 x g for at 4°C), and the supernatant introduced into a Spectrum Dialysis tube (Spectrum, Breda, The Netherlands) and dialysed against 2 l of buffer A initially for 4 h at 4°C, followed by the replacement of the buffer A (see 2.1.12.2) with a fresh buffer A and dialysed for 12 h at 4°C.

2.2.4.4 Anion exchange column (DEAE)

Prior to the chromatography, the DEAE-Sephacel column (GE-Healthcare, Chalfont St. Gilles, UK) was equilibrated in buffer A (see 2.1.12.2) and the protein solution was loaded onto the column at a flow rate of 2 ml/min. Due to the high isoelectric point of HIV-1 RT (pI = 9.3), it was not retained on the column at the pH of the running buffer, instead almost 90% of the bacterial proteins bound to the DEAE-Sephacel matrix. The RT was present in the flow-through. Fractions were collected by a GradiFrac fraction collector, analysed by SDS-PAGE, and stained with Coomassie blue stain. Those fractions containing RT were combined and further purified.

2.2.4.5 Affinity chromatography on Heparin

A Heparin Sepharose CL-6B column (GE-Healthcare, Chalfont St. Gilles, UK) was equilibrated in buffer A (see 2.1.12.2) and the pooled fractions were loaded onto the column at a flow rate of 1.0 ml/min. The column was washed with buffer A until the level of A_{280} of the flow-through reached a stable baseline. The protein was eluted using a linear gradient of 25 mM to 1 M NaCl by addition of buffer B (see 2.1.12.2). The fractions were

analysed by SDS-PAGE and stained with Coomassie blue stain. Those fractions containing RT were pooled and further processed.

2.2.4.6 Precipitation of proteins by ammonium sulphate (II)

Proteins were precipitated from the eluate by addition of ammonium sulphate as described in 2.2.4.2. After centrifugation, the protein pellet was then resuspended in gel filtration buffer (5 ml total volume).

2.2.4.7 Gel filtration

Prior to the gel filtration chromatography, a HiLoad 26/60 Superdex 75 prep grade column (GE-Healthcare, Chalfont St. Gilles, UK) was equilibrated in gel filtration buffer (see 2.1.12.2) and the resuspended proteins were loaded onto the column. Fractions were collected at a flow rate of 2 ml/min and analysed by SDS-PAGE and Coomassie blue stain. The fractions containing RT were combined and subjected to further purification.

2.2.4.8 Anion exchange chromatography (TMAE)

A Fractogel EMD TMAE-column (Merck, Darmstadt, Germany) was equilibrated in DEA buffer A (see 2.1.12.2) and the pooled fraction proteins were loaded onto the column. The column was washed with DEA buffer A until a stable baseline (A_{280}) was reached before elution with DEA buffer B (see 2.1.12.2). The fractions were collected right after the beginning of the salt gradient and were analysed for the presence of RT by SDS-PAGE and Coomassie blue stain.

The fractions containing RT were pooled and the protein concentrated using ultra filtration centrifugal filters (MWCO 30,000 kDa), according to the manufacturer's instructions (Merck, Darmstadt, Germany) followed by buffer exchange to the storage buffer (see 2.1.12.2). The protein concentration was determined (see 2.2.3.1) and the solution then shock-frozen in liquid nitrogen for storage at -80°C.

2.2.4.9 Testing for RNase contamination of protein preparations

All protein preparations were tested for RNase contamination in order to verify whether they were suitable for working with RNA. The investigated protein (5 µM) was incubated for 1 h at 37°C in the presence of 1.5 µg RNA MS2 from the bacteriophage MS2, in a total volume of 15 µl. Samples were resolved by denaturing PAGE and gels were stained with SYBR gold for 10 min and visualised by UV light. Alternatively, 10 nM of 5´-end

radiolabelled RNA (see 2.2.2.9) was incubated with 5 µM protein in a total volume of 50 µl, at 37°C for different lengths of time and the reaction products were separated by denaturing PAGE (see 2.2.2.7). Gels were exposed to a PhosphorImager screen and analysed after scanning of the screen on the Typhoon 8600.

2.2.5 Enzymatic methods

2.2.5.1 RNA-dependent DNA polymerase activity (RDDP) assay

This assay was performed in the presence and in the absence of hexanucleotides in order to test their efficacy of inhibiting RDDP activity of HIV-1. This assay was also carried out to test the functionality of other RTs, e.g. HIV-2 RT and EIAV RT. The protocol was performed as described (165). Briefly, the activity of RT was determined by monitoring the incorporation of [^{3}H]-dTTP into a poly(rA)/oligo(dT)$_{12-18}$ p/t. The RT (325 nM) was preincubated 2 min at 25°C in the presence or absence of 65 µM hexanucleotide in 1x RT binding buffer. To the solution of the reaction, 1.1 µM [^{3}H]-dTTP, 50 µM dTTP and 0.2 OD_{260}/ml poly(rA)/oligo(dT)$_{12-18}$ were added. After incubation for 10 min at 37°C or 25°C, the reaction solution was spotted in duplicate onto 2 cm^2 DEAE filters and allowed to dry. The filters were washed twice, for 5 min each time, in 1x SCC buffer to remove unincorporated free [^{3}H]-dTTP and enzyme. After a final wash in 100% (v/v) ethanol for 5 min, the filters were dried for 1 h at 80°C. As a background control, a reaction mixture lacking RT was loaded onto DEAE filters and washed together with the other filters. When dried, filters were added to 3 ml of the scintillation cocktail in a scintillation vial. The cpm were measured by a scintillation counter Wallac 1409.

2.2.5.2 DNA-dependent DNA polymerase activity (DDDP) assay

This assay was performed in the presence or absence of candidate inhibitors of HIV-1 RT. The primer Flo1 (18mer) was 5´-end-radiolabelled (see 2.2.2.9) and annealed to Flo6 template as described in 2.2.2.8. The RT (0.75 nM) was preincubated for 2 min at 25°C in the absence or presence of 30 µM hexanucleotides. An amount of 1.5 nM DNA/DNA p/t and 100 µM each dNTPs was added to the reaction mixture. The reaction was run in 1x RT binding buffer. The reaction mixture was incubated at 37°C or 25°C for different length of time (0,0.25, 0.5, 0.75, 1, 1.5, 2.5, 5, 7.5 and 10 min) and was stopped by the dilution of the sample in denaturing loading buffer and by heating for 5 min at 95°C. Products were then separated by denaturing PAGE (see 2.2.2.7). The gel was fixed in a solution of 10% (v/v) acetic acid, dried and then exposed to a PhosphorImager screen. The screen was scanned on the Typhoon 8600 scanner and the product formation was

then quantified by the program ImageQuant 5.2 (Molecular Dynamics, Sunnyvale, CA, USA).

2.2.5.3 Fidelity of HIV-1 RT during DDDP activity assay

The fidelity of HIV-1 RT in the DDDP activity assay was tested in the presence or absence of hexanucleotides. The assay was essentially performed as described in 2.2.5.2, except that one of the four dNTPs was systematically omitted in the reaction mix. To evaluate nt insertion and mispair extension of the primer by the RT, the samples were resolved by denaturing PAGE following the procedure described in 2.2.2.7.

2.2.5.4 HIV-1 RT processivity assay

Processivity assays were carried out in order to test the effect of candidate RT inhibitors on enzyme processivity during DDDP activity assay. The protocol used for this assay was modified from (178). The M13/pUC sequencing primer was 5´-end radiolabelled (see 2.2.2.9) and annealed to the M13mp18 template as described in 2.2.2.8. RT was incubated for 2 min at 25°C in the absence or presence of Hex_R in a 3,000-fold molar excess. The p/t was added to the protein solution followed by incubation for 3 min at 25°C or 37°C, in order to allow the binding of RT to its substrate. The binding mixture (15 µl) contained 10 nM HIV-1 RT, 10 nM p/t, and 30 µM hexanucleotides in 1x RT binding buffer. The primer-extension reaction was started by the addition of a solution containing a RNA trap (pseudoknot) and dNTPs to a final concentration of 1 µM and 500 µM, respectively. Under this condition, the primer was extended only once during the incubation and this was confirmed by the two control reactions with and without trap (see 3.4.4). This reaction mixture was incubated for 3 min at 37°C or 25°C, and the products were resolved by 8% denaturing PAGE (see 2.2.2.7). After separation, the gel was analysed as described in 2.2.5.2.

2.2.5.5 RNase H activity assay

In order to test the effect of hexanucleotides on RNase H activity of HIV-1 RT, a RNA/DNA hybrid duplex substrate was used, where the 5´-end of the RNA primer was radiolabelled (see 2.2.2.9). The annealing of the RNA primer sara (35mer) and of its complementary template DNA sara (52mer) was performed as described in 2.2.2.8. HIV-1 RT (0.75 nM) was incubated with or without hexanucleotide (30 µM), for 2 min at 25°C in 1x RT binding buffer. The RNA/DNA duplex substrate (1.5 nM) was added to the binding mixture and the reaction was run at 37°C or 25°C. The samples were collected

(10 µl/sample) after different time points (0, 0.25, 0.5, 0.75, 1, 1.5, 2.5, 5, 7.5 and 10 min) and the reactions were stopped by addition of denaturing loading buffer and heating for 5 min at 95°C. The products of the reaction were resolved by 10% denaturing PAGE (see 2.2.2.7) and the gel was fixed in a solution of 10% (v/v) acetic acid, dried and then exposed to a PhosphorImager screen. The screen was scanned on the Typhoon 8600 scanner and the depletion of substrate was then quantified by the program ImageQuant 5.2 (Molecular Dynamics, Sunnyvale, CA, USA).

2.2.5.6 T7 RNA polymerase activity assay

This assay was performed to verify the T7 RNA polymerase functionality. The primer T7 was 5´-end radiolabelled and annealed to the template T7 as described in 2.2.2.8. The reaction was performed in a total volume of 22 µl and the reaction solution contained 5 µM T7 RNA polymerase, 100 µM each dNTP, 0.5 µM p/t, 5 µM [5,6-^{3}H]-UTP and 0.25 U/µl RNasin in T7 transcription buffer (40 mM Tris-HCl, pH 8.0, 5 mM DTT, 20 mM $MgCl_2$ and 1 mM spermidine). The reaction mixture was incubated for 2 h at 37°C and the samples were processed as described in 2.2.5.1.

2.2.6 Binding assays

2.2.6.1 p24 core protein-ELISA

The p24-ELISA was performed in order to quantify the amount of p24 protein, and consequently the amount of HIV-1 pseudoviruses, in the cell supernatants of transfected cells as described (see 2.2.10.7). For this purpose, cells supernatant were diluted 1:5,000 (v/v) in 1x PBS_b and applied to an INNOTEST™ HIV Ag MAb ELISA kit. The protocol was performed according to the supplier's instructions (Innogenetics, Ghent, Belgium). Briefly, diluted cell supernatants containing p24 antigen were incubated in a well together with a mixture of biotinylated anti-p24 monoclonal antibodies. The wells of polystyrene microtitre plates were coated with human polyclonal antibodies to HIV. After incubation for 1.5 h at 37°C, HRP-conjugated streptavidin was added to the well and bound to the biotinylated antibodies. The addition of the peroxidase substrate to the well led to a colorimetric reaction in which the substrate was transformed into a blue colored product which turned to yellow after sulphuric acid addition. The optical density at 450 nm (OD_{450}) was measured by an ELISA-Reader and the amount of p24 protein (ng/ml) was then calculated based on a standard curve.

2.2.6.2 Filter binding assay

The filter binding assay was performed as described (164), in order to study affinities between proteins and radiolabelled nucleic acids. The rationale behind this assay is that nucleic acids being negatively charged do not bind to the nitrocellulose, which is negatively charged as well; instead most proteins have a net positive charge, and therefore bind to nitrocellulose. Consequently, the nucleic acid-protein complex is retained on the nitrocellulose and the exact amount of radiolabelled nucleic acid retained on the nitrocellulose filter is quantified by a scintillation counter. The nitrocellulose filters were pre-soaked in 1x binding buffer over night at 4°C in order to decrease the unspecific binding of nucleic acids to the filters.

Radiolabelled oligonucleotides (1 nM) (see 2.2.2.9) and target proteins (0-25 µM) were incubated in 30 µl of 1x RT binding buffer for 2 min at 25°C. An aliquot (10 µl) of this mixture was filtered under reduced pressure through a pre-wetted nitrocellulose filter BA85 (0.45 µm) and rinsed with 3 ml of 1x RT binding buffer. As a background control, a solution containing only the radiolabelled nucleic acid in 1x RT binding buffer was subjected to the same procedure. When dried, filters were added to 3 ml of the scintillation cocktail in a scintillation vial. The radioactivity retained on the filters (cpm) was measured using the scintillation counter Wallac 1409. The background value was subtracted from all the other values. Moreover, to determine the total radioactivity in the binding solution, 10 µl of binding solution containing radiolabelled nucleic acid and protein were directly poured into the scintillation cocktail (3 ml) and the radioactivity was then measured. The resulting value was set to 100% binding and used for the normalisation of the data.

2.2.6.3 Electrophoretic mobility shift assay (EMSA)

The EMSA or gel-shift assay, was performed to determine nucleic acid-protein interactions. The rationale behind this technique is that protein:nucleic acid complexes migrate more slowly than free nucleic acid molecules when subjected to non-denaturing PAGE. The protocol for the EMSA was performed as described (179).

A solution (10 µl) containing 1 nM of radiolabelled nucleic acid (see 2.2.2.9), 5 µM protein and 5% (v/v) glycerol in 1x binding buffer was incubated for 10 min at 25°C. The samples were then directly loaded into a gel and resolved by 5% (w/v) non-denaturing PAGE. The gel was dried and exposed to a PhosphorImager screen. The screen was scanned on the Typhoon 8600 scanner and analysed by the program ImageQuant 5.2 (Molecular Dynamics, Sunnyvale, CA, USA).

2.2.7 UV-crosslinking

An amount of 250 pmol of HIV-1 RT and of 100 fmol radiolabelled 4-thio U-modified Hex-$S3_R$ (at position 4) (see 2.2.2.9) were preincubated in 1x RT binding buffer for 2 min at 25°C. Samples were then transferred onto a piece of Parafilm (10 µl per drop), placed on ice and irradiated for 20 min at 366 nm using a hand-held fluotest lamp. Samples were recovered from the parafilm and transferred into a new tube. The crosslinked protein was subjected to CNBr cleavage (see 2.2.8) or directly analysed by SDS-PAGE followed by a staining of the gel with Coomassie blue (see 2.2.3.4), drying and exposure to a PhosphorImager screen. The screen was scanned on the Typhoon 8600 scanner and formation of the product was then quantified by the program ImageQuant 5.2 (Molecular Dynamics, Sunnyvale, CA, USA).

2.2.8 Cyanogen bromide (CNBr) cleavage of HIV-1 RT

The CNBr cleavage of HIV-1 RT was performed as described (180). HIV-1 RT was precipitated in 20% (w/v) TCA for 1 h at -20°C, the solution was centrifuged (15 min, 18,000 x g, 4°C), and the supernatant was discarded. The pellet was washed with 1 ml of ice-cold acetone followed by centrifugation (15 min, 18,000 x g, 4°C). The supernatant was discarded and the pellet was then air-dried and dissolved in 100 µl formic acid (70%) containing 3.5 g/l CNBr. The cleavage reaction was performed at 23°C for 24 h. Formic acid and CNBr were removed by centrifugal-lyophilisation in a Speed-vac. The pellet was dissolved in 50 mM Tris-HCl (pH 8.0) buffer and resolved by SDS-PAGE [10-20% (w/v) linear gradient] (see 2.2.3.4). Gels were stained with Coomassie blue as described in 2.2.3.4.

2.2.9 Modelling and docking studies

Modelling and docking studies were performed by T. Restle (Institute for Mol. Med., University of Lübeck). Rigid-body docking studies of HIV-1 RT (Brookhaven PDB accession No.: 1HMV, 1RTH, 1RTD and 1HVU) and Hex-$S3_R$ were performed with the program Hex 4.2 (181). Molecular graphics images were produced using the UCSF Chimera package from the Computer Graphics Laboratory, University of California, San Francisco, CA, USA (182).

2.2.10 Cell culture techniques

Standard protocols for cell cultures, e.g. media changes and cell splitting, were performed as described (183). Cell lines tested and suitable media are listed in Table 2.2.7.

Table 2.2.7: Cell lines tested and suitable media

cell line	cell culture medium
HEK293 T	DMEM with GlutaMAX I and sodium pyruvate containing 10% (v/v) FCS
HEK293	DMEM with GlutaMAX I and sodium pyruvate containing 10% (v/v) FCS
BJA-B	RPMI 1640 containing 10% (v/v) FCS

2.2.10.1 Cryopreservation of human cells

Healthy cells at the edge of confluence were harvested after trypsin treatment and counted. The cells were centrifuged (5 min, 2,000 x g, 23°C), and the supernatant was discarded. The cell pellet was resuspended to a concentration of 1 x 10^6 cells per ml by gentle mixing in cell culture medium containing 10% (v/v) DMSO. Aliquots of 1 ml each were placed into cryovials. Vials were transferred into a freezing container and placed into a -80°C freezer overnight. A day later, the vials were transferred into liquid nitrogen.

2.2.10.2 Trypan blue staining for the determination of non-viable cells

Trypan blue stain was used to distinguish viable from nonviable cells. An amount of 10 µl of cell suspension in PBS_b was mixed into an equal amount of trypan blue solution [0.4% (w/v) in 0.85% (w/v) NaCl]. Within 5 min from the adding of the staining solution the cells were counted. Viable cells excluded the dye and were not stained, while nonviable cells absorbed the dye and appeared blue.

2.2.10.3 Fluorescein diacetate (FDA) test for the determination of viable cells

The FDA is a nonfluorescent derivative of fluorescein which can be transported across cell membranes and deacetylated by nonspecific esterases in viable cells (184). The resultant fluorescein accumulates within cells allowing the fluorescence detection of living cells. For this test cells were plated in a 96-well plate, and washed twice in 1x PBS_b. The plate was placed on ice, to reduce the velocity of the reaction and a solution of 20 µM FDA in 1x PBS_b was added (50 µl per well).

Fluorescence emission was measured by Fluoroskan Microplate Reader at intervals of 1 min for 10 min in total. The excitation wavelength of the fluorescein is 488 nm and the

emission wavelength is 518 nm. The direct comparison of FDA hydrolysis rates between the investigated samples allowed the quantification of viable cells.

2.2.10.4 Lipofectamine 2000-mediated transfection of human cells

Lipofectamine 2000, a cationic lipid-based transfection reagent, was used to transfect DNA and RNA into human cells and the transfection was performed following the instructions provided by the supplier. Generally, the cells were placed into a 12-well- or 24-well-plate and transfection was performed when the cells were at a high density (70-80% confluence). The medium used for the transfection was Opti-MEM I, which is a reduced serum medium and does not interfere with nucleic acids:Lipofectamine 2000 complex formation. An appropriate amount of RNA or DNA was diluted in 50 µl of Opti-MEM I and the solution was gently mixed. Lipofectamine 2000 was diluted as well in 50 µl of Opti-MEM I to a 100 µg/ml final concentration, and the solution was incubated for 5 min at 23°C. The diluted Lipofectamine 2000 was combined with the diluted RNA or DNA and the resulting solution was incubated at 23°C for 30 min, to allow nucleic acids:Lipofectamine 2000 complexes to form. The complexes (100 µl) were diluted in 400 µl Opti-MEM I and the resulting solution was added to each well. The plate was gently mixed and the cells were incubated for 4 h at 37°C in a CO_2 incubator. The complexes were removed and fresh cell culture medium was added to the cells, followed by incubation for 24-72 h until they were ready to be assayed.

2.2.10.5 Calcium phosphate-mediated transfection of human cells

Calcium phosphate transfection was performed as described (185), to introduce DNA and RNA into cells. A precipitate containing calcium phosphate and nucleic acids was formed by slowly mixing a HEPES-buffered phosphate solution with a solution containing calcium chloride and nucleic acids. These nucleic acids precipitates are taken up by eukaryotic cells by an endocytic-type mechanism. The protocol was performed as follows. Cells were plated into a 12-well- or 24-well-plate and the transfection was performed at 70-80% cell confluence. The conditioned medium was removed, the cells were washed twice with 1x PBS_b, and 450 µl of fresh medium without FCS was added to the cells. Nucleic acids were diluted in water to 22.5 µl final volume and 2.5 µl of 2.5 M $CaCl_2$ were added to the diluted nucleic acids. The solution was well mixed and 25 µl of 2x HBS buffer were added to the cells drop-wise. After the addition of the precipitated nucleic acids, the cells were incubated at 37°C in a CO_2 incubator for 30 min. The medium was replaced by fresh cell culture medium and the cells were incubated for further 48-72 h before being assayed.

2.2.10.6 Determination of transfection efficiency by β-galactosidase assay

The β-galactosidase assay was performed in order to determine the efficiency of the transfection. The vector pcDNA 3.1 (-)/Myc-His/*lac*Z was co-transfected with the nucleic acids under investigation. This vector carries a reporter gene, the *lacZ* gene, which encodes the β-galactosidase protein that hydrolyses X-Gal into a colorless galactose and 4-chloro-3-brom-indigo, which forms an intense blue precipitate. An amount of 0.2 µg pcDNA 3.1 (-)/Myc-His/*lac*Z was used for the transfection of 200,000 cells, 24 or 48 h after transfection the cells were washed twice with 1x PBS_b and fixed for 10 min in 0.1% (v/v) glutaraldehyde, followed by washing with 1x PBS_b. The substrate solution was then added (1 ml per well) followed by incubation for 1.5 h at 37°C in a CO_2 incubator. The substrate solution contained 1 mg/ml X-Gal, 5 mM potassium hexacyanoferrate (III), 5 mM potassium hexacyanoferrate (II) trihydrate, 1 mM $MgCl_2$ in 1x PBS_b. The transfected cells could be visualised and quantified because of their intense blue color. The relative amount of transfected cells was then calculated.

2.2.10.7 HIV-1 pseudotyped viral vector assay

This assay was used for the characterisation of candidate inhibitors for reverse transcription under single-cycle conditions. For this purpose, a replication-incompetent lentiviral vector system was used (originally described by Jármy *et al.*) (174). The production of pseudotyped viral vectors was performed by calcium phosphate co-transfection of HEK293 T cells with the plasmids pczVSV-G and pGJ3-Luci, in the presence or absence of the inhibitor in different concentrations. In a 12-well plate pre-coated with fibronectin from bovine plasma (1.7 µg protein/cm^2), 200,000 cells per well were seeded, and grown in cell culture medium for 24 h before transfection. The cells were transfected by the calcium phosphate method (see 2.2.10.5) using the same amount of each plasmid (2 µg) and variable amounts of the inhibitor and were incubated for 30 min at 37°C in a CO_2 incubator. After that, the medium was exchanged and 1 ml per well of the cell culture medium and 10 mM sodium butyrate were added. Supernatants were harvested after a final incubation for 48 h and filtered through a 0.45 µm-filter to remove cell debris. HIV-1 pseudoviruses were detected and quantified by p24-ELISA, as described in 2.2.6.1, and used to infect HEK293 cells.

Packaging cells were collected and lysed for western blotting as described in 2.2.3.5. Infection of HEK293 cells with pseudovirus-containing supernatants was performed as follows. A number of 10,000 cells per well were seeded in a 96-well luminometer plate and incubated in the cell culture medium for 24 h. Then the conditioned medium was replaced with pseudovirus-containing supernatants (100 µl/well) and the

cells were incubated at 37°C in a CO_2 incubator. After 24 h, the medium was removed and the cell viability monitored by the conversion of FDA (50 µl/well) as described in 2.2.10.3. The activity and consequently the expression of the firefly luciferase enzyme was measured in a Fluoroskan Microplate Reader after addition of 50 µl of the following buffer: 28 mM Tricine (pH 7.8), 500 mM ATP, 250 mM coenzyme A, 250 mM D-luciferin, 33 mM DTT, 200 mM EDTA, 15 mM $MgSO_4$, 1.5% (v/v) Triton X-100 and 5% (v/v) glycerol.

2.2.10.8 Cell lysis protocol for western blotting

Packaging cells (see 2.2.10.7) were collected and lysed for western blotting. Conditioned medium was removed from the well and the cells were washed twice with 1x PBS_b. One ml of 1x PBS_b was added to each well and the cells were detached by scraping with a cell scraper. The cells were then harvested by centrifugation (5 min, 2,000 x g) and the cell pellet was resuspended in 40 µl of buffer containing 10 mM HEPES, 10 mM KCl, 0.1 mM EDTA, 0.1 mM EGTA, pH 7.9, and incubated on ice for 15 min. An amount of 20 µl lysis buffer [10% (v/v) NP-40 in 1x PBS_b] was added to the cell suspension, followed by vortexing for 90 s. Cell lysates were centrifuged (2 min, 14,000 x g), and supernatants were transferred into new tubes and frozen at -80°C for further western blotting.

3 Results

3.1 Binding of hexanucleotides to target proteins

3.1.1 Hexanucleotides as ligands for target proteins

In order to determine whether ´in principle´ hexanucleotides are able to interact with proteins in a way which is specific for the hexameric sequence and for the given target protein, five hexameric sequences, named Hex-1, Hex-2, Hex-S3, Hex-4 and Hex-5 (Table 3.1.1) were investigated. As target proteins, the HIV-1 RT, which naturally interacts with nucleic acids (92;131;164;165;186), the firefly luciferase and the hPrP, were included.

Table 3.1.1: Hexanucleotide sequences tested for binding to target proteins

name	RNA (5´ to 3´)	DNA (5´ to 3´)
Hex-1	UCA AAA	TCA AAA
Hex-2	UCA UGA	TCA TGA
Hex-S3	UCG UGU	TCG TGT
Hex-4	GUC UAA	GTC TAA
Hex-5	GGC AAC	GGC AAC

The hexanucleotide Hex-S3 was included for reasons of curiosity as it showed an enhanced uptake in human B cells, which indicated some kind of protein binding (33). The hexanucleotides Hex-1, Hex-2, Hex-4 and Hex-5 were chosen randomly. To study the role of the 2´-OH group at the ribose and the methyl group at the thymine for their interactions with the target proteins all hexanucleotides were investigated as RNA (designated with lower script ´R´) or DNA (designated with lower script ´D´). The binding of the hexanucleotides towards the target proteins was determined in a filter binding assay, which is based on the ability of the nitrocellulose filters to retain the nucleic acids complexed with proteins, and the results are shown in Fig. 3.1.1.

At first all hexanucleotides showed a measurable binding towards the three investigated target proteins, except for the RNA hexanucleotides, which did not bind to hPrP. This binding was specific and depended on the nt sequence, since different hexanucleotides showed a clear differential binding (Fig. 3.1.1). Among all tested sequences, Hex-S3 showed the strongest binding with a 30-fold difference over Hex-1 when incubated with HIV-1 RT as target protein. Secondly, the RNA and the DNA versions of the same sequence showed different bindings towards the same target, apart from Hex-S3 in the interaction with HIV-1 RT. This indicated that the replacement of a ribose by a deoxy-ribose or of an uracil by a thymine in the hexameric sequence led to

different binding properties (Fig. 3.1.1). This was particularly true for the hPrP, which did not bind to any of the RNA derivatives, while it showed a measurable binding to Hex-$S3_D$, Hex-4_D and Hex-5_D. The RNA and DNA versions of Hex-5, which have an identical base composition and differ only by the substitution of the sugar at the 2´-position, showed a clear differential binding to the firefly luciferase, HIV-1 RT and hPrP, underlining the importance of the 2´-OH group in these interactions. Thirdly, the binding strength of the hexameric sequences was highly specific for the target protein, as shown in Fig. 3.1.1, with all hexanucleotides preferentially binding to the HIV-1 RT.

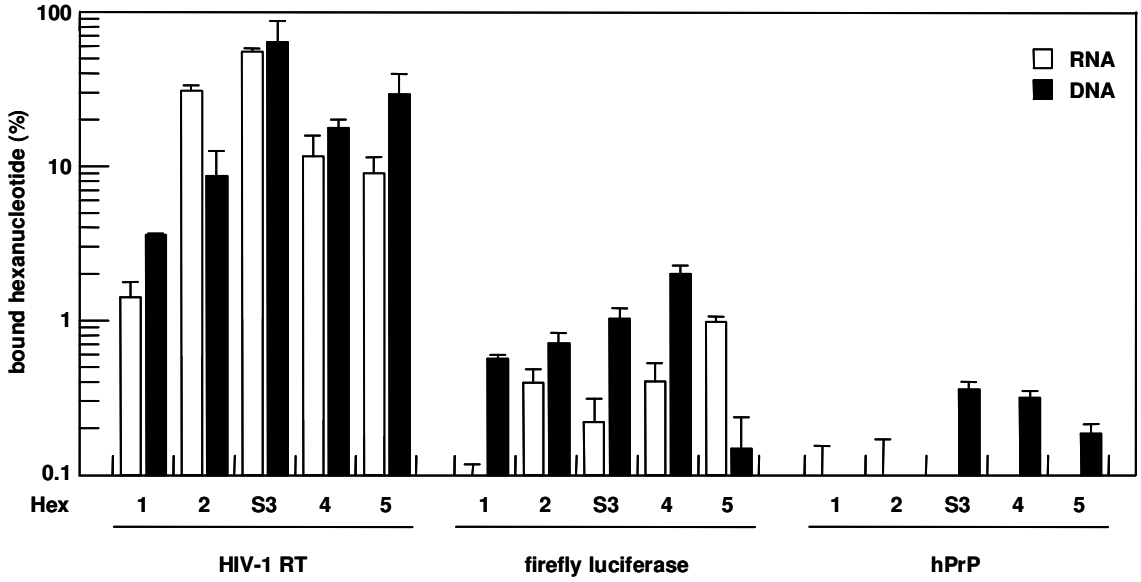

Fig. 3.1.1: Binding of hexanucleotides to target proteins. RNA or DNA hexanucleotides (1 nM) radiolabelled at their 5´-end were incubated for 2 min at 25°C with 5 µM HIV-1 RT, 5 µM firefly luciferase, or 5 µM hPrP. The assay was performed in RT binding buffer. The percentage of bound hexanucleotide was calculated based on the total amount of the input of hexanucleotide, and the values were normalised to the background level (0.05%) which was subtracted.

Taken together, these results revealed that hexanucleotides interacted with the tested proteins in a way which was specific for the nt sequence and the target protein, and that the contributions of the sugar-phosphate backbone and the functional groups of the specific bases depended on the individual interaction.

3.2 Interactions between Hex-S3 and HIV-1 RT *in vitro*

In the filter binding assay (Fig. 3.1.1), Hex-S3 showed a strong and specific binding to HIV-1 RT, therefore, this interaction was investigated in greater detail. Furthermore, HIV-1 RT presented the following advantages: (i) the 3D structure is known allowing detailed modeling studies (124;129;132), (ii) binding of high-affinity aptamers shows that, in principle, RT interacts with non-substrate like nucleic acids (92;131;164;165), (iii) in

technical terms, highly pure and active enzyme can be obtained in large amounts (175), and (iv) the availability of appropriate cell based assays for testing potential inhibitors (174).

3.2.1 Biochemical methods for studying Hex-S3-HIV-1 RT interactions

The interactions between Hex-S3 and the target protein HIV-1 RT were studied by employing a filter binding assay (164) and an EMSA (95;187). In these assays a co-incubation of Hex-S3 and RT, for 2 min at 25°C in RT binding buffer, showed the optimum results. In a filter binding assay, Hex-S3 and control hexanucleotides were incubated with HIV-1 RT. As positive controls the following sequences were included: a high-affinity RNA aptamer pseudoknot (131;163-165), a DNA aptamer RT1t49 (92). The hexanucleotide Hex-1, which proved to be a poor RT-binder in the filter binding assay (Fig. 3.1.1), was chosen as a negative control. RNA as well as DNA backbones were used in this study.

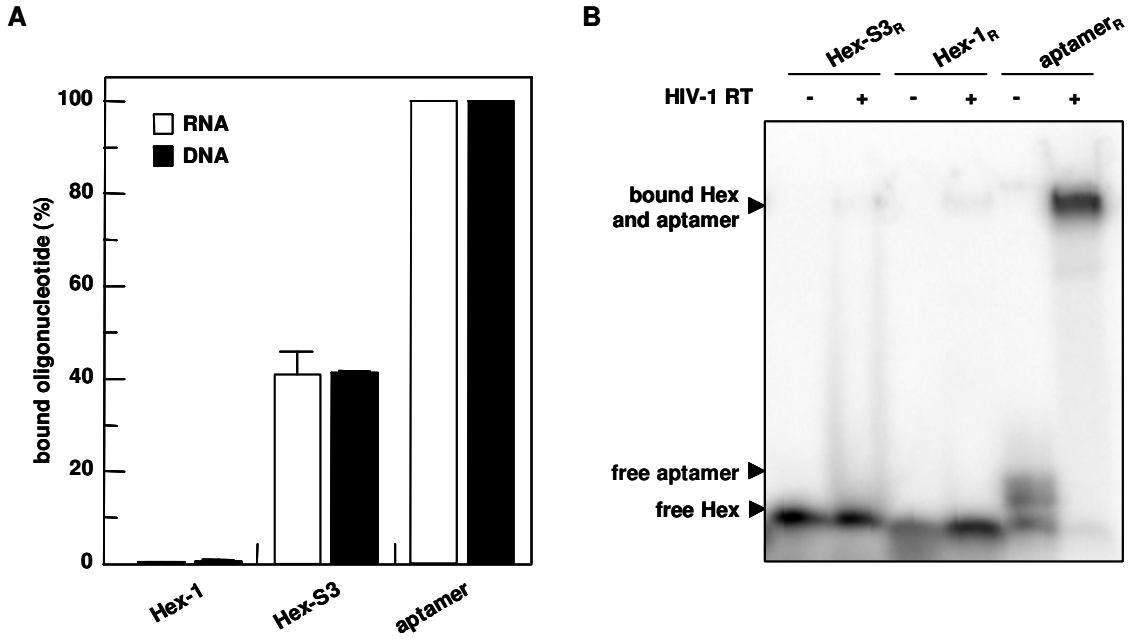

Fig. 3.2.1: Binding of hexanucleotides and controls to HIV-1 RT. (A) Relative binding of DNA and homologous RNA hexamers as well as the pseudoknot (RNA) and the RT1t49 (DNA) aptamers to RT (5 µM) determined by a filter binding assay. The percentage of bound oligonucleotide is shown relative to RT-directed aptamers (set 100%). (B) EMSA (for experimental conditions see 2.2.6.3) of radiolabelled Hex-S3$_R$ and controls (1 nM) incubated for 2 min at 25°C in the presence or absence of RT (5 µM). The binding mixtures were resolved by 5% non-denaturing PAGE. The free and the bound/shifted species are indicated.

In Fig. 3.2.1 (A) the results of the binding assay are shown. Here, no binding was seen of the negative control Hex-1, as expected. In comparison to the two RT-directed aptamers

(100% binding), only 40% of Hex-S3 bound to RT. This indicated that Hex-S3 had a lower affinity for the protein compared to the RT-directed high affinity aptamers.

The interaction between Hex-$S3_R$ and RT was further tested in an EMSA (Fig. 3.2.1 B). As negative and positive controls respectively, Hex-1_R and a RNA aptamer pseudoknot (131;164;165) were included. As shown in Fig. 3.2.1, no shift was evident when the negative control (Hex-1_R) was incubated with RT, instead a clear shift was seen in the case of the positive control ($aptamer_R$) indicating the formation of a stable complex between the RT and its high affinity ligand. The mobility of Hex-$S3_R$ was partially retarded in the presence of RT, as shown in Fig. 3.2.1 (B), and this clearly implied the formation of RT:Hex-S3 complexes, although the smearing indicated that the stability of these complexes was not sufficient to produce a clear shift as seen for the positive control. The lack of an evident retardation in Hex-S3 mobility did not render this system suitable for further studies.

3.2.2 Determination of the affinity of Hex-S3 for HIV-1 RT

The binding affinity of Hex-S3 towards RT was determined in a filter binding assay (Fig. 3.2.2). Radiolabelled Hex-$S3_R$ and Hex-$S3_D$ were titrated with increasing amounts of RT and the equilibrium affinities (K_d) were calculated from the amount of hexanucleotide (cpm) retained on the filter. For Hex-$S3_R$ and Hex-$S3_D$ K_d values of 5.3 (± 0.5) µM (Fig. 3.2.2) and 9.4 (± 2.4) µM (data not shown), respectively, were determined.

Based on the amount of radioactivity, 80% of the input of hexanucleotides was retained at the highest concentrations (20 µM protein) which indicated a saturation of the filters during the assay.

The similar affinity towards RT further supported the assumption of a highly similar binding behaviour of Hex-$S3_R$ and its homologue Hex-$S3_D$.

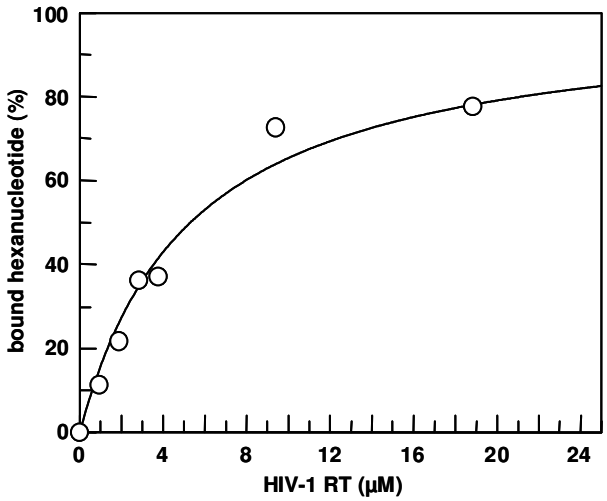

Fig. 3.2.2: Affinity of Hex-$S3_R$ for HIV-1 RT. Titration of HIV-1 RT with radiolabelled Hex-$S3_R$ (1 nM) applying a filter binding assay. Experimental data were fitted to a quadratic equation (164) using the program GraFit3 (Erithacus Software, Surrey, UK) and yielded a K_d of 5.3 (± 0.5) µM.

3.2.3 Protein-target specificity of Hex-S3

As previously shown, the binding of hexanucleotides to RT was highly specific for the nt sequence. To investigate whether Hex-S3 specifically binds to HIV-1 RT, a filter binding assay was performed in which the following proteins were compared: (i) the small subunit p51 of HIV-1 RT, (ii) HIV-2 RT which is highly homologous to the HIV-1 RT (60% aa identity plus 13% aa homology) (188), (iii) EIAV RT, (iv) T7 RNA polymerase, and (v) BSA (Fig. 3.2.3). As a negative control for Hex-S3, Hex-1_R was included. The weak or absent binding of Hex-S3 to all other control proteins proved the high specificity of this hexanucleotide for HIV-1 RT. In particular, the discrimination between the structurally and functionally closely related polymerases was remarkable. Notably, Hex-$S3_R$ and Hex-$S3_D$ showed exactly the same specificity.

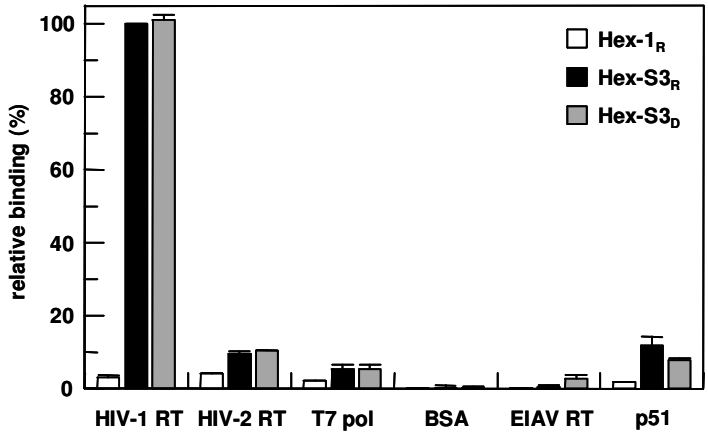

Fig. 3.2.3: Specificity of Hex-S3 for HIV-1 RT. Radiolabelled Hex-S3 and control (1 nM) were incubated for 2 min at 25°C with 5 µM protein and binding mixtures were analysed using a filter binding assay. The binding was determined relative to Hex-$S3_R$ (set 100%).

3.2.4 Importance of nucleobases, functional groups and length of Hex-S3 for binding to HIV-1 RT

The binding affinity and specificity of Hex-S3 as RNA or DNA backbone was shown to be highly comparable, indicating that the presence of the ribose rather than the deoxy-ribose, or the substitution of an uracil with a thymine in the hexameric sequence did not interfere with the binding behaviour. The importance of the nucleobases for the binding to RT was investigated by stepwise replacement of the original nt with an adenosine, which was not present in Hex-S3 (Fig. 3.2.4 A). Important contributions of the positions 3 to 6 opposed to the terminal nt at positions 1 and 2 were identified (Fig. 3.2.4 A). This showed that binding affinity and specificity required the stretch 5´-GUGU-3´ at the 3´-end of the molecule, and that the 5´-terminus was less important for the binding. Moreover, competition studies demonstrated that the phosphate group at the 5´-terminus of the hexameric sequence was not relevant for the binding to RT (data not shown).

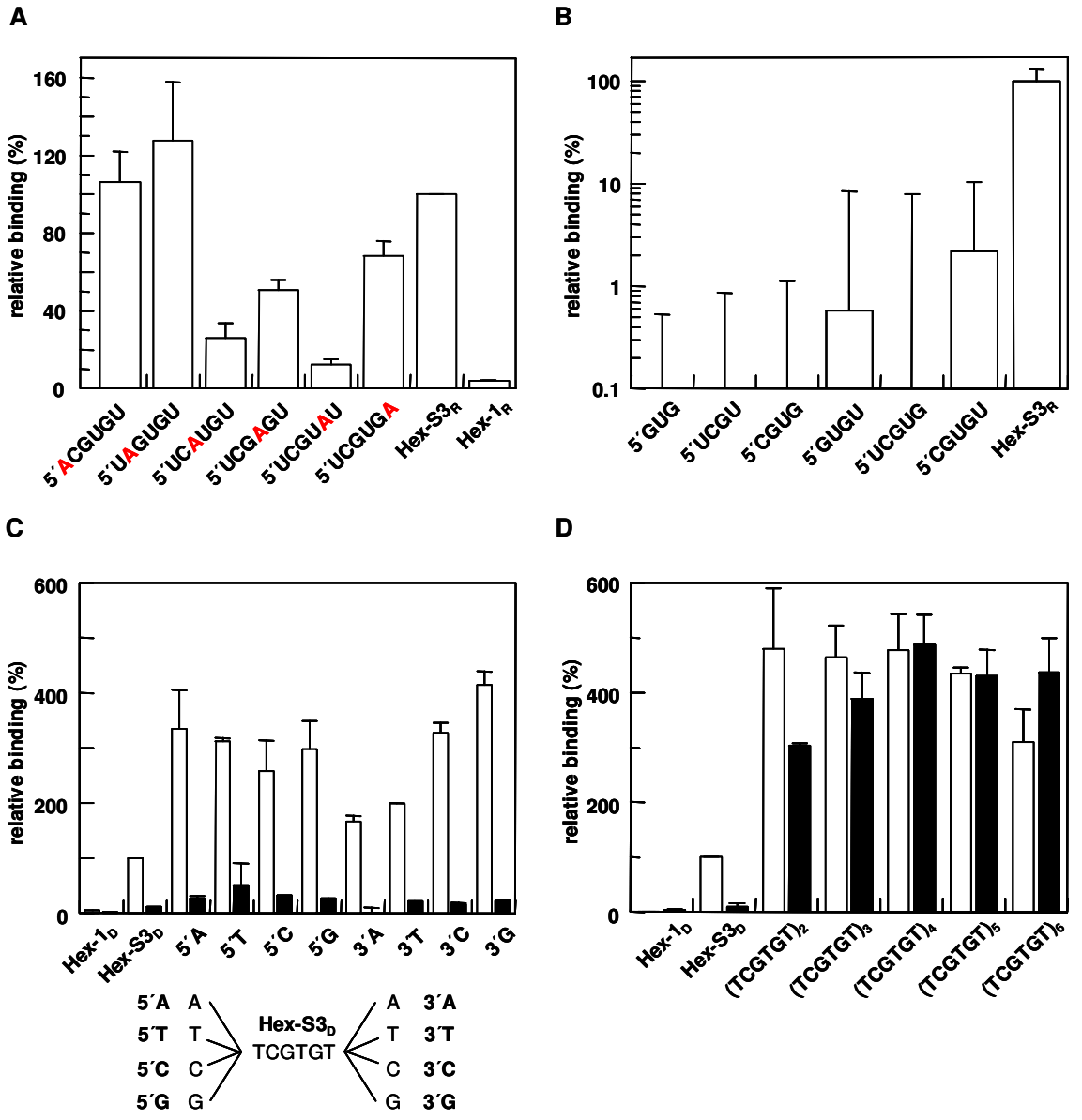

Fig. 3.2.4: Filter binding assays of positional mutants, shortened and elongated derivatives of Hex-S3 with HIV-1 RT. Radiolabelled oligonucleotides (1 nM) were incubated for 2 min at 25°C with 5 µM RT and analysed in a filter binding assay. The percentage of bound Hex-S3 was set 100%. (A) Mutational analysis of the importance of each nt position of Hex-S3$_R$ for binding to RT. An adenosine was introduced at each position replacing the original nt. Hex-1 served as a negative control. (B) Relative binding of Hex-S3$_R$-derived pentanucleotides, tetranucleotides or a trinucleotide to HIV-1 RT. (C) The relative binding of Hex-S3$_D$-derived heptanucleotides (1 nM) to 5 µM HIV-1 RT (white bars) and HIV-2 RT (back bars) was tested in a filter binding assay. Hex-1 served as negative control. The percentage of bound Hex-S3 was set 100%. (D) The relative binding of extended versions of Hex-S3$_D$ (1 nM) to 5 µM HIV-1 RT (white bars) and HIV-2 RT (black bars) was investigated using filter binding assay. Subscript numbers indicate repetitions of the Hex-S3$_D$ unit.

In order to investigate whether this was also true for the hexameric backbone, i.e. simply a phosphodiester/sugar backbone, the binding of shortened versions of Hex-S3 was tested. The shortened derivatives of Hex-S3 included two 5´- and 3´-shortened pentamers, the three tetramers and one trimer (Fig. 3.2.4 B). Under the experimental conditions used in this assay no measurable binding to RT was noticed for both Hex-S3$_R$-derived pentanucleotides and for the other shortened versions, as shown in Fig. 3.2.4 (B).

These findings suggested that a hexameric backbone was necessary for efficient binding to RT. Elongated versions of Hex-S3 were also tested for binding to RT and target specificity. All possible eight derivatives of Hex-S3 elongated by one nt at either terminus showed up to 4-fold stronger binding to RT while still being specific for the target, i.e. for HIV-1 RT *versus* HIV-2 RT (Fig. 3.2.4 C). However, extension to a 12mer or 18mer was accompanied, besides further increase in affinity, by a progressive decrease in specificity (Fig. 3.2.4 D).

3.2.5 Binding of derivatives of Hex-S3 to HIV-1 RT and HIV-2 RT

Next, the effect of specific chemical modifications of the sugar moiety and the phosphate backbone of hexanucleotides on the binding to HIV-1 RT and their target specificity was examined. The LNA, 2´-O-Me, PS and 2´-F modified hexanucleotides are known to exhibit an increased nuclease stability when compared to natural nt. Therefore, the binding of such chemically modified hexanucleotides and controls to the RT of HIV-1 and HIV-2 was tested in a filter binding assay (Table 3.2.1).

Table 3.2.1: Relative binding of chemically modified Hex-S3 and Hex-1 to HIV-1 or HIV-2 RTs

Name	HIV-1 RT	HIV-2 RT
Hex-1_D	3.0 ± 0.6	4.1 ± 0.2
Hex-$S3_D$	101 ± 1.4	10.4 ± 0.1
Hex-1_D -2´-O-Me	11.5 ± 2.1	nd[a)]
Hex-$S3_D$ -2´-O-Me	24.8 ± 1.7	nd
Hex-$S3_D$ –LNA	53.6 ± 5.6	nd
Hex-1_D –PS	256.7 ± 36.4	159.2 ± 9.0
Hex-$S3_D$ –PS	651.8 ± 121.0	307.7 ± 43.1
Hex-1_R	2.5 ± 0.6	0.0 ± 0.1
Hex-$S3_R$	100 ± 0.0	9.1 ± 2.6
Hex-1_R -2´-F	12.3 ± 1.4	12.6 ± 3.2
Hex-$S3_R$ -2´-F	140.0 ± 34.8	0.3 ± 0.0
4-thio U-Hex-$S3_R$	110.7 ± 6.2	5.0 ± 5.0

[a)] nd, not determined.

Radiolabelled hexanucleotides were incubated as described (see 2.2.6.2). The percentage of bound Hex-S3 was set 100% binding. As previously shown the 2´-OH group did not substantially contribute to binding, whereas 2´-O-Me and LNA derivatives bound to RT with lower affinity. Furthermore, a 4-thio uracil at position 4 of Hex-S3 had no effect on binding affinity and specificity. An increased affinity to RT was observed for the PS derivatives of Hex-S3 and Hex-1. However, Hex-$S3_D$-PS showed only 2.5-fold stronger binding to RT compared to Hex-1_D-PS, while the unmodified Hex-$S3_D$ showed a 34-fold

stronger binding in comparison to the unmodified Hex-1_D. Furthermore, the PS-derivatives also bound HIV-2 RT, thus a loss of specificity was observed. The 2´-F derivatives showed a binding strength and a target specificity which was comparable to the unmodified nt, indicating that the replacement of the 2´-OH group with 2´-fluoro did not have a substantial effect. Nevertheless, in comparison to the unmodified nt a lower binding to HIV-2 RT was observed for the Hex-S3-2´-F, resulting in an enhanced specificity of this hexanucleotide towards HIV-1 RT.

3.2.6 Identification of the binding site of Hex-S3 on HIV-1 RT

In order to locate the binding site on HIV-1 RT, a 4-thio uracil derivative of Hex-$S3_R$ (4-thio uracil at position 4), which proved to bind with the same affinity as the unmodified Hex-$S3_R$ (Table 3.2.1), was crosslinked by UV-treatment to HIV-1 RT. This experiment showed that only the large subunit p66 was crosslinked (Fig. 3.2.5 A).

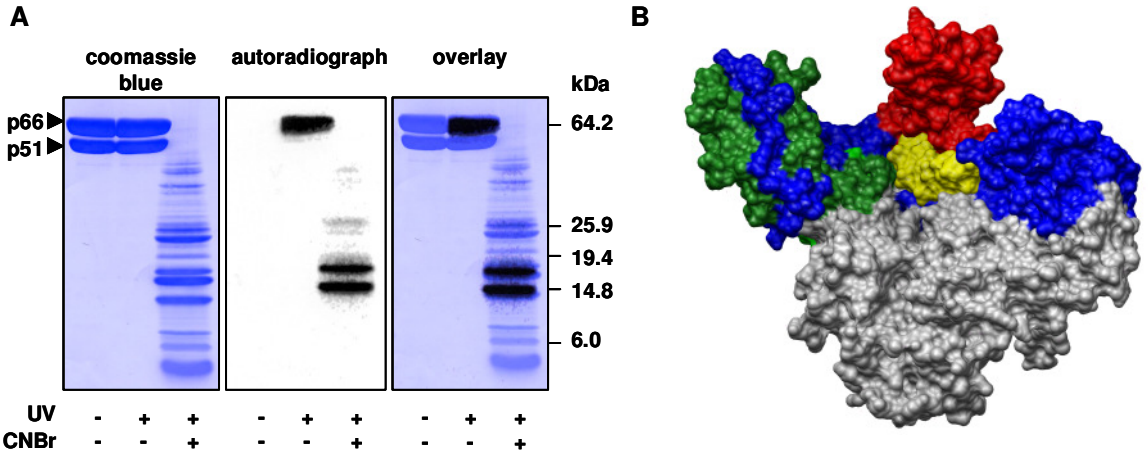

Fig. 3.2.5: Site-specific binding of Hex-S3 to RT determined by UV-crosslinking and CNBr cleavage. (A) The UV-crosslinking was performed as described in detail in 2.2.7. Samples were separated by 10-20% linear gradient SDS-PAGE. Left panel, Coomassie blue-stained gel; middle panel, autoradiograph; right panel, overlay. After crosslinking, samples were subjected to CNBr cleavage. (B) 3D model of the binding site of RT for Hex-S3 based on docking studies and the constraints explained in 2.2.9. Color code: yellow, Hex-S3; green, CNBr fragment (aa 42-183); red, CNBr fragment (aa 231-356); blue, remaining portions of the large subunit p66; grey, small subunit p51.

The following CNBr treatment and the separation of the resulting fragments by SDS-PAGE led to the identification of about 25 peptides having a molecular weight between 1.7 and 50 kDa. Considering the mechanism of the CNBr cleavage, in theory, only eight fragments of 1.7, 2.4, 2.9, 5.6, 8.63, 14.1, 14.7 and 23.07 kDa in size were expected after CNBr treatment of HIV-1 RT. The larger number of fragments obtained probably resulted from an incomplete cleavage of the protein. Among these fragments, only two were radiolabelled, namely a fragment of 14.7 kDa and a fragment of 16.5 kDa,

which was derived from the incomplete separation of the fragments 14.1 kDa and 2.4 kDa. These two peptides were isolated from the gel and their N-terminal amino acid sequence determined. One fragment (aa 42-183, indicated by green color in Fig. 3.2.5 B) carried approximately one third and the second fragment (aa 231-356, indicated by red color in Fig. 3.2.5 B) about two thirds of the label (Fig. 3.2.5 A).

Further information on the binding site of Hex-S3 was derived from competition experiments with a 18/36mer Flo1/Flo6 p/t (186), a RNA aptamer (131;163;164), as well as the non-nucleoside inhibitor S-TIBO (189). TIBO has been shown to stabilise an open conformation of RT, i.e. rotation of the p66 thumb domain of about 30-40° generating a large nucleic acid binding site (126;136), whereas the RNA aptamer induces a closed conformation. These competition studies showed that S-TIBO increased the binding strength of the hexanucleotide towards RT (Fig. 3.2.6 A) no matter if it was added prior to or after the incubation of Hex-$S3_R$ with the protein. These results showed that Hex-S3 had a higher affinity to RT when the enzyme had an open conformation. The p/t and aptamer competed for hexanucleotide binding but not vice versa (Fig. 3.2.6 A and B).

In this case no difference was seen after the addition of the competitors p/t and aptamer prior to or after the incubation of the radiolabelled hexanucleotide with RT. Increasing amounts of Hex-$S3_R$ did not compete with the radiolabelled p/t for binding to RT (Fig. 3.2.6 B). Rigid-body docking studies of HIV-1 RT and Hex-S3 based on the experimentally derived constraints were performed by T. Restle (Fig. 3.2.5 B, 3.2.6 C and D). According to the model derived thereof, Hex-S3 bound the p66 subunit at the bottom of the thumb domain pointing towards the nucleic acid binding cleft of the viral polymerase. Binding of this hexanucleotide ligand required the thumb domain to be in an upright position.

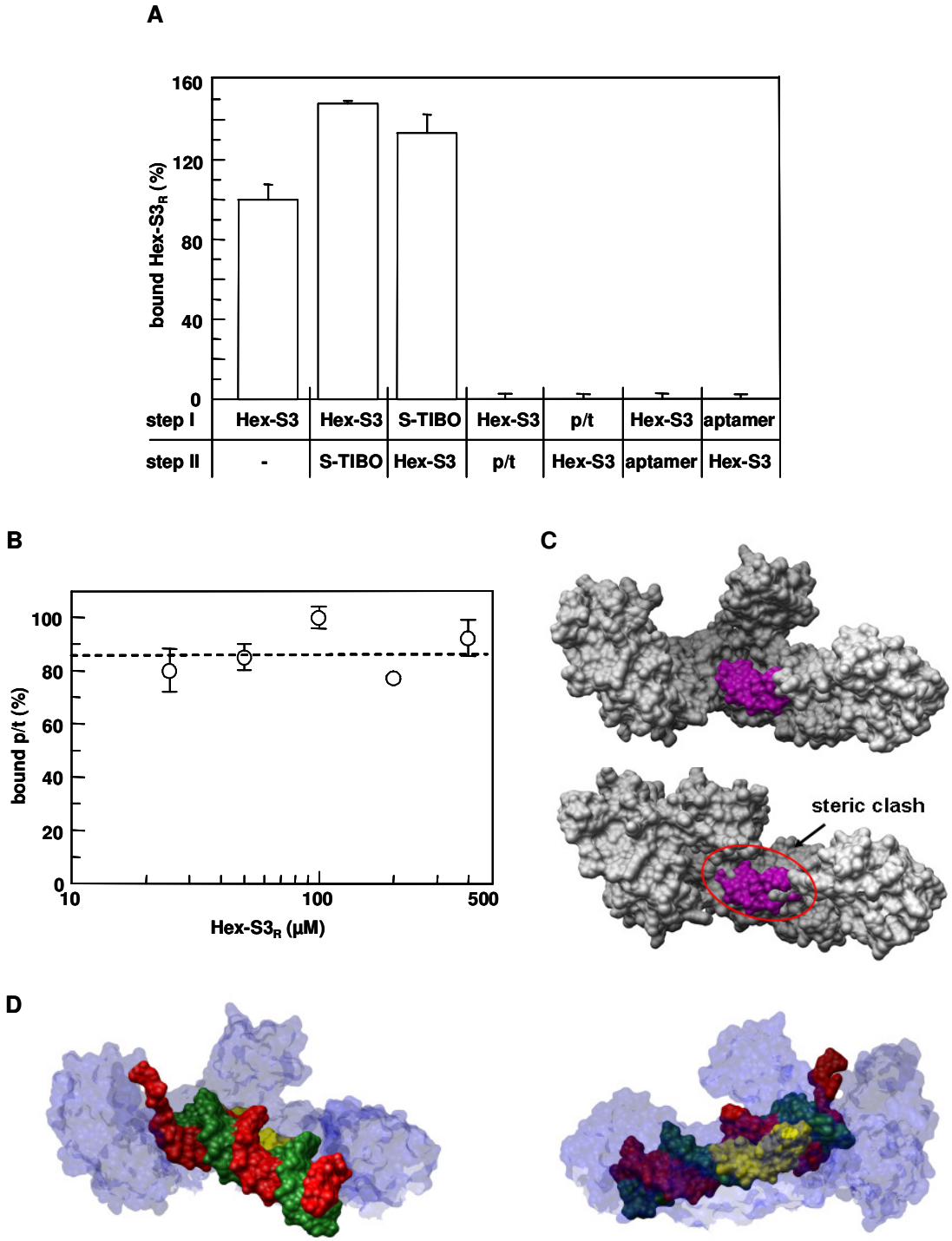

Fig. 3.2.6: Competition study and structure of the p66 subunit of HIV-1 RT complexed with Hex-S3. (A) The competition of Hex-$S3_R$ with S-TIBO, p/t and aptamer pseudoknot for the binding to RT was determined by a filter binding assay. Radiolabelled Hex-$S3_R$ (1 nM) was incubated for 2 min at 25°C with 5 µM RT in the presence or absence of 20 µM S-TIBO, 20 µM p/t or 20 µM aptamer. The competitors were added prior to or after the incubation of Hex S3 with RT. The percentage of bound hexanucleotides was determined and normalised to the amount of input of hexanucleotide. (B) Radiolabelled p/t (1 nM) was incubated with RT (5 µM) in the presence of an increasing amount of Hex-$S3_R$. (C) Surface rendering of p66 showing Hex-S3 complexed with the enzyme in an open conformation (PDB: 1RTH, top panel) or close conformation (PBD: 1HMV and 1HVU, bottom panel). Color code: magenta, Hex-S3 and gray, p66 subunit. (D) Surface rendering of p66 complexed with a DNA/DNA p/t substrate (1RTD) and Hex-S3; front view (left panel) and back view (right panel). Color code: yellow, Hex-S3; green and red, p/t substrate; blue, large subunit p66 of HIV-1 RT. Modelling studies performed as described in 2.2.9.

3.3 Use of Hex-S3 as HIV-1 inhibitor in human cells

The low cellular uptake and rapid degradation in physiological fluids are the two main factors which limit the application of nucleic acid-based drugs (190;191). Due to their small size hexanucleotides may be less prone to enzymatic degradation. Furthermore, they may be more readily taken up by cells in comparison to longer nucleic acids (> 20 nt). Several experiments were thus performed to investigate their resistance against endo- and exonucleases and their cellular internalisation. Moreover, Hex-$S3_R$ which showed a high specific binding to HIV-1 RT was tested in human cells by using a recombinant replication-incompetent proviral HIV-1 construct (174).

3.3.1 Determination of the stability of unmodified hexanucleotides

In order to determine whether hexanucleotides may be less prone to enzymatic degradation in comparison to longer nucleic acids (> 20 nt) and may be suited to the *in vitro* application, e.g. as inhibitors using a replication-incompetent HIV-1-based system, and to the *in vivo* application, the intracellular stability and the stability in fetal calf serum and cell culture media were tested.

3.3.1.1 Stability in fetal calf serum and cell culture media

The serum stability of hexanucleotides with an unmodified phosphodiester backbone was determined and compared to longer nucleic acids (24mer). The longer oligonucleotides consisted of tetrameric repeats of hexameric sequences in order to exclude sequence-specific influences on the nuclease resistance. Radiolabelled RNA and DNA hexanucleotides or Hex-S3-derived 24mers were incubated in standard binding buffer containing 1% (v/v) FCS at 37°C. The fraction of uncleaved oligonucleotides plotted over time is shown in Fig. 3.3.1 (A). The unmodified hexamers showed an increased nuclease resistance when compared with 24mers, which was particularly true for the RNA. The half-life times ($t_{1/2}$) of Hex-$S3_R$, $(\text{Hex-S3}_R)_4$, Hex-$S3_D$, $(\text{Hex-S3}_D)_4$ were 1.2 (± 0.2) min, 0.1 (± 0.1) min, 3.4 (± 0.3) min and 2.5 (± 0.2) min, respectively. Thus, the Hex-$S3_D$ was the most resistant one (15-fold) whereas the $t_{1/2}$ of Hex-$S3_R$ was increased 6-fold in comparison to the 24mer. Despite the higher resistance of the hexanucleotides compared to the longer oligonucleotides to nuclease degradation, their $t_{1/2}$ was in the order of a few minutes which was not sufficient for their application *in vivo*. However, for the *in vitro* application of hexanucleotides, the stability in serum was not relevant since human cells could be incubated and treated with inhibitors in customised culture media which do not

contain serum. Therefore, the stability of Hex-S3 and of a chemically modified 2´-F derivative in cell culture media was tested (Fig. 3.3.1 B).

The 2´-F derivative of Hex-S3 showed a binding strength and a target specificity which was comparable to the unmodified ones (Table 3.2.1), thus combining the advantages of an increased nuclease resistance with a chemical modification that did not affect binding behaviour. In this assay, radiolabelled hexanucleotides (10 nM) were incubated at 37°C in cell culture media (DMEM, RPMI 1640, 199 medium) and the samples collected after different time points were analysed by PAGE. In all tested media both unmodified and 2´-F modified hexanucleotides were stable during the incubation time (Fig. 3.3.1 B). Consequently they could be applied *in vitro* without loss of activity.

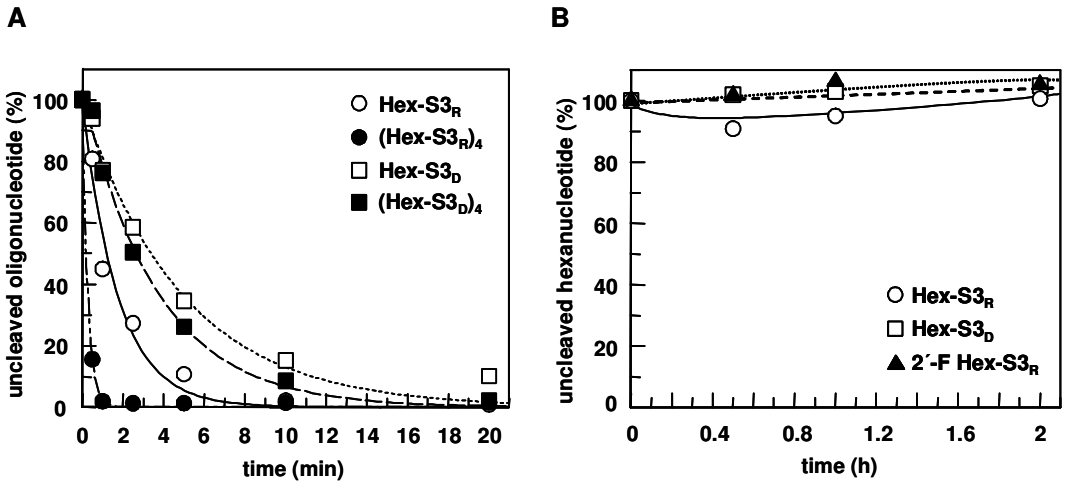

Fig. 3.3.1: Stability of hexa- and oligonucleotides in FCS or cell culture media. (A) Hex-$S3_R$ or Hex-$S3_D$ were compared to the respective derivatives, $(Hex\text{-}S3_R)_4$ and $(Hex\text{-}S3_D)_4$, for their resistance to nucleases in FCS. Radiolabelled oligonucleotides (10 nM) were incubated with 1% (v/v) FCS at 37°C. Reactions were stopped at intervals (0, 0.5, 1, 2.5, 5, 10 and 20 min) and samples were separated by 20% denaturing PAGE. In the graph, the fraction of uncleaved oligonucleotides was plotted as a function of time. (B) Unmodified Hex-S3 and the 2´-F Hex-$S3_R$ derivative were tested for nuclease resistance in 199 cell culture medium. Samples were collected after 0, 0.5, 1 or 2 h from the beginning of the incubation and resolved by 20% denaturing PAGE. In the graph, the fraction of uncleaved hexanucleotides was plotted as a function of time.

3.3.1.2 Intracellular stability

The intracellular stability of the hexanucleotides and thus their biological availability as inhibitors were determined after calcium phosphate-mediated transfection of HEK293T cells with fluorescently labelled hexanucleotides. The degradation of internalised Hex-$S3_R$ (6-FAM label at the 5´-end, 5´-6-FAM) (Fig. 3.3.2) was determined by fluorescence measurement of the band corresponding to the undegraded hexanucleotide (6mer). The amount of Hex-$S3_R$ at time 0 after the transfection was set to 100%. After 1 h, 70% on the internalised hexanucleotide was degraded. After 2, 4, 6 and 24 h, the amounts of intact Hex-$S3_R$ in the cells were 14, 3, 3 and 2%, respectively. The pattern of the degradation

products clearly indicated a degradation process rather than a loss of the fluorescent label. Since 5´-FAM-6 Hex-1_R and 3´-Cy5 Hex-$S3_R$ showed an intracellular stability identical to the 5´-6-FAM Hex-$S3_R$ the degradation process was independent of the hexanucleotide sequence and of the position or chemical nature of the fluorescent label (data not shown). The amount of hexanucleotide internalised at time 0 min after transfection was determined to be about 2.5 x 10^5 (100%) molecules per cell, thus, after 24 h about 5 x 10^3 (2%) molecules were still present in each cell. Despite the fact that the hexanucleotides were subjected to a rapid intracellular degradation, these results showed that a considerable number of hexameric molecules was still bioavailable even after a long time of incubation.

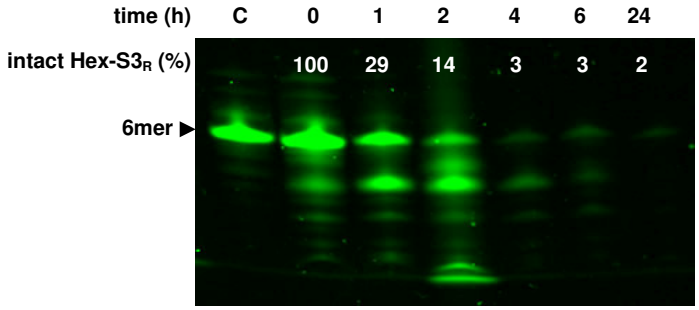

Fig. 3.3.2: Intracellular stability of Hex-$S3_R$. HEK293T cells (2.0 x 10^5 cells) were transfected, by calcium phosphate-mediated transfection, with 8 µM Hex in a 500 µl final volume. After transfection, the cells were washed and collected by centrifugation (2,000 x g, 3 min) at different time points (0, 1, 2, 4, 6 and 24 h). The cell pellets were lysed by resuspension in SideStep lysis and stabilisation buffer which protects RNA from degradation. The samples were resolved by 20% denaturing PAGE and the gels were scanned by a Typhoon 8600 scanner. The amount of Hex-$S3_R$ at time 0 h after transfection was set to 100%. ´C´, control 5´-FAM-6 Hex-$S3_R$ not applied to the cells.

3.3.2 Cellular uptake of naked hexa- and oligonucleotides

One of the major obstacles in developing nucleic acid-based drugs is their delivery across the cell membrane to the cytoplasm where they can act. Naked nucleic acids are known to penetrate the cell membrane inefficiently, with only a few molecules gaining entry in to the cell (192). These data were obtained for oligonucleotides longer than 20 nt. Therefore, small molecules, such as hexanucleotides, may show an enhanced cellular delivery compared to longer nucleic acids. Thus, the cellular uptake of hexanucleotide was compared to longer oligonucleotides. In this assay the BJA-B cell line was used since it is able to take up nucleic acids readily from the extracellular milieu (33). Unmodified phosphodiester backbone Hex-S3 RNA or DNA and Hex-S3-derived oligonucleotides (24mer) were compared. RNA and DNA hexanucleotides or Hex-S3-derived 24mers were radiolabelled and applied to the cells. After incubation for 30 min at 37°C in FCS-free medium (Opti-MEM I), the cells were washed for 30 min at 37°C with 1% (v/v) FCS to ascertain the degradation of oligonucleotides adherent to the outer

surface of the cell membrane. Thus false positive signals were avoided allowing the quantification of internalised oligonucleotides by PAGE (Fig. 3.3.3). No uptake of hexanucleotides was apparent, whereas for the Hex-S3-derived 24mers a small band was visible, indicating an enhanced uptake of longer oligonucleotides by BJA-B cells in comparison to hexanucleotides. These findings showed that only longer oligonucleotides were readily taken up by the cells, but no spontaneous internalisation of hexanucleotides was observed. Therefore, the mechanism of cell entry employed by the longer oligonucleotides is not available for the shorter ones.

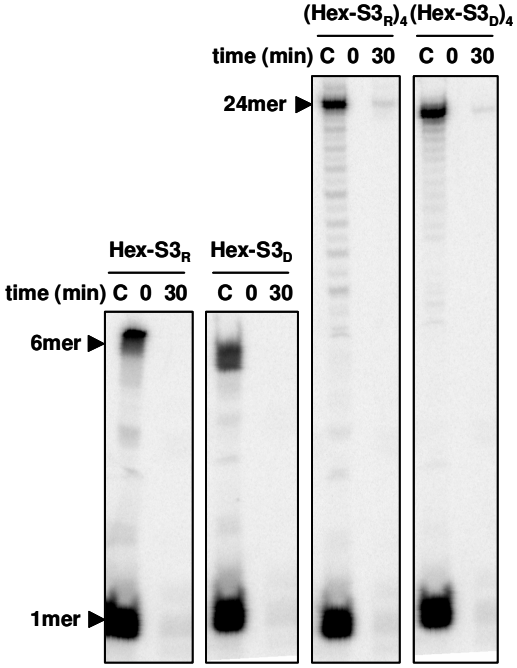

Fig. 3.3.3: Uptake of naked hexa- and oligonucleotides. BJA-B cells (6.0×10^5 cells) were incubated in 500 µl Opti-MEM I medium containing 1 nM 5´-end radiolabelled Hex-S3 RNA or DNA and respective Hex-S3-derived 24mers [$(Hex\text{-}S3_R)_4$ and $(Hex\text{-}S3_D)_4$]. After 0 or 30 min of incubation, the cells were washed with 1x PBS_b and incubated for 30 min at 37°C with Opti-MEM I containing 1% (v/v) FCS. Cells were lysed by the resuspension in SideStep lysis and stabilisation buffer which protects RNA and DNA from degradation. Samples were resolved by 20% denaturing PAGE. ´C´, control $Hex\text{-}S3_R$, $Hex\text{-}S3_D$, $(Hex\text{-}S3_R)_4$ or $(Hex\text{-}S3_D)_4$ not applied to the cells.

3.3.3 Biological activity of Hex-S3 in a self-inactivating HIV-1 system

In order to investigate whether Hex-S3 was able to exert biological effects, i.e. to interfere with the production of HIV-1 viral particles and their infectivity in human cells in a negative way, a recombinant replication-incompetent proviral HIV-1 construct [pGJ3-luci, (174)] was used. This system is based on a replication-defective HIV-1 viral vector which contains a defective HIV-1 genome in which the envelope (*env*) and most of the regulatory and accessory genes of HIV-1 were removed and which, instead, contains the firefly luciferase as a marker gene (Fig. 3.3.4 A). The cells were co-transfected together with the pczVSV-G vector which encoded for the vesicular stomatitis virus G glycoprotein (VSV-G) (Fig. 3.3.4 A). Pseudoviruses produced by the transfected cells contains the rudimentary HIV-1 RNA genome with the marker gene, RT and PR proteins surrounded by CA and MA proteins from HIV-1. The viral envelope was a VSV-G-containing membrane.

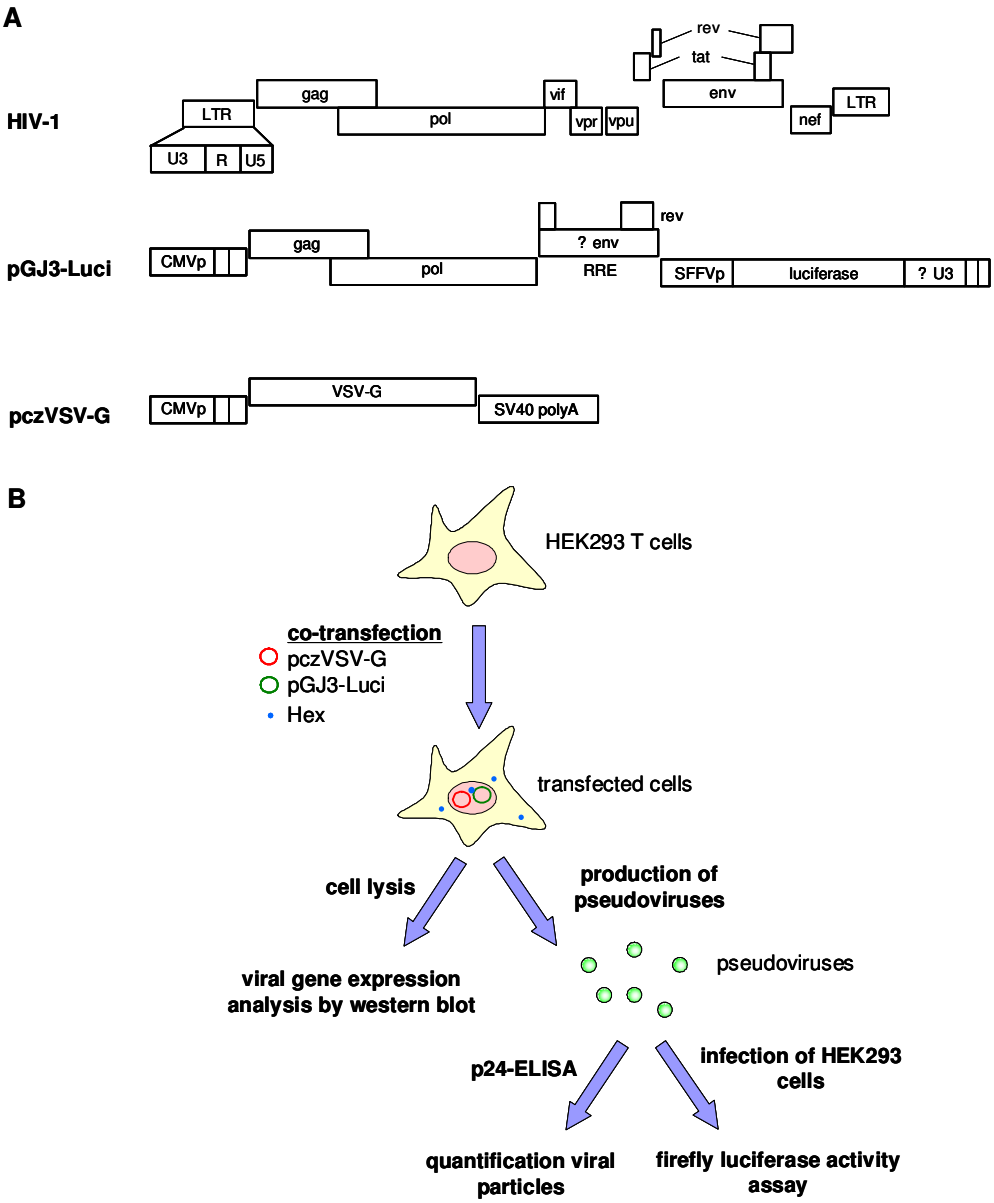

Fig. 3.3.4: Replication-defective HIV-1 viral vector system. (A) Genome organisation of HIV-1 and schematic drawings of the two plasmid constructs used in the assays. The vector pGJ3-luci encodes a defective HIV-1 genome and contains the firefly luciferase as a marker gene, the pczVSV-G vector encodes for the vesicular stomatitis virus G glycoprotein (VSV-G). (B) Schematic representation of the assay. HEK293T cells were co-transfected with the two vectors (pGJ3-luci and pczVSV-G) and hexanucleotides. The viral gene expression was analysed by western blotting of the packaging cell lysates. The pseudoviruses produced by the packaging cells were quantified by p24-ELISA and used to infect HEK293 cells. Their infectivity was determined by measurement of the firefly luciferase activity.

The viral particles represent infectious, replication-incompetent derivatives of HIV-1 capable of a single round of infection. Packaging HEK293T cells were co-transfected with the luciferase-harbouring defective HIV-1 genome and the plasmid-encoded packaging functions, which led to the release of infectious recombinant particles that were subsequently used to infect recipient cells in which the luciferase gene expression was determined to monitor infectivity (Fig. 3.3.4 B). The viral gene expression pattern was

analysed in ´packaging cells´ as described (see 3.3.3.2). The quantity of pseudoviruses released from the transfected cells was monitored by a p24-specific ELISA.

3.3.3.1 Effect of Hex-S3 on viral particles infectivity

The effect of Hex-S3 on the infectivity was tested in the replication-defective HIV-1 viral vector system described above (see 3.3.3). The cells were co-transfected with the two vectors and increasing amounts of hexanucleotides. The pseudoviruses produced were used to infect recipient cells and the infectivity was monitored by the activity of the firefly luciferase and the results are shown in Fig. 3.3.5 (A) (the initial experiment was performed by Sandra D. Laufer) (193). Increasing amounts of Hex-$S3_R$ were related to a strong, concentration-dependent decrease of firefly luciferase activity in infected HEK293 cells, but not in case of the control Hex-1_R. The half-maximal inhibitory concentration (IC_{50}) value for Hex-$S3_R$ was calculated by GraFit5 (Erithacus Software, Surrey, UK) and determined to be 1.8 (± 0.2) µM.

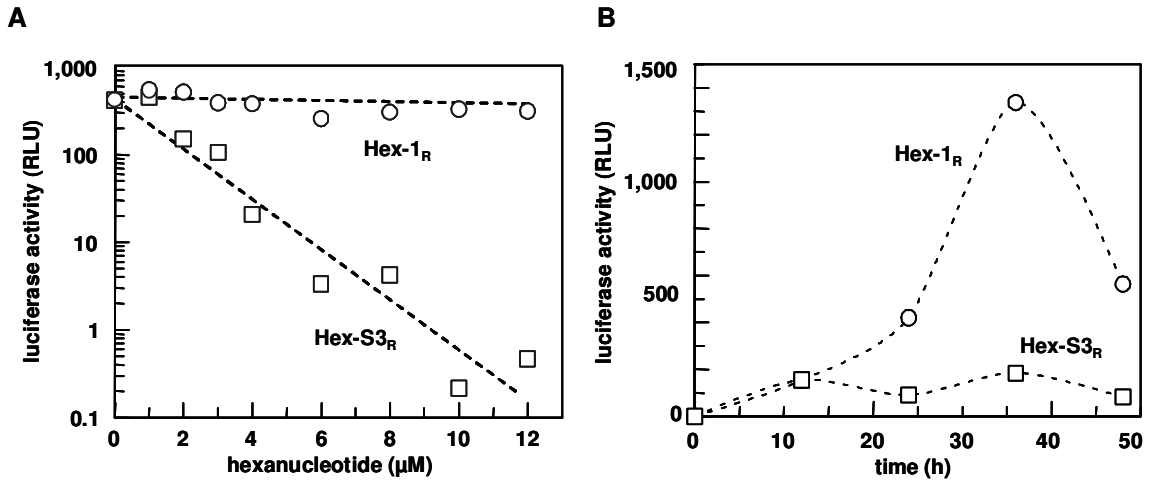

Fig. 3.3.5: Biological activity of Hex-$S3_R$ in a self-inactivating HIV-1 system (193)**.** (A) Packaging HEK293T cells were co-transfected with Hex-$S3_R$ (□) or Hex-1_R (○), with a luciferase-harbouring defective HIV-1 genome and with plasmid-encoded packaging functions. Released infectious recombinant particles after 48 h were used in a consecutive step to infect recipient cells. The hexanucleotides were co-transfected in the first step at increasing concentrations and the luciferase activity was measured after the infection of HEK293T cells. The data were normalised to the number of viable cells. (B) Supernatants of packaging cells transfected with 12 µM Hex-$S3_R$ (□) or Hex-1_R (○) were collected at different time points (0, 10, 24, 36 and 48 h) and used to infect HEK293 cells. The infectivity was monitored by the luciferase activity and values were normalised to the number of viable cells.

In order to follow the effect of Hex-S3 on viral particles infectivity over the course of 48 h after transfection, a time-course experiment was performed. Cells were transfected with 12 µM Hex-$S3_R$ or Hex-1_R, a dose which has been proved for Hex-$S3_R$ to inhibit luciferase activity up to 1,000-fold in comparison to the control Hex-1_R. The supernatants from the packaging cells were collected at different time points and used to infect recipient cells.

The infectivity of viral particles was time-dependent as shown in Fig. 3.3.5 (B), and reached a maximum level in 36 h after transfection. Pseudoviruses produced by cells which were treated with Hex-$S3_R$, showed a persistent low level of luciferase activity, indicating a constant and long-term influence of Hex-S3 on the infectivity of viral particles.

Regarding an assessment of the particular step of the viral life cycle that could be affected by Hex-$S3_R$, a number of additional experiments were performed with the following results: the co-transfection of hexanucleotides together with packaging functions of HIV-1 using the single-round replication systems described, yielded a reduced amount of viral particles released from transfected cells, as monitored by a p24-specific ELISA, when Hex-$S3_R$ was used *versus* a control hexamer (Hex-1_R), as shown in Fig. 3.3.6 (white bars). Moreover, the infectivity of these viral particles was investigated in an infectivity assay, and the activity of the firefly luciferase for both hexanucleotides, as shown in Fig. 3.3.6 (black bars), was comparable to their relative amount, determined by p24-ELISA.

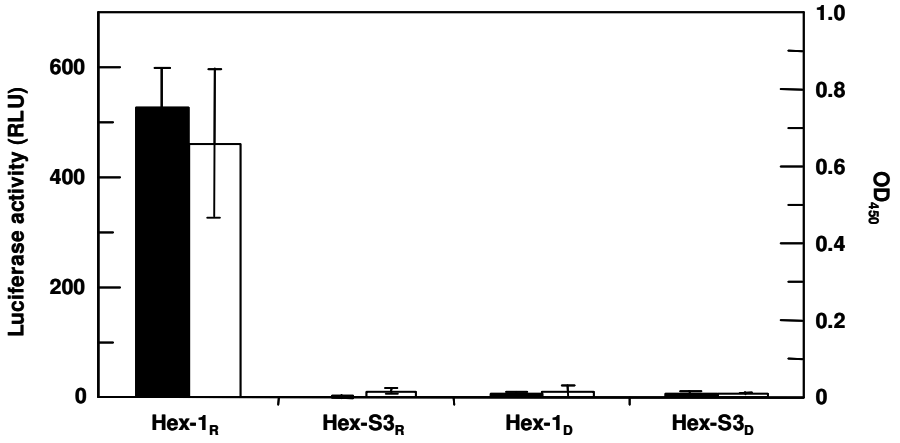

Fig. 3.3.6: Comparison of viral particles infectivity *versus* viral particles amount. The cell supernatants from packaging cells treated with Hex-S3 as RNA or DNA and Hex-1 as RNA or DNA were used in an infection assay, and the infectivity was monitored by the luciferase activity (black bars). They were also tested in a p24-ELISA assay to determine the amount of p24, (amount of viral particles) in the cell supernatants (white bars). The p24 amount was monitored by the optical density value measured at 450 nm (OD_{450}), obtained after the colorimetric reaction described in detail in 2.2.6.1.

In spite of this, when equal amounts of p24 antigen, corresponding to an equal number of viral particles (produced in the presence of Hex-$S3_R$ or a control hexanucleotide) were subsequently applied to infect HEK293T cells, there was no difference to the observed reporter gene activity (data not shown). This strongly suggested that the Hex-S3-specific inhibitory step occurred in packaging cells rather than during the second round of infection. Additionally, Hex-$S3_D$ and negative control Hex-1_D were tested in this system, the infectivity and the amount of the viral particles released by transfected cells were strongly reduced in both cases. The transfection efficiency of the two vectors was unaffected by the addition of either DNA or RNA hexanucleotides, suggesting a

sequence-unspecific involvement of the DNA hexanucleotides in a step which affects the production of viral particles and their release.

3.3.3.2 Effect of Hex-S3 on viral gene expression

The Hex-S3-specific inhibitory effect of Hex-S3$_R$ on the production of viral particles and their release was further investigated by an analysis of the viral gene expression in the packaging cells. This was achieved by western blotting using a goat polyclonal Ab directed against HIV-1 viral components and a rabbit polyclonal Ab specific for the p24 protein (CA) and for the Gag precursor (194;195).

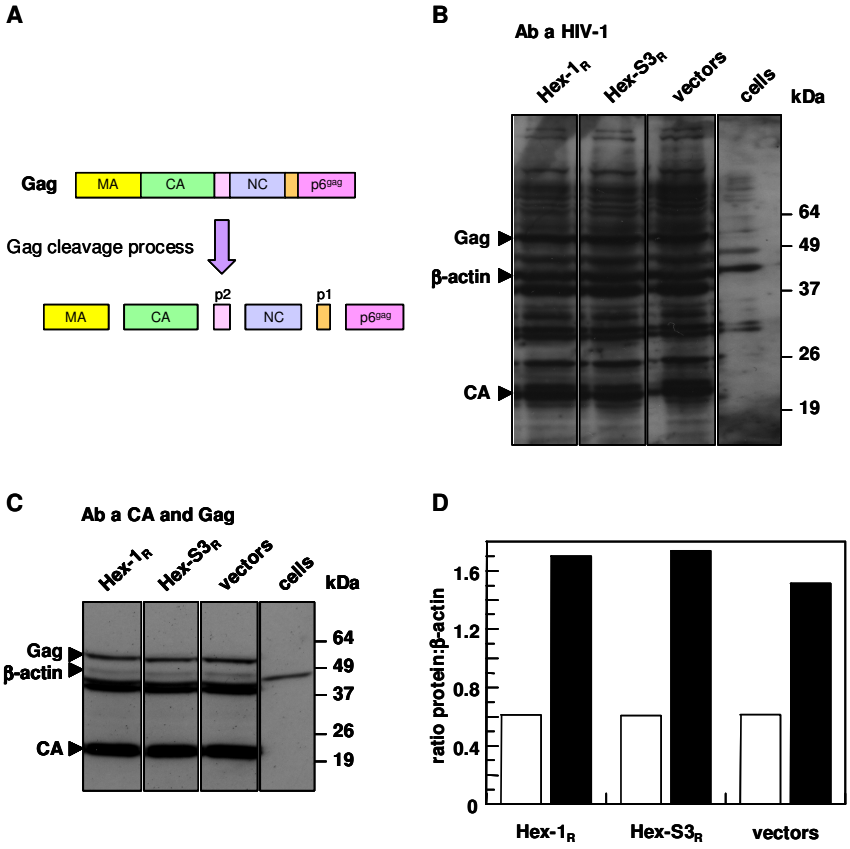

Fig. 3.3.7: Effect of Hex-S3$_R$ on viral gene expression and Gag processing. (A) The schematic drawing of the Gag precursor (55 kDa) and of its processing into the CA, MA, p2, NC, p1 and p6^{gag} viral proteins. (B) The detection of HIV-1 proteins in packaging cell lysates by western blotting by using a polyclonal Ab directed against the whole HIV-1 viral components. The lines ´Hex-1$_R$´, ´Hex-S3$_R$´, ´vectors´ and ´cells´ indicate cell lysates from packaging cells treated with 12 µM Hex-1$_R$, 12 µM Hex-S3$_R$, only vectors or non-transfected cells, respectively. Samples were resolved by a 12% SDS-PAGE. The secondary Ab used in this assay was conjugated to the HRP, and the development of the signals was performed by using the ECL system. The β-actin was used as a loading control. (C) The same samples were resolved by a 15% SDS-PAGE, and a western blotting was performed by using a polyclonal Ab specific for the CA and the Gag viral proteins. Proteins were detected after incubation with a HRP-conjugated secondary Ab. The β-actin was used as a control. (D) Quantification of western blot bands in figure C and determination of the ratio between Gag and β-actin (white bars) or CA and β-actin (black bars).

The specificity of the first Ab towards all HIV-1 proteins allowed the direct comparison of the viral protein synthesis among differently treated packaging cells. The second Ab, which was specific for the CA and Gag proteins, was used to investigate the processing of Gag precursor as shown in Fig. 3.3.7 (A).

The Gag precursor is a polyprotein with a molecular mass of about 55 kDa, which undergoes to cleavage at specific sites by the viral PR to produce the CA (24 kDa), the MA, the NC and other viral proteins. Briefly, HEK293T cells were transfected with the described vectors encoding the viral proteins and 12 µM Hex-$S3_R$ or Hex-1_R. The cells were collected and lysed 48 h after the transfection. The lysates were analysed by western blotting using the antiserum against HIV-1 (Fig. 3.3.7 B) or the antiserum directed against CA/Gag proteins (Fig. 3.3.7 C). The pattern and the intensity of bands obtained from the cells treated with Hex-$S3_R$ or Hex-1_R or only vectors were identical, which indicated that Hex-$S3_R$ did not affect viral protein expression (Fig. 3.3.7 B and C). To test the effect of Hex-$S3_R$ on Gag precursor processing, the amount of CA and Gag proteins was determined and normalised to β-actin, loading control (Fig. 3.3.7 D). The ratio between CA and Gag proteins was the same in all samples, without an evident accumulation of Gag precursor, which showed that Hex-$S3_R$ had no influence on the processing of the precursor.

3.4 Effect of Hex-S3 on HIV-1 RT enzymatic activities and functions

Based on the experimental results which showed that Hex-S3 was able to reduce HIV-1 infectivity and bound with a low micromolar affinity to HIV-1 RT, enzymatic assays were performed to elucidate whether Hex-$S3_R$ was an inhibitor of enzymatic activity and functions of HIV-1 RT. Therefore, standard RT assays were performed in the presence or absence of Hex-$S3_R$ and using Hex-1_R as a negative control. Some of these biochemical assays imitated distinct steps of the viral genome replication (Fig. 1.7.2 B), like the RDDP, the DDDP and the RNase H assays. Others were based on the intrinsic properties of RT, namely the RT processivity and fidelity. All assays were performed at 25°C, the optimum temperature for the binding of Hex-$S3_R$ to the RT (see 3.2.1), or at physiological temperature, 37°C. In each experiment, the RT was preincubated for 2 min at 25°C in the absence or presence of Hex-$S3_R$ or Hex-1_R to allow the binding of the hexanucleotides to the protein and consequent formation of RT:Hex_R complexes.

3.4.1 The RDDP assay

The effect on the RDDP enzymatic activity of RT by Hex-S3$_R$ was tested in a standard RT assay using poly(rA)/oligo(dT)$_{12-18}$ as p/t (Fig. 3.4.1 A). The RT was preincubated in the absence or presence of Hex$_R$ and the reaction was started by addition of p/t, [^{3}H]-dTTP and unlabelled dTTP to the binding mixture. The assay was performed at 25°C or at 37°C and the reaction time was 10 min. The activity of RT alone or preincubated with Hex-S3$_R$ or Hex-1$_R$ was determined by monitoring the incorporation of [^{3}H]-dTTP into the growing chain (Fig. 3.4.1 B). Hex-S3$_R$ did not affect the RDDP activity of RT, since the amount of incorporated [^{3}H]-dTMP was comparable to the one obtained with RT alone (control) or incubated with Hex-1$_R$.

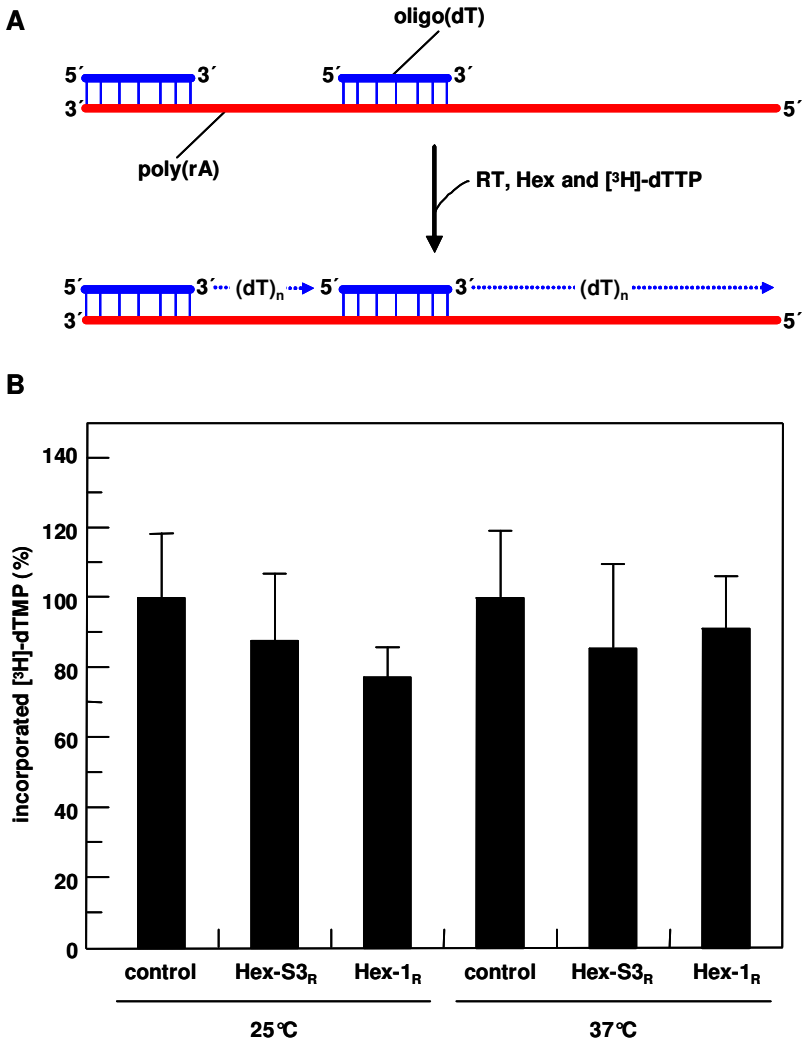

Fig. 3.4.1: RDDP activity of RT in the presence of Hex-S3$_R$. (A) Schematic depiction of the RDDP assay. Poly(rA) template is in red and the oligo(dT) primers in blue. (B) The assay was performed at 25°C and 37°C and the RT activity was determined by the quantification of incorporated [^{3}H]-dTMP in percentage. In the ´control´ experiment, RT alone (325 nm) was incubated with the p/t (0.2 OD$_{260}$/ml) and the values were set 100%. In ´Hex-S3$_R$´ or ´Hex-1$_R$´, RT was preincubated with 65 µM Hex-S3$_R$ or Hex-1$_R$, respectively, before addition of the p/t.

3.4.2 The DDDP assay

The ability of Hex-S3 to affect the DDDP activity of HIV-1 RT was assayed by measuring the decrease in the formation of extension product from a p/t substrate (Fig. 3.4.2 A).

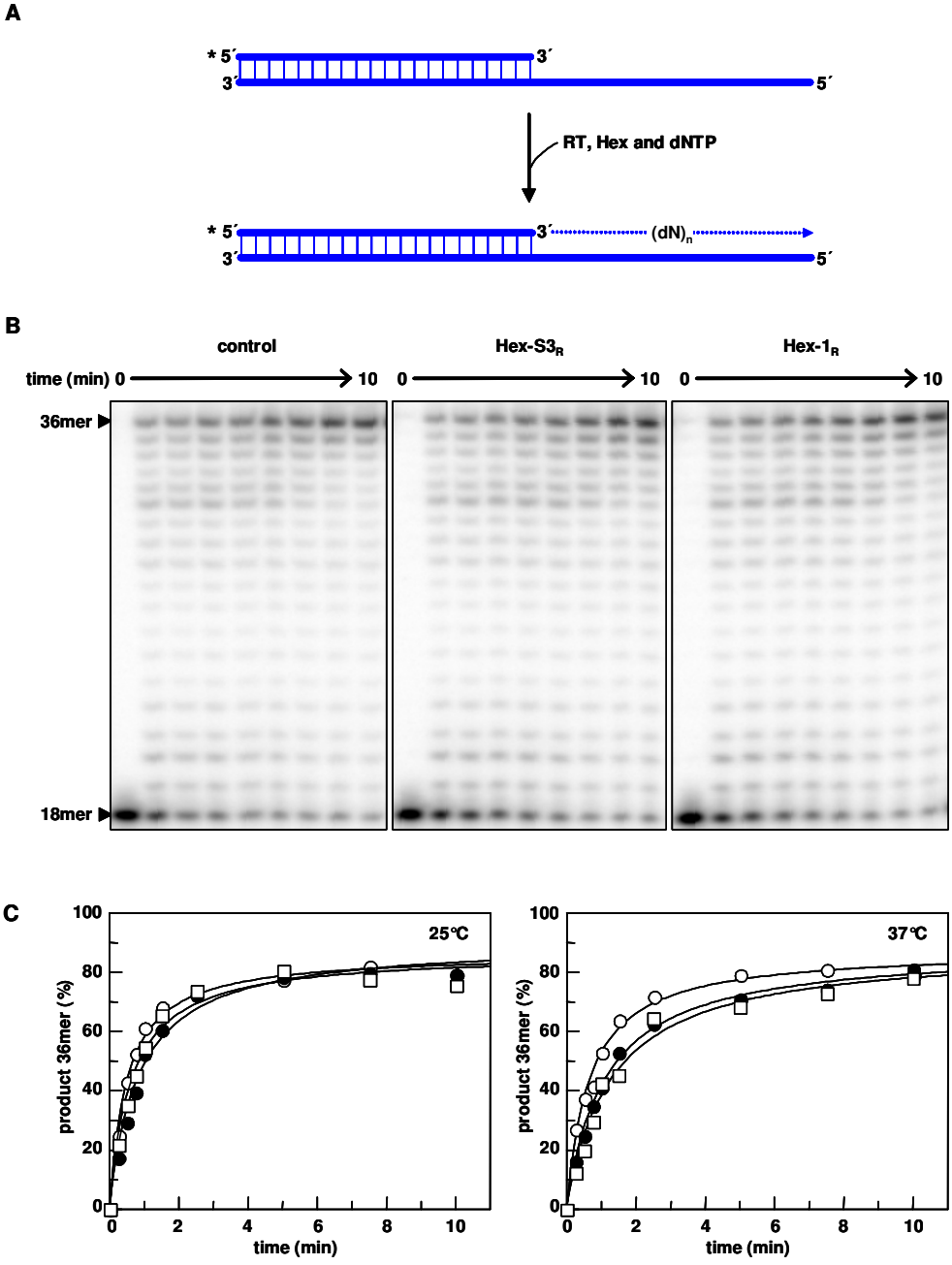

Fig. 3.4.2: DDDP activity of RT in the presence of Hex-S3$_R$. (A) Schematic representation of the DDDP assay. The template Flo6 (36mer) annealed to a 5´-radiolabelled (*) Flo1 primer (18mer) was used in this assay. Both strands are DNA and indicated in blue. (B) The reaction was performed by RT (0.75 nM) at 25°C in the absence of hexanucleotides, panel ´control´, or in the presence of 30 µM Hex-S3$_R$, middle panel, or of 30 µM Hex-1$_R$, right panel. The samples were collected after different periods of time from the beginning of the reaction (0, 0.25, 0.5, 0.75, 1, 1.5, 2.5, 5, 7.5 and 10 min). (C) Primer-elongation profiles of RT ´control´ (○), RT treated with Hex-S3$_R$ (●), or RT treated with Hex-1$_R$ (□). The reactions were performed at 25°C, left panel, or at 37°C, right panel. The percentage of 36mer product was calculated and plotted as a function of time. All reactions were analysed by 10% denaturing PAGE and quantified.

The Flo1 primer (18mer) was radiolabelled at the 5´-terminus and annealed to Flo6 template (36mer) (186).

The RT was preincubated in the absence or presence of Hex-$S3_R$ or Hex-1_R (negative control). The p/t (1.5 nM) was added to the binding mixture, the reaction was started by the addition of dNTPs and the assay was performed at 25°C or 37°C. In Fig. 3.4.2 (B) is shown the extension of the radiolabelled primer as a function of time. The amount of the 36mer product was comparable to reactions in which only RT was used (control) or where RT was preincubated with Hex-$S3_R$ in large molar excess. The amount of product was quantified and plotted over the time, as shown in Fig. 3.4.2 (C). The primer-elongation profiles produced by RT with or without Hex-$S3_R$ were identical, thus Hex-S3 did not affect the DDDP activity of the enzyme.

3.4.3 The RT fidelity assay

The HIV-1 RT is particularly error-prone since it lacks 3´→5´ proofreading activity (196;197). The insertional fidelity of RT, i.e. the ability of the enzyme to misincorporate nt during the polymerisation, was determined during a DDDP assay in the presence or absence of Hex-$S3_R$ or Hex-1_R. The p/t (Flo1/Flo6) used in this assay (Fig. 3.4.2 A and 3.4.3 A) (186), was correctly paired and the primer Flo1 was 5´-end radiolabelled. RT was preincubated in the absence or presence of Hex_R. The p/t was added to the binding mixture and the reaction was started by the addition of all four or only three dNTPs. The result of the misincorporation assay performed at 25°C and at 37°C, in the presence or absence of Hex_R is shown in Fig. 3.4.3 (B). When all four dNTPs were available in the reaction mixture, RT elongated the 18mer primer to a 36mer final product. However, when one of the four dNTPs was missing the primer-elongation mainly stopped at the specific nt-sites. To a certain extent RT was able to incorporate a wrong nt, proceeding the polymerisation to a 36mer final product. For each reaction, the amount of product (36mer) was calculated as a percentage of the amount obtained in the control reaction, as shown in Fig. 3.4.3 (C).

The primer-elongation profiles did not differ between RT alone, RT complexed with Hex-$S3_R$ or RT incubated with Hex-1_R, indicating that the fidelity of the enzyme was unaffected.

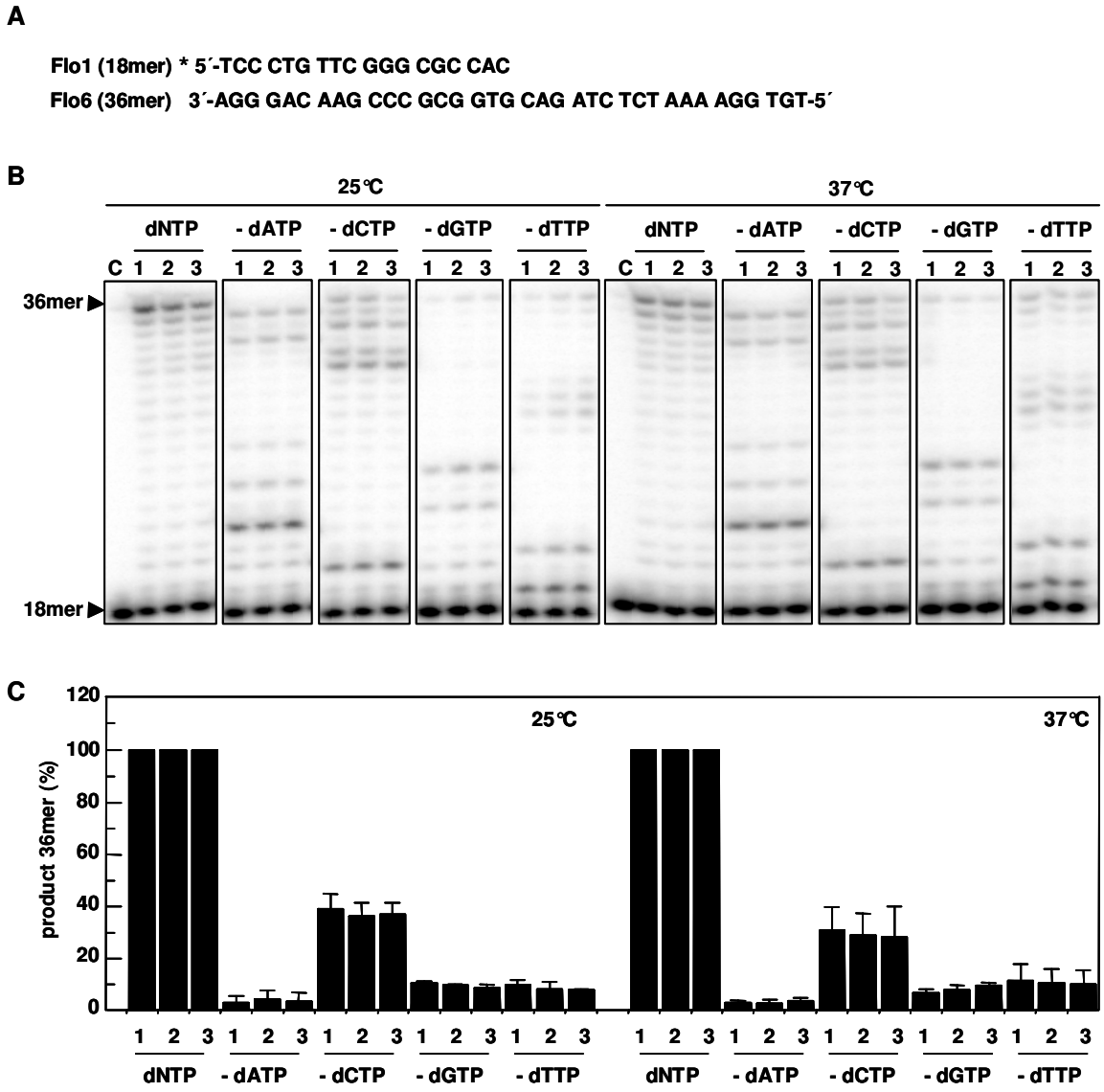

Fig. 3.4.3: Fidelity of RT in the presence of Hex-S3$_R$. (A) Sequences of the template (Flo6) and of the annealed primer (Flo1) 5´-end radiolabelled (*). (B) The misincorporation assay was performed at 25°C, left panel, or at 37°C, right panel. The reaction mixtures contained all four dNTPs, lane ´dNTP´, or only three dNTPs, lanes ´- dATP´, ´- dCTP´, ´- dGTP´, and ´- dTTP´. Control reactions ´C´ were performed without the addition of dNTPs, as ´1´ only RT, as ´2´ RT incubated with Hex-S3$_R$, and as ´3´ RT incubated with Hex-1$_R$. The primer-extension reactions were analysed by 10% denaturing PAGE. (C) For each reaction the amount of product (36mer) was calculated as a percentage of the amount obtained in the control reaction.

3.4.4 The RT processivity assay

The ability of Hex-S3$_R$ to alter RT processivity was tested in a DDDP assay (Fig. 3.4.2 A). The M13/pUC primer (24mer) was 5´-end radiolabelled and annealed to the M13mp18 template (7.25 kb). The assay was performed under conditions which allowed a single-round of primer-extension. Briefly, RT was preincubated in the absence or presence of Hex-S3$_R$ or Hex-1$_R$. The p/t was added to the protein solution followed by incubation for 3 min at 25°C or 37°C, to allow the binding of RT to the p/t. The extension

reaction was started by the addition of a mixture containing the RNA trap (pseudoknot) (131;164;165) and dNTP followed by incubation for 3 min at 25°C or 37°C. The RNA trap bound to RT and blocked the p/t binding site, preventing a further interaction and elongation of the substrate by the RT. As shown in Fig. 3.4.4 (lines marked ´P´, processivity), the primer (24mer) was extended by RT up to 600 nt.

The reaction was performed at 25°C or at 37°C. However, neither at 25°C nor at 37°C Hex-$S3_R$ interfered with RT processivity. To confirm the single-round primer-extension during the processivity assay, two additional control experiments were performed (Fig. 3.4.4). In the first control experiment, indicated as lines ´- trap´, RT was preincubated with or without Hex_R, as described above, followed by the addition of the p/t and incubation for 3 min at 25°C or at 37°C. The reaction was started by adding dNTPs and stopped after 3 min. The absence of the trap allowed multiple rounds of primer-extension, as shown in Fig. 3.4.4, and more primer could be extended than in a single-round extension experiment. In the second control experiment, the binding of the enzyme to the p/t was blocked as follows. A trap solution containing RNA trap, p/t and dNTPs was added to RT or RT:Hex_R, followed by incubation for 3 min at 25°C or at 37°C. This experiment was performed to test the ability of the RNA trap, pseudoknot, to really act as a trap for RT, blocking the p/t binding site on the enzyme, and the results are shown in Fig. 3.4.4, lines ´+ trap´.

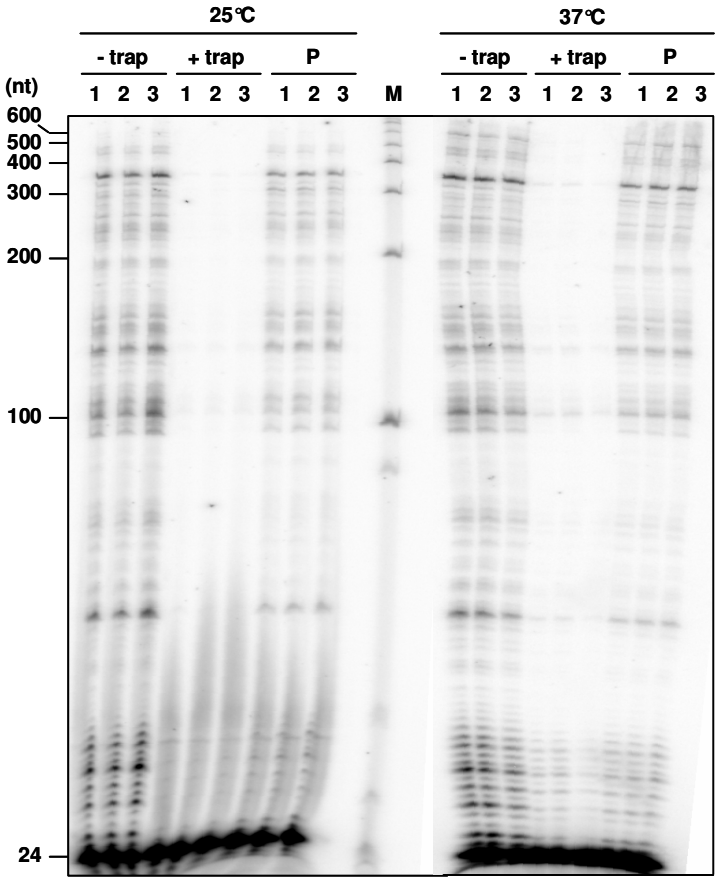

Fig. 3.4.4: Processivity of HIV-1 RT in the presence of Hex-$S3_R$. The assay was performed at 25°C (left) or at 37°C (right). The template M13mp18 (ssDNA) annealed to a 5´-radiolabelled M13/pUC primer (24mer) was used in this assay. The line ´1´ indicates RT (10 nM) without preincubation with hexanucleotides, and the lines ´2´ and ´3´ indicate RT (10 nM) incubated with 30 µM Hex-$S3_R$ or with 30 µM Hex-1_R, respectively. In the lines indicated with ´- trap´, RT or RT:Hex complexes were premixed with p/t (10 nM), and then the reaction was started by the addition of dNTP, allowing multiple rounds of primer-extension. In the line indicated ´+ trap´, RT or RT:Hex complexes were mixed with a trap mixture containing the RNA trap (1 µM), p/t and dNTP. This condition inhibited the binding of RT to the labelled p/t. In the lines indicated as ´P´ (processivity), the p/t was preincubated with RT or RT:Hex complexes, and the reaction was started by the addition of a trap solution containing RNA trap, and dNTP. All reactions were analysed by 8% denaturing PAGE. ´M´, ssDNA mass ladder.

3.4.5 The RNase H activity assay

HIV-1 RT exhibits RNase H activity, which specifically degrades the RNA in RNA/DNA hybrid duplexes. To determine the effect of Hex-$S3_R$ on RNase H activity of RT, the enzyme was preincubated with or without Hex_R and the reaction was started by the addition of a RNA/DNA heteroduplex substrate, in which the 5´-end of the RNA primer (35mer) was radiolabelled (Fig. 3.4.5 A). In this assay the dNTPs were omitted from the reaction mixture and the assay was performed at 25°C or at 37°C. The pattern of the RNA cleavage by RT in the presence or absence of hexanucleotides when the assay was performed at 25°C is shown in Fig. 3.4.5 (B).

Samples were collected at different time points, the hydrolysis profiles were quantified and the percentage of intact RNA primer was determined for all reactions as shown in Fig. 3.4.5 (C).

The ability of RT to hydrolyse the RNA primer was comparable at 25°C or at 37°C. The $t_{1/2}$ for the substrate was determined and is summarised in Table 3.4.1.

Table 3.4.1: Half-life of RNA in RNA/DNA hybrid duplexes during incubation with HIV-1 RT in the presence of Hex-$S3_R$ and controls

sample	$t_{1/2}$ (± SD) min, at 25°C	$t_{1/2}$ (± SD) min, at 37°C
control	1.63 (± 0.13)	1.84 (± 0.19)
Hex-$S3_R$	1.15 (± 0.10)	2.10 (± 0.15)
Hex-1_R	1.01 (± 0.10)	1.22 (± 0.10)

Both Hex-$S3_R$ and Hex-1_R affected the RNase H activity of RT at 25°C, leading to a faster degradation of the RNA substrate. This effect was clearly unspecific and independent of the hexameric sequence. At 37°C Hex-$S3_R$ did not affect the RNase H activity of RT as shown by the substrate-degradation profiles and by the $t_{1/2}$ values, which did not differ significantly from the ones obtained with RT alone (control). However, RT treated with the non-binder Hex-1_R showed a reduced $t_{1/2}$ value, which reflected an enhanced RNase H activity.

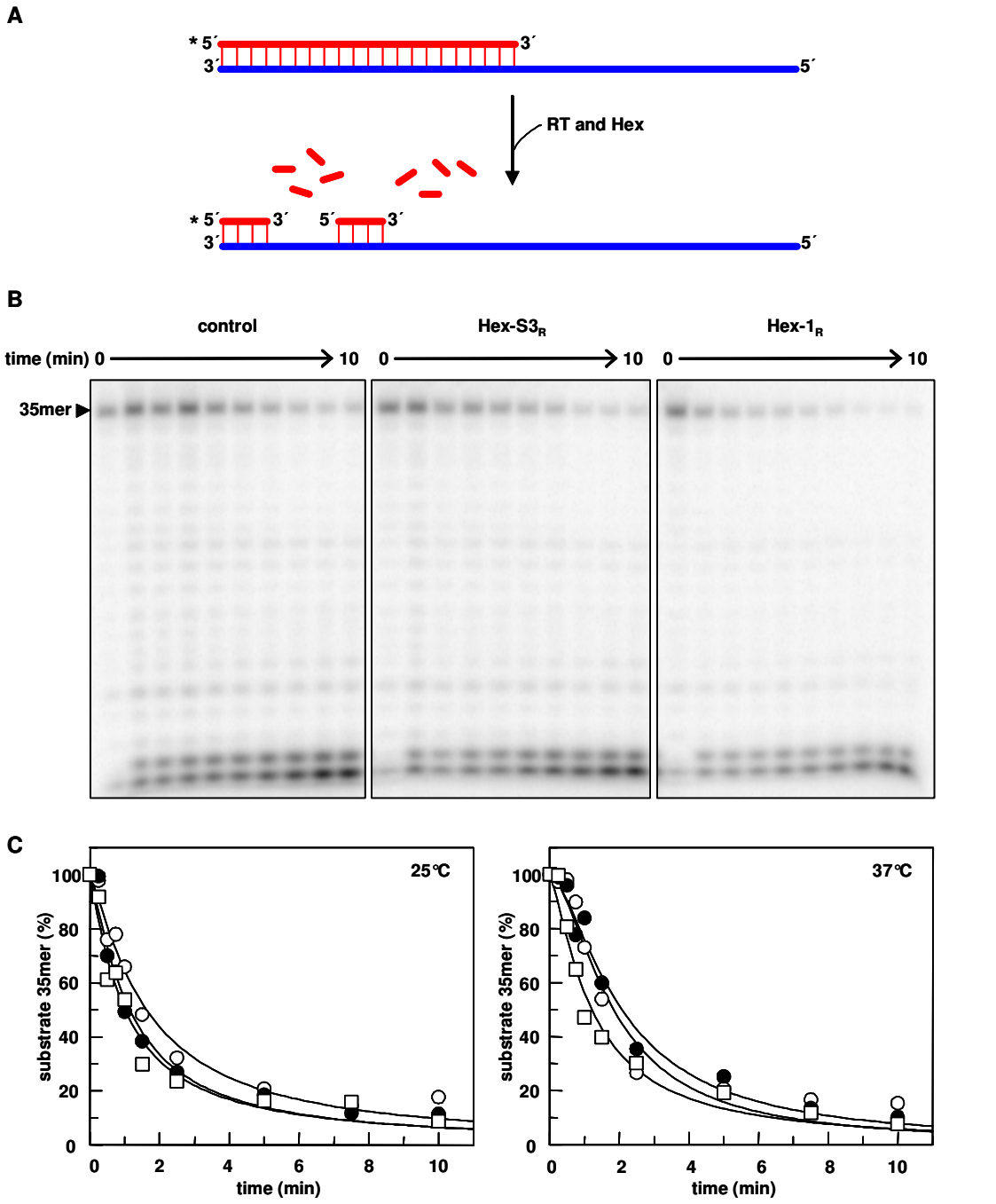

Fig. 3.4.5: RNase H activity in the presence of Hex-S3$_R$. (A) Schematic depiction of the RNase H assay. In the heteroduplex, the RNA strand is radiolabelled at the 5´-end (*) and indicated in red while the DNA is in blue. (B) A 10% denaturing PAGE showing the RT-mediated RNase H cleavage of the RNA primer (35mer) 5´-end radiolabelled. The reaction was performed using RT (0.75 nM) at 25°C in the absence of hexanucleotides, panel ´control´, or in the presence of 30 µM Hex-S3$_R$, middle panel, or 30 µM Hex-1$_R$, right panel. Samples were collected after different periods of time from the beginning of the reaction (0, 0.25, 0.5, 0.75, 1, 1.5, 2.5, 5, 7.5 and 10 min). (C) RNase H hydrolysis profiles of RT ´control´ (○), RT treated with Hex-S3$_R$ (●), or RT treated with Hex-1$_R$ (□). The reactions were performed at 25°C, left panel, or at 37°C, right panel. The percentage of intact primer was calculated and plotted as a function of time.

3.5 Combinatorial selection of hexanucleotide ligands in solution for HIV-1 RT

The experimental data obtained in the use of Hex-S3 as a ligand for HIV-1 RT, as well as an inhibitor of HIV-1 viral particles production *in vitro*, supported the fact that even very short oligonucleotides were able to bind specifically to a given target protein and exert biological activity.

Based on these findings, it would be advantageous to be able to select the target-specific hexanucleotides from a random pool of all possible sequences. As targets relevant pathology-related proteins could be used and the best-binding hexameric species would be tested for their ability to interfere with the activity of the target. In order to establish whether a combinatorial approach for the selection of hexanucleotide ligands binding to HIV-1 RT, chosen as model target, was feasible several methods were evaluated, comprising chromatographic methods, the selection using microbeads, and a filter binding approach (see 3.5.1 and 3.5.3).

In this study the development of a combinatorial approach in solution is described. In addition, the sequencing of the selected hexanucleotides required the development of a cloning strategy which involved their elongation by a terminal transferase and primer-ligation by the T4 RNA ligase (see 3.5.3.1). Attempts to use the RNA analogs, i.e. hexaribonucleotides as substrates for terminal deoxynucleotidyl transferase, poly(dA) polymerase, and T4 RNA ligase showed extremely little product or failed, indicating that very short RNAs were poor substrates for those enzymes. Therefore, the following experiments were performed with hexanucleotides having a DNA backbone.

3.5.1 Comparison of in vitro selection approaches for the identification of HIV-1 RT-binding hexanucleotides

In order to select HIV-1 RT-binding hexameric DNA species, several combinatorial selection approaches were employed, namely chromatographic methods, a microbead-based approach and a filter binding-based method (Fig. 3.5.1). All methods were at first tested for their stringency, which was evaluated based on the background level obtained by use of appropriate controls, i.e. Hex-S3 as binder and Hex-1 as non-binder for HIV-1 RT. In each system RT was incubated either with radiolabelled Hex-S3 or Hex-1 and the RT:Hex complexes were subjected to selection.

The first approach was based on gel filtration chromatography using ´MicroSpin™ G-50´ columns with a MWCO of 50 kDa. This allowed the separation of preformed RT:Hex complexes, which presented a MW greater than 50 kDa, from the free and unbound hexanucleotides (MW about 2 kDa).

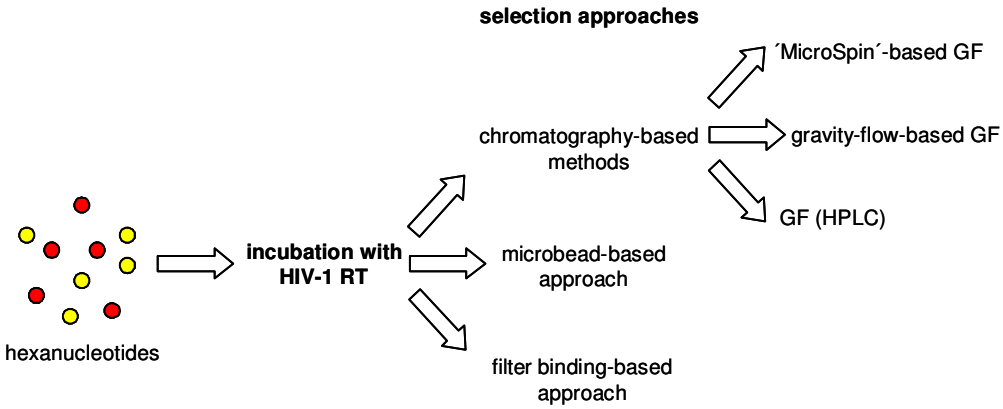

Fig. 3.5.1: Selection approaches for the search of target-specific hexanucleotides. Schematic drawing of the different selection approaches tested in this study. Hex-S3 and Hex-1 were incubated with HIV-1 RT and the binding mixture was subjected to a selection procedure based on chromatography, the capture on microbeads or on filter. Three gel filtration (GF) chromatographic methods were tested, i.e. ´Microspin´, gravity-flow-based GF and GF under high performance liquid chromatography (HPLC) conditions.

HIV-1 RT (10 µM) was incubated either with radiolabelled Hex-$S3_D$ (10 nM) or with radiolabelled Hex-1_D (10 nM), which served as a negative control. The binding mixtures (50 µl) were incubated for 2 min at 25°C, in RT binding buffer, which were the optimal experimental conditions for the binding of Hex-S3 to RT (see 3.2.1). The mixtures were applied to the columns, followed by a centrifugation. The eluted radioactive RT:Hex complexes were then measured by a scintillation counter Wallac 1409. The percentage of eluted radioactivity, which was calculated in relation to the total radioactivity applied to the column, was similar for Hex-$S3_D$ (25%) and for Hex-1_D (20%), rendering the system unsuitable for the separation of binders for RT from non-binders (data not shown).

Other chromatographic methods tested were a gravity-flow-based gel filtration chromatography and a HPLC. Resins used for the gravity flow were Sephadex G-15, G-25 and G-75 (GE Healthcare). For the HPLC a Superdex 200 HR 10/30 (GE Healthcare) was used. In the first case, when radiolabelled Hex-$S3_D$ or Hex-1_D were incubated with the HIV-RT and applied to gravity-flow chromatographic columns, the retention time of both hexanucleotides/RT mixtures was the same, without any discrimination between the binder and the non-binder species (data not shown). For the HPLC gel chromatography, 10 µM unlabelled Hex-$S3_D$ or Hex-1_D were incubated with or without 10 µM HIV-1 RT, in a total volume of 50 µl, under the conditions described above. The retention times of free HIV-1 RT or free hexanucleotide were 15 min and 29 min, respectively. Using this system, no RT:Hex complexes were detected in the chromatogram (data not shown).

Furthermore, a microbead-based approach was performed, in which nickel-nitrilotriacetic acid (Ni-NTA) magnetic agarose beads (Qiagen) were used. In this approach, HIV-1 RT containing an affinity tag of six consecutive histidine residues (6xHis tag) was immobilised

on the beads. Immobilised RT (2.5 µM) was incubated with 20 nM radiolabelled hexanucleotides in a total volume of 55 µl, under the experimental conditions described above. The purification of RT:Hex complexes from free, unbound hexanucleotides was performed by the collection of the microbeads with a magnet, which was followed by washing with RT binding buffer and elution of the bound hexanucleotides using a 1M NaCl solution. The main disadvantage of this approach was the presence of Ni^{2+} on the surface of the beads, since nucleic acids showed affinity for this metal ion. This did not allow a separation of hexanucleotides bound to RT from the ones interacting with the metal ion.

The last approach in solution employed for the selection of hexanucleotides against RT was a filter binding-based system, which was successfully used to select of aptamers against various targets (37;37;163) and which is described in detail in 3.5.2.

3.5.2 Selection of HIV-1 RT-binding hexanucleotides by filter binding

In a combinatorial selection approach based on a filter binding method, a radiolabelled randomised pool of hexanucleotides, containing all 4,096 (4^6) existing hexameric species, was subjected to selection for binding to HIV-1 RT on nitrocellulose filters. Hexanucleotides (10 nM) were incubated for 10 min at 37°C with 10 µM HIV-1 RT, in a total volume of 40 µl and in buffer containing 50 mM Tris-HCl (pH 8.0), 50 mM KCl and 6 mM $MgCl_2$. An aliquot (20 µl) of this mixture was filtered under reduced pressure through a pre-wetted nitrocellulose filter BA85 (0.45 µM) and rinsed with 3 ml of buffer.

In order to optimise the elution of hexanucleotides from the filters, a variety of conditions were compared. Initially, the extraction step was performed as described (37) by using a solution containing 2 M urea, 6 mM sodium citrate (pH 5.0), 0.3 mM EDTA and 70% (v/v) phenol (pH 5.2). In a separate experiment only 70% (v/v) phenol in water was used. The filter was transferred to a microcentrifuge tube and vortexed after the addition of the extraction solution. The extracted hexanucleotides were collected from the upper phase after centrifugation. Alternatively, 100% (v/v) acetone was applied to the filter, and the extracted hexanucleotides were lyophilised. All these methods involved the use of phenol or acetone, which proved to dissolve the nitrocellulose filters. The fragmented nitrocellulose was difficult to separate from the eluted hexanucleotides without the loss of a large amount of sample. Therefore, an alternative method was employed, in which hexanucleotides were eluted from the filter via addition of 1 ml water to the filter, followed by heating at 95°C for 10 min. The amount of DNA recovered was about 90% (cpm) of the DNA bound to the filter prior to the elution, which correspond to 0.3% (600 amol) of the input DNA. The level of background was determined by filtering hexanucleotides in the absence of RT, and the unspecifically bound DNA was calculated to be

the 0.04% of the input DNA. Accordingly, approximately 15% of ´selected´ hexanucleotides were unspecifically retained by the nitrocellulose filter.

3.5.3 Processing and identification of selected hexanucleotides

3.5.3.1 Poly(dC) tailing, primer ligation, amplification and cloning of selected hexamers

Selected hexanucleotides were subjected to poly(dC) tailing at the 3´-terminus by the terminal deoxynucleotidyl transferase, followed by primer ligation at the 5´-end and amplification of elongated hexanucleotides by PCR, as schematically represented in Fig. 3.5.2 (A).

The tailing reaction performed by the terminal deoxynucleotidyl transferase was very efficient since the number of dCMT incorporated at the 3´-end of the hexanucleotides was in a range of 40 to 90 nt, as shown in Fig. 3.5.2 (B). Tailed products were then precipitated in ethanol and ligated at their 5´-terminus with a primer PA (sequence shown in Table 2.1.1). Tailed hexanucleotides were incubated for 20 h at 25°C with 0.5 units T4 RNA ligase, 50 µg/ml BSA, 1 mM ATP, 25% (w/v) PEG 8000, and 50 nM primer PA in 20 µl final volume. The reaction was stopped by heating at 95°C for 5 min. Ligated products were precipitated in ethanol and amplified by PCR in the presence of *Taq* polymerase and primers PA, PB and adaptor PB (sequences shown in Table 2.1.1). The PCR products were resolved by TAE-agarose gel electrophoresis (Fig. 3.5.2 C), cloned in the pCRII-TOPO or pGEM-T easy vectors and sequenced.

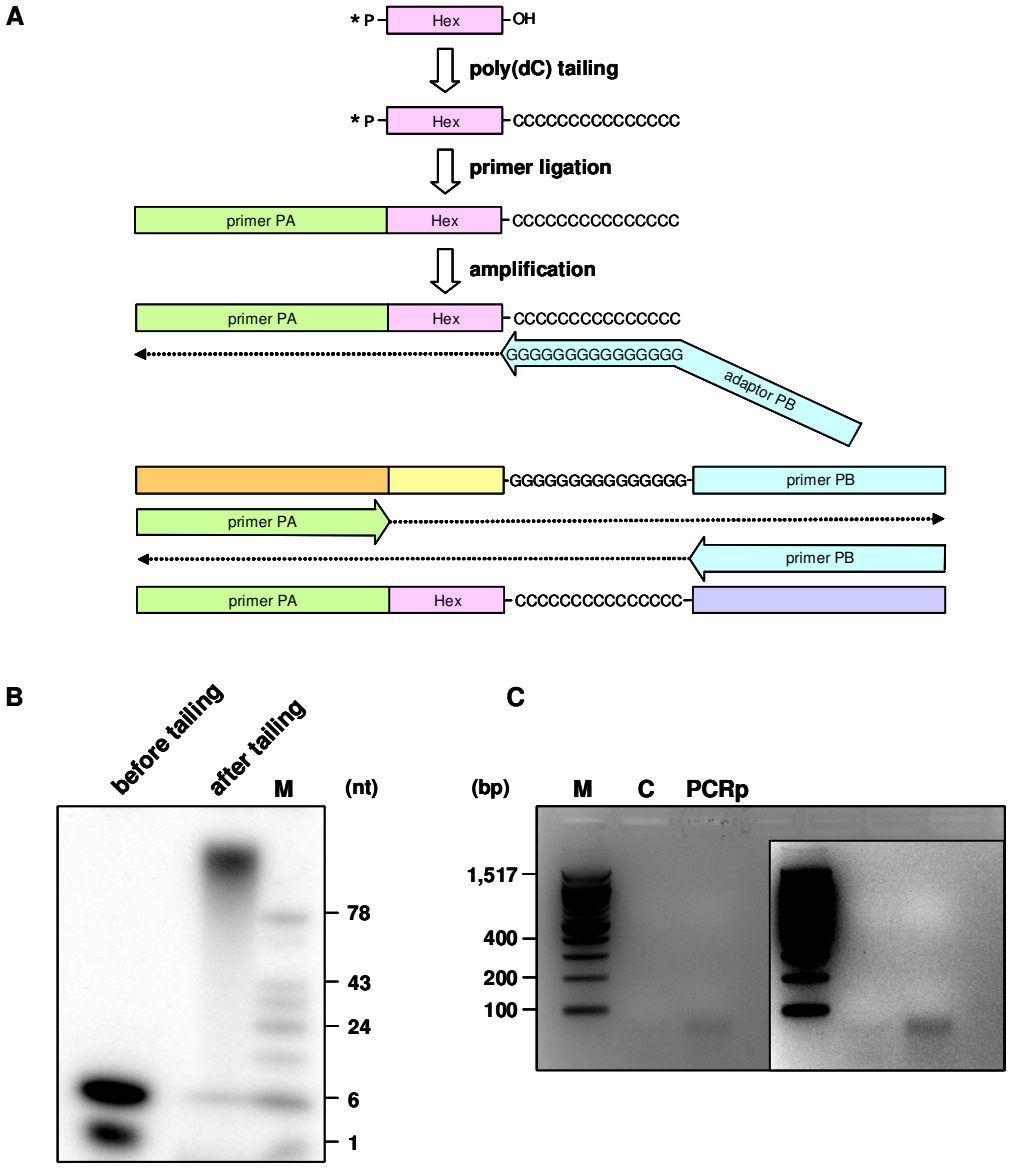

Fig. 3.5.2: Processing of the selected hexanucleotides. (A) Schematic drawing of the cloning strategy for the sequencing of hexanucleotides. A poly(dC) tail was introduced at the 3´-end of the selected species, followed by ligation at their 5´-end with the primer PA and amplification via *Taq* polymerase and primers PA, PB and adaptor PB. (B) The tailing reaction was performed for 10 min at 37°C using 1 unit of terminal deoxynucleotidyl transferase and 7.5 µM dCTP in a final volume of 20 µl. Tailed products were resolved by 15% denaturing PAGE. As a control, hexanucleotides prior to the tailing reaction are shown. (C) Ligated and tailed hexanucleotides were subjected to PCR, as follows. Briefly, elongated hexanucleotides were amplified in the presence of 0.02 units/µl of *Taq* polymerase, 0.8 mM dNTP, 0.5 µM primer PA, 0.5 µM primer PB, 0.1 nM adaptor PB. PCR products, ´PCRp´, were resolved by 3% TAE-agarose gel electrophoresis. The frame on the right shows lanes ´M´, ´C´ and ´PCRp´ of the gel after scanning with a longer exposure time. ´C´, PCR reaction in which water replaced the hexanucleotide solution. ´M´, mass ladder.

3.5.3.2 Analysis of selected sequences

From 130 clones analysed, 35 contained selected hexanucleotide sequences. The sequence analysis of the cloned species revealed seven different sequences, five hexamers and two pentamers (Fig. 3.5.3). The two pentamers probably resulted from a truncation phenomenon during the processing of the selected species. The most

abundant species were Hex-FB1 and Hex-FB2, which were found in 46% and 28% of the clones respectively.

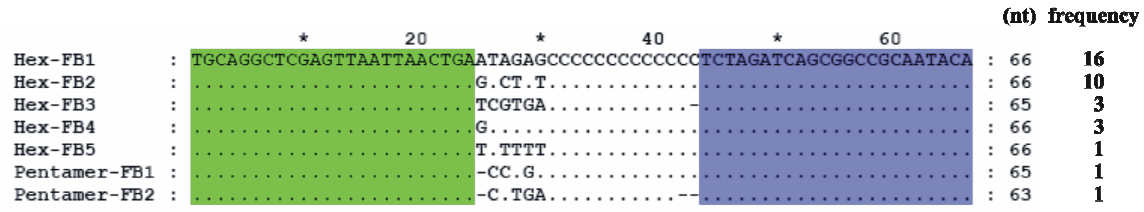

Fig. 3.5.3: Aligned sequences from the HIV-1 RT binding pool after the selection round. The numbers indicate the length (nt) of the cloned inserts and the frequency of occurrence of the individual sequence. The primer fixed sequences are shaded in green and blue. Sequences were aligned using the program Genedoc (198) and only the differences are shown. Identical and missing nt are represented by dots and dashes, respectively.

As further control the random pool of hexanucleotides was also subjected to processing and sequencing in order to determine whether there was a bias for certain sequences (performed by W. Wünsche). The sequence analysis of the 61 cloned species showed that Hex-FB1 was present in two clones, Hex-FB4 in one clone, while none of the other selected species were found (data not shown). The nt frequencies in percentage found at each varied position and the derived consensus sequence are presented in Table 3.5.1.

Table 3.5.1: Nucleotide frequencies at each position and derived consensus sequence

nucleotide	position (5´ to 3´)					
	I	II	III	IV	V	VI
A	41	21	54	25	33	3
C	39	25	13	16	26	10
G	10	38	23	51	20	75
T	8	16	8	7	10	10
N[a)]	2	0	2	2	0	2
consensus sequence	A	G	A	G	A	G

[a)] ambiguous sequencing result.

3.5.4 Binding of selected hexanucleotides and controls to HIV-1 RT

The interaction of the seven selected sequences and controls with HIV-1 RT was analysed by a filter binding assay. In this assay, selected species were incubated with RT under the conditions which were used during the selection procedure (in selection buffer, high salt, at 37°C, 10 min), or under conditions which were established to be the optimum for the binding of Hex-S3 to RT (in RT binding buffer, low salt, at 25°C, 2 min). The results are shown in Fig. 3.5.4.

As controls, Hex-$S3_D$ and Hex-S1 were included. The Hex-S1 was identified by W. Wünsche and showed a moderate affinity towards RT. The Hex-0, which was also

included as a control, was the consensus sequence derived from the starting pool of hexanucleotides (Table 3.5.1). At high temperature and salt conditions, the binding of the hexamers and pentamers to RT was below 5% binding, as shown in Fig. 3.5.4,

Hex-S3 and Hex-S1 showed a 1.5% binding, while Hex-0 showed 0.15% binding to RT. Among the selected species, Hex-FB4 and Pentamer-FB2 showed a comparable binding to RT, whereas Hex-FB1, Hex-FB2, Hex-FB3, Hex-FB5 and Pentamer-FB1 bound more strongly to RT than Hex-S3 (Fig. 3.5.4).

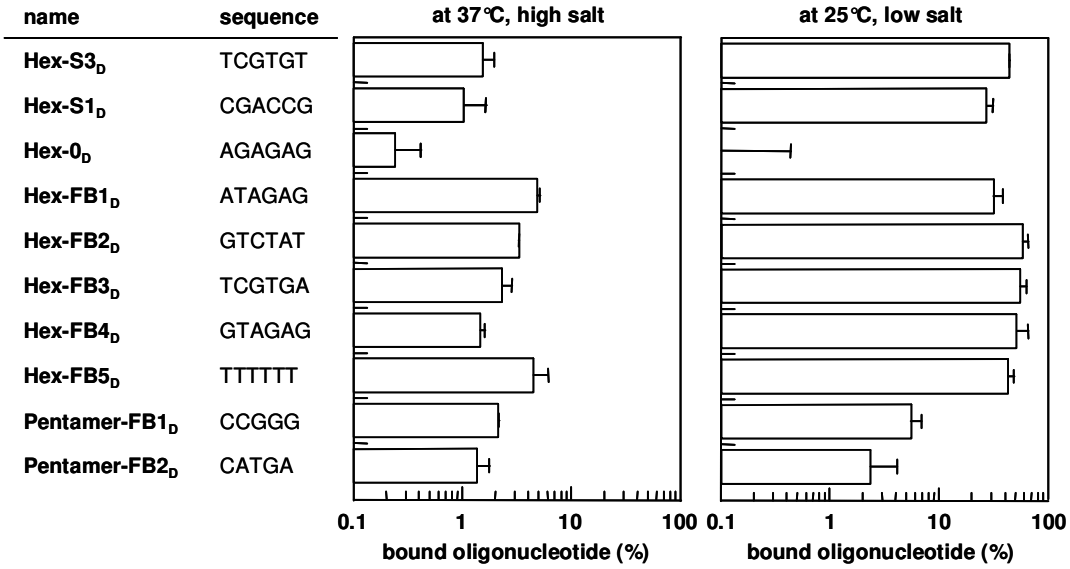

Fig. 3.5.4: Filter binding assay of selected sequences with HIV-1 RT. The investigated species and respective sequences are shown on the left panel. The radiolabelled oligonucleotides (1 nM) and HIV-1 RT (5 µM) were incubated in a final volume of 30 µl under two different conditions, namely at 37°C, high salt or 25°C, low salt. The percentage of binding of each sequence was determined by normalisation to the total input of hexanucleotide.

At a low temperature and ionic strength the two pentameric species showed about one-tenth of the binding in comparison to hexameric species (Fig. 3.5.4). Under these conditions, 0.1% Hex-0 bound to RT, while the three hexanucleotides, Hex-FB2, Hex-FB3 and Hex-FB5 showed a higher binding to RT compared to Hex-S3. The Hex-FB4 and Hex-FB1 respectively, showed the same binding or lower binding to enzyme when compared to the control Hex-S3. Interestingly, Hex-FB4 and Hex-0, which differed by only one nt at the second position from the 5´-end, showed a completely different binding behaviour. This clearly implied the loss of binding properties by the replacement in that sequence context of a T with a G at the second position from the 5´-end. Hex-FB4, too, differed from Hex-FB1 by a single nt and the replacement of an A with a G at the first position from the 5´-end, did not prove to affect the binding at a high temperature and high ionic strength, while it led to almost 2-fold increased binding at a low temperature and salt concentration. Moreover, the selected Hex-FB3 differed from the control Hex-$S3_D$ by one

nt (T *versus* A at the 3´-end). The binding strength of the selected Hex-FB3 was slightly higher than for Hex-$S3_D$ under both tested experimental conditions, indicating that the replacement of the last nt with an A increased binding strength for RT.

3.6 Development of an oligonucleotide-based array

As a more specific and systematic alternative to the *in vitro* selection of target-specific hexameric species, a hexanucleotide array-based approach was conceived. This approach would circumvent the cloning steps for sequencing and eliminate the introduced bias, furthermore truncated sequences would not occur and a large number of targets could be screened simultaneously. This array would contain all possible 4,096 (4^6) hexameric sequences, and allow the rapid and specific detection of target proteins bound to immobilised hexanucleotides, combining the advantages of applying a very limited amount of sample to the possibility of high-throughput screening. Accordingly, to test whether such an array-based approach was feasible, an oligonucleotide-based array, including selected oligo- and hexanucleotides was developed, and its features and processing described in the following chapter.

3.6.1 Oligonucleotide-based array design

As a first approach and for establishing the conditions under which an array-based selection can be successfully performed a small array containing ten oligo- and hexameric sequences was designed. The sequences were chosen based on their binding behaviour in solution towards HIV-1 RT and control proteins, i.e. Hex non-RT-binders (Hex-1 and Hex-0), Hex RT-binders (Hex-S3, Hex-S1 and Hex-4) and oligonucleotides [ss-45mer, $(Hex\text{-}S3_D)_4$, $(Hex\text{-}S3_DC{\rightarrow}A)_4$, $ODN2080_D$ and a RT-directed DNA aptamer] (sequences shown in Table 3.6.1).

Hexanucleotides were included in the array as DNA or RNA backbones. The DNA oligonucleotides, and particularly the well-characterised high-affinity RT-directed DNA aptamer, called RT1t49 (92), served as positive controls for the binding of HIV-1 RT to immobilised single-stranded nucleic acids. As further control for the protein-binding specificity, two oligonucleotides, namely the $(Hex\text{-}S3)_4$, and the ODN2080 were chosen on the basis of their ability to interact with the TLR9 *in vitro* (33), whereas $(Hex\text{-}S3_DC{\rightarrow}A)_4$ was described as not being able to interact and therefore included as a negative control.

Table 3.6.1: Sequences used in this study

nucleic acid	sequence (5´ to 3´)
Hex-1	TCA AAA
Hex-0	AGA GAG
Hex-S3	TCG TGT
Hex-S1	CGA CCG
Hex-4	GTC TAA
ss-45mer DNA	T_{20}CT GTA CAG GTA GCA ATG GCA GGT GC
$(Hex\text{-}S3_D)_4$	TCG TGT TCG TGT TCG TGT TCG TGT
$(Hex\text{-}S3_DC{\rightarrow}A)_4$	TAG TGT TAG TGT TAG TGT TAG TGT
$ODN2080_D$	TCG TCG TTC CCC CCC CCC CCC CCC
DNA aptamer (RT1t49)	ATC CGC CTG ATT AGC GAT ACT CAG AAG GAT AAA CTG TCC AGA ACT TGG A

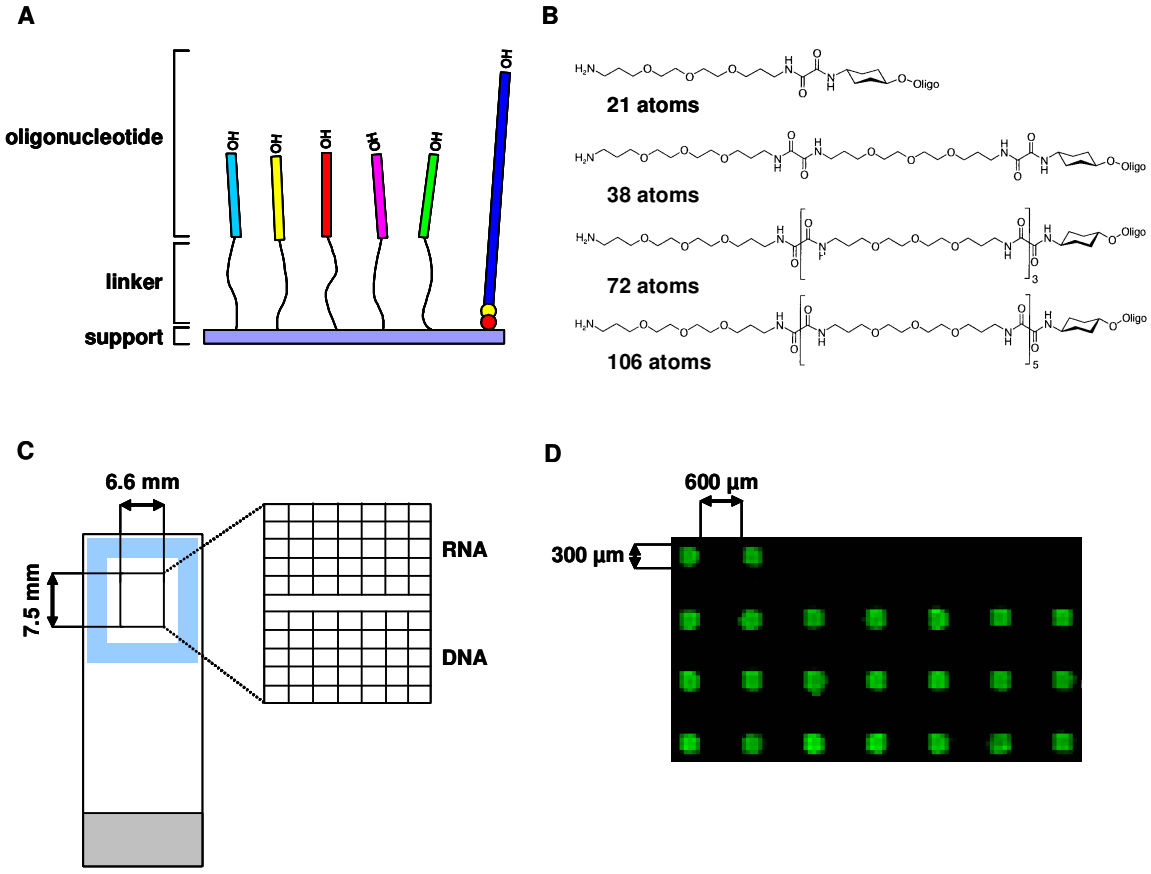

Fig. 3.6.1: Features of the oligonucleotide array. (A) Schematic representation of printed hexameric and oligomeric nucleic acids. The hexanucleotides were covalently linked by their 5´-end to the surface by a tether, while control oligonucleotides were immobilised at their 5´-termini through a biotin-streptavidin interaction. (B) Chemistry of the linkers used for the array. Four different linkers of increasing lengths were used (21-, 38-, 72- and 106-atoms). (C) Schematic drawing of the array. The nucleic acids were spotted on the matrix within an area of 6.6 mm per 7.5 mm, and the space assigned to the DNA or RNA nucleic acids is shown. (D) Quality control of spotted nucleic acids. Unspecific binding sites were blocked with 2% (w/v) casein, the array washed and incubated for 10 min at 37°C with 3.33 µM fluorescein-12-ddCTP and 100 units of terminal deoxynucleotidyl transferase in a total volume of 100 µl. The reaction was stopped by the addition of 10 mM EDTA, the array was then washed, fixed in acetone for a few seconds and scanned on a Typhoon scanner.

The hexameric sequences were linked at their 5´-termini by a tether to a solid surface. Long control oligonucleotides were 5´-end biotinylated and bound to the support via immobilised streptavidin, as shown in Fig. 3.6.1 (A). Linkers having a length of 21-, 38-, 72- and 106-atoms (Fig. 3.6.1 B) were tested in order to examine the influence of the tether dimension on the binding efficiency and specificity. The arrays were developed on glass slides coated by matrix, namely nitrocellulose, epoxy or CodeLink. The nucleic acids were spotted on the matrix within an area of 6.6 mm per 7.5 mm, as shown in Fig. 3.6.1 C, and DNA as well as RNA hexameric- backbones were used. The amount of nucleic acid per spot was determined to be about 1 fmol, each nucleic acid was printed in duplicate per slide, with a spot diameter of 300 µM and a distance between two spots of 600 µM (Fig. 3.6.1 D). The quality of the printed spots was determined via analysis of quantity and density of the hexa- and oligonucleotides immobilised within each spot on the array. This was performed by 3´-end fluorescent labelling of the immobilised nucleic acids followed by scanning and analysis of the fluorescent signals. The identically arrayed spots of the different sequences after fluorescent labelling are shown in Fig. 3.6.1 (D).

3.6.2 Establishment of experimental conditions for the array analysis

Conditions for the array processing were established to investigate in an unequivocal and highly specific way the differential binding of HIV-1 RT and control proteins to the selected hexameric species. Therefore, several experimental conditions were investigated to minimise unspecific binding of the target, to increase detection sensitivity, and resolution.

3.6.2.1 Strategies for the detection of bound target protein

In order to monitor the binding of HIV-1 RT to immobilised hexanucleotides and controls, two detection strategies were employed. First radio- or fluorescent-labelled proteins were applied to the array. Alternatively unlabelled proteins were detected by fluorescently labelled Ab directed against the bound protein (Fig. 3.6.2).

The HIV-1 RT was labelled with ^{125}I as described in detail in 2.2.3.6. The iodinated protein was resolved by SDS-PAGE, the gels were exposed to a PhosphorImager screen and scanned on a Typhoon 8600 scanner (Fig. 3.6.3 A). The labelling efficiency of the smaller subunit p51 of HIV-1 RT was much greater than for the larger subunit, p66. The lower limit of detection was determined to be 150 amol protein. The radiolabelled protein was applied to the array, following the experimental conditions described in 3.6.3.

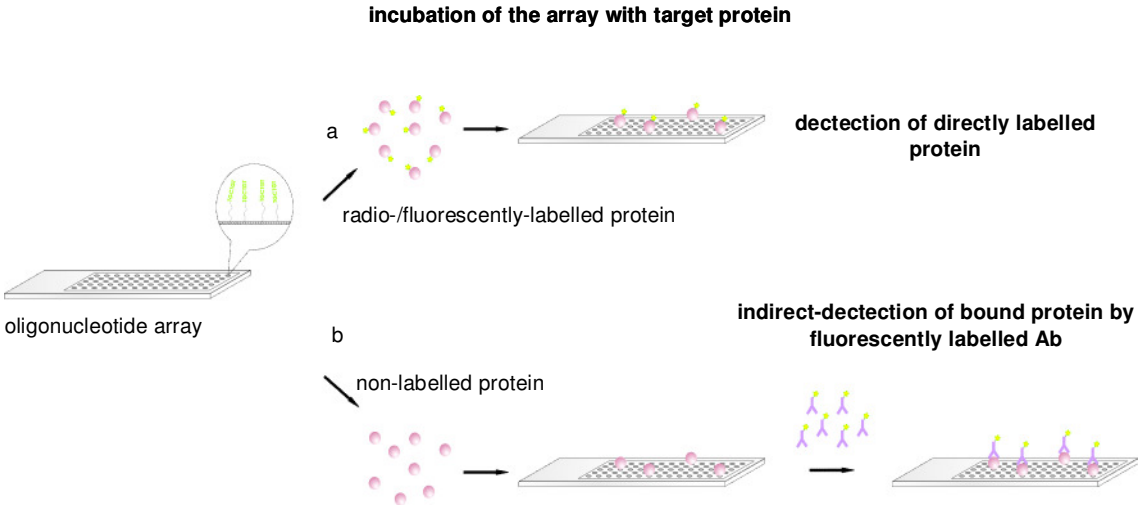

Fig. 3.6.2: Schematic depiction of an array-based screen for protein-hexamer interactions. Arrays, before incubation with the target protein, were incubated with an optimised blocking solution for 2 h in order to decrease unspecific binding of the protein to the matrix. The binding was monitored by using radio- or fluorescently-labelled protein (a) or unlabelled protein followed by detection of bound protein with a fluorescently-labelled protein-directed Ab (b). After the binding step, arrays were washed and dried, and signals were detected by a Typhoon 8600 scanner.

After washing and drying, the array was exposed for 2 h to a PhosphorImager screen and the screen was then scanned. As shown in Fig. 3.6.3 (B), via exposing the array to the screen, the radioactive signal was spread over the whole surface of the array. Therefore, a second labelling system was employed, which was based on the fluorescent-labelling of protein. Site-directed Alexa^{488} labelled RT, as well as cysteine- or lysine-specific fluorescein-labelled proteins were used. The Alexa^{488} labelled HIV-1 RT was a kind gift from T. Restle, and a fluorochrom was introduced at amino acid position 194 or 287 of the p66 subunit (p66^{E194C}Alexa^{488}/p51 and p66^{K287C}Alexa^{488}/p51) or at position 281 of the p51 subunit (p66/p51^{K281C}Alexa^{488}). These proteins were shown earlier to preserve all enzymatic activities (136;164;199). The lower detection limit with fluorescently labelled protein was determined to be between 1 fmol and 100 amol (Fig. 3.6.3 C). The arrays were incubated with fluorescently labelled RT, washed and the fluorescence intensity was detected by a Typhoon 8600 scanner (Alexa^{488}: 495/519 nm excitation/emission, fluorescein: 494/518 nm excitation/emission). The employment of fluorescently labelled protein combined the advantages of a low background with a very clear differential binding of the protein to immobilised oligo- and hexameric sequences, as shown in Fig. 3.6.3 D and A. Independent of the label chemistry, position or amount, the binding behaviour was identical among the tested RTs indicating that the binding characteristics were not affected by the fluorescent moiety of the protein (data not shown).

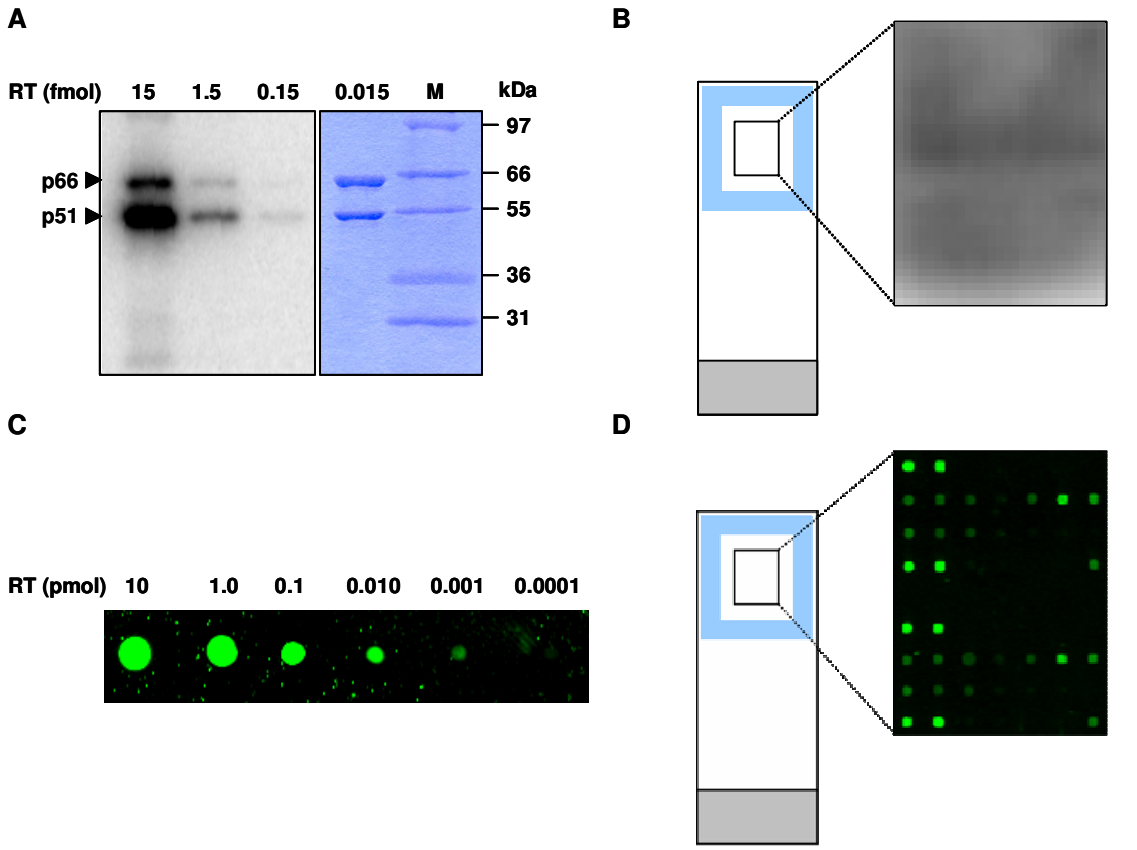

Fig. 3.6.3: Detection of fluorescently labelled protein. (A) The detection limit of radiolabelled RT was determined by an analysis of radiolabelled protein via 15% SDS-PAGE, followed by exposure for 2 h of the gel to a screen and the scanning of the screen. Three different amounts of labelled RT were used, i.e. 0.15, 1.5 and 15 fmol. The two subunits of RT are indicated as ´p66´ and ´p51´. The autoradiograph (left panel) and coomassie blue stained gel (right panel). ´M´, mass ladder. (B) Result obtained with an array incubated with 500 nM radiolabelled RT, after exposure to a PhosphorImager screen (2 h) and scanning. (C) The detection limit of fluorescently labelled protein was determined by scanning of spotted p66/p51^{K281C}Alexa^{488} in different amounts on a CodeLink matrix. (D) The results obtained with an array treated with 500 nM p66/p51^{K281C}Alexa^{488}.

Alternatively, the arrays were incubated with unlabelled RT followed by the detection of the bound protein via a FITC-conjugated RT-specific monoclonal Ab (MAb 20) (172). The array was incubated with unlabelled RT, washed and incubated with FITC-labelled Ab, followed by scanning (FITC: 506/529 nM excitation/emission) on a fluorescence scanner. The direct comparison between the direct and the indirect detection systems is shown in Fig. 3.6.4. The protein bound to the immobilised hexanucleotides and the controls is highlighted in green (upper panel) and the intensity of each spot was determined (lower panel). By using the direct detection system (Fig. 3.6.4 A), the experiment showed a strong binding of RT to the oligonucleotides as well as a binding to the hexamers Hex-S1, Hex-4 and Hex-S3, while no signal was detected for the non-binders, Hex-0 and Hex-1, which was consistent with the binding data observed in solution. In contrast, using an indirect detection system (Fig. 3.6.4 B), only the strong interaction between RT and the longer oligonucleotides was clearly visible. However, the differences in the binding between the hexanucleotides were diminished and close to background level.

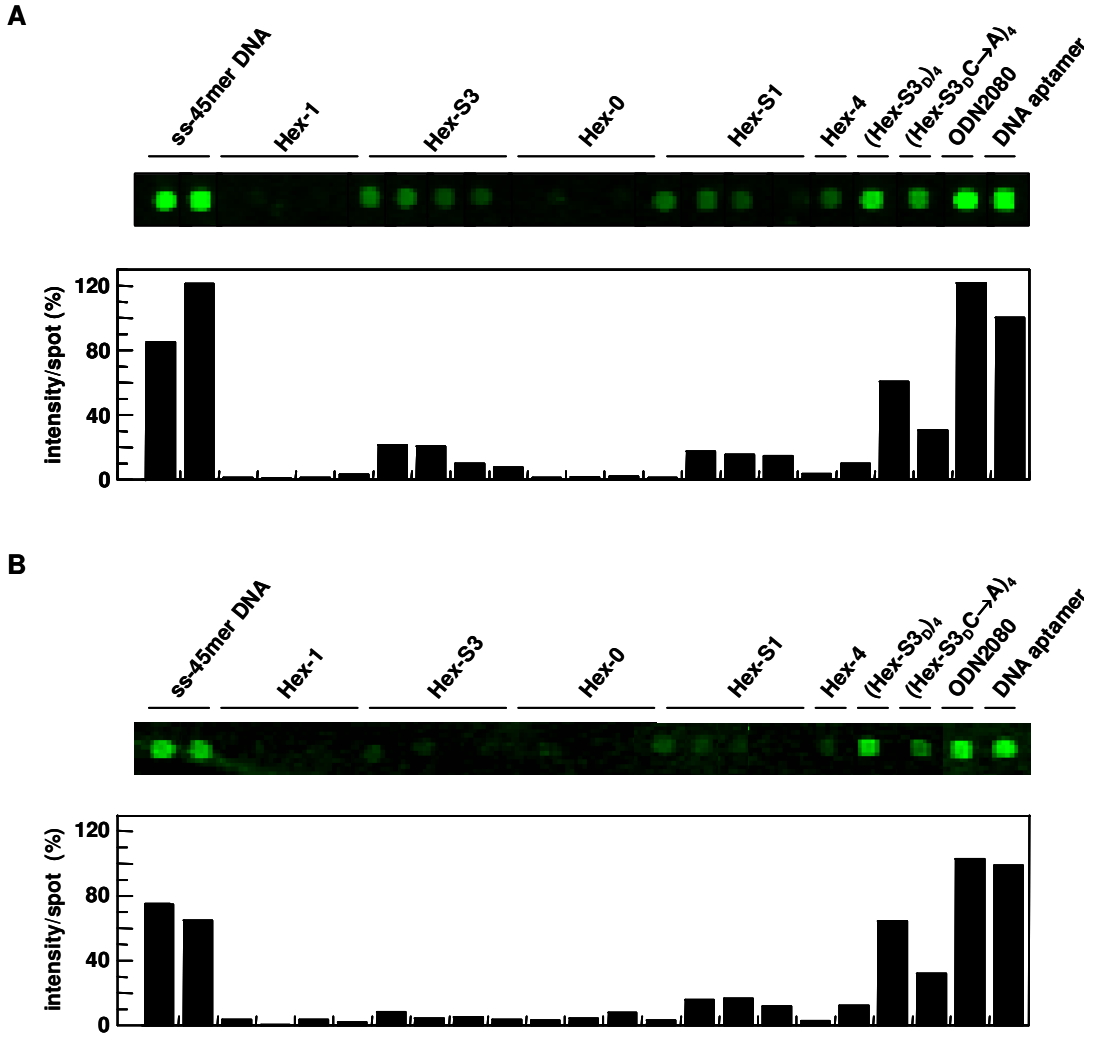

Fig. 3.6.4: Comparison between direct and indirect detection methods of bound protein. (A) An array treated with 500 nM p66/p51^{K281C}Alexa^{488} was scanned and the intensity of each spot was determined and normalised to the DNA aptamer value which was set to 100% intensity/spot. (B) Results obtained with an array incubated with 500 nM unlabelled RT, followed by washing and incubation with 500 nM FITC-labelled RT-directed Ab. The intensity of the spots was determined and normalised as described in (A). All oligo- and hexameric sequences examined were DNA.

3.6.2.2 Importance of surface chemistry and of the linker length on RT binding efficiency and specificity

As previously described, the nucleic acids were printed on glass slides coated with three different matrixes, namely nitrocellulose, epoxy and CodeLink matrixes. This was performed in order to determine which of the three matrixes would fulfill the requirements of specificity, sensitivity and resolution. The testing of the different matrixes was performed by W. Wünsche and the best results were achieved by using the CodeLink surface (data not shown), which was then employed for all further experiments. The

CodeLink matrix (GE Healthcare) consisted of a hydrophilic polymer containing *N*-hydroxysuccinimide ester groups designed to minimise unspecific binding.

Furthermore, the effect of the linker length on RT binding specificity and efficiency was evaluated. The linkers used in this study are shown in Fig. 3.6.1 (B). As described previously, hexanucleotides immobilised at their 5´-end via a 21-, 38-, 72- or 108-atoms linker to the surface were incubated with fluorescently labelled RT. The bound protein was detected via a scanning of the array on a fluorescence scanner and the results are summarised in Fig. 3.6.5 (A). Interestingly, the intensity of the signal per spot decreased proportionally with increasing linker length. This was true for the two RT-binding species, Hex-S3 and Hex-S1, but did not apply to Hex-0 and Hex-1 (negative controls) which did not show any signal. Both 21- and 38-atoms long linkers gave rise to the best signals, indicating that longer linkers may fold on themselves or sterically inhibit the binding of the protein. Moreover, the fluorescence signals were specific for the linker-bound oligonucleotides since nuclease treatment prior to the binding of RT abolished the fluorescence on the solid matrix and the linker alone did not give rise to any signal as well (Fig. 3.6.5 B).

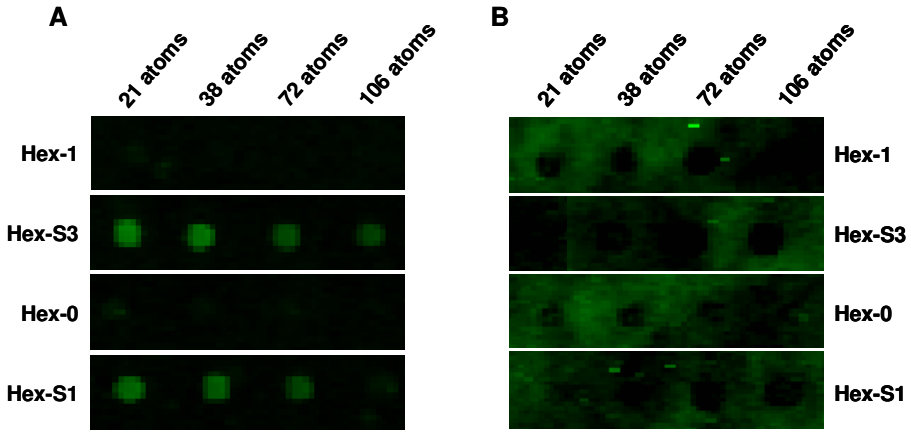

Fig. 3.6.5: Comparison of different linker lengths for the binding of RT to immobilised hexanucleotides. (A) Hexanucleotides covalently attached to 21-, 38-, 72- or 106-atoms linkers were incubated with 500 nM p66/p51^{K281C}Alexa^{488} and the binding results were directly compared. (B) Previous to the incubation with 500 nM p66/p51^{K281C}Alexa^{488}, the array was treated with a solution containing 400 units of Mung Bean- and 400 units of S1-nucleases in a total volume of 100 µl. The reaction was stopped by the addition of 10 mM EDTA and the array was then incubated with the labelled protein, washed and scanned by a fluorescence scanner.

3.6.2.3 Procedures for blocking the array-slides and incubation conditions

To minimise unspecific binding of fluorescently labelled proteins to the CodeLink coated slides, several blocking solutions and conditions were tested. The experiments concerning the optimisation of the blocking procedure were performed by W. Wünsche. Blocking solutions were prepared in RT binding buffer and contained either 1% (w/v) BSA

(RNase-free or non-RNase-free), 2% (w/v) skim milk or 2% (w/v) casein from bovine milk. Additionally, the Array-block (BF-BIOlabs) blocking reagent of unknown composition was also tested. The arrays were incubated in the blocking solution up to 20 h. Already after 2 h of incubation at 23°C, the background level reached a minimum. Among all tested blocking solutions the 2% (w/v) casein in RT binding buffer was the most efficient in saturating the unspecific binding sites on the coated surface and was therefore used in all further experiments. One of the disadvantages in the use of the 2% (w/v) casein was its contamination with nucleases, which led to a very rapid degradation of the RNA hexanucleotides. Therefore, the binding of RT to RNA hexanucleotides could not be tested under these experimental conditions. On the contrary, the DNA hexanucleotides immobilised on the array or free in solution showed a very high stability against nucleases when incubated for 4 h in this blocking solution. Moreover, as a further control, the binding of casein to printed oligo- and hexamers or to radiolabelled oligonucleotides free in solution was also tested, respectively, via the incubation of the array with fluorescein-labelled casein or via filter binding assay. As expected, casein showed very little affinity towards the oligonucleotides and without any significant sequence-specificity.

Experiments were performed in order to improve the binding of RT to printed hexanucleotides. The binding of a protein to a given ligand depends on the ionic composition and strength of the incubation buffer, hence several binding solutions were tested, which included RT binding buffer, RT binding buffer containing 0.1% (v/v) Tween 20, PBS_b with or without 0.1% (v/v) Tween 20, 1x PBS_b containing 100 µg/ml BSA, or customised PBS_b solution containing 100 mM, 50 mM or 5 mM NaCl. The binding of fluorescently labelled RT was compared to control proteins. The solution which yielded the highest specificity with a very high signal/noise ratio was the modified PBS_b solution with 100 mM NaCl and 0.1% (v/v) Tween 20.

Fluorescently labelled RT was incubated up to 16 h on the array for an optimisation of the incubation time. This long incubation led to degradation of the immobilised nucleic acids, but already after 10 s from the beginning of the incubation, RT showed a moderate and differential binding to the oligo- and hexamers. The prolongation of the incubation yielded a proportional increase in the spot intensity, but the relative signal intensities between the investigated species remained the same.

The washing step was also optimised and varied from a few seconds up to 48 h. A proportional detachment of protein was detected during the washing time, but a complete detachment was not seen even after 48 h of washing step.

This array-based method proved to be extremely sensitive since as little as 5 nM fluorescently labelled RT needed to be applied to the array leading to get a clear and specific pattern of highlighted spots. Furthermore, a FITC-conjugated firefly directed-Ab

used as a control protein proved to bind preferentially specific sequences on the array (see 3.6.3) when incubated in RT binding buffer. However, the Ab did not show any binding towards radiolabelled hexa- and oligomers in solution in a filter binding assay under the same experimental conditions.

3.6.3 Binding of HIV-1 RT and control proteins to printed hexanucleotides

A variety of conditions was tested to achieve an unequivocal detection of proteins which bound specifically to the immobilised oligo- and hexamers. The main steps in the array processing are summarised in Table 3.6.2.

Table 3.6.2: Main steps in the array processing

step	duration	solution
1. blocking	2 h at 23°C	2% (w/v) casein in RT binding buffer
2. washing	3x, 10 s each	PBS_b, with 100 mM NaCl and 0.1% (v/v) Tween 20
3. incubation with RT	2 min at 23°C	PBS_b with 100 mM NaCl and 0.1% (v/v) Tween 20
4. washing	3 x, 10 s each	PBS_b, with 100 mM NaCl and 0.1% (v/v) Tween 20
5. fixing	2x, 10 each	100% (v/v) acetone
6. drying	2 min at 23°C	
7. scanning	2 min/array	

The binding of p66/p51^{K281C}Alexa^{488} and of a FITC-conjugated firefly directed-Ab (control) was monitored under two different experimental conditions, i.e. in RT binding buffer or in PBS_b, low NaCl (100 mM NaCl). The two buffers differed in their salt content, with the RT binding buffer containing a lower amount of salt. The control FITC-conjugated firefly luciferase directed-Ab showed specific binding to Hex-$S3_D$, Hex-$S1_D$, Hex-4_D, (Hex-$S3_D$)$_4$, (Hex-$S3_D$C→A)$_4$ and ODN2080, when incubated in RT binding buffer. No binding was seen in PBS_b, low NaCl buffer (Fig. 3.6.6 A). Under both experimental conditions, RT showed a strong binding towards the DNA RT-directed aptamer, the ODN2080 and all the oligonucleotides, as well as the binding to the hexamers Hex-$S1_D$, Hex-$S3_D$ and Hex-4_D (Fig. 3.6.6 A and B), which was consistent with the binding data of Hex-S3 observed in solution (see 3.1.1 and 3.5.4). A similarly clear consistency was observed in the use of the non-binders Hex-0 and Hex-1, albeit the unspecific binding of RT to the negative controls was higher in lower salt conditions (Fig. 3.6.6 B).

In addition, competition experiments were carried out in order to examine whether the binding of the RT towards immobilised Hex-$S3_D$ could be competed by the addition of free Hex-$S3_D$. The array was incubated with fluorescently labelled RT in the presence of a large molar excess (5 x 10^6:1) of free Hex-$S3_D$ or Hex-1_D to the immobilised hexamer. The Hex-1_D served as a negative control. After the incubation, the arrays were scanned and

the results obtained showed an unexpected and clear lack of competition between the free and bound Hex-S3$_D$.

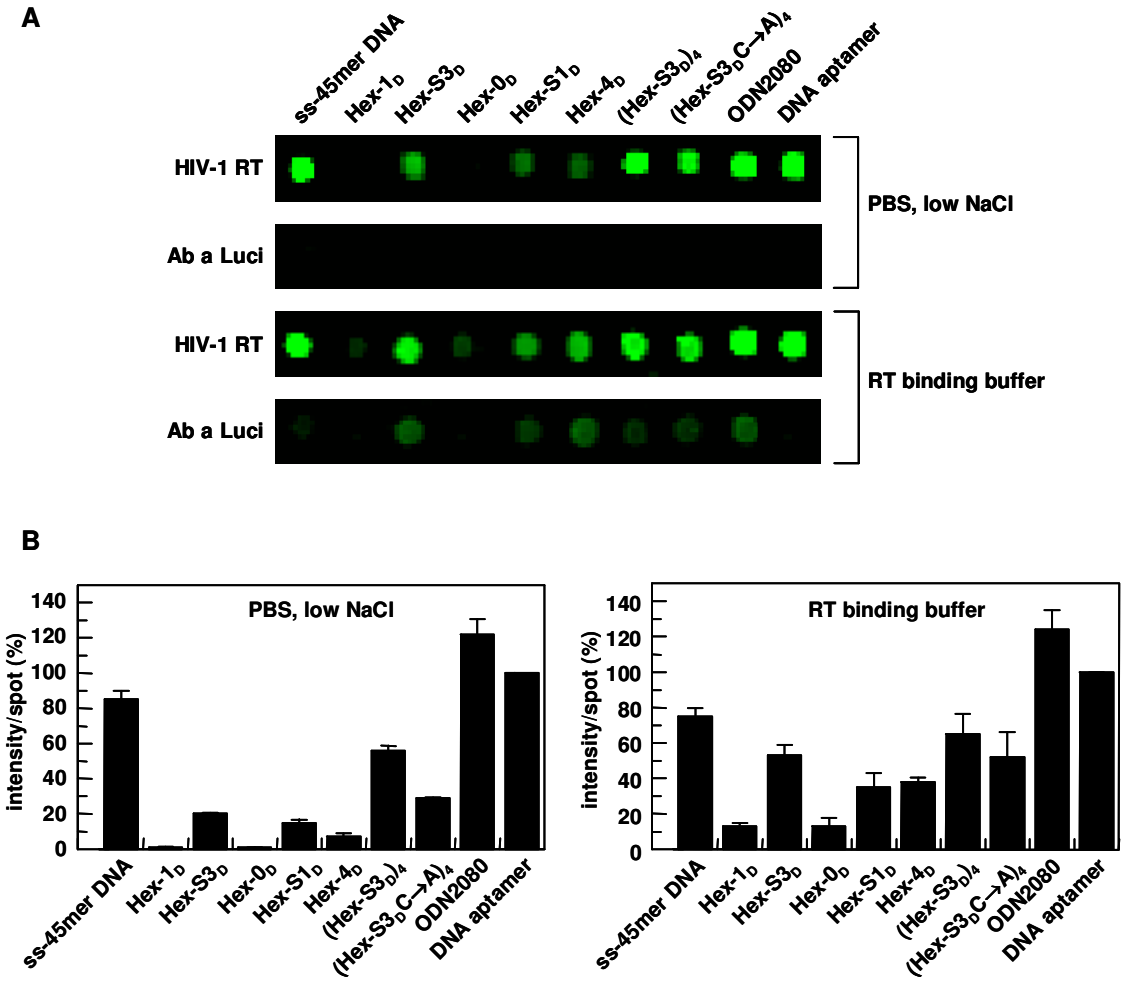

Fig. 3.6.6: Binding of RT and control protein to immobilised hexa- and oligomers under two different experimental conditions. (A) Arrays incubated with 500 nM p66/p51^{K281C}Alexa^{488} or FITC-conjugated firefly luciferase directed-Ab (Ab α Luci) (100 µl total volume) in PBS$_b$, low salt or RT binding buffer. Shown are hexanucleotides linked with a 21-atoms tether. (B) Quantification of arrays incubated with p66/p51^{K281C}Alexa^{488} in PBS$_b$, low salt or RT binding buffer. The intensity per spot in percentage was obtained as the average value of two different spots of the same sequence linked with a 21-atoms tether, and normalised to the DNA aptamer control which was set 100% intensity/spot.

Other control proteins were used in these assays including the T7 RNA polymerase, the BSA, the HIV-2 RT, the TLR9 and the p51 subunit of HIV-1 RT. In all cases, direct fluorescent-labelling of the proteins was performed, and only for a few, i.e. HIV-2 RT and TLR9, the indirect detection via a fluorescently labelled Ab was also employed. In RT binding buffer, and at 500 nM protein concentration, T7 RNA polymerase and HIV-2 RT showed some binding to the printed sequences, with a pattern which resembled the one obtained with HIV-1 RT. However, the ratio between the signal and the noise was very low, making an interpretation of the data difficult. Instead, when incubated in PBS$_b$, low

NaCl buffer, none of those proteins showed any binding to the immobilised hexa- and oligomers.

3.6.4 Recycling of used arrays

Due the high cost of the arrays, a number of procedures for their regeneration was tested. Used arrays were treated with proteinase K or trypsin in order to degrade the bound protein, otherwise the bound protein was denatured by urea treatment. All methods proved to be effective only ta a certain percentage of the recycled array, and a comparable efficiency (data not shown). Briefly, arrays were incubated for 2 h at 37°C in the presence of 2 mg of proteinase K or of a solution containing 0.05% (w/v) trypsin and 0.025% (w/v) EDTA. The proteinases were inactivated by the addition of 5 mM PMSF, followed by incubation for 15 min at 23°C. Alternatively, used arrays were incubated with 7 M urea for 2 h at 23°C. After an extensive washing recycled arrays were scanned to test the complete removal of the bound protein (Fig. 3.6.7). To test whether the degradation or denaturation processes affected the integrity of the oligo- and hexamers immobilised on the surface, a few treated arrays were reincubated with fluorescently labelled RT, followed by a scanning of the bound protein on a Typhoon scanner. The results are shown in Fig. 3.6.7 where a representative array treated with proteinase K, was reused. Although the recycling methods showed a certain effectiveness, the background level on reused arrays was higher when compared to new arrays.

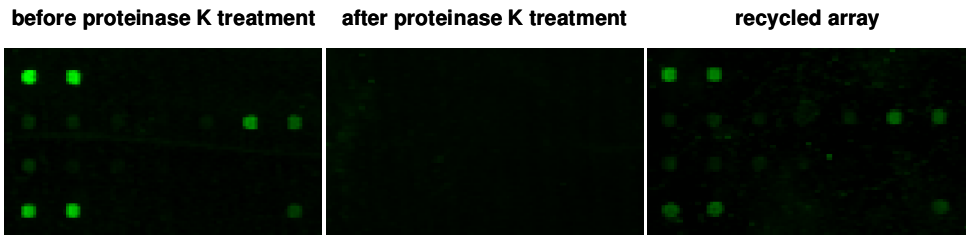

Fig. 3.6.7: Recycling of used arrays. An array incubated with $p66^{E194C}Alexa^{488}$/p51 was scanned prior (left panel) and after (middle panel) the treatment with proteinase K. After inactivation of the protease by PMSF and extensive washing, the array was reincubated with $p66^{E194C}Alexa^{488}$/p51 and the results are shown in the right panel.

4 Discussion

4.1 Proof of concept: hexanucleotides as a promising class of nucleic acid-based therapeutics

This work shows that interactions between hexanucleotides and target proteins occur (see 3.1) and that the binding was highly specific to the nt sequence and to the target protein (see 3.1 and 3.2). Here the HIV-1 RT and the hexanucleotide Hex-S3 (UCGUGU) were chosen for the proof of concept. The affinity of this hexanucleotide in the low micromolar range was related to biological activity in a cell culture system (see 3.3).

This strongly suggests to consider hexanucleotides as a yet unexplored class of nucleic acid-based therapeutics, which may serve as lead compounds for drug development.

This has to be seen in view of the fact that the chemical nature of nucleic acids allows them to take part in a variety of specific and biologically relevant interactions with different classes of molecules, which lay the basis for essential cellular processes. These interactions can be highly specific to the nt sequence, the 3D shape of the nucleic acid or a combination of both.

In the specific case of protein-nucleic acid interactions, the binding and the stabilisation of the complexes are given by a large number of electrostatic interactions, van der Waals interactions, hydrogen bonds and salt bridges between the molecules (59;65). Many proteins bind to nucleic acids in a sequence-independent fashion, others, in contrast, have specifically evolved to bind particular nucleic acid sequences (59;60). For example, sequence-specific binding occurs during the recognition of transcriptional factors or restriction enzymes to their target DNA sequences (62;63). In this case, in order to achieve the necessary specificity the recognition and binding of the two molecules require a large number of contacts. In contrast, only a few contacts are needed to provide strong and specific binding in the interaction between small molecules, such as mono- and dinucleotide and their cognate nucleotide-binding proteins (200;201).

As an extension of mono- and dinucleotides, it was attractive to speculate about a sequence-specific binding of short nucleic acids, such as hexanucleotides, to target proteins. This concept may allow the identification of hexanucleotides, which specifically bind to a target protein, and the interactions between the two molecules may be strong enough to interfere with the activity of the target protein. Thus, these results would be of fundamental importance for clinical drug discovery contributing to the development of novel drugs against the action of relevant pathology-related molecules and of novel tools in molecular biology as well.

Hexanucleotides as a distinct class of potential nucleic acid-based tools and drugs offer several major technical advantages that are not shared by almost all of other classes of nucleic acid-based drugs, such as for example aptamers, ribozymes and siRNA. Hexanucleotides are accessible to large scale chemical synthesis at low prices due to the possibility of solution synthesis. On the level of drug design, the structure-function relationship is simple for hexamer-target recognition. This promotes the screening of systematic libraries to identify lead compounds, and the chances of success of a rational drug design. In pharmacological terms such small molecules may be less prone to nuclease degradation and may show an enhanced cellular delivery compared to longer nucleic acids, leading to an improved pharmacokinetic profile.

At a first glance the possible sequence space composed by hexanucleotides looks rather limited. However, if one considers the currently wide repertoire of chemical modifications of the sugar moiety, the nucleobases, and the internucleotide phosphates or linkages, then the sequence space that can be include in systematic combinatorial approaches is substantially increased.

This is a proof of concept study in the use of an intracellular target protein, which immediately raises the problem of cellular and intracellular delivery. However, one should be aware of the fact that most pharmaceutically relevant targets are located at the cell surface. Therefore, promising future targets should include structures which are accessible from the extracellular site (receptors, e.g. ICAM-1) or the inner site of vesicles such as endosomes (receptors, e.g. TLR9).

Moreover, molecules of only six nt in length are not assumed to fold into any secondary or tertiary structure, thus target specificity might occur through contacts along the quasi linear hexameric molecule. The study of such complexes would lead to new general insights into the field of protein-nucleic acids recognition and interactions.

So far, the selection of nucleic acid ligands towards target proteins has been realised using the SELEX approach (see 1.5.2). In this case, high-affinity nucleic acid ligands are selected from large sequence spaces (~ 10^{15}) against a given target protein. The resulting aptamers are long nucleic acids (30-200 nt), which bind their targets by adaptive recognition. Their high affinity and specificity is based on their ability to fold into complex, 3D shapes which fit into the architecture of the target binding sites (26;40). Previous studies have described the interactions between short chemically-modified oligonucleotides and target proteins. Pinskaya *et al.* (88) selected a PS-modified octanucleotide, which bound to HIV-1 IN with a high affinity, while Wyatt *et al.* (89) showed that an 11mer coupled with an acridine group was able to bind the surface glycoprotein gp120 of HIV-1 and inhibit gp120-mediated cell fusion. However, binding

affinity in those cases was not due to specific primary sequences, but rather to the ability of the PS-modified oligonucleotides to form higher quadruplex structures or the presence of a hydrophobic moiety in the molecule, respectively.

With regard to those binding characteristics the work described here indicates a ´real´ sequence specificity of target recognition.

Effect of Hex-S3 on HIV-1 RT enzymatic activities and functions: The results of the crosslinking experiments and the binding assays indicated that Hex-S3 might be able to inhibit the enzymatic functions of HIV-1 RT despite the high K_d in comparison to the natural substrate p/t. Several assays which comprise RDDP, DDDP and the RNase H activities were performed to test this hypothesis (see 3.4). These assays imitated distinct steps of the viral genome replication. Additionally, the effect on the RT processivity and fidelity were studied. All assays were performed at optimum conditions for the binding of Hex-S3 to RT and under physiological conditions. The hexanucleotide was used in large excess over the p/t substrate and was complexed with RT prior to the addition of the p/t. In none of these assays Hex-S3 affected RT activity and functions. A possible explanation can be derived from the competition experiments, which showed that p/t competed for hexanucleotide binding but not *vice versa*. Apparently, the different affinities towards the enzyme for the p/t (K_d ~ 1 nM) and the Hex-S3 (K_d ~ 5 µM) precluded an inhibitory effect.

Effect of Hex-S3 on viral particle formation and infectivity - Hex-S3 as anti-HIV-1 agent in human cells: Hex-S3 was also tested in human cells by using a recombinant proviral HIV-1 construct (174) (see 3.3). Prior to this experiment, in order to determine whether Hex-S3 could be suited to this application, the stability and the cellular uptake *in vitro* were tested (see 3.3).

Nucleic acid-based drugs are characterised by a low cellular uptake and rapid degradation in physiological fluids, which are the two main limitations for their application *in vivo* (190;191). Due to their small size, hexanucleotides may be less prone to enzymatic degradation and more readily taken up by cells in comparison to longer nucleic acids. Hence, the serum stability of hexanucleotides with an unmodified phosphodiester backbone was determined and compared to longer nucleic acids (24mers) (Fig. 3.3.1 A). The unmodified hexamers showed an increased nuclease resistance (Hex-$S3_R$ $t_{1/2}$ ~ 1.2 min, Hex-$S3_D$ $t_{1/2}$ ~ 3.4 min) compared to the longer oligonucleotides [$(Hex\text{-}S3_R)_4$ $t_{1/2}$ ~ 0.2 min, $(Hex\text{-}S3_D)_4$ $t_{1/2}$ ~ 2.5 min], which was particularly true for the RNA. It appears that such short molecules are less readily recognised as substrate by exo- and endonucleases than longer oligonucleotides. Despite the enhanced nuclease-resistance of the hexanucleotides, the $t_{1/2}$ of these molecules in serum was in the order of a few minutes,

which is not sufficient for an adequate cellular delivery *in vivo*. Thus, for the therapeutic application of hexanucleotides, the insertion of chemical modifications (Fig. 1.3.1) that confers stability against exo- and endonucleases is necessary (28;53;54).

For the *in vitro* application of hexanucleotides, the serum stability was not relevant since human cells could be incubated and treated with inhibitors in customised culture media which did not contain serum. Therefore, the stability of hexanucleotides in such cell culture media was tested (Fig. 3.3.1 B) and the results showed that they were stable during the incubation time (up to 2 h), and consequently could be applied *in vitro* without loss of activity.

Next, the intracellular stability of the hexanucleotides and thus their biological availability was determined. The results showed that at time 0 h after transfection, an amount of about 2.5 x 10^5 molecules was present in each cell, but already after 4 h it was reduced to 7.5 x 10^3 molecules per cell. Interestingly, after 24 h about 5 x 10^3 molecules were still present in each cell, indicating that hexanucleotides were subjected to intracellular degradation, yet only up to a certain extent. Considering that for siRNAs only 300 molecules per cell are needed to lead to a half maximal target suppression, this amount might be sufficient to be biologically active [(202) and our own observation].

The delivery of nucleic acids into cells is a key obstacle for their *in vivo* application, and has to fulfil a number of criteria: (i) the delivery should be cell type-specific, (ii) the nucleic acid should be able to gain entry to the cell through the plasma membrane, and (iii) once intracellular, it should encounter its target. Naked nucleic acids are known to inefficiently penetrate the cellular lipid membrane with only a few molecules gaining entry into the cell (191;192). In cultured cells, exogenously administered naked nucleic acids were proven to enter cells by a combination of fluid-phase (pinocytosis), adsorptive and receptor-mediated endocytosis (192). These data were obtained for oligonucleotides longer than 20 nt. Thus, it is conceivable that small molecules, such as hexanucleotides, may show an enhanced cellular delivery compared to longer nucleic acids. To address this question, the cellular uptake of naked hexanucleotide and longer oligonucleotides (24mers) was examined and compared (Fig. 3.3.3). Surprisingly, only longer oligonucleotides were readily taken up by cells, whereas no internalisation of hexanucleotides was observed. A possible explanation could be that due to their size longer oligonucleotides may be able via direct interaction to activate a specific cell membrane molecule such as a ´channel´ or ´receptor´ that somehow leads to their cellular uptake. Several studies described evidences for a ´receptor´-mediated naked DNA delivery, however none of these studies led to the identification of this receptor (203;204). On the contrary, hexanucleotides may be too small to activate this transport mechanism efficiently. Therefore, for the efficient *in vitro* and *in vivo* application of hexanucleotides,

there is the necessity of employing delivery systems in order to facilitate their cellular internalisation. *In vitro* this can be achieved, for example, via the complexation of hexanucleotides with cationic lipids (e.g. Lipofectamine 2000), or co-precipitation with calcium phosphate.

In conclusion, the extended half-life in culture medium without serum, and the use of a delivery system allowed studying biological effects of hexanucleotides *in vitro*.

The ability of Hex-S3 to exert biological effects, i.e. to negatively interfere with the production of HIV-1 viral particles and their infectivity in human cells, was analysed by using a recombinant proviral construct (174). This system is based on a replication-defective HIV-1 viral vector which contains a rudimentary HIV-1 genome where the env and most of the regulatory and accessory genes of HIV-1 are removed and which contains the firefly luciferase as a marker gene (Fig. 3.3.4 A). In this study, packaging HEK293T cells were co-transfected with the luciferase-harbouring defective HIV-1 genome, the plasmid-encoded VSV-G-envelope protein and hexanucleotides. Transfected cells released infectious recombinant particles that were subsequently used to infect recipient cells in which the luciferase gene expression was determined to monitor infectivity (Fig. 3.3.4 B). The results showed that increasing amounts of Hex-$S3_R$ led to a strong, concentration-dependent decrease in firefly luciferase activity, which reflected infectivity, in newly infected HEK293 cells. The IC_{50} value for Hex-$S3_R$ was determined to be 1.8 (± 0.2) µM (Fig. 3.3.5 A). If one compares this IC_{50} value with the ones observed, using the same viral system, for the two strong RT inhibitors, AZT (79 nM) and S-TIBO (101 nM) (193), the approximately 10-fold difference in comparison to these drugs is surprisingly low.

Further experiments showed that the infectivity of the viral particles produced in the presence of only parental vectors was time-dependent (Fig. 3.3.5 B) and reached a maximum level at 36 h after the transfection. In contrast, pseudoviruses produced by the cells treated with Hex-$S3_R$, showed a persistent low level of luciferase activity, indicating a constant and long-term influence of Hex-S3 on the infectivity of viral particles.

To investigate at which stage of the HIV-1 life cycle the Hex-$S3_R$ interfered leading up to 1,000-fold decrease in viral particle infectivity, several aspects of the viral cycle were analysed. Fist, the production and release of pseudoviruses by packaging cells treated with Hex-$S3_R$ was monitored by a p24-specific ELISA. The results showed that treatment with Hex-$S3_R$ yielded a reduced total number of viral particles released (Fig. 3.3.6). However, when normalised to the amount of p24, those particles showed the same infectivity in comparison to particles produced in the presence of the negative control, Hex-1_R. This strongly indicates that the Hex-$S3_R$-specific inhibitory step occurred in

packaging cells rather than during the early steps of the infection, and that Hex-$S3_R$ was not incorporated into the viral particles causing inhibition of reverse transcription during the infection step. Hexanucleotides having a DNA backbone were also tested in this system. Interestingly, the infectivity and the amount of the viral particles released by the cells were strongly reduced by the treatment with each DNA hexanucleotide, independent of their sequence. Since the transfection efficiency of the two vectors was unaffected by the addition of either DNA or RNA hexanucleotides, this strong unspecific inhibition by the DNA hexanucleotides suggests a sequence-unspecific effect on viral particles production and release.

Since no reverse transcription takes place in the packaging cells and Hex-$S3_R$ was unable to inhibit RT *in vitro*, the possibility was considered that Hex-$S3_R$ interfered with viral gene expression or the maturation of the Gag precursor. These two processes are essential for viral production and release, and in particular, alterations in Gag polyprotein processing were shown to strongly affect viral particle assembly and maturation (205;206). To address these possibilities, the viral gene expression and Gag precursor processing in packaging cells treated with Hex-$S3_R$ was investigated by western blotting. The results showed that Hex-$S3_R$ neither affected viral protein expression nor the Gag precursor processing (Fig. 3.3.7 B and C), suggesting an alternative mechanism whereby Hex-$S3_R$ interfered with the viral particle release. Importantly, the Ab used in this study was specific only for the Gag precursor and not for the GagPol precursor, therefore no data are available concerning the processing of the longer precursor, which could also be a step affected by Hex-$S3_R$.

Interestingly, the HIV-1 RT-directed aptamer pseudoknot was shown to interfere with viral particles production in a similar way as shown for the Hex-$S3_R$ (165), leading to a reduction of about 75% in viral particle production in cells co-transfected with infectious proviral HIV-1 DNA. In this system reverse transcription did not take place either, indicating that beyond its effect on RT and reverse transcription, this aptamer may be involved in alternative pathways which interfered with viral particle production.

It is conceivable that Hex-$S3_R$ and pseudoknot may affect viral packaging by direct binding to the RT domain within the premature GagPol precursor. In this scenario the binding of Hex-$S3_R$ or pseudoknot to the GagPol precursor may interfere with the formation of Gag/GagPol complexes leading to altered Gag/GagPol ratios within the complexes. The ratio between the two precursors has been shown to play an important role in RNA genome dimerisation and packaging, and its alteration was shown to reduce infectivity of progeny viruses (207-210). Alternatively, the binding of Hex-$S3_R$ and pseudoknot to GagPol may interfere with the trafficking of those precursor complexes to the host cell plasma membrane. Mutations within the highly conserved residues in the

primer grip domain of RT gene caused similar effects (211). Another possibility could be that the binding of the inhibitors to the GagPol precursor may affect selective packaging of the $tRNA^{Lys3}$ primer into the viral particles (212-214).

It is noteworthy that all the attempts to test Hex-$S3_R$ during the infection step failed, since the transfection of cells with Hex-$S3_R$, prior or subsequent to their infection with viral particles led to a dramatic loss in cell fitness, leading to cell death (data not shown).

Taken together these results showed that Hex-$S3_R$ blocked the assembly of infectious particles probably by physical interaction with RT within the GagPol precursor, although it was unable to interfere with the enzymatic activities of the viral polymerase *in vitro*.

4.2 Combinatorial selection approaches for target-specific hexanucleotides

The findings obtained in the use of Hex-S3 as ligand for HIV-1 RT, as well as inhibitor of HIV-1 viral particles production *in vitro*, support the view that even short oligonucleotides are able to bind specifically to a given target protein and exert biological activity. Thus, hexanucleotides may be considered an as yet unexplored class of compounds with a number of highly promising characteristics for drug development, such as simple chemical features, they are amenable for chemical optimisation, and accessible to large scale chemical synthesis. Furthermore, the option of screening systematic libraries to identify lead compounds and the possibility of a rational drug design exist.

Their limited sequence space 4^6 (4,096) provides the possibility to perform a fast and systematic search for hexanucleotides that bind to a given target in a sufficiently specific and tight manner, thereby representing a first lead.

One of the most crucial findings of this work is the high degree of consistency in qualitative terms between the sequence-specific binding of hexanucleotides to RT in solution *versus* the array-based setup which was surprising (see 3.6.3). Even though this may not be reflected by absolute affinities this finding suggests to make use of the array technology as a powerful and suitable tool for systematic and highly efficient search for hexanucleoitde binders. On the more mechanistic and academic level it seems to be worth to have a closer look and the thermodynamics and kinetics of the interaction of surface-bound hexamer and target. In terms of improvements of novel technology this study suggests to develop an array technology that is suitable to measure binding of very short oligonulceotides to proteins and other entities of pharmaceutical and biomedical interest, such as carbohydrate structures or lipoproteins.

As a combinatorial extension of this study, a selection approach in solution for the search of hexanucleotide ligands to HIV-1 RT was established (see 3.5). This approach involved cloning steps for sequencing which introduced a certain bias, therefore as a more reliable and sensitive alternative to this method, a hexanucleotide array-based approach was conceived. Accordingly, to test whether such an array-based approach was feasible, an oligonucleotide-based array, including selected oligo- and hexanucleotides was developed (see 3.6).

Combinatorial selection in solution of HIV-1 RT-directed hexanucleotides: For the selection of target-directed hexanucleotides a SELEX based-approach (37) cannot be performed because flanking regions would be required, which serve as primers for the subsequent amplification by PCR. Very recently, a non-SELEX approach has been described (87) and applied for the selection of non-amplifiable libraries. In this system the steps of amplification and strand separation were omitted and the partitioning was performed via capillary electrophoresis. Remarkably, only three rounds of selection led to the identification of oligonucleotides (80 nt in length) with high affinity (K_d in the order of nM) for the target protein.

In order to establish a combinatorial approach for the selection of hexanucleotides which bind to HIV-1 RT in solution, several methods were tested including chromatographic-, microbeads-, and filter binding-based approaches (Fig. 3.5.1). All methods were first tested for their stringency, whose evaluation was based on the background level when Hex-S3 was used as a positive and Hex-1 as a negative control. The attempts to use methods based on chromatography failed, since Hex-S3 and Hex-1 showed the same retention time in the presence of HIV-1 RT using MicroSpin- and gravity-flow-based gel filtration chromatography, indicating that the systems were not stringent enough for an efficient separation of bound from unbound hexanucleotides. In HPLC RT:Hex complexes were not stable during the chromatography and were eluted as separate fractions. A microbead-based approach in which HIV-1 RT was immobilised on Ni^{2+}-coated beads was unsuccessful because the nucleic acids bound to the surface of the beads. In a filter binding-based system which was previously successfully applied to select aptamers against various targets (37;163;215), about 50% of Hex-S3 and only less than 1% of Hex-1 bound to RT (Fig. 3.1.1), indicating that this system was sufficiently stringent and allowed the discrimination between binders and non-binders. However, only hexanucleotides having a DNA backbone could be used in this approach, since the cloning strategy, necessary for the sequencing of the selected species, required the use of enzymes, such as the terminal transferase and the T4 RNA ligase, which did not recognise RNA hexanucleotides as substrates.

A randomised pool of hexanucleotides having a DNA backbone, containing all possible 4,096 (4^6) different sequences, was subjected to the selection procedure. After cloning, the sequence analysis of the selected species revealed seven different sequences, five hexamers (Hex-FB1, ATAGAG; Hex-FB2, GTCTAT; Hex-FB3, TCGTGA; Hex-FB4, GTAGAG; Hex-FB5, TTTTTT) and two pentamers (Pentamer-FB1, CCGGG; Pentamer-FB2, CATGA) (Fig. 3.5.3). The two pentamers resulted probably from a truncation during the cloning procedure. The most abundant species were Hex-FB1 and Hex-FB2, which were found in 46% and 28% of the clones, respectively.

To determine whether in the starting random pool of hexanucleotides there was a bias for certain sequences, it was also subjected to cloning and sequencing. The sequence analysis of the starting pool showed that Hex-FB1 was present in two clones, Hex-FB4 in one clone, while none of the other selected species was found (data not shown). Based on the nt frequencies at each position a consensus sequence Hex-0 (AGAGAG) could be derived (Table 3.5.1), which suggested that there was a bias for certain sequences in the original random pool. It is at present not clear whether the bias had already been introduced during the chemical synthesis of the starting pool or in subsequent cloning steps. Interestingly, the selected Hex-FB3 was almost identical to the control Hex-$S3_D$ (A *versus* T at the 3´-end), and Hex-FB2 differed only by one nt from Hex-4_D (T *versus* A at the 3´-end) (Fig. 3.1.1 and Table 3.1.1).

Thus, the selection from the random pool of hexanucleotides was successful and allowed the identification of novel species and sequences, which were very similar to known HIV-1 RT-binding hexanucleotides.

In order to evaluate the relative affinities of the selected sequences for RT, they were compared in a filter binding assay. Under the conditions used during the selection procedure (high temperature and high salt conditions), the amount of the hexamers and pentamers bound to RT was below 5% of the input (Fig. 3.5.4). The Hex-S3 and Hex-S1, which were included as positive controls, showed a 1.5% binding, while Hex-0 showed 0.15% binding to RT. Among the selected species, Hex-FB4 and Pentamer-FB2 showed a comparable binding to RT, whereas Hex-FB1 (5%), Hex-FB2 (3.5%), Hex-FB3 (2.5%), Hex-FB5 (4%) and Pentamer-FB1 (2%) bound more strongly to RT than Hex-S3. This showed clearly that the very stringent conditions applied during the selection procedure allowed the successful identification of a number of species which bound more tightly than Hex-S3 to the enzyme.

The binding assay was also performed under the conditions established to be optimal for the binding of Hex-S3 to RT (low temperature and low ionic strength) (Fig. 3.5.4). In this case, all selected hexanucleotides and the control Hex-S3 showed

between 30% and 60% binding. The affinity of the two pentameric species was about one-tenth in comparison to the hexameric species (Fig. 3.5.4). Under these conditions, 0.1% Hex-0 bound to RT, while the three hexanucleotides, Hex-FB2, Hex-FB3 and Hex-FB5 showed a higher binding (~ 60%) to RT compared to Hex-S3 (~ 50%). The Hex-FB4 and Hex-FB1 respectively showed the same binding (~ 50%) or lower binding (~ 35%) to enzyme when compared to the control Hex-S3. Additionally, Hex-S1 showed lower binding (30%) to RT in comparison to Hex-S3. Accordingly, also under these milder experimental conditions three selected hexanucleotides (Hex-FB2, Hex-FB3 and Hex-FB5) bound with a higher affinity to RT than Hex-S3. However, for Hex-FB1, which, at high temperature and high ionic strength, showed almost 3-fold stronger binding to RT than Hex-S3, at lower stringency a loss of affinity was observed in comparison to Hex-S3. Instead, the Hex-FB4 and Hex-S3 displayed a similar binding behaviour under both experimental conditions. On the contrary, the binding of the pentameric sequences did not substantially change under different experimental conditions, indicating that even at a low temperature and ionic strength pentanucleotides were not tight binders for RT. This confirmed the previous results of filter binding assays using the truncated versions of Hex-S3 (Fig. 3.2.4 B). Interestingly, the replacement of a T with a G at the 2 position from the 5´-end in the sequence of Hex-FB1 (which led to the Hex-0 sequence), affected dramatically its affinity for the protein under both experimental conditions. The Hex-FB1 too, differed from Hex-FB4 by a single nt and the replacement of an A with a G at the first position from the 5´-end, did not affect the binding at high temperature and salt conditions, while it led to almost 2-fold increased binding at low temperature and salt conditions. Moreover, the selected Hex-FB3 differed from the control Hex-$S3_D$ by one nt (T *versus* A at the 3´-end). Under both tested experimental conditions, the binding strength of the selected Hex-FB3 was slightly higher than for Hex-$S3_D$. Also Hex-FB2 and Hex-4 (Fig. 3.1.1) differed by one nt at their 3´-end (T *versus* A) and the replacement of a T with an A, in this case led to a 3.5-fold decreased binding towards RT. These data indicated a contribution of the 3´-end nucleotide to the binding. In the filter binding assay of the mutated (U *versus* A at the 3´-end) Hex-$S3_R$ and HIV-1 RT (Fig. 3.2.4 A) the same replacement led to a slight decrease of the affinity, providing further evidence in support of this assumption. However, the opposite effects in Hex-FB2 and Hex-FB3 point to a dominant role of the remaining sequence and thus confirmed the initial results of the filter binding assay (Fig. 3.2.4 A) with systematically mutated Hex-$S3_R$ hexanucleotides. Additionally, the individual hexanucleotides were different in their sensitivity towards the experimental conditions, and thus, there is an indication for different modes of binding.

Although the sequences may not have been equally represented in the original library, the applied selection procedure was able to overcome the bias since only two of the five identified hexanucleotides had a similar sequence.

Towards an array-based selection of target-specific hexanucleotides; development of an oligonucleotide-based array: In order to facilitate the analysis and selection of hexanucleotides which bind to HIV-1 RT with high affinity, an array-based approach was conceived. This approach would render the cloning steps unnecessary. Furthermore truncated sequences would not occur, a large number of targets could be screened in parallel, and RNA could be investigated. This array would contain all possible 4,096 (4^6) hexameric sequences, and allow the rapid and specific detection of target proteins bound to immobilised hexanucleotides. Therefore, to test whether such an array-based approach is feasible, an oligonucleotide-based array, which included ten selected oligo- and hexanucleotides was designed and validated through a ´proof of concept´ RT binding assay.

The sequences printed on the array included non-RT-binding hexanucleotides (Hex-1 and Hex-0), RT-binding hexanucleotides (Hex-S3, Hex-S1 and Hex-4) and RT-binding oligonucleotides [ss-45mer, $(\text{Hex-S3}_\text{D})_4$, $(\text{Hex-S3}_\text{D}\text{C}\rightarrow\text{A})_4$, ODN2080_D and a RT-directed RT1t49 aptamer (92)] (Table 3.6.1). The hexameric sequences were linked at their 5´-termini by a tether to the solid surface. The long oligonucleotides were 5´-end biotinylated and bound to the support via immobilised streptavidin. Each hexameric sequence was included as DNA or RNA. Attempts to detect the RNA homologues failed, since they had been subjected to a rapid degradation in the presence of blocking solution. Therefore, only the hexadeoxynucleotides could be tested for binding to RT.

Several experimental conditions for the array processing were investigated to minimise unspecific binding of the target, increase the detection sensitivity, and resolution. A number of surface chemistries, linker lengths, blocking and binding conditions, and detection strategies were compared for affinity and specificity to the protein. Highest specificity, sensitivity and resolution, was observed when using a CodeLink surface (GE Healthcare), which consisted of a hydrophilic polymer containing NHS ester groups designed to minimise unspecific binding. Additionally, four different linker lengths (21-, 38-, 72- or 108-atoms) were compared (Fig. 3.6.1 B). Interestingly, both short linkers gave rise to stronger signals compared to the longer ones, suggesting that longer linkers may fold on themselves and sterically hinder the binding of RT (Fig. 3.6.5 A). A nuclease treatment prior to the binding of RT abolished the fluorescent-signal and the linker alone did not give rise to a signal. Therefore, the fluorescent-signals were specific to the linker-coupled oligonucleotides (Fig. 3.6.5 B).

The unspecific binding to the matrix of fluorescently labelled RT was minimised by using an optimised blocking solution [2% (w/v) casein], which did not show a bias for the tested hexa- and oligonucleotides in control binding assays.

The binding interactions between immobilised hexa- and oligonucleotides and RT or control proteins, i.e. FITC-conjugated firefly directed-Ab were highly dependent on the ionic strength. The buffer which led to the highest specificity with a very high signal/noise ratio was the modified PBS_b solution with 100 mM NaCl and 0.1% (v/v) Tween 20. Interestingly, when the amount of the salt was below 100 mM, unspecific binding of the control proteins could be detected, while above 100 mM NaCl RT showed almost no binding towards the hexanucleotides (Fig. 3.6.6 A and B). This suggested that the ionic interactions played a fundamental role for the binding between hexanucleotides and proteins, by influencing the electrostatic component of these interactions.

As detection strategies two methods were tested, i.e. a direct approach using labelled RT and an indirect approach in which bound RT was detected by a fluorescently labelled RT-directed Ab (Fig. 3.6.2). In the direct detection system two different labelling methods were applied, i.e. radio- and fluorescent-labelling.

Despite its very high sensitivity (lower limit of detection = 150 amol protein), the use of ^{125}I-radiolabelled RT proved to be unsuited for this application (Fig. 3.6.3 B) due to the detection procedure, which required the exposure of the array to a PhosphorImager screen prior to scanning, resulting in radioactive signal spread over the whole surface of the array. Therefore, a second labelling system was employed, which was based on the fluorescent-labelling of the protein (lower limit of detection = 0.1-1 fmol) (Fig. 3.6.3 C). In this case, a high binding specificity and low background were observed (Fig. 3.6.3 D and 3.6.4 A). A second advantage of the direct detection was the fact that the binding behaviour of RT was unaffected by the chemistry, position or amount of a fluorescent-label. On the contrary, a reduced fluorescent-intensity per spot compared to the directly labelled RT was observed when using an indirect detection approach (Fig. 3.6.4 B). Accordingly, only the strong interactions between RT and the longer oligonucleotides were still visible, while the differences in the binding among the hexanucleotides were diminished and closed to background level.

Under the optimised conditions HIV-1 RT showed a strong binding towards the DNA RT-directed aptamer, the ODN2080 and all the oligonucleotides, as well as binding to the hexamers Hex-$S1_D$, Hex-$S3_D$ and Hex-4_D (Fig. 3.6.6 A and B), which was consistent with binding data of Hex-S3 observed in solution (see 3.1.1 and 3.5.4). Similar consistency was observed in the use of the non-binders Hex-0 and Hex-1 (Fig. 3.6.6 B). So far, for unknown reasons, the strong binding of RT to the immobilised hexanucleotides has been unable to be competed by the addition of free hexanucleotides. A possible explanation

would be an increased affinity of the proteins towards the densely immobilised hexanucleotides.

In conclusion, the conceived array-based approach for the selection of hexanucleotides is possible in principle. Furthermore, it has been shown that such arrays can be reused by removing bound protein, considerably reducing the costs. However, the optimisation of the blocking solution for the use of an RNA array remains an unsolved question. It remains to be seen whether hexanucleotides which bind to other proteins can be identified via this approach. Nevertheless, this should be possible in principle. Conditions which have to be met are the availability of labelled functional protein or of antibodies against these targets which do not compete for the binding to hexanucleotides.

4.3 A detailed analysis of the interactions between target proteins and hexanucleotides

Characterisation of the interactions between hexanucleotides and target proteins: In this study, to investigate whether specific interactions between short and unstructured hexanucleotides and given target proteins occur, a set of hexameric sequences were chosen, having either an RNA or a DNA backbone and their binding capability and specificity were compared. The RNA hexanucleotides were chosen, since the 2´-OH group at the ribose ring may allow additional contacts compared to the deoxy-ribose. In addition, RNA is known to interact with a variety of molecules, and displays a higher flexibility, which allows it to adopt a greater number of conformations. However, generally RNA is more prone to degradation than DNA due to the presence of the 2´-OH, making it less suitable for *in vivo* applications.

As target model targets, two proteins which play a major role in the development of important diseases were chosen, namely the HIV-1 RT (see 1.7.2) and the hPrP. The hPrP is a normal ubiquitous protein in mammalian cells, which through a posttranslational process can be converted into the human prion protein disease-related scrapie form ($hPrP^{Sc}$), leading to fatal neurodegenerative diseases (216;217). The firefly luciferase, which was also chosen as a model target, catalyses a reaction which yields visible light, and has a broad range of application as a tool in molecular and cellular biology (218). The three proteins used as targets in this ´proof of concept´, have completely different characteristics and the only one which is known to naturally interact with nucleic acids is the HIV-1 RT.

To analyse the interactions between hexanucleotides and target proteins a filter binding assay was employed, in which the five different hexameric sequences were incubated with the target proteins. The results of this assay revealed that hexanucleotides

interacted with target proteins in a way which was specific to the nt sequence and the target protein (Fig. 3.1.1). All hexanucleotides preferentially bound HIV-1 RT (up to 80% bound hexanucleotide) rather than firefly luciferase and hPrP proteins (< 2% bound hexanucleotide), and this could be explained by the natural predisposition of RT to interact with nucleic acids, which the other two proteins lack. In addition, different sequences displayed different specificity and affinity towards the target proteins. This strongly indicated that the interactions were dependent on the pattern of functional groups at the bases. Furthermore, the RNA and the DNA versions of the same sequence showed, in most of the cases, a differential binding towards a given protein. This suggests that the functional groups at the 2´-position of the ribose and at the 5-position of the thymidine and uracil bases play important roles in dictating the affinity and specificity of these molecules. This was particularly true for the hPrP which bound only to hexanucleotides having a DNA backbone.

Remarkably, the binding of Hex-S3 (UCGUGU and TCGTGT) to the RT was the only complex which was not affected by the replacement of those chemical moieties, since both RNA and DNA versions of Hex-S3 bound to RT with a comparable affinity. This suggested that in this case the six 2´-OH groups and the three 5-methyl groups in the hexameric RNA molecule did not influence its binding affinity towards RT and seemed to be dispensable for the binding to RT.

Interestingly, the DNA and RNA versions of Hex-5 (GGCAAC), which have an identical base composition and differ only because of the replacement of deoxy-ribose with ribose, displayed a differential binding towards the target proteins. In this case, the lack of a 2´-OH led to a higher affinity towards HIV-1 RT and hPrP, while it reduced the binding to the firefly luciferase, indicating the importance of the functional group at the 2´-position of the ribose in the interaction with these proteins.

Taken together, this experimental evidence indicated that the contributions of the sugar-phosphate backbone and the functional groups of the specific bases depended on the individual interaction and a general rule could not be deduced. Each hexameric sequence has specific moieties that provide a special chemical signature to the molecule, which is differentially recognised by the target proteins.

The strong binding of Hex-S3 to RT and the similarity in binding behaviour of its DNA and RNA versions to RT, made this hexanucleotide very attractive for further studies, and a more detailed analysis on this species was performed. The interactions between Hex-S3 and RT were studied in depth, and affinity, specificity, binding site and biological effects of Hex-S3 for the protein were determined.

Affinity and specificity of Hex-S3 for HIV-1 RT: The filter binding and the EMSA approaches, which are widely used to study nucleic acid-protein interactions, were employed to investigate the formation of Hex-S3-RT complexes (Fig. 3.2.1 A and B). The first method is based on the ability of the nitrocellulose filters to retain nucleic acids complexed with proteins, while the EMSA approach is based on the retardation in the mobility of nucleic acid-protein complexes compared to unbound nucleic acid when subjected to electrophoresis. The two positive controls, the RNA aptamer pseudoknot (131;164;165) and DNA aptamer RT1t49 (92) aptamers directed against RT, bound with a high affinity to RT in the filter binding assay and produced a clear shift in the EMSA. This could be explained by the high stability of the aptamer:RT complexes which display an off-rate in the order of 0.0002 s^{-1} ($t_{1/2}$ ~ 1 h) (164), and by the high affinity of the two aptamers towards RT, which is reflected by K_d values of 25 pM (164) and 4 nM (92), respectively for the RNA and DNA aptamers. In both assays, the negative control, Hex-1, as expected, did not bind to RT, while Hex-S3 in the filter binding assay showed a relatively strong binding (40%) to RT in comparison to the aptamers (100%), and only a partial retardation in its mobility in the EMSA. These findings suggest that the stability of the complexes, probably reflected by a very fast off-rate of the hexanucleotide, may not be sufficient to allow the detection of RT:Hex-S3 complexes under the stringent EMSA conditions, but sufficient to be detected in a ´quick´ filter binding assay.

Equilibrium binding experiments, employing a filter binding assay, radiolabelled Hex-S3 and RT yielded apparent K_d values of 5.3 (± 0.5) µM for the Hex-$S3_R$ and 9.4 (± 2.4) µM for Hex-$S3_D$ (Fig. 3.2.2). These findings further suggested a high similarity in binding behaviour between Hex-$S3_R$ and the homologue Hex-$S3_D$. Surprisingly, the maximum of bound hexanucleotide was reached at 80% and not at 100% as one would have expected. For this reason, as control experiments, equilibrium titrations of RT in the presence of RNA/DNA p/t were performed (data not shown) and led to an identical plateau ending at 80% maximum binding. This was possibly due to a saturation of the filters during the filter binding assay or to a detachment of the bound nucleic acid during the extensive washing step.

The high specificity of Hex-S3 for HIV-1 RT in comparison to hPrP and the firefly luciferase raised the question whether this was also true for other proteins including structurally and functionally related polymerases. Therefore, binding studies were performed with: (i) the small subunit p51 of HIV-1 RT, (ii) HIV-2 RT (iii) EIAV RT, (iv) T7 RNA polymerase, and (v) BSA (Fig. 3.2.3). The results showed a highly specific binding of the DNA and RNA versions of Hex-S3 towards HIV-1 RT and a weak or absent binding to

all other proteins. This great reduction in binding in comparison to HIV-1 RT was especially surprising for HIV-2 RT which is highly homologous to the HIV-1 enzyme (60% identity and 13% homology) (188;219). The EIAV RT also exhibits a high sequence identity (42%) to HIV-1 RT (220). In addition, all three RTs are heterodimers with a large subunit (66 kDa) and a small (51-58 kDa) that share a common amino terminus (221). The T7 RNA polymerase is less related to HIV-1 RT than the other RTs, but still it displays extensive structural homology to the HIV-1 RT (222;223). The lack of binding of Hex-S3 to the smaller subunit of HIV-1 RT suggested that the binding site on RT maybe be located on the p66 subunit on a surface created by the association of the two subunits in the heterodimer. The ability of Hex-S3 to differentiate between the structural and functional closely related polymerases was remarkable, and implied that a site-specific interaction between HIV-1 RT and Hex-S3 occurs.

Role of the functional groups and hexameric backbone of Hex-S3 on the interactions with HIV-1 RT: The binding affinity and specificity of Hex-S3 was shown to be unaffected by the exchange of ribose with deoxy-ribose, or the substitution of an uracil with a thymine. To elucidate the importance of the single nucleobases for the binding to RT a stepwise replacement of the original nt with an adenosine, which is absent in the Hex-S3 sequence, was performed and the Hex-S3 derivatives were assayed for binding to HIV-1 RT in a filter binding assay (Fig. 3.2.4 A). The result clearly indicated that the positions 3 to 6 (GUGU) played an important role in the interaction with RT, opposed to the terminal nt at positions 1 and 2. Thus, bases towards the 3´-terminus of the molecule were required for binding, while the 5´-terminus was less important. Furthermore, it was also demonstrated that the phosphate group at the 5´-terminus of the hexameric sequence was not relevant for the binding to RT and could be replaced by a 5´-OH group.

The importance of the hexameric sugar/phosphate backbone in the interaction with the protein was also determined. The shortened derivatives of Hex-S3 tested showed no significant binding to RT (Fig. 3.2.4 B). This clearly implied that the hexameric backbone of Hex-S3 was essential for the interaction with RT.

Heptanucleotides derived from Hex-S3 by addition of one nt at either terminus showed up to 4-fold stronger binding to RT while still being specific to the target, i.e. to HIV-1 RT *versus* HIV-2 RT (Fig. 3.2.4 C). The extension of the hexameric molecule to a 12mer or 18mer showed a further increased affinity, but was accompanied by a loss of specificity (Fig. 3.2.4 D). A possible explanation for the loss of specificity and increased affinity is that the binding mode of Hex-S3, i.e. binding to a specific pocket on the protein surface, changes at increasing chain length in such a way that it resembles natural substrates of this polymerase.

Further studies using chemically modified Hex-S3-derivatives led to additional information on the role of functional groups on the Hex-S3 molecule for affinity and specificity towards RT (Table 3.2.1). The replacement of the 2´-H at the 2´-position of ribose with an O-methyl group led to a dramatic decrease in binding strength towards RT, while the substitution of the 2´-H with 2´-fluoro did not affect the affinity and a slight increase in specificity was observed. These findings implied that small groups at the 2´-position were tolerated, while bulkier groups such as an O-methyl were unfavourable due to steric hindrance. The LNA derivative modified at position 1 showed a decreased affinity to RT and this could be explained by a change in conformation of the hexameric molecule after the insertion of this nt which is modified by an extra bridge connecting 2´- and 4´-carbons, locking the ribose in 3´-endo conformation (Fig. 1.3.1) (28).

The PS derivatives of Hex-S3 were also tested. These analogs have a sulfur atom in place of one non-bridging oxygen at each inter-nucleotide linkage (Fig. 1.3.1), and are isoelectronic with natural sugar-phosphate backbone. An increased affinity and a decreased specificity towards RT were observed, which is not surprising, since other studies described, besides the high affinity of PS-modified oligonucleotides toward their targets, their unspecific interaction with certain proteins, particularly those that interact with polyanions, and the reason behind this unspecificity is not yet fully understood (54). Furthermore, the substitution of oxygen with sulfur at position 4 of the uracil at position 4 of the hexameric molecule had no effect on binding affinity and specificity. This derivative was chosen for further crosslinking experiments and the position 4 of the hexameric molecule was shown to play an important role in the binding to RT.

Taken together these findings indicated that a hexameric backbone and the stretch 5´-GUGU-3´ of Hex-S3 were necessary for efficient binding to RT. The elongation of the hexamer by one nt at either terminus increased affinity without affecting specificity. Further, the 2´-position at the sugar could tolerate small functional groups and at the bases could tolerate the presence of a methyl group at 5 position of thymine and the replacement at the uracil ring of the oxygen at the 4 position with a sulphur without changes in the binding behaviour.

The binding site of Hex-S3 on HIV-1 RT: In order to map the binding site on HIV-1 RT, a 4-thio uracil derivative of Hex-$S3_R$, which was proven to bind with the same affinity and specificity as the unmodified Hex-$S3_R$, was crosslinked by UV treatment to HIV-1 RT. The free-radical intermediate generated by photo-activation of 4-thio uracil is known to crosslink only at very close range (several Å) and to be quite indiscriminate with respect to reacting groups within a polypeptide chain (224). Therefore, this method allows the mapping of specific RNA-protein contacts. As described here, the fact that Hex-S3 did not

bind to the p51subunit of HIV-1 RT in a filter binding assay (Fig. 3.2.3), suggested that the binding site on RT may be located on the p66 subunit on a surface created by the association of the two subunits in the heterodimer. This first experimental evidence was confirmed by the results of the crosslinking experiment, since only the large subunit p66 was crosslinked (Fig. 3.2.5 A). To determine whether Hex-S3 had a specific binding site within the p66 subunit, a CNBr treatment of the crosslinked protein was performed and among the resulting fragments only two were labelled, i.e. one fragment of 141 aa (aa 42-183, indicated by green color in Fig. 3.2.5 B), which carried approximately one third of the label and the second fragment of 125 aa (aa 231-356, indicated by red color in Fig. 3.2.5 B), which carried about two thirds of the label (Fig. 3.2.5 A). The 141 aa fragment included part of the fingers and the palm subdomains, while the 125 aa fragment included the thumb and part of the palm subdomains of the polymerase domain. These findings implied a binding site of Hex-S3 in the vicinity of both labelled fragments, but pointing more in the direction of the thumb subdomain, since the 125 aa fragment carried 60% of the label.

Additional information on the binding site of Hex-S3 were derived from competition experiments with a 18/36mer Flo1/Flo6 p/t (186), a RNA pseudoknot aptamer (131;163;164), as well as the non-nucleoside inhibitor S-TIBO (189). The TIBO compounds belong to the class of the NNRTIs and block the RT reaction through interaction with a hydrophobic pocket adjacent to the polymerase active site on the p66 subunit. This interaction causes structural modifications, which lead to a decreased nt incorporation rate (122;125;156;157). TIBO have been shown to stabilise an open conformation of the RT, i.e. a rotation of the p66 thumb domain of about 30-40°, generating a large nucleic acid binding site (126;225), which leads to an increased affinity of the enzyme for the p/t (122;226). Experimental evidence described in this study showed that S-TIBO increased the binding strength of the hexanucleotide towards RT (Fig. 3.2.6 A), indicating that the binding of this hexanucleotide ligand required the thumb domain to be in an upright position. The RNA pseudoknot aptamer, which was also used in this study, induces and stabilises a closed conformation of the polymerase through extensive electrostatic interactions with several basic residues of the p66 thumb and in the p66 fingers domain (131). This aptamer seems to inhibit RT by binding to a site that partly overlaps the p/t binding site (131;164). The competition studies showed that p/t and aptamer competed for hexanucleotide binding but not *vice versa* (Fig. 3.2.6). The inability of Hex-S3 to inhibit the interactions of RT with the natural p/t substrate or an aptamer (Fig. 3.2.6 B) is probably the result of the different affinity of the p/t (K_d in the range of low nM) and aptamer (K_d = 25 pM) (164) for the protein compared to the one of the hexanucleotide (K_d ~ 5.3 µM). Additionally, the binding of Hex-S3 was affected by the addition of p/t and

when the p/t was bound to the enzyme no binding was noticed for the Hex-S3. This indicated that the bound p/t blocks the binding site of the hexanucleotide on the RT. On the other hand, when the hexanucleotide was bound to the RT the high affinity of the p/t for the protein displaced the hexanucleotide from its binding site, probably inducing a close conformation and so obliterating the binding site of the hexanucleotide on the protein that, as described above, binds to RT preferentially in a open conformation.

A model was derived by rigid-body docking studies of HIV-1 RT and Hex-S3 based on these experimentally derived constraints (Fig. 3.2.6 C). According to this model, Hex-S3 bound the p66 subunit at the bottom of the thumb subdomain pointing towards the nucleic acid binding cleft of the viral polymerase, and the binding of Hex-S3 required the thumb domain to be in an upright position.

5 Conclusions and Perspectives

Taken together, the findings described in this thesis strongly suggest that hexanucleotides might be considered as an as yet unexplored class of compounds with a number of highly promising characteristics for drug development. The results observed for Hex-S3, indicated that hexanucleotides in general may provide high specificity and sufficient binding affinity for a given target and, thus, represent attractive lead compounds.

Several strategies can be envisaged to further increase the binding affinity and, hence, the biological activity of Hex-S3. First, rational drug design in the classical sense could be based on docking studies with the known 3D structure of HIV-1 RT. Second, saturation transfer difference nuclear magnetic resonance (STD NMR) (227) could be exploited to determine the critical residues for binding of Hex-S3 to RT, which in turn can be chemically modified potentially leading to increased binding strength. Third, systematic pools of unmodified or chemically modified hexanucleotides can be tested for specific binding to RT or any other target of interest in an array-based selection approach. This array would include all 4,096 hexanucleotides, and the positive and negative controls tested in the ´trial´ array. The results obtanined in the use of the ´trial´array further suggest a linker length of 21- or 38-atoms and a DNA backbone. This would allow, in principle, to perform an extremely rapid and systematic search for hexanucleotides that bind to a given target sufficiently specific and tight, thereby representing a first lead. Interesting targets would certainly be proteins which play an important role in diseases, e.g. the TLR9 (228-230) and the intercellular adhesion molecule-1 (ICAM-1) (231;232), which are involved in inflammation and autoimmunity, and viral proteins, such as the hepatitis C virus RNA-dependent RNA polymerase (HCV polymerase) (233;234) and the hepatitis A virus 3C proteinase (HAV 3C proteinase) (235;236), which are important in viral infections.

6 Summary

The work described in this thesis addressed the question whether small nt were able to exhibit specific binding for target proteins with an affinity which is high enough to be biologically relevant. Such compounds might be suitable for drug development against a variety of infectious and other diseases.

As a ´proof of concept´ I investigated the highly specific binding of the hexanucleotide UCGUGU (Hex-S3) to the HIV-1 RT, a key enzyme for viral replication. The results revealed that Hex-S3 interacted with HIV-1 RT in a way which was highly specific to the nt sequence and the target protein, since Hex-S3 did not bind to the highly related HIV-2 and EIAV RTs. Binding studies using a set of Hex-S3 derivatives indicated that the specific interaction depended on the length and sequence of the nt and occurred with an affinity of ~ 5.3 µM (K_d). Competition experiments and UV-crosslinking studies suggested a site-specific binding of Hex-S3 to the large subunit of RT (p66) at the bottom of the thumb subdomain pointing towards the substrate binding cleft of the viral polymerase.

In human cells, Hex-S3 proved to suppress in a dose-dependent manner (IC_{50} ~ 1.8 µM) HIV-1 viral particle production by up to three orders of magnitude, indicating that it exerted specific and biologically relevant activity. However, *in vitro* biochemical analyses of the enzymatic activity of RT in the presence of Hex-S3 did not indicate a difference that could explain the observed strong inhibition of HIV-1 infectivity in cell culture. Thus, short hexanucleotides, can be selected which possess a high specificity for a given target protein and exert biological effects.

In order to develop a method for the identification of hexanucleotide ligands from a random library covering the whole sequence space (4,096), which bind with high affinity to different proteins, the feasibility of combinatorial selection approaches was investigated. A selection approach in solution allowed the identification of seven different sequences, and five of them showed an improved affinity for HIV-1 RT, proving that the combinatorial selection of hexanucleotides can be successfully performed. However, this approach involved cumbersome cloning steps for sequencing that potentially might lead to the introduction of a bias for certain sequences, which are preferentially accepted by the cloning enzymes. Furthermore, an erroneous amplification might occur, leading to wrong sequence information and this approach is limited to DNA based hexanucleotides. Therefore, to overcome these limitations, a hexanucleotide array-based approach was conceived as a more reliable and sensitive alternative. A test array containing selected oligo- and hexanucleotides was designed and after an optimisation of the conditions for the analysis, shown to be a valid and promising alternative to the selection in solution.

7 Zusammenfassung

Spezifische Wechselwirkungen von Nukleinsäuren mit Proteinen sind von fundamentaler Bedeutung für den Metabolismus und die biologische Funktion aller lebenden Zellen. Auch für die Diagnostik- und Therapie-orientierte medizinische Forschung besitzen Nukleinsäureliganden von zellulären Proteinen eine große Bedeutung (44;45). Dementsprechend ist die Identifizierung und mechanistische Aufklärung natürlicher sowie im Labor entwickelter Nukleinsäureliganden Gegenstand intensiver aktueller Forschung.

Insbesondere die Bindung von Nukleinsäuren an lösliche und membranständige Proteine ist in pharmakologischer und therapeutischer Sicht von Interesse und aus bisherigen Untersuchungen ist bekannt, dass die molekularen Wechselwirkungen von der Primärsequenz der Nukleinsäuren, ihrer dreidimensionalen Struktur (Konformation) oder einer Kombination aus beiden bestimmt sein können, jedoch lässt sich bislang kein allgemein gültiges Prinzip ableiten (59-64).

Zur Identifizierung von Nukeinsäureliganden, die mit hoher Affinität an Proteine binden, wurden verschiedene Strategien entwickelt. Hierzu zählen das *Systematic Evolution of Ligands by Exponential Enrichment* (SELEX) Verfahren (39) und *Microarray*-basierte Verfahren. Unter Verwendung von SELEX konnten *in vitro* aus randomisierten Bibliotheken einige hundert Nukleotide große RNA und DNA Aptamere von biomedizinischer Bedeutung (38) identifiziert werden. Die Aufklärung der 3D Struktur einiger Aptamere hat ergeben, dass ihre Spezifität auf einer stark angepassten, stabilen 3D Struktur beruht (40;46). Grundsätzlich ist die *Microarray*-Technologie ebenfalls geeignet, die Bindung von Nukleinsäuren an Proteine *in vitro* nachzuweisen (80;86). Hierbei wird eine große Anzahl von Nukleinsäuren unterschiedlicher Sequenz auf einem Träger in einem *Spot*-Verfahren immobilisiert und die Bindung von Proteinen anschließend durch direkte oder indirekte (z.B. sekundäre markierte Antikörper) Methoden nachgewiesen (86).

Die intrinsische Instabilität von Nukleinsäuren in physiologischen Flüssigkeiten und ihre begrenzte Aufnahme durch Zellen limitiert ihren Einsatz bislang *in vivo*. Um diese Einschränkungen zu überwinden, sind verbesserte Wirkstoff-Transportsysteme sowie chemisch veränderte Nukleinsäurederivate entwickelt worden, die bei einer unveränderten biologischen Aktivität eine erhöhte Stabilität gegenüber Exo- und Endonukleasen aufweisen (28;54;55). Verschiedene hochaffine Nukleinsäureliganden sind gegen die Reverse Transkriptase des HIV-1 (HIV-1 RT) entwickelt worden, das eine zentrale Rolle im Infektionszyklus dieses Virus einnimmt und somit einen geeigneten Ansatzpunkt zur Therapie der HIV-1 Infektion darstellt (74;156 158;163). Unter Verwendung des SELEX konnten Tuerk *et al.* (164) ein RNA Molekül (RNA pseudoknot) identifizieren, welches mit einer

sehr hohen Affinität (K_d = 25 pM) an die HIV-1 RT gebunden hat und eine starke inhibitorische Wirkung gegenüber dem HIV-1 aufwies (165;166). Bei diesen inhibitorisch aktiven Nukleinsäuren handelte es sich im Allgemeinen um relativ große Moleküle, die in Lösung eine stabile Tertiärstruktur ausbilden.

Auf der Basis dieser Ergebnisse, war es zunächst das Ziel meiner Arbeit zu untersuchen, ob auch relativ kleine Hexanukleotide, die in wässriger Lösung eine größere strukturelle Flexibilität besitzen, eine ausreichende Spezifität und Affinität in der Bindung an Proteine aufweisen können, um in der medizinischen Diagnostik oder Therapie erfolgreich eingesetzt werden zu können. Um diese Frage zu untersuchen, habe ich als Modellsystem die HIV-1 RT gewählt, da gegen dieses Enzym bereits erfolgreich hoch affine Nukleinsäureliganden isoliert werden konnten (s.o.) und es gleichermaßen ein zentrales Enzym des Replikationszyklus des HIV-1 ist, was die biologische Funktion bzw. deren Hemmbarkeit mit Hexameren erleichtern sollte. Weitergehend sollte die Interaktion u. a. unter Verwendung chemisch modifizierter Nukleotidliganden biochemisch charakterisiert werden, um einen tieferen Einblick in die molekularen Grundlagen der Bindung von kleinen Oligonukleotiden an Proteine zu erhalten. Es wurden u.a. DNA(Hex_D)- und RNA(Hex_R)-basierte Hexanukleotide, sowie 2´-Deoxy-2´-Fluoro, 2´-O-Methyl, Phosphorthioate, *Locked Nucleic Acid* (LNA) und 4-thio-Uracil modifizierte Derivate eingesetzt. Bindende Hexanukleotide sollten anschließend auf ihre inhibitorische Wirkung gegenüber den Enzymaktivitäten der Reversen Transkriptase sowie auf ihre antiviralen und pharmakologischen Eigenschaften, wie z.B. Serumresistenz, Membrangängigkeit und Halbwertszeit im Zytoplasma, untersucht werden. Da es unter Verwendung geeigneter Selektionsverfahren gelingen könnte, aus synthetischen Hexanukleotid-Bibliotheken Liganden gegen biomedizinisch relevante Proteine im allgemeinen zu identifizieren, war ein weiteres wichtiges Ziel meiner Arbeit, technische Bedingungen zu etablieren, unter denen eine derartige Selektion erfolgreich durchgeführt werden kann.

Um die spezifische Bindung von Hexanukleotiden an die HIV-1 RT, die Luciferase der amerikanischen *firefly* (*Photinus pyralis*) und dem humanen Prion Protein (hPrP), nachweisen zu können, wurden Filterbindungsassays sowie der *Electrophoretic Mobility Shift Assay* (EMSA) eingesetzt. Vergleichende Bindungsstudien unter Verwendung von Hex_R und Hex_D unterschiedlicher Sequenz ergaben, dass alle ausgewählten Hexanukleotide eine messbare Bindung an die drei untersuchten Proteine zeigten. Diese Bindung war sequenzabhängig und spezifisch für das jeweilige Protein, wobei die Beteiligung des Ribosephosphat-Gerüsts und der funktionellen Gruppen der Basen von der jeweiligen Interaktion abhingen und keine allgemein gültigen Aussagen gemacht werden konnten. Es konnte gezeigt werden, dass das Hexanukleotid Hex-S3 (Hex-$S3_R$, UCGUGU;

Hex-S3$_D$, TCGTGT) eine vergleichsweise hohe Affinität und Spezifität für die Bindung an die HIV-1 RT aufwies.

Aus diesem Grund wurde dieser Komplex näher untersucht und die Affinität, Spezifität, die Bindungsstelle und biologische Wirkungen des Hex-S3 bestimmt. Die Affinitätsmessung von Hex-S3$_R$ und Hex-S3$_D$ ergab K_d Werte von 5.3 (± 0.5) µM and 9.4 (± 2.4) µM. Besonders bemerkenswert war die Beobachtung, dass das Hex-S3 keine Bindung an die strukturell und funktionell verwandten HIV-2 RT, *equine infectious anemia virus* (EIAV) RT und die T7 RNA-Polymerase zeigte.

Die Bedeutung der einzelnen Basen, der funktionellen Gruppen sowie der Länge des Hex-S3 für die Bindung an HIV-1 RT wurde durch Einsatz synthetischer Derivate untersucht. Die 5´-terminale Sequenz 5´-GUGU-3´ sowie eine Länge des Backbones von sechs Phosphodiester-Bausteinen des Hexanukleotids waren für die Bindung von essenzieller Bedeutung, da Positionsmutanten und kürzere Nukleotide eine deutlich verringerte Bindung aufwiesen. Um die Bindungsstelle des Hex-S3 näher zu bestimmen, wurde eine Photoaffinitätsmarkierung mit einem radioaktiv markierten 4-thio-Uracilderivat (an Position 4) von Hex-S3$_R$, gefolgt von einer CNBr-Spaltung, durchgeführt. Das Ergebnis deutete darauf hin, dass das Hex-S3 an die p66 Untereinheit an der Basis der „Daumenuntereinheit“ gebunden hat. Kompetitive Hemmexperimente mit einem 18/36mer *primer/template* (191), einem RNA Aptamer (164), sowie dem Nicht-Nukleosid Inhibitor S-TIBO (192) ergaben, dass sich das Hex-S3 unterhalb der Nukleinsäure-Bindestelle der viralen Polymerase erstreckte und dass sich die Daumenuntereinheit in einer horizontalen Position befand.

Aufgrund der Bindungsdaten, war es vielversprechend die hemmende Wirkung des Hex-S3 in der Zellkultur auf die Produktion viraler Partikel und ihrer Infektiosität zu untersuchen. Hierzu wurde ein rekombinantes Replikations-inkompetentes HIV-1-System mit dem proviralen HIV-1 Konstrukt [pGJ3 luci (243)] in einem zellulären Assay eingesetzt. In diesem System werden HEK293 T-Zellen (*packaging cells*) mit zwei Vektoren ko-transfiziert, welche die Bildung von Pseudoviren bewirken. Diese Viren sind infektiös, bilden jedoch nach Re-infektion keine infektiösen Partikel. Die virale Genexpression nach Transduktion wurde mit einem Luciferase-Reporterassay bestimmt. Die von den transfizierten Zellen freigesetzten Pseudoviren wurden mittels ELISA unter Verwendung eines Antikörpers gegen das p24-Kapsidprotein quantifiziert und die virale Genexpression mittels Western Blot Analyse mit anti-HIV-1 Antikörpern bestimmt. Die Zugabe steigender Mengen von Hex-S3$_R$ bei Transfektion von *Packaging*-Zellen führte zu einer starken konzentrationsabhängigen Verringerung der Zahl infektiöser Partikel, wobei der IC_{50} Wert des Hex-S3$_R$ 1.8 (± 0.2) µM betrug. Des Weiteren zeigten die Hex-S3$_R$ Zellen eine

durchweg geringere Luciferase-Aktivität. Dies deutet darauf hin, dass die Hex-S3-spezifische Hemmung der Bildung infektiöser Partikel in den *Packaging*-Zellen stattfand und nicht in der zweiten Infektionsrunde, wobei die virale Genexpression in den *Packaging*-Zellen und die Prozessierung des Gag-Vorläufermoleküls von der Wirkung des Hex-S3 unbeeinträchtigt waren. Da in den *Packaging*-Zellen keine reverse Transkription stattfindet und Hex-$S3_R$ RT *in vitro* nicht inhibieren konnte, wäre eine mögliche Erklärung die, dass Hex-$S3_R$ durch Interaktionen mit der RT innerhalb des Gag-Pol-Vorläufermoleküls das „Assembly" viraler Partikel beeinträchtigt.

Die hemmende Wirkung des Hexanukleotids Hex-S3 auf die Bildung infektiöser viraler Partikel *in vitro* sowie die in Bindungsassays und im *Crosslinking* Experiment gezeigte spezifische Bindung an die HIV-1 RT, legten eine Beeinträchtigung einer der enzymatischen Aktivitäten des Enzyms nahe. Aus diesem Grund wurden Enzymaktivitätsmessungen mit unterschiedlichen natürlichen Substraten durchgeführt. Obwohl Hex-S3 die HIV-1 Infektiosität signifikant verringerte und mit mikromolarer Affinität (K_d ~ 5 µM) HIV-1 RT gebunden wurde, konnte keine Hemmung der enzymatischen Aktivitäten und Funktionen der HIV-1 RT *in vitro* nachgewiesen werden. Eine Erklärung hierfür ist wahrscheinlich eine nicht ausreichende Affinität des Hex-S3 im Vergleich zu der des p/t Substrats (K_d ~ 1 nM), wodurch keine kompetitive Hemmung bei der eingesetzten Konzentration erreicht wurde.

Aufgrund der spezifischen Bindung von Hexanukleotiden an Proteine, sah ich die Möglichkeit der Selektion von HIV-1 RT spezifischen Hexanukleotiden aus einer randomisierten Bibliothek aller möglichen Sequenzen. Hierzu wurden zunächst Experimente in Lösung durchgeführt, in denen HIV-1 RT mit der Hexanukleotid-Bibliothek (4^6 = 4.096 Spezies) ko-inkubiert wurden und anschließend das Protein mit gebundenen Hexamer-Spezies mitels eines Filters abgetrennt und isoliert wurden. Nach Elution der gebundenen Hexanukleotide konnten deren Sequenzen in einem speziellen Klonierungsverfahren bestimmt werden. Hierdurch gelang die Identifizierung von Sequenzen, die mit deutlich höherer Affinität als das Hex-S3 an die HIV-1 RT gebunden wurden. Somit ist die Selektion von bindenden Hexanukleotiden in einem kombinatorischen Ansatz grundsätzlich möglich. Das Verfahren zur Klonierung ist jedoch methodisch aufwendig und intrinsisch mit Fehlern behaftet. Um eine Verbesserung des Verfahrens zu erreichen, habe ich die Methodik für ein *Array*-Verfahren etabliert, in dem der Klonierungsschritt umgangen werden kann. Für diesen Ansatz wurde zunächst ein Versuchsarray entwickelt, auf dem selektierte Oligonukleotide mit bekannten Bindungseigenschaften immobilisiert wurden. Nach Inkubation des Arrays mit dem Protein konnte die Bindung direkt, bei Einsatz von fluoreszenzmarkierter HIV-1 RT, oder durch fluoreszenzmarkierte sekundäre Antikörper

nachgewiesen werden. Hingegen war der Einsatz radioaktiv markierten Proteins technisch unbefriedigend. Nach Optimierung der Blockierungsmethode des Arrays und der Waschbedingungen nach den Bindungsschritten konnten eindeutige Bindungsdaten erhalten werden. Die Ergebnisse zeigten, dass das Bindungsverhalten den Ergebnissen der Filterbindungsexperimente entsprach. Somit erscheint die Anwendung eines *Array*-Verfahrens grundsätzlich möglich und vielversprechend.

Zusammenfassend konnte gezeigt werden, dass Hexanukleotide trotz ihrer geringen Größe und ihrer hieraus resultierenden flexiblen Struktur grundsätzlich in der Lage sind, spezifisch an Proteine zu binden. Dies wurde für die HIV-1 RT beispielhaft gezeigt. Gleichermaßen besaß das hier untersuchte Hexanukleotid Hex-S3 *in vitro* eine hemmende Wirkung gegenüber der Bildung infektiöser viraler Partikel des HIV-1. Dennoch konnte keine hemmende Wirkung der enzymatischen Aktivitäten beobachtet werden. Kompetitive Bindungsexperimente lassen vermuten, dass keine ausreichende Affinität im Vergleich zum normalen Substrat erreicht wurde. Die erfolgreiche Selektion von weiteren hochspezifischen Sequenzen aus einer randomisierten Bibliothek von Hexanukleotiden in einem Filterbindungsexperiment sowie die Etablierung der Methodik für ein *Array*-basiertes Verfahren haben die Basis gelegt, um Sequenzen zu identifizieren, die verbesserte Bindungseigenschaften aufweisen. Die beobachtete biologische Wirkung legt jedoch nahe, dass Hexanukleotide eine Klasse von Molekülen darstellen, die eine Reihe von Charakteristika aufweisen, die sie für die Medikamentenentwicklung als geeignet erscheinen lassen. Hierzu zählen eine einfache synthetische Chemie, die eine Optimierung durch rationales *Drug Design* ermöglichen, der Zugang zur chemischen Synthese im großen Maßstab und insbesondere die Option des systematischen Durchsuchens von Bibliotheken, um Basisstrukturen zu identifizieren, die in ihren biomedizinischen Eigenschaften beliebig verändert werden können und als Grundlage für die Entwicklung neuartiger Medikamente dienen können.

8 References

1. Hershey,A.D. and Chase,M. (1952) Independent functions of viral protein and nucleic acid in growth of bacteriophage. *J.Gen.Physiol*, **36**, 39-56.

2. Alberts,B. (2003) DNA replication and recombination. *Nature*, **421**, 431-435.

3. Krieg,A.M. (2006) Therapeutic potential of Toll-like receptor 9 activation. *Nat.Rev.Drug Discov.*, **5**, 471-484.

4. Opalinska,J.B. and Gewirtz,A.M. (2002) Nucleic-acid therapeutics: basic principles and recent applications. *Nat.Rev.Drug Discov.*, **1**, 503-514.

5. Doudna,J.A. and Lorsch,J.R. (2005) Ribozyme catalysis: not different, just worse. *Nat.Struct.Mol.Biol.*, **12**, 395-402.

6. Fedor,M.J. and Williamson,J.R. (2005) The catalytic diversity of RNAs. *Nat.Rev.Mol.Cell Biol.*, **6**, 399-412.

7. Schroeder,R., Barta,A. and Semrad,K. (2004) Strategies for RNA folding and assembly. *Nat.Rev.Mol.Cell Biol.*, **5**, 908-919.

8. Noller,H.F. (2005) RNA structure: reading the ribosome. *Science*, **309**, 1508-1514.

9. Moore,P.B. and Steitz,T.A. (2003) After the ribosome structures: how does peptidyl transferase work? *RNA.*, **9**, 155-159.

10. Mandal,M. and Breaker,R.R. (2004) Gene regulation by riboswitches. *Nat.Rev.Mol.Cell Biol.*, **5**, 451-463.

11. Kaempfer,R. (2003) RNA sensors: novel regulators of gene expression. *EMBO Rep.*, **4**, 1043-1047.

12. Tucker,B.J. and Breaker,R.R. (2005) Riboswitches as versatile gene control elements. *Curr.Opin.Struct.Biol.*, **15**, 342-348.

13. Schwalbe,H., Buck,J., Furtig,B., Noeske,J. and Wohnert,J. (2007) Structures of RNA switches: insight into molecular recognition and tertiary structure. *Angew.Chem.Int.Ed Engl.*, **46**, 1212-1219.

14. Cheah,M.T., Wachter,A., Sudarsan,N. and Breaker,R.R. (2007) Control of alternative RNA splicing and gene expression by eukaryotic riboswitches. *Nature*, **447**, 497-500.

15. Matera,A.G., Terns,R.M. and Terns,M.P. (2007) Non-coding RNAs: lessons from the small nuclear and small nucleolar RNAs. *Nat.Rev.Mol.Cell Biol.*, **8**, 209-220.

16. Kugel,J.F. and Goodrich,J.A. (2007) An RNA transcriptional regulator templates its own regulatory RNA. *Nat.Chem.Biol.*, **3**, 89-90.

17. Goodrich,J.A. and Kugel,J.F. (2006) Non-coding-RNA regulators of RNA polymerase II transcription. *Nat.Rev.Mol.Cell Biol.*, **7**, 612-616.

18. Kiss,T. (2002) Small nucleolar RNAs: an abundant group of noncoding RNAs with diverse cellular functions. *Cell*, **109**, 145-148.

19. Caprara,M.G. and Nilsen,T.W. (2000) RNA: versatility in form and function. *Nat.Struct.Biol.*, **7**, 831-833.

20. Rana,T.M. (2007) Illuminating the silence: understanding the structure and function of small RNAs. *Nat.Rev.Mol.Cell Biol.*, **8**, 23-36.

21. Sarnow,P., Jopling,C.L., Norman,K.L., Schütz,S. and Wehner,K.A. (2006) MicroRNAs: expression, avoidance and subversion by vertebrate viruses. *Nat.Rev.Microbiol.*, **4**, 651-659.

22. Irvine,D.V., Zaratiegui,M., Tolia,N.H., Goto,D.B., Chitwood,D.H., Vaughn,M.W., Joshua-Tor,L. and Martienssen,R.A. (2006) Argonaute slicing is required for heterochromatic silencing and spreading. *Science*, **313**, 1134-1137.

23. Noma,K., Sugiyama,T., Cam,H., Verdel,A., Zofall,M., Jia,S., Moazed,D. and Grewal,S.I. (2004) RITS acts in cis to promote RNA interference-mediated transcriptional and post-transcriptional silencing. *Nat.Genet.*, **36**, 1174-1180.

24. Dawe,R.K. (2004) RNA interference on chromosomes. *Nat.Genet.*, **36**, 1141-1142.

25. Rassoulzadegan,M., Grandjean,V., Gounon,P., Vincent,S., Gillot,I. and Cuzin,F. (2006) RNA-mediated non-mendelian inheritance of an epigenetic change in the mouse. *Nature*, **441**, 469-474.

26. Breaker,R.R. (2004) Natural and engineered nucleic acids as tools to explore biology. *Nature*, **432**, 838-845.

27. Breaker,R.R. (1997) DNA enzymes. *Nat.Biotechnol.*, **15**, 427-431.

28. Bumcrot,D., Manoharan,M., Koteliansky,V. and Sah,D.W. (2006) RNAi therapeutics: a potential new class of pharmaceutical drugs. *Nat.Chem.Biol.*, **2**, 711-719.

29. Corey,D.R. (2007) RNA learns from antisense. *Nat.Chem.Biol.*, **3**, 8-11.

30. Stein,C.A. and Cheng,Y.C. (1993) Antisense oligonucleotides as therapeutic agents-is the bullet really magical? *Science*, **261**, 1004-1012.

31. Gewirtz,A.M., Sokol,D.L. and Ratajczak,M.Z. (1998) Nucleic acid therapeutics: state of the art and future prospects. *Blood*, **92**, 712-736.

32. Nagatsugi,F., Sasaki,S., Seidmen,M.M. and Miller,P.S. (2002) Mutagenesis targeted by triple-helix forming oligonucleotides containing a reactive nucleoside analogue. *Nucleic Acids Res.Suppl*, 31-32.

33. Mende,M., Hopert,A., Wünsche,W., Overhoff,M., Detzer,A., Borngen,K., Schlenke,P., Kirchner,H. and Sczakiel,G. (2007) A hexanucleotide selected for increased cellular uptake in cis contains a highly active CpG-motif in human B cells and primary peripheral blood mononuclear cells. *Immunology*, **120**, 261-272.

34. Nimjee,S.M., Rusconi,C.P. and Sullenger,B.A. (2005) Aptamers: an emerging class of therapeutics. *Annu.Rev.Med.*, **56**, 555-583.

35. Sullenger,B.A. and Gilboa,E. (2002) Emerging clinical applications of RNA. *Nature*, **418**, 252-258.

36. Ellington,A.D. and Szostak,J.W. (1990) In vitro selection of RNA molecules that bind specific ligands. *Nature*, **346**, 818-822.

37. Tuerk,C. and Gold,L. (1990) Systematic evolution of ligands by exponential enrichment: RNA ligands to bacteriophage T4 DNA polymerase. *Science*, **249**, 505-510.

38. Hermann,T. and Patel,D.J. (2000) Adaptive recognition by nucleic acid aptamers. *Science*, **287**, 820-825.

39. Morris,K.N., Jensen,K.B., Julin,C.M., Weil,M. and Gold,L. (1998) High affinity ligands from in vitro selection: complex targets. *Proc.Natl.Acad.Sci.U.S.A*, **95**, 2902-2907.

40. Bunka,D.H. and Stockley,P.G. (2006) Aptamers come of age - at last. *Nat.Rev.Microbiol.*, **4**, 588-596.

41. Patel,D.J. and Suri,A.K. (2000) Structure, recognition and discrimination in RNA aptamer complexes with cofactors, amino acids, drugs and aminoglycoside antibiotics. *J.Biotechnol.*, **74**, 39-60.

42. Que-Gewirth,N.S. and Sullenger,B.A. (2007) Gene therapy progress and prospects: RNA aptamers. *Gene Ther.*, **14**, 283-291.

43. Blank,M. and Blind,M. (2005) Aptamers as tools for target validation. *Curr.Opin.Chem.Biol.*, **9**, 336-342.

44. Proske,D., Blank,M., Buhmann,R. and Resch,A. (2005) Aptamers - basic research, drug development, and clinical applications. *Appl.Microbiol.Biotechnol.*, **69**, 367-374.

45. Jayasena,S.D. (1999) Aptamers: an emerging class of molecules that rival antibodies in diagnostics. *Clin.Chem.*, **45**, 1628-1650.

46. Cerchia,L., Hamm,J., Libri,D., Tavitian,B. and de Franciscis, V. (2002) Nucleic acid aptamers in cancer medicine. *FEBS Lett.*, **528**, 12-16.

47. Famulok,M. and Mayer,G. (2005) Intramers and aptamers: applications in protein-function analyses and potential for drug screening. *Chembiochem.*, **6**, 19-26.

48. Gold,L. (2002) RNA as the catalyst for drug screening. *Nat.Biotechnol.*, **20**, 671-672.

49. McNamara,J.O., Andrechek,E.R., Wang,Y., Viles,K.D., Rempel,R.E., Gilboa,E., Sullenger,B.A. and Giangrande,P.H. (2006) Cell type-specific delivery of siRNAs with aptamer-siRNA chimeras. *Nat.Biotechnol.*, **24**, 1005-1015.

50. Ng,E.W., Shima,D.T., Calias,P., Cunningham,E.T., Jr., Guyer,D.R. and Adamis,A.P. (2006) Pegaptanib, a targeted anti-VEGF aptamer for ocular vascular disease. *Nat.Rev.Drug Discov.*, **5**, 123-132.

51. Patil,S.D., Rhodes,D.G. and Burgess,D.J. (2005) DNA-based therapeutics and DNA delivery systems: a comprehensive review. *AAPS.J.*, **7**, E61-E77.

52. Wiznerowicz,M., Szulc,J. and Trono,D. (2006) Tuning silence: conditional systems for RNA interference. *Nat.Methods*, **3**, 682-688.

53. Soutschek,J., Akinc,A., Bramlage,B., Charisse,K., Constien,R., Donoghue,M., Elbashir,S., Geick,A., Hadwiger,P., Harborth,J. *et al.* (2004) Therapeutic silencing of an endogenous gene by systemic administration of modified siRNAs. *Nature*, **432**, 173-178.

54. Kurreck,J. (2003) Antisense technologies. Improvement through novel chemical modifications. *Eur.J.Biochem.*, **270**, 1628-1644.

55. De Paula,D., Bentley,M.V. and Mahato,R.I. (2007) Hydrophobization and bioconjugation for enhanced siRNA delivery and targeting. *RNA.*, **13**, 431-456.

56. Kim,D.H. and Rossi,J.J. (2007) Strategies for silencing human disease using RNA interference. *Nat.Rev.Genet.*, **8**, 173-184.

57. Dorsett,Y. and Tuschl,T. (2004) siRNAs: applications in functional genomics and potential as therapeutics. *Nat.Rev.Drug Discov.*, **3**, 318-329.

58. Song,E., Zhu,P., Lee,S.K., Chowdhury,D., Kussman,S., Dykxhoorn,D.M., Feng,Y., Palliser,D., Weiner,D.B., Shankar,P. *et al.* (2005) Antibody mediated in vivo delivery of small interfering RNAs via cell-surface receptors. *Nat.Biotechnol.*, **23**, 709-717.

59. Garvie,C.W. and Wolberger,C. (2001) Recognition of specific DNA sequences. *Mol.Cell*, **8**, 937-946.

60. Halford,S.E. and Marko,J.F. (2004) How do site-specific DNA-binding proteins find their targets? *Nucleic Acids Res.*, **32**, 3040-3052.

61. Holstege,F.C. and Clevers,H. (2006) Transcription factor target practice. *Cell*, **124**, 21-23.

62. Singh,R. and Valcarcel,J. (2005) Building specificity with nonspecific RNA-binding proteins. *Nat.Struct.Mol.Biol.*, **12**, 645-653.

63. Luscombe,N.M. and Thornton,J.M. (2002) Protein-DNA interactions: amino acid conservation and the effects of mutations on binding specificity. *J.Mol.Biol.*, **320**, 991-1009.

64. Luscombe,N.M., Laskowski,R.A. and Thornton,J.M. (2001) Amino acid-base interactions: a three-dimensional analysis of protein-DNA interactions at an atomic level. *Nucleic Acids Res.*, **29**, 2860-2874.

65. Jones,S., Daley,D.T., Luscombe,N.M., Berman,H.M. and Thornton,J.M. (2001) Protein-RNA interactions: a structural analysis. *Nucleic Acids Res.*, **29**, 943-954.

66. Doudna,J.A. (2000) Structural genomics of RNA. *Nat.Struct.Biol.*, **7 Suppl**, 954-956.

67. Draper,D.E. (1999) Themes in RNA-protein recognition. *J.Mol.Biol.*, **293**, 255-270.

68. Galas,D.J. and Schmitz,A. (1978) DNAse footprinting: a simple method for the detection of protein-DNA binding specificity. *Nucleic Acids Res.*, **5**, 3157-3170.

69. Choo,Y. and Klug,A. (1993) A role in DNA binding for the linker sequences of the first three zinc fingers of TFIIIA. *Nucleic Acids Res.*, **21**, 3341-3346.

70. Choo,Y. and Klug,A. (1994) Toward a code for the interactions of zinc fingers with DNA: selection of randomized fingers displayed on phage. *Proc.Natl.Acad.Sci.U.S.A*, **91**, 11163-11167.

71. Pollock,R. and Treisman,R. (1990) A sensitive method for the determination of protein-DNA binding specificities. *Nucleic Acids Res.*, **18**, 6197-6204.

72. Brockman,J.M., Frutos,A.G. and Corn,R.M. (1999) A Multistep Chemical Modification Procedure To Create DNA Arrays on Gold Surfaces for the Study of Protein-DNA Interactions with Surface Plasmon Resonance. *J.Am.Chem.Soc.*, **121**, 8044-8051.

73. Bulyk,M.L., Huang,X., Choo,Y. and Church,G.M. (2001) Exploring the DNA-binding specificities of zinc fingers with DNA microarrays. *Proc.Natl.Acad.Sci.U.S.A*, **98**, 7158-7163.

74. Hoheisel,J.D. (2006) Microarray technology: beyond transcript profiling and genotype analysis. *Nat.Rev.Genet.*, **7**, 200-210.

75. Young,R.A. (2000) Biomedical discovery with DNA arrays. *Cell*, **102**, 9-15.

76. Bulyk,M.L. (2006) DNA microarray technologies for measuring protein-DNA interactions. *Curr.Opin.Biotechnol.*, **17**, 422-430.

77. Ren,B., Robert,F., Wyrick,J.J., Aparicio,O., Jennings,E.G., Simon,I., Zeitlinger,J., Schreiber,J., Hannett,N., Kanin,E. *et al.* (2000) Genome-wide location and function of DNA binding proteins. *Science*, **290**, 2306-2309.

78. Iyer,V.R., Horak,C.E., Scafe,C.S., Botstein,D., Snyder,M. and Brown,P.O. (2001) Genomic binding sites of the yeast cell-cycle transcription factors SBF and MBF. *Nature*, **409**, 533-538.

79. Liu,X.S., Brutlag,D.L. and Liu,J.S. (2002) An algorithm for finding protein-DNA binding sites with applications to chromatin-immunoprecipitation microarray experiments. *Nat.Biotechnol.*, **20**, 835-839.

80. Mukherjee,S., Berger,M.F., Jona,G., Wang,X.S., Muzzey,D., Snyder,M., Young,R.A. and Bulyk,M.L. (2004) Rapid analysis of the DNA-binding specificities of transcription factors with DNA microarrays. *Nat.Genet.*, **36**, 1331-1339.

81. Li,Y., Lee,H.J. and Corn,R.M. (2006) Fabrication and characterization of RNA aptamer microarrays for the study of protein-aptamer interactions with SPR imaging. *Nucleic Acids Res.*, **34**, 6416-6424.

82. Collett,J.R., Cho,E.J. and Ellington,A.D. (2005) Production and processing of aptamer microarrays. *Methods*, **37**, 4-15.

83. McCauley,T.G., Hamaguchi,N. and Stanton,M. (2003) Aptamer-based biosensor arrays for detection and quantification of biological macromolecules. *Anal.Biochem.*, **319**, 244-250.

84. Zhang,Z., Blank,M. and Schluesener,H.J. (2004) Nucleic acid aptamers in human viral disease. *Arch.Immunol.Ther.Exp.(Warsz.)*, **52**, 307-315.

85. Vater,A., Jarosch,F., Buchner,K. and Klussmann,S. (2003) Short bioactive Spiegelmers to migraine-associated calcitonin gene-related peptide rapidly identified by a novel approach: tailored-SELEX. *Nucleic Acids Res.*, **31**, e130.

86. Brody,E.N. and Gold,L. (2000) Aptamers as therapeutic and diagnostic agents. *J.Biotechnol.*, **74**, 5-13.

87. Berezovski,M., Musheev,M., Drabovich,A. and Krylov,S.N. (2006) Non-SELEX selection of aptamers. *J.Am.Chem.Soc.*, **128**, 1410-1411.

88. Pinskaya,M., Romanova,E., Volkov,E., Deprez,E., Leh,H., Brochon,J.C., Mouscadet,J.F. and Gottikh,M. (2004) HIV-1 integrase complexes with DNA dissociate in the presence of short oligonucleotides conjugated to acridine. *Biochemistry*, **43**, 8735-8743.

89. Wyatt,J.R., Vickers,T.A., Roberson,J.L., Buckheit,R.W., Jr., Klimkait,T., DeBaets,E., Davis,P.W., Rayner,B., Imbach,J.L. and Ecker,D.J. (1994) Combinatorially selected guanosine-quartet structure is a potent inhibitor of human immunodeficiency virus envelope-mediated cell fusion. *Proc.Natl.Acad.Sci.U.S.A*, **91**, 1356-1360.

90. Toulmé,J.J., Di Primo,C. and Boucard,D. (2004) Regulating eukaryotic gene expression with aptamers. *FEBS Lett.*, **567**, 55-62.

91. James,W. (2007) Aptamers in the virologists' toolkit. *J.Gen.Virol.*, **88**, 351-364.

92. Schneider,D.J., Feigon,J., Hostomsky,Z. and Gold,L. (1995) High-affinity ssDNA inhibitors of the reverse transcriptase of type 1 human immunodeficiency virus. *Biochemistry*, **34**, 9599-9610.

93. Burke,D.H., Scates,L., Andrews,K. and Gold,L. (1996) Bent pseudoknots and novel RNA inhibitors of type 1 human immunodeficiency virus (HIV-1) reverse transcriptase. *J.Mol.Biol.*, **264**, 650-666.

94. DeStefano,J.J. and Cristofaro,J.V. (2006) Selection of primer-template sequences that bind human immunodeficiency virus reverse transcriptase with high affinity. *Nucleic Acids Res.*, **34**, 130-139.

95. Joshi,P. and Prasad,V.R. (2002) Potent inhibition of human immunodeficiency virus type 1 replication by template analog reverse transcriptase inhibitors derived by SELEX (systematic evolution of ligands by exponential enrichment). *J.Virol.*, **76**, 6545-6557.

96. Andreola,M.L., Pileur,F., Calmels,C., Ventura,M., Tarrago-Litvak,L., Toulmé,J.J. and Litvak,S. (2001) DNA aptamers selected against the HIV-1 RNase H display in vitro antiviral activity. *Biochemistry*, **40**, 10087-10094.

97. Hannoush,R.N., Min,K.L. and Damha,M.J. (2004) Diversity-oriented solid-phase synthesis and biological evaluation of oligonucleotide hairpins as HIV-1 RT RNase H inhibitors. *Nucleic Acids Res.*, **32**, 6164-6175.

98. Freed,E.O. (2001) HIV-1 replication. *Somat.Cell Mol.Genet.*, **26**, 13-33.

99. Newton,I.S. (2003) RNA Virus Genome Replication and mRNA Production. In Flint,S.J., Enquist,L.W., Racaniello,V.R. and Skalka,A.M. (eds.), *Principles of Virology: Molecular Biology, Pathogenesis, and Control of Animal Viruses*. ASM Press, Washington, D.C., pp. 183-214.

100. Gallo,R.C., Salahuddin,S.Z., Popovic,M., Shearer,G.M., Kaplan,M., Haynes,B.F., Palker,T.J., Redfield,R., Oleske,J., Safai,B. *et al.* (1984) Frequent detection and isolation of cytopathic retroviruses (HTLV-III) from patients with AIDS and at risk for AIDS. *Science*, **224**, 500-503.

101. Barré-Sinoussi,F., Chermann,J.C., Rey,F., Nugeyre,M.T., Chamaret,S., Gruest,J., Dauguet,C., Axler-Blin,C., Vezinet-Brun,F., Rouzioux,C. *et al.* (1983) Isolation of a T-lymphotropic retrovirus from a patient at risk for acquired immune deficiency syndrome (AIDS). *Science*, **220**, 868-871.

102. Turner,B.G. and Summers,M.F. (1999) Structural biology of HIV. *J.Mol.Biol.*, **285**, 1-32.

103. Freed,E.O. (1998) HIV-1 gag proteins: diverse functions in the virus life cycle. *Virology*, **251**, 1-15.

104. Frankel,A.D. and Young,J.A. (1998) HIV-1: fifteen proteins and an RNA. *Annu.Rev.Biochem.*, **67**, 1-25.

105. Balvay,L., Lopez,L.M., Sargueil,B., Darlix,J.L. and Ohlmann,T. (2007) Translational control of retroviruses. *Nat.Rev.Microbiol.*, **5**, 128-140.

106. Lederman,M.M., Offord,R.E. and Hartley,O. (2006) Microbicides and other topical strategies to prevent vaginal transmission of HIV. *Nat.Rev.Immunol.*, **6**, 371-382.

107. Dimitrov,D.S. (2004) Virus entry: molecular mechanisms and biomedical applications. *Nat.Rev.Microbiol.*, **2**, 109-122.

108. Smith,A.E. and Helenius,A. (2004) How viruses enter animal cells. *Science*, **304**, 237-242.

109. Moore,J.P. and Doms,R.W. (2003) The entry of entry inhibitors: a fusion of science and medicine. *Proc.Natl.Acad.Sci.U.S.A*, **100**, 10598-10602.

110. Briz,V., Poveda,E. and Soriano,V. (2006) HIV entry inhibitors: mechanisms of action and resistance pathways. *J.Antimicrob.Chemother.*, **57**, 619-627.

111. Moore,J.P. and Stevenson,M. (2000) New targets for inhibitors of HIV-1 replication. *Nat.Rev.Mol.Cell Biol.*, **1**, 40-49.

112. Bukrinskaya,A.G. (2004) HIV-1 assembly and maturation. *Arch.Virol.*, **149**, 1067-1082.

113. Paillart,J.C., Shehu-Xhilaga,M., Marquet,R. and Mak,J. (2004) Dimerization of retroviral RNA genomes: an inseparable pair. *Nat.Rev.Microbiol.*, **2**, 461-472.

114. D'Souza,V. and Summers,M.F. (2005) How retroviruses select their genomes. *Nat.Rev.Microbiol.*, **3**, 643-655.

115. Cimarelli,A. and Darlix,J.L. (2002) Assembling the human immunodeficiency virus type 1. *Cell Mol.Life Sci.*, **59**, 1166-1184.

116. Cen,S., Niu,M. and Kleiman,L. (2004) The connection domain in reverse transcriptase facilitates the in vivo annealing of tRNALys3 to HIV-1 genomic RNA. *Retrovirology.*, **1**, 33.

117. Li,L., Li,H.S., Pauza,C.D., Bukrinsky,M. and Zhao,R.Y. (2005) Roles of HIV-1 auxiliary proteins in viral pathogenesis and host-pathogen interactions. *Cell Res.*, **15**, 923-934.

118. Mariani,R., Chen,D., Schröfelbauer,B., Navarro,F., König,R., Bollman,B., Münk,C., Nymark-McMahon,H. and Landau,N.R. (2003) Species-specific exclusion of APOBEC3G from HIV-1 virions by Vif. *Cell*, **114**, 21-31.

119. Schröfelbauer,B., Yu,Q. and Landau,N.R. (2004) New insights into the role of Vif in HIV-1 replication. *AIDS Rev.*, **6**, 34-39.

120. Sluis-Cremer,N., Arion,D., Abram,M.E. and Parniak,M.A. (2004) Proteolytic processing of an HIV-1 pol polyprotein precursor: insights into the mechanism of reverse transcriptase p66/p51 heterodimer formation. *Int.J.Biochem.Cell Biol.*, **36**, 1836-1847.

121. Rodgers,D.W., Gamblin,S.J., Harris,B.A., Ray,S., Culp,J.S., Hellmig,B., Woolf,D.J., Debouck,C. and Harrison,S.C. (1995) The structure of unliganded reverse transcriptase from the human immunodeficiency virus type 1. *Proc.Natl.Acad.Sci.U.S.A*, **92**, 1222-1226.

122. Esnouf,R., Ren,J., Ross,C., Jones,Y., Stammers,D. and Stuart,D. (1995) Mechanism of inhibition of HIV-1 reverse transcriptase by non-nucleoside inhibitors. *Nat.Struct.Biol.*, **2**, 303-308.

123. Kohlstaedt,L.A., Wang,J., Friedman,J.M., Rice,P.A. and Steitz,T.A. (1992) Crystal structure at 3.5 A resolution of HIV-1 reverse transcriptase complexed with an inhibitor. *Science*, **256**, 1783-1790.

124. Ren,J., Esnouf,R., Garman,E., Somers,D., Ross,C., Kirby,I., Keeling,J., Darby,G., Jones,Y., Stuart,D. *et al.* (1995) High resolution structures of HIV-1 RT from four RT-inhibitor complexes. *Nat.Struct.Biol.*, **2**, 293-302.

125. Smerdon,S.J., Jäger,J., Wang,J., Kohlstaedt,L.A., Chirino,A.J., Friedman,J.M., Rice,P.A. and Steitz,T.A. (1994) Structure of the binding site for nonnucleoside inhibitors of the reverse transcriptase of human immunodeficiency virus type 1. *Proc.Natl.Acad.Sci.U.S.A*, **91**, 3911-3915.

126. Das,K., Ding,J., Hsiou,Y., Clark,A.D., Jr., Moereels,H., Koymans,L., Andries,K., Pauwels,R., Janssen,P.A., Boyer,P.L. *et al.* (1996) Crystal structures of 8-Cl and 9-Cl TIBO complexed with wild-type HIV-1 RT and 8-Cl TIBO complexed with the Tyr181Cys HIV-1 RT drug-resistant mutant. *J.Mol.Biol.*, **264**, 1085-1100.

127. Pata,J.D., Stirtan,W.G., Goldstein,S.W. and Steitz,T.A. (2004) Structure of HIV-1 reverse transcriptase bound to an inhibitor active against mutant reverse transcriptases resistant to other nonnucleoside inhibitors. *Proc.Natl.Acad.Sci.U.S.A*, **101**, 10548-10553.

128. Jacobo-Molina,A., Ding,J., Nanni,R.G., Clark,A.D., Jr., Lu,X., Tantillo,C., Williams,R.L., Kamer,G., Ferris,A.L., Clark,P. *et al.* (1993) Crystal structure of human immunodeficiency virus type 1 reverse transcriptase complexed with double-stranded DNA at 3.0 A resolution shows bent DNA. *Proc.Natl.Acad.Sci.U.S.A*, **90**, 6320-6324.

129. Huang,H., Chopra,R., Verdine,G.L. and Harrison,S.C. (1998) Structure of a covalently trapped catalytic complex of HIV-1 reverse transcriptase: implications for drug resistance. *Science*, **282**, 1669-1675.

130. Sarafianos,S.G., Das,K., Tantillo,C., Clark,A.D., Jr., Ding,J., Whitcomb,J.M., Boyer,P.L., Hughes,S.H. and Arnold,E. (2001) Crystal structure of HIV-1 reverse transcriptase in complex with a polypurine tract RNA:DNA. *EMBO J.*, **20**, 1449-1461.

131. Jäger,J., Restle,T. and Steitz,T.A. (1998) The structure of HIV-1 reverse transcriptase complexed with an RNA pseudoknot inhibitor. *EMBO J.*, **17**, 4535-4542.

132. Wang,J., Smerdon,S.J., Jäger,J., Kohlstaedt,L.A., Rice,P.A., Friedman,J.M. and Steitz,T.A. (1994) Structural basis of asymmetry in the human immunodeficiency virus type 1 reverse transcriptase heterodimer. *Proc.Natl.Acad.Sci.U.S.A*, **91**, 7242-7246.

133. Restle,T., Müller,B. and Goody,R.S. (1992) RNase H activity of HIV reverse transcriptases is confined exclusively to the dimeric forms. *FEBS Lett.*, **300**, 97-100.

134. Restle,T., Müller,B. and Goody,R.S. (1990) Dimerization of human immunodeficiency virus type 1 reverse transcriptase. A target for chemotherapeutic intervention. *J.Biol.Chem.*, **265**, 8986-8988.

135. Morris,M.C., Berducou,C., Mery,J., Heitz,F. and Divita,G. (1999) The thumb domain of the P51-subunit is essential for activation of HIV reverse transcriptase. *Biochemistry*, **38**, 15097-15103.

136. Kensch,O., Restle,T., Wöhrl,B.M., Goody,R.S. and Steinhoff,H.J. (2000) Temperature-dependent equilibrium between the open and closed conformation of the p66 subunit of HIV-1 reverse transcriptase revealed by site-directed spin labelling. *J.Mol.Biol.*, **301**, 1029-1039.

137. Held,D.M., Kissel,J.D., Saran,D., Michalowski,D. and Burke,D.H. (2006) Differential susceptibility of HIV-1 reverse transcriptase to inhibition by RNA aptamers in enzymatic reactions monitoring specific steps during genome replication. *J.Biol.Chem.*, **281**, 25712-25722.

138. Götte,M., Li,X. and Wainberg,M.A. (1999) HIV-1 reverse transcription: a brief overview focused on structure-function relationships among molecules involved in initiation of the reaction. *Arch.Biochem.Biophys.*, **365**, 199-210.

139. Kleiman,L. (2002) tRNA(Lys3): the primer tRNA for reverse transcription in HIV-1. *IUBMB.Life*, **53**, 107-114.

140. Liu,H.W., Cosa,G., Landes,C.F., Zeng,Y., Kovaleski,B.J., Mullen,D.G., Barany,G., Musier-Forsyth,K. and Barbara,P.F. (2005) Single-molecule FRET studies of important intermediates in the nucleocapsid-protein-chaperoned minus-strand transfer step in HIV-1 reverse transcription. *Biophys.J.*, **89**, 3470-3479.

141. Beltz,H., Clauss,C., Piemont,E., Ficheux,D., Gorelick,R.J., Roques,B., Gabus,C., Darlix,J.L., de Rocquigny,H. and Mely,Y. (2005) Structural determinants of HIV-1 nucleocapsid protein for cTAR DNA binding and destabilization, and correlation with inhibition of self-primed DNA synthesis. *J.Mol.Biol.*, **348**, 1113-1126.

142. Cancio,R., Spadari,S. and Maga,G. (2004) Vif is an auxiliary factor of the HIV-1 reverse transcriptase and facilitates abasic site bypass. *Biochem.J.*, **383**, 475-482.

143. De Clercq,E. (2004) Antivirals and antiviral strategies. *Nat.Rev.Microbiol.*, **2**, 704-720.

144. Lengauer,T. and Sing,T. (2006) Bioinformatics-assisted anti-HIV therapy. *Nat.Rev.Microbiol.*, **4**, 790-797.

145. Stevens,M., De Clercq,E. and Balzarini,J. (2006) The regulation of HIV-1 transcription: molecular targets for chemotherapeutic intervention. *Med.Res.Rev.*, **26**, 595-625.

146. Sticht,J., Humbert,M., Findlow,S., Bodem,J., Müller,B., Dietrich,U., Werner,J. and Kräusslich,H.G. (2005) A peptide inhibitor of HIV-1 assembly in vitro. *Nat.Struct.Mol.Biol.*, **12**, 671-677.

147. Strayer,D.S., Akkina,R., Bunnell,B.A., Dropulic,B., Planelles,V., Pomerantz,R.J., Rossi,J.J. and Zaia,J.A. (2005) Current status of gene therapy strategies to treat HIV/AIDS. *Mol.Ther.*, **11**, 823-842.

148. Jacque,J.M., Triques,K. and Stevenson,M. (2002) Modulation of HIV-1 replication by RNA interference. *Nature*, **418**, 435-438.

149. Lee,N.S. and Rossi,J.J. (2004) Control of HIV-1 replication by RNA interference. *Virus Res.*, **102**, 53-58.

150. Konstantinova,P., de Vries,W., Haasnoot,J., ter Brake,O., de Haan,P. and Berkhout,B. (2006) Inhibition of human immunodeficiency virus type 1 by RNA interference using long-hairpin RNA. *Gene Ther.*, **13**, 1403-1413.

151. Wolkowicz,R. and Nolan,G.P. (2005) Gene therapy progress and prospects: novel gene therapy approaches for AIDS. *Gene Ther.*, **12**, 467-476.

152. Elmén,J., Zhang,H.Y., Zuber,B., Ljungberg,K., Wahren,B., Wahlestedt,C. and Liang,Z. (2004) Locked nucleic acid containing antisense oligonucleotides enhance inhibition of HIV-1 genome dimerization and inhibit virus replication. *FEBS Lett.*, **578**, 285-290.

153. Nielsen,M.H., Pedersen,F.S. and Kjems,J. (2005) Molecular strategies to inhibit HIV-1 replication. *Retrovirology.*, **2**, 10.

154. Tarrago-Litvak,L., Andréola,M.L., Nevinsky,G.A., Sarih-Cottin,L. and Litvak,S. (1994) The reverse transcriptase of HIV-1: from enzymology to therapeutic intervention. *FASEB J.*, **8**, 497-503.

155. Pomerantz,R.J. and Horn,D.L. (2003) Twenty years of therapy for HIV-1 infection. *Nat.Med.*, **9**, 867-873.

156. Vivet-Boudou,V., Didierjean,J., Isel,C. and Marquet,R. (2006) Nucleoside and nucleotide inhibitors of HIV-1 replication. *Cell Mol.Life Sci.*, **63**, 163-186.

157. De Clercq,E. (2004) Non-nucleoside reverse transcriptase inhibitors (NNRTIs): past, present, and future. *Chem.Biodivers.*, **1**, 44-64.

158. Sarafianos,S.G., Das,K., Hughes,S.H. and Arnold,E. (2004) Taking aim at a moving target: designing drugs to inhibit drug-resistant HIV-1 reverse transcriptases. *Curr.Opin.Struct.Biol.*, **14**, 716-730.

159. Turner,D. and Wainberg,M.A. (2006) HIV transmission and primary drug resistance. *AIDS Rev.*, **8**, 17-23.

160. Menendez-Arias,L. (2002) Targeting HIV: antiretroviral therapy and development of drug resistance. *Trends Pharmacol.Sci.*, **23**, 381-388.

161. Carr,A. (2003) Toxicity of antiretroviral therapy and implications for drug development. *Nat.Rev.Drug Discov.*, **2**, 624-634.

162. Pinti,M., Salomoni,P. and Cossarizza,A. (2006) Anti-HIV drugs and the mitochondria. *Biochim.Biophys.Acta*, **1757**, 700-707.

163. Tuerk,C., MacDougal,S. and Gold,L. (1992) RNA pseudoknots that inhibit human immunodeficiency virus type 1 reverse transcriptase. *Proc.Natl.Acad.Sci.U.S.A*, **89**, 6988-6992.

164. Kensch,O., Connolly,B.A., Steinhoff,H.J., McGregor,A., Goody,R.S. and Restle,T. (2000) HIV-1 reverse transcriptase-pseudoknot RNA aptamer interaction has a binding affinity in the low picomolar range coupled with high specificity. *J.Biol.Chem.*, **275**, 18271-18278.

165. Chaloin,L., Lehmann,M.J., Sczakiel,G. and Restle,T. (2002) Endogenous expression of a high-affinity pseudoknot RNA aptamer suppresses replication of HIV-1. *Nucleic Acids Res.*, **30**, 4001-4008.

166. Sluis-Cremer,N. and Tachedjian,G. (2002) Modulation of the oligomeric structures of HIV-1 retroviral enzymes by synthetic peptides and small molecules. *Eur.J.Biochem.*, **269**, 5103-5111.

167. Morris,M.C., Robert-Hebmann,V., Chaloin,L., Mery,J., Heitz,F., Devaux,C., Goody,R.S. and Divita,G. (1999) A new potent HIV-1 reverse transcriptase inhibitor. A synthetic peptide derived from the interface subunit domains. *J.Biol.Chem.*, **274**, 24941-24946.

168. Depollier,J., Hourdou,M.L., Aldrian-Herrada,G., Rothwell,P., Restle,T. and Divita,G. (2005) Insight into the mechanism of a peptide inhibitor of HIV reverse transcriptase dimerization. *Biochemistry*, **44**, 1909-1918.

169. Menezes,J., Leibold,W., Klein,G. and Clements,G. (1975) Establishment and characterization of an Epstein-Barr virus (EBC)-negative lymphoblastoid B cell line (BJA-B) from an exceptional, EBV-genome-negative African Burkitt's lymphoma. *Biomedicine.*, **22**, 276-284.

170. DuBridge,R.B., Tang,P., Hsia,H.C., Leong,P.M., Miller,J.H. and Calos,M.P. (1987) Analysis of mutation in human cells by using an Epstein-Barr virus shuttle system. *Mol.Cell Biol.*, **7**, 379-387.

171. Graham,F.L., Smiley,J., Russell,W.C. and Nairn,R. (1977) Characteristics of a human cell line transformed by DNA from human adenovirus type 5. *J.Gen.Virol.*, **36**, 59-74.

172. Restle,T., Pawlita,M., Sczakiel,G., Müller,B. and Goody,R.S. (1992) Structure-function relationships of HIV-1 reverse transcriptase determined using monoclonal antibodies. *J.Biol.Chem.*, **267**, 14654-14661.

173. Wöhrl,B.M., Krebs,R., Thrall,S.H., Le Grice,S.F., Scheidig,A.J. and Goody,R.S. (1997) Kinetic analysis of four HIV-1 reverse transcriptase enzymes mutated in the primer grip region of p66. Implications for DNA synthesis and dimerization. *J.Biol.Chem.*, **272**, 17581-17587.

174. Jármy,G., Heinkelein,M., Weissbrich,B., Jassoy,C. and Rethwilm,A. (2001) Phenotypic analysis of the sensitivity of HIV-1 to inhibitors of the reverse transcriptase, protease, and integrase using a self-inactivating virus vector system. *J.Med.Virol.*, **64**, 223-231.

175. Müller,B., Restle,T., Weiss,S., Gautel,M., Sczakiel,G. and Goody,R.S. (1989) Co-expression of the subunits of the heterodimer of HIV-1 reverse transcriptase in Escherichia coli. *J.Biol.Chem.*, **264**, 13975-13978.

176. http://www.expasy.org/tools/protparam.html . 2007.

177. Laemmli,U.K. (1970) Cleavage of structural proteins during the assembly of the head of bacteriophage T4. *Nature*, **227**, 680-685.

178. Kim,B., Ayran,J.C., Sagar,S.G., Adman,E.T., Fuller,S.M., Tran,N.H. and Horrigan,J. (1999) New human immunodeficiency virus, type 1 reverse transcriptase (HIV-1 RT) mutants with increased fidelity of DNA synthesis. Accuracy, template binding, and processivity. *J.Biol.Chem.*, **274**, 27666-27673.

179. Arts,E.J., Miller,J.T., Ehresmann,B. and Le Grice,S.F. (1998) Mutating a region of HIV-1 reverse transcriptase implicated in tRNA(Lys-3) binding and the consequences for (-)-strand DNA synthesis. *J.Biol.Chem.*, **273**, 14523-14532.

180. Morris,G.E., Frost,L.C., Newport,P.A. and Hudson,N. (1987) Monoclonal antibody studies of creatine kinase. Antibody-binding sites in the N-terminal region of creatine kinase and effects of antibody on enzyme refolding. *Biochem.J.*, **248**, 53-59.

181. Mustard,D. and Ritchie,D.W. (2005) Docking essential dynamics eigenstructures. *Proteins*, **60**, 269-274.

182. Pettersen,E.F., Goddard,T.D., Huang,C.C., Couch,G.S., Greenblatt,D.M., Meng,E.C. and Ferrin,T.E. (2004) UCSF Chimera - a visualization system for exploratory research and analysis. *J.Comput.Chem.*, **25**, 1605-1612.

183. Phelan,M.C. Basic Techniques for Mammalian Cell Tissue Culture. 2002. New Yersey, John Wiley & Sons, Inc. Current Protocols in Cell Biology. Bonifacino, J. S., Dasso, M., Harford, J. B., Lippincott-Schwartz, J., and Yamada, K. M.

184. Jones,K.H. and Senft,J.A. (1985) An improved method to determine cell viability by simultaneous staining with fluorescein diacetate-propidium iodide. *J.Histochem.Cytochem.*, **33**, 77-79.

185. Albright, L., Coen, D. M., Smith, C. L., Varki, A., and Wildermuth, M. C. (5). 2007. New York, John Wiley & Sons, Inc. Current Protocols in Molecular Biology. Harkinis, E. W.

186. Wöhrl,B.M., Krebs,R., Goody,R.S. and Restle,T. (1999) Refined model for primer/template binding by HIV-1 reverse transcriptase: pre-steady-state kinetic analyses of primer/template binding and nucleotide incorporation events distinguish between different binding modes depending on the nature of the nucleic acid substrate. *J.Mol.Biol.*, **292**, 333-344.

187. Arion,D., Harada,R., Li,X., Wainberg,M.A. and Parniak,M.A. (1996) HIV-1 reverse transcriptase shows no specificity for the binding of primer tRNA(Lys3). *Biochem.Biophys.Res.Commun.*, **225**, 839-843.

188. Ren,J., Bird,L.E., Chamberlain,P.P., Stewart-Jones,G.B., Stuart,D.I. and Stammers,D.K. (2002) Structure of HIV-2 reverse transcriptase at 2.35-A resolution and the mechanism of resistance to non-nucleoside inhibitors. *Proc.Natl.Acad.Sci.U.S.A*, **99**, 14410-14415.

189. Pauwels,R., Andries,K., Desmyter,J., Schols,D., Kukla,M.J., Breslin,H.J., Raeymaeckers,A., Van Gelder,J., Woestenborghs,R., Heykants,J. *et al.* (1990) Potent and selective inhibition of HIV-1 replication in vitro by a novel series of TIBO derivatives. *Nature*, **343**, 470-474.

190. Uprichard,S.L. (2005) The therapeutic potential of RNA interference. *FEBS Lett.*, **579**, 5996-6007.

191. Li,C.X., Parker,A., Menocal,E., Xiang,S., Borodyansky,L. and Fruehauf,J.H. (2006) Delivery of RNA interference. *Cell Cycle*, **5**, 2103-2109.

192. Hughes,M.D., Hussain,M., Nawaz,Q., Sayyed,P. and Akhtar,S. (2001) The cellular delivery of antisense oligonucleotides and ribozymes. *Drug Discov.Today*, **6**, 303-315.

193. Mescalchin,A., Wünsche,W., Laufer,S.D., Grohmann,D., Restle,T. and Sczakiel,G. (2006) Specific binding of a hexanucleotide to HIV-1 reverse transcriptase: a novel class of bioactive molecules. *Nucleic Acids Res.*, **34**, 5631-5637.

194. von Schwedler,U.K., Stuchell,M., Müller,B., Ward,D.M., Chung,H.Y., Morita,E., Wang,H.E., Davis,T., He,G.P., Cimbora,D.M. *et al.* (2003) The protein network of HIV budding. *Cell*, **114**, 701-713.

195. Stuchell,M.D., Garrus,J.E., Müller,B., Stray,K.M., Ghaffarian,S., McKinnon,R., Kräusslich,H.G., Morham,S.G. and Sundquist,W.I. (2004) The human endosomal sorting complex required for transport (ESCRT-I) and its role in HIV-1 budding. *J.Biol.Chem.*, **279**, 36059-36071.

196. Roberts,J.D., Bebenek,K. and Kunkel,T.A. (1988) The accuracy of reverse transcriptase from HIV-1. *Science*, **242**, 1171-1173.

197. Preston,B.D., Poiesz,B.J. and Loeb,L.A. (1988) Fidelity of HIV-1 reverse transcriptase. *Science*, **242**, 1168-1171.

198. Nicholas,K.B., Nicholas,H.B.J. and Deerfield,D.W., II (1997) GeneDoc: Analysis and Visualization of Genetic Variation. *EMBNEW.NEWS*, **4**, 14.

199. Rothwell,P.J., Berger,S., Kensch,O., Felekyan,S., Antonik,M., Wöhrl,B.M., Restle,T., Goody,R.S. and Seidel,C.A. (2003) Multiparameter single-molecule fluorescence spectroscopy reveals heterogeneity of HIV-1 reverse transcriptase:primer/template complexes. *Proc.Natl.Acad.Sci.U.S.A*, **100**, 1655-1660.

200. Allende,J.E. (1988) GTP-mediated macromolecular interactions: the common features of different systems. *FASEB J.*, **2**, 2356-2367.

201. Sternlicht,H., Yaffe,M.B. and Farr,G.W. (1987) A model of the nucleotide-binding site in tubulin. *FEBS Lett.*, **214**, 226-235.

202. Veldhoen,S., Laufer,S.D., Trampe,A. and Restle,T. (2006) Cellular delivery of small interfering RNA by a non-covalently attached cell-penetrating peptide: quantitative analysis of uptake and biological effect. *Nucleic Acids Res.*, **34**, 6561-6573.

203. Basner-Tschakarjan,E., Mirmohammadsadegh,A., Baer,A. and Hengge,U.R. (2004) Uptake and trafficking of DNA in keratinocytes: evidence for DNA-binding proteins. *Gene Ther.*, **11**, 765-774.

204. Budker,V., Budker,T., Zhang,G., Subbotin,V., Loomis,A. and Wolff,J.A. (2000) Hypothesis: naked plasmid DNA is taken up by cells in vivo by a receptor-mediated process. *J.Gene Med.*, **2**, 76-88.

205. Wiegers,K., Rutter,G., Kottler,H., Tessmer,U., Hohenberg,H. and Kräusslich,H.G. (1998) Sequential steps in human immunodeficiency virus particle maturation revealed by alterations of individual Gag polyprotein cleavage sites. *J.Virol.*, **72**, 2846-2854.

206. Pettit,S.C., Everitt,L.E., Choudhury,S., Dunn,B.M. and Kaplan,A.H. (2004) Initial cleavage of the human immunodeficiency virus type 1 GagPol precursor by its activated protease occurs by an intramolecular mechanism. *J.Virol.*, **78**, 8477-8485.

207. Buxton,P., Tachedjian,G. and Mak,J. (2005) Analysis of the contribution of reverse transcriptase and integrase proteins to retroviral RNA dimer conformation. *J.Virol.*, **79**, 6338-6348.

208. Shehu-Xhilaga,M., Crowe,S.M. and Mak,J. (2001) Maintenance of the Gag/Gag-Pol ratio is important for human immunodeficiency virus type 1 RNA dimerization and viral infectivity. *J.Virol.*, **75**, 1834-1841.

209. Shehu-Xhilaga,M., Hill,M., Marshall,J.A., Kappes,J., Crowe,S.M. and Mak,J. (2002) The conformation of the mature dimeric human immunodeficiency virus type 1 RNA genome requires packaging of pol protein. *J.Virol.*, **76**, 4331-4340.

210. Wang,S.W. and Aldovini,A. (2002) RNA incorporation is critical for retroviral particle integrity after cell membrane assembly of Gag complexes. *J.Virol.*, **76**, 11853-11865.

211. Yu,Q., Ottmann,M., Pechoux,C., Le Grice,S. and Darlix,J.L. (1998) Mutations in the primer grip of human immunodeficiency virus type 1 reverse transcriptase impair proviral DNA synthesis and virion maturation. *J.Virol.*, **72**, 7676-7680.

212. Huang,Y., Khorchid,A., Wang,J., Parniak,M.A., Darlix,J.L., Wainberg,M.A. and Kleiman,L. (1997) Effect of mutations in the nucleocapsid protein (NCp7) upon Pr160(gag-pol) and tRNA(Lys) incorporation into human immunodeficiency virus type 1. *J.Virol.*, **71**, 4378-4384.

213. Mak,J., Jiang,M., Wainberg,M.A., Hammarskjold,M.L., Rekosh,D. and Kleiman,L. (1994) Role of Pr160gag-pol in mediating the selective incorporation of tRNA(Lys) into human immunodeficiency virus type 1 particles. *J.Virol.*, **68**, 2065-2072.

214. Khorchid,A., Javanbakht,H., Wise,S., Halwani,R., Parniak,M.A., Wainberg,M.A. and Kleiman,L. (2000) Sequences within Pr160gag-pol affecting the selective packaging of primer tRNA(Lys3) into HIV-1. *J.Mol.Biol.*, **299**, 17-26.

215. Tuerk,C., Eddy,S., Parma,D. and Gold,L. (1990) Autogenous translational operator recognized by bacteriophage T4 DNA polymerase. *J.Mol.Biol.*, **213**, 749-761.

216. Caughey,B. and Baron,G.S. (2006) Prions and their partners in crime. *Nature*, **443**, 803-810.

217. Weissmann,C. (2004) The state of the prion. *Nat.Rev.Microbiol.*, **2**, 861-871.

218. Baldwin,T.O. (1996) Firefly luciferase: the structure is known, but the mystery remains. *Structure.*, **4**, 223-228.

219. Sevilya,Z., Loya,S., Adir,N. and Hizi,A. (2003) The ribonuclease H activity of the reverse transcriptases of human immunodeficiency viruses type 1 and type 2 is modulated by residue 294 of the small subunit. *Nucleic Acids Res.*, **31**, 1481-1487.

220. Rubinek,T., Loya,S., Shaharabany,M., Hughes,S.H., Clark,P.K. and Hizi,A. (1994) The catalytic properties of the reverse transcriptase of the lentivirus equine infectious anemia virus. *Eur.J.Biochem.*, **219**, 977-983.

221. Souquet,M., Restle,T., Krebs,R., Le Grice,S.F., Goody,R.S. and Wöhrl,B.M. (1998) Analysis of the polymerization kinetics of homodimeric EIAV p51/51 reverse transcriptase implies the formation of a polymerase active site identical to heterodimeric EIAV p66/51 reverse transcriptase. *Biochemistry*, **37**, 12144-12152.

222. Sousa,R., Chung,Y.J., Rose,J.P. and Wang,B.C. (1993) Crystal structure of bacteriophage T7 RNA polymerase at 3.3 A resolution. *Nature*, **364**, 593-599.

223. Patel,P.H., Jacobo-Molina,A., Ding,J., Tantillo,C., Clark,A.D., Jr., Raag,R., Nanni,R.G., Hughes,S.H. and Arnold,E. (1995) Insights into DNA polymerization mechanisms from structure and function analysis of HIV-1 reverse transcriptase. *Biochemistry*, **34**, 5351-5363.

224. Mishima,Y. and Steitz,J.A. (1995) Site-specific crosslinking of 4-thiouridine-modified human tRNA(3Lys) to reverse transcriptase from human immunodeficiency virus type I. *EMBO J.*, **14**, 2679-2687.

225. Ren,J., Esnouf,R., Hopkins,A., Ross,C., Jones,Y., Stammers,D. and Stuart,D. (1995) The structure of HIV-1 reverse transcriptase complexed with 9-chloro-TIBO: lessons for inhibitor design. *Structure.*, **3**, 915-926.

226. Rittinger,K., Divita,G. and Goody,R.S. (1995) Human immunodeficiency virus reverse transcriptase substrate-induced conformational changes and the mechanism of inhibition by nonnucleoside inhibitors. *Proc.Natl.Acad.Sci.U.S.A*, **92**, 8046-8049.

227. Meyer,B. and Peters,T. (2003) NMR spectroscopy techniques for screening and identifying ligand binding to protein receptors. *Angew.Chem.Int.Ed Engl.*, **42**, 864-890.

228. Liew,F.Y., Xu,D., Brint,E.K. and O'Neill,L.A. (2005) Negative regulation of toll-like receptor-mediated immune responses. *Nat.Rev.Immunol.*, **5**, 446-458.

229. Cook,D.N., Pisetsky,D.S. and Schwartz,D.A. (2004) Toll-like receptors in the pathogenesis of human disease. *Nat.Immunol.*, **5**, 975-979.

230. Rifkin,I.R., Leadbetter,E.A., Busconi,L., Viglianti,G. and Marshak-Rothstein,A. (2005) Toll-like receptors, endogenous ligands, and systemic autoimmune disease. *Immunol.Rev.*, **204**, 27-42.

231. Nishibori,M., Takahashi,H.K. and Mori,S. (2003) The regulation of ICAM-1 and LFA-1 interaction by autacoids and statins: a novel strategy for controlling inflammation and immune responses. *J.Pharmacol.Sci.*, **92**, 7-12.

232. Weitz-Schmidt,G., Welzenbach,K., Brinkmann,V., Kamata,T., Kallen,J., Bruns,C., Cottens,S., Takada,Y. and Hommel,U. (2001) Statins selectively inhibit leukocyte function antigen-1 by binding to a novel regulatory integrin site. *Nat.Med.*, **7**, 687-692.

233. Mo,H., Lu,L., Pilot-Matias,T., Pithawalla,R., Mondal,R., Masse,S., Dekhtyar,T., Ng,T., Koev,G., Stoll,V. *et al.* (2005) Mutations conferring resistance to a hepatitis C virus (HCV) RNA-dependent RNA polymerase inhibitor alone or in combination with an HCV serine protease inhibitor in vitro. *Antimicrob.Agents Chemother.*, **49**, 4305-4314.

234. Zhong,W., An,H., Barawkar,D. and Hong,Z. (2003) Dinucleotide analogues as novel inhibitors of RNA-dependent RNA polymerase of hepatitis C Virus. *Antimicrob.Agents Chemother.*, **47**, 2674-2681.

235. Cohen,L., Benichou,D. and Martin,A. (2002) Analysis of deletion mutants indicates that the 2A polypeptide of hepatitis A virus participates in virion morphogenesis. *J.Virol.*, **76**, 7495-7505.

236. Peters,H., Kusov,Y.Y., Meyer,S., Benie,A.J., Bäuml,E., Wolff,M., Rademacher,C., Peters,T. and Gauss-Müller,V. (2005) Hepatitis A virus proteinase 3C binding to viral RNA: correlation with substrate binding and enzyme dimerization. *Biochem.J.*, **385**, 363-370.

9 Acknowledgements

First and foremost, I would like to thank my Ph.D. supervisor Prof. Dr. Georg Sczakiel, who has given me the opportunity to work at his Institute, for his guidance, advice and support throughout this study.

I would also like to express my gratitude to Prof. Dr. Tobias Restle who first of all provided several proteins and compounds without which this study would not have been possible. The docking study he performed on the hexanucleotide and HIV-1 RT gave me an insight into this interaction in the third dimension and helped to understand the crosslinking experiment. Furthermore, I am grateful for his comments and suggestions.

I am also very grateful to Mr. Winfried Wünsche for his contributions within the ´hexanucleotide world´, for the helpful discussions and for laying the basis of many experimental approaches applied here.

Part of this study would not have been possible without the help of Dr. Dina Grohmann and Mrs. Sandra D. Laufer, who introduced me to the RDDP and RNase H HIV-1 RT activity assays and the HIV-based cell system. Sandra D. Laufer in particular performed the initial experiment using hexanucleotides in the cell-based system.

I would also like to thank Mrs. Kathrin Theil and Mr. Philip Seibler, who during their Bachelour thesis and Master training, respectively, worked with me to study the interactions between hexanucleotides and RT.

I would also like to express my gratitude to all the members of the Institute of Molecular Medicine for giving time, insight, ideas and suggestions during my work and for an excellent atmosphere, which made my work enjoyable and fulfilling.

I appreciated the help of Mrs. Gabriele Kreutzfeldt in improving my German, despite there is still a little bit of work to do. I am particularly grateful to Mrs. Petra Höltig for the support she gave me during all the paperwork.

I thank Dr. Eicke Latz (University of Massachusetts Medical School, Worcester, USA) for providing us with the TLR9 recombinant protein used in this study, Dr. Barbara Müller (Dep. of Virology, Heidelberg) for the anti-p24 Ab and Dr. Patrick Zeltz (BF Biolabs, Freiburg) for pieces of advice in the use of the arrays.

This work was financially supported by the Institute of Molecular Medicine (Lübeck), the K-DDTM (Lübeck), the Werner und Klara Kreitz-Stiftung (Kiel) and since the beginning of this year by the grant of the ´Medizinische Fakultät, Lübeck´ (FKZ: A26:2007).

10 Curriculum Vitae

Personal data

Name:	Alessandra Mescalchin
Date of birth:	13.10.1975
Place of birth:	Dolo (Ve), Italy
Nationality:	Italian
Family status:	unmarried

Study and Ph.D. thesis

Sep. 1989 - Jul. 1994	High school degree (Diploma Scuola Superiore) “ITIS Pacinotti”, Mestre (Ve), Italy.
Oct. 1994 - Mar. 2001	Diploma study in Biology at the University of Padua, Italy.
	Degree: Master of Biology (Laurea), 110/110 cum laude.
	Master thesis: “A dominant-negative mutant of Zebrafish myostatin inhibits the secretion of the wild-type protein” under the tutorship of Prof. Dr. Lorenzo Colombo, Laboratory of Comparative Endocrinology, Biology Department, University of Padua, Italy.
Mar. 2001 - Sep. 2001	Professional training period Professor Dr. Lorenzo Colombo, Laboratory of Comparative Endocrinology, Biology Department, University of Padua, Italy.
May 2004 - present	Ph.D. studentship under the supervision of Prof. Dr. Georg Sczakiel, Institute of Molecular Medicine, University of Lübeck, Germany.
	Project: Selection and characterisation of short oligonucleotides which bind to target proteins.

Employment: industrial experience

Oct. 2001 - Apr. 2004	Researcher at Cutech Srl, Padua, Italy.
	Project: Effects of hair growth modulators on human hair follicles. Isolation of hair follicle cell populations and

development of new screening systems to test the effect of candidate drugs.

Teaching experience

Nov. 2005 – present	Instructor of Bachelor theses in “Molecular Life Science”, University of Lübeck, Germany.
Nov. 2005 - present	Instructor of lab courses in Master course “Molecular Life Science”, University of Lübeck, Germany.

Grants

Apr. 2006	Grant for the research project “Zelluläre Einschleusung von therapeutischen Oligonukleotiden” together with Dr. Marita Overhoff by the “Werner und Klara Kreitz-Stiftung”, Kiel (2006: € 5,000).
Sep. 2006	Grant for the research project “Development of hexanucleotides as a novel class of small oligomeric nucleic acid tools and drugs” by the Forschunsförderung der Medizinischen Fakultät, Universität zu Lübeck (2007–2008: € 37,500). FKZ: A26-2007.

Publications

B. Havlickova, T. Bíró, A. Mescalchin, P. Arenberger and R. Paus. Towards optimization of an organotypic assay system that imitates human hair follicle-like epithelial-mesenchymal interactions. British Journal of Dermatology (2004) 151:753-765.

E. Bodó, T. Bíró, A. Telek, G. Czifra, Z. Griger, B.I. Tóth, A. Mescalchin, T. Ito, A. Bettermann, L. Kovács and R. Paus. A hot new twist to hair biology involvement of vanilloid receptor-1 (VR1/TRPV1) signalling in human hair growth control. American Journal of Pathology (2005) 166:985-998.

A. Mescalchin, W. Wünsche, S.D. Laufer, D. Grohmann, T. Restle, and G. Sczakiel. Specific binding of a hexanucleotide to HIV-1 reverse transcriptase: a novel class of bioactive molecules. Nucleic Acids Research (2006) 34:5631-5637.

A. Mescalchin, A. Detzer, M. Wecke, M. Overhoff, W. Wünsche and G. Sczakiel. Delivery and intracellular release are major obstacles to the therapeutic application of siRNA: novel options by phosphorothioate-stimulated delivery. Manuscript submitted.

B. Havlickova, T. Bíró, A. Mescalchin, M. Tschirschmann, H. Mollenkopf, A. Bettermann, P. Pertile, R. Lauster and R. Paus. A novel human folliculoid microsphere assay for exploring epithelial-mesenchymal interactions that mimic intrafollicular communication pathways. Manuscript submitted.

Patent

A. Mescalchin, W. Wünsche, S.D. Laufer, D. Grohmann, T. Restle, G. Sczakiel. Oligonucleotide active substances. Patent: Publication No.: WO/2006/122701, International Application No.: PCT/EP2006/004439, Publication Date: 23.11.2006, International Filing Date: 11.05.2006.

Posters and Abstracts

S. Vianello, L. Brazzoduro, A. Mescalchin**,** P. Belvedere and L. Colombo (2001). A dominant negative mutant of Zebrafish myostatin inhibits the secretion of the wild-type protein. Program of the 14th International Congress of the Comparative Endocrinology, Sorrento (NA) Italy, 26-30 May 2001.

A. Mescalchin, A. Zambon Bertoja, P. Pertile and R. Paus (2003). Human hair follicle organ culture as a screening tool for "hair drug" discovery: a reconsideration. Program of the annual meeting of the Arbeitsgemeinschaft Dermatologische Forschung (ADF), Frankfurt Germany, 27 February-1 March 2003.

A. Zambon Bertoja, A. Mescalchin, P. Pertile and R. Paus (2003). Human hair follicle organ culture as a screening tool for "hair drug" discovery: a reconsideration. Program of the 1st Joint Meeting of the International Congress for Bioengineering and the International Society for Skin Imaging, Hamburg Germany, 21-23 May 2003.

A. Mescalchin, M. Massironi, A. Bettermann, R. Paus and P. Pertile (2004). Human hair follicle organ culture as a screening tool for "hair drug" discovery: applications, limitations and optimization. The Society of Investigative Dermatology, Providence, Rhode Island, 28 April-1 May 2004.

A. Mescalchin, M. Massironi, A. Bettermann, R. Paus and P. Pertile (2004). Human hair follicle organ culture as a screening tool for "hair drug" discovery. The 4th Intercontinental Meeting of Hair Research Societies, Berlin, 17-19 June 2004.

A. Mescalchin, W. Wünsche, T. Restle and G. Sczakiel. Identification of a hexanucleotide which specifically binds to HIV-1 reverse transcriptase. First meeting of the Oligonucleotide Therapeutics Society in New York, 15-18 September 2005.

A. Mescalchin, W. Wünsche, S. Laufer, T. Restle and G. Sczakiel. Hexanucleotides as target-specidic drugs. International Workshop on Discovery of Antiviral Compounds. Lübeck, Germany, 26-29 April 2006.

A. Mescalchin, W. Wünsche, S.D. Laufer, T. Restle and G. Sczakiel. Hexanucleotides as target-specific drugs. RNA Biochemistry & Workshop on microRNAs. Kassel, Germany, 12-15 October 2006.

A. Mescalchin, W. Wünsche and G. Sczakiel. Specific binding of the selected hexanucleotide UCGUGU to HIV-1 reverse transcriptase: development of a hexamer array. The 7th International Meeting on Recognition Studies in Nucleic Acids (NACON VII). University of Sheffield, UK, 1-5 April 2007.